I. Collective Behavior, From Particles to Fields

I.A Introduction

The object of the first part of this course was to introduce the principles of statistical mechanics which provide a bridge between the fundamental laws of microscopic physics, and observed phenomena at macroscopic scales.

Microscopic Physics is characterized by large numbers of degrees of freedom; for example, the set of positions and momenta $\{\vec{p}_i, \vec{q}_i\}$, of particles in a gas, configurations of spins $\{\vec{s}_i\}$, in a magnet, or occupation numbers $\{n_i\}$, in a grand canonical ensemble. The evolution of these degrees of freedom is governed by an underlying Hamiltonian $\mathcal{H}$.

Macroscopic Physics is usually described by a few equilibrium state variables such as pressure P, volume V, temperature T, internal energy E, entropy S, etc., which obey the laws of thermodynamics.

Statistical Mechanics provides a probabilistic connection between the two realms. For example, in a canonical ensemble of temperature T, each micro-state μ, of the system occurs with a probability $p(\mu) = \exp\big(-\beta\mathcal{H}(\mu)\big)/Z$, where $\beta = (k_B T)^{-1}$. To insure that the total probability is normalized to unity, the *partition function* $Z(T)$ must equal $\sum_\mu \exp\big(-\beta\mathcal{H}(\mu)\big)$. Thermodynamic information about the *macroscopic* state of the system is then extracted from the *free energy* $F = -k_B T \ln Z$.

The above program can in fact be fully carried out only for a limited number of simple systems; mostly describing non–interacting collections of particles where the partition function can be calculated exactly. Some effects of interactions can be included by perturbative treatments around such exact solutions. However, even for the relatively simple case of an imperfect gas, the perturbative approach breaks down close to the condensation point. One the other hand, it is precisely the multitude of new phases and prperties resulting from interactions that renders macroscopic physics interesting. In particular, we would like to address the following questions:

(1) In the thermodynamic limit ($N \to \infty$), strong interactions lead to new phases of matter. We studied the simplest example of the liquid gas transition in some detail, but there are in fact many other interesting phases such as solids, liquid–crystals, magnets, superconductors, etc. How can we describe the emergence of such distinct macroscopic behavior from the interactions of the underlying particles? What are the thermodynamic variables that describe the macroscopic state of these phases; and

what are their identifying signatures in measurements of bulk response functions (heat capacity, susceptibility, etc.)?

(2) What are the characteristic low energy excitations of the system? As in the case of phonons in solids or in superfluid helium, low energy excitations are typically *collective modes*, which involve the coordinated motions of many microscopic degrees of freedom (particles). These modes are easily excited by thermal fluctuations, and probed by scattering experiments.

The underlying microscopic Hamiltonian for the interactions of particles is usually quite complicated, making an *ab initio* particulate approach to the problem intractable. However, there are many common features in the macroscopic behavior of many such systems that can still be fruitfully studied by the methods of statistical mechanics. Although, the interactions between particles are very different at the microscopic scale, one may hope that averaging over sufficiently many particles leads to a simpler description. (In the same sense that the central limit theorem ensures that the sum over many random variables has a simple Gaussian distribution.) This expectation is indeed justified in many cases where the collective behavior of the interacting system becomes more simple at long wavelengths and long times. (This is sometimes called *hydrodynamic limit* by analogy to the Navier–Stokes equations for a fluid of particles.) The averaged variables appropriate to these length and time scales are no longer the discrete set of particle degrees of freedom, but slowly varying continuous *fields*. For example, the velocity field that appears in the Navier–Stokes equations is quite distinct from the velocities of the individual particles in the fluid. Hence the productive method for the study of collective behavior in interacting systems is the Statistical Mechanics of Fields. Thus the program of this course is,

- **Goal:** To learn to describe and classify states of matter, their collective properties, and the mechanisms for transforming from one phase to another.
- **Tools:** Methods of classical field theories; use of symmetries, treatment of nonlinearities by perturbation theory, and the renormalization group (RG) method.
- **Scope:** To provide sufficient familiarity with the material so that you can follow the current literature on such subjects as phase transitions, growth phenomena, polymers, superconductors, etc.

I.B Phonons and Elasticity

The theory of elasticity represents one of the simplest examples of a field theory. We shall demonstrate how certain properties of an elastic medium can be obtained, either by

the complicated method of starting from first principles, or by the much simpler means of appealing to symmetries of the problem. As such, it represents a prototype of how much can be learned from a phenomenological approach. The actual example has little to do with the topics that will be covered in this course, but it fully illustrates the methodology that will be employed. The problem of computing the low temperature heat capacity of a solid can be studied by both *ab initio* and *phenomenological* methods.

(i) *Ab initio* **(particulate) approach:** Calculating the heat capacity of a solid material from first principles is rather complicated. We breifly sketch some of the steps:

• The *ab initio* starting point is the Schrödinger equation for electrons and ions which can only be treated approximately, say by a density functional formalism. Instead, we start with a many body potential energy for the *ionic* coordinates $\mathcal{V}(\vec{q}_1, \vec{q}_2, \cdots, \vec{q}_N)$, which may itself be the outcome of such a quantum mechanical treatment.

• Ideal lattice positions at zero temperature are obtained by minimizing $\mathcal{V}$, typically forming a lattice $\vec{q}^{\,*}(\ell, m, n) = [\ell\hat{a} + m\hat{b} + n\hat{c}] \equiv \vec{q}^{\,*}_{\vec{r}}$, where $\vec{r} = \{\ell, m, n\}$ is a triplet of integers, and $\hat{a}$, $\hat{b}$, and $\hat{c}$ are unit vectors.

• Small fluctuations about the ideal positions (due to finite temperature or quantum effects) are included by setting $\vec{q}_{\vec{r}} = \vec{q}^{\,*}_{\vec{r}} + \vec{u}(\vec{r})$. The cost of deformations in the potential energy is given by

$$\mathcal{V} = \mathcal{V}^* + \frac{1}{2} \sum_{\substack{\vec{r},\vec{r}\,' \\ \alpha,\beta}} \frac{\partial^2 \mathcal{V}}{\partial q_{\vec{r},\alpha} \partial q_{\vec{r}\,',\beta}} u_\alpha(\vec{r})\; u_\beta(\vec{r}\,') + O(u^3), \tag{I.1}$$

where the indices α and β denote spatial components. (Note that the first derivative of $\mathcal{V}$ vanishes at the equilibrium position.) The full Hamiltonian for small deformations is obtained by adding the kinetic energy $\sum_{\vec{r},\alpha} p_\alpha(\vec{r})^2/2m$ to eq.(I.1), where $p_\alpha(\vec{r})$ is the momentum conjugate to $u_\alpha(\vec{r})$.

• The next step is to find the normal modes of vibration (phonons) by diagonalizing the matrix of derivatives. Since the ground state configuration is a regular lattice, the elements of this matrix must satisfy various translation and rotation symmetries. For example, they can only depend on the difference between the position vectors of ions $\vec{r}$ and $\vec{r}\,'$, i.e.

$$\frac{\partial^2 \mathcal{V}}{\partial q_{\vec{r},\alpha} \partial q_{\vec{r}\,',\beta}} = K_{\alpha\beta}(\vec{r} - \vec{r}\,'). \tag{I.2}$$

This translational symmetry allows us to at least partially diagonalize the Hamiltonian by using the Fourier modes,

$$u_\alpha(\vec{r}) = \sum_{\vec{k}}{}' \frac{e^{i\vec{k}\cdot\vec{r}}}{\sqrt{N}} u_\alpha(\vec{k}). \tag{I.3}$$

(Only *wavevectors* $\vec{k}$ inside the first *Brillouin zone* contribute to the sum.) The Hamiltonian then reads

$$\mathcal{H} = \mathcal{V}^* + \frac{1}{2}\sum_{\vec{k},\alpha,\beta}\left[\frac{|p_\alpha(\vec{k})|^2}{m} + K_{\alpha\beta}(\vec{k})u_\alpha(\vec{k})u_\beta(\vec{k})^*\right]. \tag{I.4}$$

While the precise form of the Fourier transformed matrix $K_{\alpha\beta}(\vec{k})$ is determined by the microscopic interactions, it has to respect the underlying symmetries of the crystallographic point group. Let us assume that diagonalizing this 3×3 matrix yileds eigenvalues $\{\kappa_\alpha(k)\}$ The quadratic part of the Hamiltonian is now decomposed into a set of independent (non–interacting) harmonic oscillators.

- The final step is to quantize each oscillator, leading to

$$\mathcal{H} = \mathcal{V}^* + \sum_{\vec{k},\alpha}\hbar\omega_\alpha(\vec{k})\left(n_\alpha(\vec{k}) + \frac{1}{2}\right), \tag{I.5}$$

where $\omega_\alpha(\vec{k}) = \sqrt{\kappa_\alpha(\vec{k})/m}$, and $\{n_\alpha(\vec{k})\}$ are the set of occupation numbers. The average energy at a temperature T is given by

$$E(T) = \mathcal{V}^* + \sum_{\vec{k},\alpha}\hbar\omega_\alpha(\vec{k})\left(\left\langle n_\alpha(\vec{k})\right\rangle + \frac{1}{2}\right), \tag{I.6}$$

where we know from elementary statistical mechanics that the average occupation numbers are given by $\langle n_\alpha(\vec{k})\rangle = 1/\big(\exp(\frac{\hbar\omega_\alpha}{k_B T}) - 1\big)$. Clearly $E(T)$, and other macroscopic functions, have a complex behavior, dependent upon microscopic details through $\{\kappa_\alpha(k)\}$. Are there any features of these functions (e.g. the functional dependence as $T \to 0$) that are independent of microscopic features? The answer is positive, and illustrated with a one dimensional example.

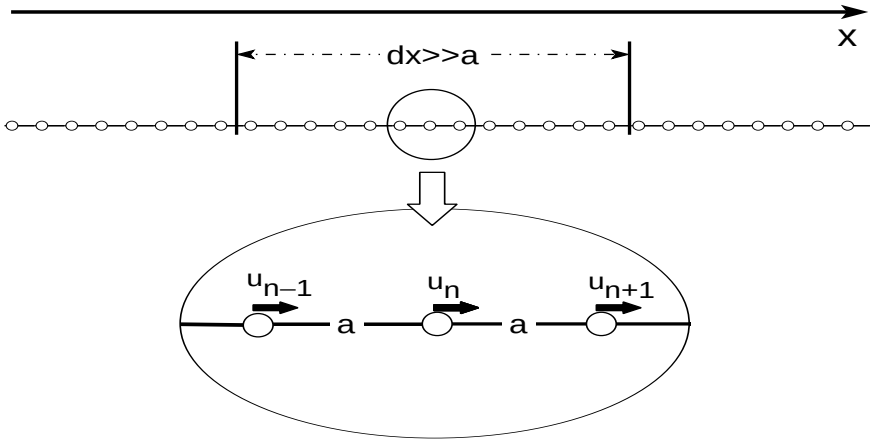

I.1. Displacements of a one–dimensional chain, and coarse–graining.

Consider a chain of particles, constrained to move in one dimension. A most general quadratic potential energy for deformations $\{u_n\}$, around an average separation of a, is

$$\mathcal{V} = \mathcal{V}^* + \frac{K_1}{2}\sum_n (u_{n+1} - u_n)^2 + \frac{K_2}{2}\sum_n (u_{n+2} - u_n)^2 + \cdots . \tag{I.7}$$

The decomposition to normal modes is obtained via

$$u_n = \int_{-\pi/a}^{\pi/a} \frac{dk}{2\pi} e^{-ikna} u(k), \quad \text{where} \quad u(k) = a\sum_n e^{ikna} u_n \ . \tag{I.8}$$

(Note the difference in normalizations from eq. (I.3).) The resulting potential energy is,

$$\mathcal{V} = \mathcal{V}^* + \frac{K_1}{2}\sum_n \int_{-\pi/a}^{\pi/a} \frac{dk}{2\pi}\frac{dk'}{2\pi}(e^{ika} - 1)(e^{ik'a} - 1)e^{-i(k+k')na} u(k)u(k') + \cdots . \tag{I.9}$$

Using the identity $\sum_n e^{-i(k+k')na} = \delta(k + k')2\pi/a$, and noting that $u(-k) = u^*(k)$, we obtain

$$\mathcal{V} = \mathcal{V}^* + \frac{1}{2a}\int_{-\pi/a}^{\pi/a} \frac{dk}{2\pi}\left[K_1(2 - 2\cos ka) + K_2(2 - 2\cos 2ka) + \cdots\right] |u(k)|^2 . \tag{I.10}$$

The frequency of normal modes, given by $\omega(k) = \sqrt{\left[2K_1(1 - \cos ka) + \cdots\right]/m}$, is depicted below. In the limit $k \to 0$, $\omega(k) \to v|k|$, where the 'sound velocity' v equals $a\sqrt{K/m}$ (see below).

The internal energy of these excitations, for a chain of N particles, is

$$E(T) = \mathcal{V}^* + Na\int_{-\pi/a}^{\pi/a} \frac{dk}{2\pi} \frac{\hbar\omega(k)}{\exp\left(\hbar\omega(k)/k_B T\right) - 1)} . \tag{I.11}$$

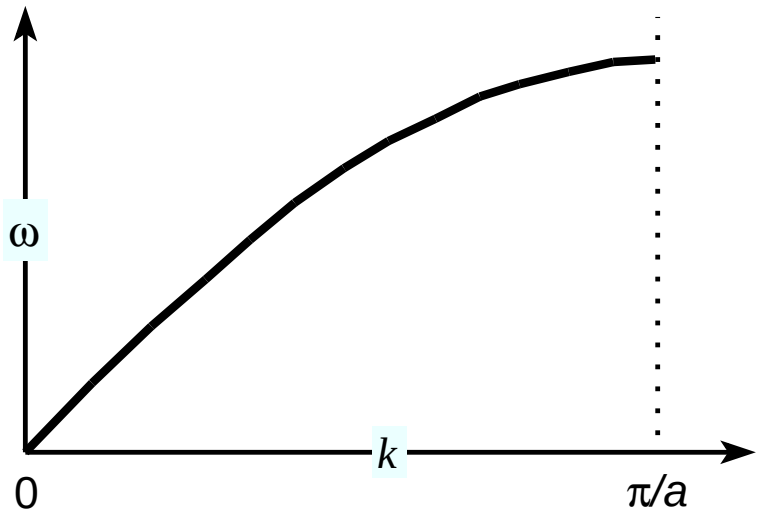

I.2. The dispersion of phonon modes for a linear chain.

As $T \to 0$, only modes with $\hbar\omega(k) < k_B T$ are excited. Hence only the $k \to 0$ part of the excitation spectrum is important and $E(T)$ simplifies to

$$E(T) = \mathcal{V}^* + Na \int_{-\infty}^{\infty} \frac{dk}{2\pi} \frac{\hbar v|k|}{\exp(\hbar v|k|/k_B T) - 1} = \mathcal{V}^* + Na \frac{\pi^2}{6\hbar v} (k_B T)^2. \tag{I.12}$$

Note:

(1) The full spectrum of excitation energies is

$$\frac{K(k)}{2} = K_1(1 - \cos ka) + K_2(1 - \cos 2ka) + \cdots \Longrightarrow \frac{\bar{K}}{2} k^2 \quad \text{as} \quad k \to 0, \tag{I.13}$$

Further neighbor interactions change the speed of sound, but not the form of the dispersion relation as $k \to 0$.

(2) The heat capacity $C(T) = dE/dT$ is proportional to T. This dependence is a *universal* property, i.e. not material specific, and independent of the choice of the interatomic interactions.

(3) The T^2 dependence of energy comes from excitations with $k \to 0$ (or $\lambda \to \infty$), i.e. from collective modes involving many particles. These are precisely the modes for which statistical considerations may be meaningful.

(ii) Phenomenological (field) approach: We now outline a mesoscopic approach to the same problem, and show how it provides additional insights and is easily generalized to higher dimensions. Typical excitations at low temperatures have wavelengths $\lambda > \lambda(T) \approx (\hbar v/kT) \gg a$, where a is a lattice spacing. We can eliminate the unimportant short wavelength modes by an averaging process known as **coarse graining**. The idea is

consider a point x, and an interval $a \ll dx \ll \lambda(T)$ around it (Fig. I.1). In dx all the displacements u are approximately the same; and we can define an average deformation field $u(x)$. The kinetic energy is now related to the density $\rho = m/a$ via $\rho \int dx \dot{u}(x)^2/2$. Note that $u(x)$ is treated as a continuous function, but it certainly does not have any variations over distances smaller than the lattice spacing a.

What is the most general potential energy functional $\mathcal{V}[u]$, for the chain? A priori, we don't know much about the form of $\mathcal{V}[u]$, but we can construct it using the following general principles:

Locality: In most situations, the interactions between particles are short range, allowing us to define a potential energy *density* Φ at each point x, with $\mathcal{V}[u] = \int dx \Phi\big(u(x), du/dx, \cdots\big)$. Naturally, by including all derivatives we can also describe long-range interactions. In this context, the term *locality* implies that the higher derivative terms are less significant.

Translational symmetry: A uniform translation of the chain does not change its internal energy, and hence the energy density must satisfy the constraint $\Phi[u(x) + c] = \Phi[u(x)]$. This implies that Φ cannot depend directly on $u(x)$, but only on its derivatives du/dx, $d^2u/dx^2, \cdots$.

Stability: Since the fluctuations are around the *equilibrium* solution, there can be no linear terms in u or its derivatives. (Stability further requires that the quadratic part of $\mathcal{V}[u]$ must be positive definite.)

The most general potential consistent with these constraints is

$$\mathcal{V}[u] = \int dx \left[\frac{K}{2} \left(\frac{\partial u}{\partial x} \right)^2 + \frac{L}{2} \left(\frac{\partial^2 u}{\partial^2 x} \right)^2 + \cdots + M \left(\frac{\partial u}{\partial x} \right)^3 + \cdots \right], \tag{I.14}$$

which after Fourier transformation gives

$$\begin{aligned} \mathcal{V}[u] = \int \frac{dk}{2\pi} \left[\frac{K}{2} k^2 + \frac{L}{2} k^4 + \cdots \right] |u(k)|^2 \\ - iM \int \frac{dk_1}{2\pi} \frac{dk_2}{2\pi} k_1 k_2 (k_1 + k_2) u(k_1) u(k_2) u(-k_1 - k_2) + \cdots . \end{aligned} \tag{I.15}$$

As $k \to 0$, higher order gradient terms (such as L) become unimportant. Also, for small deformations we may neglect terms beyond second order in u (such as M). Adding the kinetic energy, we get a simple one dimensional field theory, with a Hamiltonian

$$\mathcal{H} = \frac{\rho}{2} \int dx \left[\left(\frac{\partial u}{\partial t} \right)^2 + v^2 \left(\frac{\partial u}{\partial x} \right)^2 \right].$$

This is a one–dimensional elastic (string) theory with material dependent constants ρ and $v = \sqrt{K/\rho}$. While the phenomenological approach cannot tell us the value of these parameters, it does show that the low energy excitations satisfy the dispersion relation $\omega = v|k|$.

We can now generalize the elastic theory of the string to arbitrary dimensions d: The discrete particle deformations $\vec{u}_n$ are coarse grained into a continuous deformation field $\vec{u}(\vec{x})$. For an *isotropic* material the potential energy $\mathcal{V}[\vec{u}]$, must be invariant under both rotations and translations $u_\alpha(\vec{x}) \mapsto R_{\alpha\beta}u_\beta(\vec{x}) + c_\alpha$, where $R_{\alpha\beta}$ is a rotation matrix. A useful local quantity is the symmetric *strain field*,

$$u_{\alpha\beta}(\vec{x}) = \frac{1}{2}\left(\frac{\partial u_\alpha}{\partial x_\beta} + \frac{\partial u_\beta}{\partial x_\alpha}\right), \tag{I.16}$$

in terms of which the most general quadratic deformation Hamiltonian is

$$\mathcal{H} = \sum_{\alpha,\beta} \int d^d\vec{x} \left[\frac{\rho}{2}\frac{\partial u_\alpha}{\partial t}\frac{\partial u_\alpha}{\partial t} + \frac{2\mu}{2}u_{\alpha\beta}u_{\alpha\beta} + \frac{\lambda}{2}u_{\alpha\alpha}u_{\beta\beta}\right]. \tag{I.17}$$

The elastic constants μ and λ are known as *Lame coefficients*. Summing over the repeated indices ensures that the result is rotationally invariant. This rotational invariance is more transparent in the Fourier basis, $\vec{u}(\vec{k}\,) = \int d^d\vec{x} e^{i\vec{k}.\vec{x}}\vec{u}(\vec{x})$, since the Hamiltonian

$$\mathcal{H} = \int \frac{d^d\mathbf{k}}{(2\pi)^d}\left[\frac{\rho}{2}|\dot{\vec{u}}(\vec{k}\,)|^2 + \frac{\mu}{2}k^2|\vec{u}(\vec{k}\,)|^2 + \frac{\mu+\lambda}{2}\big(\vec{k}.\vec{u}(\vec{k}\,)\big)^2\right], \tag{I.18}$$

manifestly includes only rotationally invariant quantities $\vec{k}\cdot\vec{k}$, $\vec{u}\cdot\vec{u}$, and $\vec{k}\cdot\vec{u}$. We can further decompose the Hamiltonian into two types of sound modes: *longitudinal modes* where $\vec{k} \parallel \vec{u}$, with $v_\ell = \sqrt{(2\mu+\lambda)/\rho}$, and *transverse modes* with $\vec{k} \perp \vec{u}$, where $v_t = \sqrt{\mu/\rho}$. The internal energy is then given by

$$E(t) = L^d \int \frac{d^d\mathbf{k}}{(2\pi)^d}\left[\frac{\hbar v_\ell k}{\exp(\hbar v_\ell k/k_BT)-1} + \frac{(d-1)\hbar v_t k}{\exp(\hbar v_t k/k_BT)-1}\right] \approx \mathcal{A}(v_\ell, v_t)L^d(k_BT)^{d+1}. \tag{I.19}$$

The specific heat vanishes as $C \propto T^d$, as $T \to 0$.

Note:

(1) All material dependent parameters end up in the coefficient $\mathcal{A}$, while the scaling with T is *universal*.

(2) The universal exponent originates from the (hydrodynamic) modes with $\vec{k} \to 0$. The high frequency (short wavelength) modes come into play only at high temperatures.

(3) The scaling exponent depends on dimensionality and the range of interactions. (Long–range Coulomb interactions lead to a different result.)

(4) Experimental observation of a power law alerts us to the physics. For example, in superfluid helium, the observation of $C \propto T^3$ (as opposed to $C \propto T^{3/2}$ expected for an ideal Bose gas), immediately implies phonon–like excitations as noted by Landau.

$\star$ There are many other well known examples demonstrating the universality and importance of power laws. For example, consider a cloud of tracers moving in some unspecified medium. The scaling of some characteristic dimension x with time t can alert us to the possible dynamics that governs the motion of the particles. Three simple possibilities are:

(1) *Diffusion,* in which case $x \propto \sqrt{Dt}$.

(2) *Dissipate transport,* where $x \propto vt$.

(3) *Free forced motion,* where $x \propto gt^2/2$, as in a gravitational field.

The Navier–Stokes equation for fluid flow is yet another example. We can use these examples to construct general guidelines for setting up and analysing phenomenological field theories. Some of steps in the procedure are:

(1) **Input** for construction of the coarse grained Hamiltonian comes from symmetry, range of interactions, and dimensionality.

(2) Unlike the above example, in general nonlinearities cannot be ignored in the resulting effective field theory. We shall learn how to treat such nonlinearities by the methods of perturbation theory and the renormalization group.

(3) **Output** of the analysis is expressed in terms of universal exponents, and other functional dependances that can be directly compared with experiments.

I.C Phase Transitions

The most spectacular consequence of interactions among particles is the appearance of new phases of matter whose collective behavior bears little resemblance to that of a few particles. How do the particles then transform from one macroscopic state to a completely different one. From a formal perspective, all macroscopic properties can be deduced from the free energy or the partition function. Since phase transitions typically involve dramatic changes in various response functions they must correspond to singularities in the free energy. The canonical partition function for a finite collection of particles is always an analytical function. Hence phase transitions, and their associated non–analyticities, are only obtained for infinitely many particles, i.e. in the *thermodynamic limit*, $N \to \infty$. The study of phase transitions is thus related to finding the origin of various singularities in the free energy and characterizing them.

The classical example of a phase transition is the condensation of a gas into a liquid. Some important features of the liquid–gas condensation transition are:

(1) In the temperature/pressure plane, (T, P), the phase transition occurs along a line that terminates at a *critical point* (T_c, P_c).

(2) In the volume/pressure plane, $(P, v \equiv V/N)$, the transition appears as a *coexistence interval*, corresponding to a mixture of gas and liquids of densities $\rho_g = 1/v_g$, and $\rho_l = 1/v_l$, at temperatures $T < T_c$.

(3) Due to the termination of the coexistence line, it is possible to go from the gas phase to the liquid phase continuously (without a phase transition) by going around the critical point. Thus there are no fundamental differences between liquid and gas phases.

From a mathematical perspective, the free energy of the system is an analytical function in the (P, T) plane, except for some form of branch cut along the phase boundary. Observations in the vicinity of the critical point further indicate that:

(4) The difference between the densities of coexisting liquid and gas phases vanishes on approaching T_c, i.e. $\rho_{\rm liquid} \to \rho_{\rm gas}$, as $T \to T_c^-$.

(5) The pressure versus volume isotherms become progressively more flat on approaching T_C from the high temperature side. This implies that the isothermal compressibility, $\kappa_T = -\left.\partial V/\partial P\right|_T /V$, diverges as $T \to T_c^+$.

(6) The fluid appears "milky" close to criticality. This phenomenon, known as *critical opalescence*, suggests collective fluctuations in the gas at long enough wavelengths to scatter visible light. These fluctuations must necessarily involve many particles, and a coarse graining procedure may thus be appropriate to their description.

A related, but possibly less familiar, phase transition occurs between paramagnetic and ferromagnetic phases of certain substances such as iron or nickel. These materials become spontaneously magnetized below a Curie temperature T_c. There is a discontinuity in magnetization of the substance as the magnetic field h, goes through zero for $T < T_c$. The phase diagram in the (h, T) plane, and the magnetization isotherms $M(h)$, have much in common with their counterparts in the condensation problem. In both cases a line of discontinuous transitions terminates at a critical point, and the isotherms exhibit singular behavior in the vicinity of this point. The phase diagram of the magnet is simpler in appearance, because the symmetry $h \mapsto -h$ ensures that the critical point occurs at $h_c = M_c = 0$.

I.D Critical Behavior

The singular behavior in the vicinity of a critical point is characterized by a set of *critical exponents*. These exponents describe the non–analyticity of various thermodynamic functions. The most commonly encountered exponents are listed below:

• **The Order Parameter:** By definition, there is more than one equilibrium phase on a coexistence line. The order parameter is a thermodynamic function that is different in each phase, and hence can be used to distinguish between them. For a magnet, the magnetization

$$m(T) = \frac{1}{V} \lim_{h \to 0} M(h, T),$$

serves as the order parameter. In zero field, m vanishes for a paramagnet and is non–zero in a ferromagnetic, i.e.

$$m(T, h = 0) \propto \begin{cases} 0 & \text{for} \quad T > T_c, \\ |t|^\beta & \text{for} \quad T < T_c, \end{cases} \tag{I.20}$$

where $t = (T_c - T)/T_c$ is the *reduced temperature*. The singular behavior of the order parameter along the coexistence line is therefore indicated by the exponent β. The singular behavior of m along the critical isotherm is indicated by another exponent δ, defined through

$$m(T = T_c, h) \propto h^{1/\delta}. \tag{I.21}$$

The two phases along the liquid–gas coexistence line are differentiated by their density, and the density difference $\rho - \rho_c$, where ρ_c is the critical density, serves the role of the order parameter.

• **Response Functions:** The critical system is quite sensitive to external perturbations, as typified by the infinite compressibility at the liquid–gas critical point. The divergence in the response of the order parameter to a field conjugate to it is indicated by an exponent γ. For example, in a magnet,

$$\chi_{\pm}(T, h = 0) \propto |t|^{-\gamma_{\pm}}, \tag{I.22}$$

where in principle two exponents γ_+ and γ_- are necessary to describe the divergences on the two sides of the phase transition. Actually in almost all cases, the same singularity governs both sides and $\gamma_+ = \gamma_- = \gamma$. The heat capacity is the thermal response function, and its singularities at zero field are described by the exponent α, i.e.

$$C_{\pm}(T, h = 0) \propto |t|^{-\alpha_{\pm}}. \tag{I.23}$$

• **Long–range Correlations:** Since the response functions are related to equilibrium fluctuations, their divergence in fact implies that fluctuations are correlated over long distances. We shall prove this statement by considering the magnetic susceptibility. Starting from the (Gibbs) partition function in a field h, $Z(h) = \mathrm{tr}\{\exp[-\beta\mathcal{H}_0 + \beta h M]\}$, the magnetization can be computed as $\langle M\rangle = \partial \ln Z/\partial(\beta h) = \mathrm{tr}\{M \exp[-\beta\mathcal{H}_0 + \beta h M]\}/Z$. The susceptibility is then related to the variance of magnetization by

$$\begin{aligned}\chi = \frac{\partial M}{\partial h} =& \beta \left\{ \frac{1}{Z} \mathrm{tr}\left[M^2 \exp\left(-\beta\mathcal{H}_0 + \beta h M\right)\right] - \frac{1}{Z^2} \mathrm{tr}\left[M \exp\left(-\beta\mathcal{H}_0 + \beta h M\right)\right]^2 \right\} \\ =& \frac{1}{k_B T} \left(\left\langle M^2 \right\rangle - \langle M\rangle^2 \right).\end{aligned} \tag{I.24}$$

The overall magnetization is obtained by adding contributions from different parts of the system, i.e.

$$M = \int d^3\,\vec{r}\, m(\vec{r}). \tag{I.25}$$

(For the time being we treat the magnetization as a scalar quantity.) Substituting the above into eq.(I.24) gives

$$k_B T\, \chi = \int d^3\vec{r}\, d^3\vec{r}\,' \left(\langle m(\vec{r}) m(\vec{r}\,')\rangle - \langle m(\vec{r})\rangle \langle m(\vec{r}\,')\rangle \right). \tag{I.26}$$

Translational symmetry of a homogeneous system implies that $\langle m(\vec{r})\rangle = m$ is a constant, while $\langle m(\vec{r}) m(\vec{r}\,')\rangle = G(\vec{r} - \vec{r}\,')$ depends only on the separation. We can express the result in terms of the *connected* correlation function, defined as

$$\langle m(\vec{r}) m(\vec{r}\,')\rangle_c \equiv \langle (m(\vec{r}) - \langle m(\vec{r})\rangle)\,(m(\vec{r}\,') - \langle m(\vec{r}\,')\rangle)\rangle = G(\vec{r} - \vec{r}\,') - m^2. \tag{I.27}$$

Integrating over the center of mass coordinates in eq.((I.26)) results in a factor of volume V, and the susceptibility is given by

$$\chi = \beta V \int d^3\vec{r}\, \langle m(\vec{r})m(0)\rangle_c \,. \tag{I.28}$$

The connected correlation function is a measure of how the local fluctuations in one part of the system effect those of another part. Typically such influences occur over a characteristic distance ξ, called the *correlation length*. (It can be shown rigorously that this function must decay to zero at large separations; in many cases $G_c(\vec{r}) \equiv \langle m(\vec{r})m(0)\rangle_c$ decays as $\exp(-|\vec{r}|/\xi)$ at separations $|\vec{r}| > \xi$.) Let g denote a typical value of the correlation function for $|\vec{r}| < \xi$. It then follows from eq.(I.28) that $k_B T\chi/V < g\xi^3$; and $\chi \to \infty$, necessarily implies $\xi \to \infty$. This divergence of the correlation length also explains the observation of critical opalescence. The correlation function can be measured by scattering probes and its divergence

$$\xi_\pm(T, h = 0) \propto |t|^{-\nu_\pm}, \tag{I.29}$$

is controlled by exponents $\nu_+ = \nu_- = \nu$.

II. THE LANDAU–GINZBURG APPROACH

II.A Introduction

We noted in the previous section that the singular behavior of thermodynamic functions at a critical point (the termination of a coexistence line) can be characterized by a set of critical exponents $\{\alpha, \beta, \gamma, \cdots\}$. Experimental observations indicate that these exponents are quite *universal*, i.e. independent of the material under investigation, and to some extent, of the nature of the phase transition. For example, the vanishing of the coexistence boundary in the condensation of CO_2 has the same singular behavior as that of the phase separation of protein solutions into dilute and dense components. This universality of behavior needs to be explained. We also noted that the divergence of the response functions, as well as direct observations of fluctuations via scattering studies, indicate that the correlations become long ranged in the vicinity of the critical point. Such correlated fluctuations involve many particles ($\xi \gg a$, where a is a typical inter-particle spacing), and a coarse graining approach, in the spirit of the theory of elasticity, may be appropriate to their description. Here we shall construct such a *statistical field theory*.

We shall frame the discussion in the language of a magnetic system, whose symmetries are more transparent, although the results are of more general applicability. Consider a metal, say iron, close to its Curie point. The microscopic origin of magnetism is quantum mechanical, involving such elements as itinerant electrons, their spin, and the exclusion principle. Clearly a microscopic approach is rather complicated, and material dependent. Such a theory is necessary to find out which elements are likely to produce ferromagnetism. However, given that there is such behavior, the microscopic theory is not necessarily useful to describe its disappearance as a result of thermal fluctuations. This is because the (quantum) statistical mechanics of the collection of interacting electrons is excessively complicated. The important degrees of freedom close to the Curie point, whose statistical mechanics is responsible for the phase transition, are long wavelength collective excitations of spins (much like the long wavelength phonons that dominate the heat capacity at low temperatures). We can thus coarse grain the magnet to a scale much larger than the lattice spacing, and define a magnetization field $\vec{m}(\mathbf{x})$, which represents the average of the elemental spins in the vicinity of a point $\mathbf{x}$. It is important to emphasize that while $\mathbf{x}$ is treated as a continuous variable, the functions $\vec{m}$ do not exhibit any variations at distances

of the order of the lattice spacing, i.e. their Fourier transforms involve only wave-numbers less than some upper cutoff $\Lambda \sim 1/a$.

In describing other types of phase transitions, the role of $\vec{m}(\mathbf{x})$ is played by the appropriate order parameter density. It is then useful to examine a generalized magnetization for n-component spins, existing in d-dimensional space, i.e.

$$\mathbf{x} \equiv (x_1, x_2, ..., x_d) \in \Re^d \qquad \text{(space)} \quad , \quad \vec{m} \equiv (m_1, m_2, ..., m_n) \in \Re^n \qquad \text{(spin)}.$$

Some specific problems covered in this framework are:
$n = 1$ describes liquid–gas transitions, binary mixtures, as well as uniaxial magnets;
$n = 2$ applies to superfluidity, superconductivity, and planar magnets;
$n = 3$ corresponds to classical magnets.
While most physical situations occur in three–dimensional space ($d = 3$), there are also important phenomena on surfaces ($d = 2$), and in wires ($d = 1$). Relativistic field theory is described by a similar structure, but in $d = 4$.

As in the case of a deformed solid, we construct a local effective Hamiltonian $\beta\mathcal{H}[\vec{m}] = \int d^d\mathbf{x}\Phi[\vec{m}(\mathbf{x})]$, on the basis of appropriate symmetries. We shall assume that the material is *uniform* and *isotropic*, so that all locations and directions in $\mathbf{x}$ space are equivalent. In the absence of an external magnetic field, all directions for magnetization are equivalent, and hence $\mathcal{H}[R_n\vec{m}(\mathbf{x})] = \mathcal{H}[\vec{m}(\mathbf{x})]$, where R_n is a rotation in the n-dimensional space. Some of the terms consistent with these symmetries that can appear in the expansion of $\Phi[\vec{m}(\mathbf{x})]$ are

$$m^2(\mathbf{x}) \equiv \vec{m}(\mathbf{x}) \cdot \vec{m}(\mathbf{x}) \equiv \sum_{i=1}^{n} m_i(\mathbf{x}) m_i(\mathbf{x}) \quad , \quad m^4(\mathbf{x}) \equiv \left(m^2(\mathbf{x})\right)^2 \quad , \quad m^6(\mathbf{x}) \quad , \quad \cdots \quad ,$$

$$(\nabla\vec{m})^2 \equiv \sum_{i=1}^{n}\sum_{\alpha=1}^{d} \partial_\alpha m_i \partial_\alpha m_i \quad , \quad (\nabla^2\vec{m})^2 \quad , \quad m^2(\nabla\vec{m})^2 \quad , \quad \cdots \quad .$$

Including a small magnetic field $\vec{h}$, that breaks the rotational symmetry, the lowest order terms in the expansion of Φ lead to,

$$\beta\mathcal{H} = \int d^d\mathbf{x} \left[\frac{t}{2} m^2(\mathbf{x}) + u m^4(\mathbf{x}) + \frac{K}{2}(\nabla m)^2 + \cdots - \vec{h} \cdot \vec{m}(\mathbf{x}) \right], \tag{II.1}$$

which is known as the *Landau–Ginzburg* Hamiltonian. (The magnetic field also generates terms proportional to $m^2\vec{m} \cdot \vec{h}$, which are of higher order, and actually less important than the um^4 term.)

Eq.(II.1) is constructed on the basis of symmetry alone, and depends on a set of *phenomenological* parameters $\{t, u, K, \cdots\}$. These parameters are non-universal functions of microscopic interactions, *as well as external parameters such as temperature and pressure*. It is essential to fully appreciate the latter point, which is usually the source of much confusion. The probability for a particular configuration of the field is given by the Boltzmann weight $\exp\{-\beta\mathcal{H}[\vec{m}(\mathbf{x})]\}$. This *does not imply* that all terms in the exponent are proportional to $(k_B T)^{-1}$. Such dependence holds only for the true microscopic Hamiltonian. The Landau–Ginzburg Hamiltonian is more correctly an effective free energy obtained by integrating over (coarse graining) the microscopic degrees of freedom, while constraining their average to $\vec{m}(\mathbf{x})$. It is precisely because of the difficulty of carrying out such a first principles program that we postulate the form of the resulting effective free energy on the basis of symmetries alone. The price paid is that the phenomenological parameters have an unknown functional dependence on the original microscopic parameters, as well as such on external constraints as temperature (since we have to account for the entropy of the short distance fluctuations lost in the coarse graining process).

II.B Saddle Point Approximation, and Mean–Field Theory

The original problem has been simplified considerably by focusing only on the coarse grained magnetization field described by the Landau–Ginzburg Hamiltonian in eq.(II.1). Various thermodynamic functions (and their singular behavior) can now be obtained from the associated partition function

$$Z = \int \mathcal{D}\vec{m}(\mathbf{x}) \exp\{-\beta\mathcal{H}[\vec{m}(\mathbf{x})]\}. \tag{II.2}$$

Since the degrees of freedom appearing in the Hamiltonian are functions of $\mathbf{x}$, the symbol $\int \mathcal{D}\vec{m}(\mathbf{x})$ refers to a *functional integral*. In actuality, the functional integral should be regarded as a limit of discrete integrals. After discretizing the coordinate x into a lattice of $\mathcal{N}$ points i, at a distance a from each other,

$$\int \mathcal{D}m(x)\mathcal{F}\left[m(x), \frac{\partial m}{\partial x}, \cdots\right] \equiv \lim_{\mathcal{N}\to\infty} \prod_{i=1}^{\mathcal{N}} dm_i \mathcal{F}\left[m_i, \frac{m_{i+1}-m_i}{a}, \cdots\right].$$

(There are some mathematical concerns regarding the existence of functional integrals. The problems are associated with having too many degrees of freedom at short distances, allowing rather badly behaved functions. These issues need not concern us since we know

that the underlying problem has a well defined lattice spacing that restricts the short distance behavior.)

It is still difficult to calculate the Landau–Ginzburg partition function. As a first step, we perform a *saddle point approximation* in which the integral in eq.(II.2) is replaced by the maximum value of the integrand. The natural tendency of interactions in a magnet is to keep the magnetizations vectors parallel, and hence we expect the parameter K in eq.(II.1) to be positive. The configuration of $\vec{m}$ that maximizes the integrand is then uniform, and

$$\beta F = -\ln Z \approx V \min\{\Psi(m)\}_m. \tag{II.3}$$

The uniform magnetization occurs for $\vec{m}(\mathbf{x}) = \bar{m}\hat{h}$, which minimizes

$$\Psi(m) \equiv \frac{t}{2}m^2 + um^4 + \cdots - \vec{h}.\vec{m}. \tag{II.4}$$

In the vicinity of the critical point, m is a small quantity, and it is justified to keep only the lowest powers in the expansion of $\Psi(m)$. (We can later check self consistently that the terms left out are indeed small corrections.) The behavior of $\Psi(m)$ depends strongly on the sign of the parameter t.

(1) For $t > 0$, we can ignore the quartic term, and the minimum occurs for $\vec{m} \approx \vec{h}/t$. The vanishing of magnetization as $\vec{h} \to 0$ signals paramagnetic behavior. The susceptibility $\chi = 1/t$, diverges as $t \to 0$.

(2) For $t < 0$, a quartic term with a positive value of u is required to insure stability (i.e. a finite magnetization). The function $\Psi(m)$ now has degenerate minima, at a non–zero value of $\bar{m}$. There is thus a spontaneous magnetization, even at $\vec{h} = 0$ indicating ferromagnetic behavior. The direction of the $\vec{m}$ is determined by the systems preparation, and can be realigned by an external field $\vec{h}$.

Thus a saddle point evaluation of the Landau–Ginzburg partition function results in paramagnetic behavior for $t > 0$, and ferromagnetic behavior for $t < 0$. Hence we can map the phase diagram of the Landau–Ginzburg Hamiltonian to that of a magnet by setting

$$\begin{aligned} t(T, \cdots) =& a(T - T_c) + \mathcal{O}(T - T_c)^2, \\ u(T, \cdots) =& u + u_1(T - T_c) + \mathcal{O}(T - T_c)^2, \end{aligned} \tag{II.5}$$

where a and u are unknown positive constants, dependent upon material properties. The basic idea is that the phenomenological parameters are functions of temperature that can be expanded in a Taylor series in $T - T_c$. The minimal conditions needed to reproduce the

experimental phase diagram are contained in eqs.(II.5). It is of course possible that some other terms in the expansion, e.g. a or u are also zero. However, these are non-generic situations which can presumably be removed by changing some other system parameter.

We now examine the singular behaviors predicted by eqs.(II.3) and (II.4).

• **Magnetization:** In zero field, from $\partial\Psi/\partial m = t\bar{m} + 4u\bar{m}^3 = \bar{m}(t + 4u\bar{m}^2) = 0$, and we obtain

$$\bar{m} = \begin{cases} 0 & \text{for } t > 0, \\ \sqrt{\frac{-t}{4u}} & \text{for } t < 0. \end{cases} \tag{II.6}$$

We thus find a universal exponent $\beta = 1/2$, while the amplitude is material dependent.

• **Heat Capacity:** The free–energy is given by ($h = 0$)

$$\frac{\beta F}{V} = \min \Psi(m) = \begin{cases} 0 & \text{for } t > 0, \\ -\frac{t^2}{16u} & \text{for } t < 0. \end{cases} \tag{II.7}$$

Since $t = a(T - T_c) + \cdots$; $\partial/\partial T \propto \partial/\partial t$, and

$$C = -T\frac{\partial^2 f}{\partial T^2} \propto -\frac{\partial^2}{\partial t^2}\left(\frac{\beta F}{V}\right) = \begin{cases} 0 & \text{for } t > 0, \\ \frac{1}{8u} & \text{for } t < 0. \end{cases} \tag{II.8}$$

We observe a discontinuity, rather than a divergence, in the heat capacity. If we insist upon describing the singularity by a power law, we have to choose the exponent $\alpha = 0$.

• **Susceptibility:** In the presence of $\vec{h}$, we expect $\vec{m} = \bar{m}(h)\hat{h}$, and from $\partial\Psi/\partial m = 0$, we obtain $t\bar{m} + 4u\bar{m}^3 = h$. Hence

$$\chi_\ell^{-1} = \left.\frac{\partial h}{\partial \bar{m}}\right|_{h=0} = t + 12u\bar{m}^2 = \begin{cases} t & \text{for } t > 0, \\ -2t & \text{for } t < 0. \end{cases} \tag{II.9}$$

Thus the singularity in susceptibility is describable by $\chi_\pm \sim A_\pm |t|^{-\gamma_\pm}$, with $\gamma_+ = \gamma_- = 1$. Although the amplitudes $A_\pm$ are material dependent, their ratio is predicted to be universal, with $A_+/A_- = 2$. (As we shall see later, what we have calculated so far is a *longitudinal susceptibility*. There is also a *transverse susceptibility* that is always infinite below T_c.)

• **Equation of State:** On the critical isotherm $t = 0$, the magnetization behaves as $\bar{m} = (h/4u)^{1/3}$, i.e.

$$\bar{m}(t = 0, h) \sim h^{1/\delta}, \quad \text{with} \quad \delta = 3. \tag{II.10}$$

II.C Spontaneous Symmetry Breaking and Goldstone Modes

For zero field, $\vec{h} = 0$, although the microscopic Hamiltonian has full rotational symmetry, the low–temperature phase does not. As a specific direction in n–space is selected for the net magnetization $\vec{M}$, there is a *spontaneously broken symmetry*, and a corresponding *long–range order* is established in the system. The original symmetry is still present globally, in the sense that if all local magnetizations $\vec{m}(\mathbf{x})$, are rotated together (i.e. if $\vec{m}(\mathbf{x}) \mapsto \Re\vec{m}(\mathbf{x})$), there is no change in energy. Such a rotation transforms one ordered state into an equivalent one. If a uniform rotation costs no energy, by continuity we expect a rotation that is slowly varying in space (e.g. $\vec{m}(\mathbf{x}) \mapsto \Re(\mathbf{x})\vec{m}(\mathbf{x})$, where $\Re(\mathbf{x})$ only has long wavelength variations) to cost very little energy. Such low energy excitations are called *Goldstone modes*. They are present in any system with a broken *continuous symmetry*. There are no Goldstone modes when a discrete symmetry is broken, since it is impossible to produce slowly varying rotations from one state to an equivalent one. Phonons are an example of Goldstone modes, corresponding to the breaking of translation and rotation symmetries by a crystal structure.

Let us explore the origin and consequences of Goldstone modes in the context of *superfluidity*. In analogy to Bose condensation, the superfluid phase has a macroscopic occupation of a single quantum ground state. The order parameter,

$$\psi(\mathbf{x}) \equiv \psi_{\Re} + i\psi_{\Im} \equiv |\psi(\mathbf{x})|e^{i\theta(\mathbf{x})}, \tag{II.11}$$

is the ground state component (overlap) of the actual wavefunction in the vicinity of $\mathbf{x}$. The phase of the wavefunction is not an observable quantity and should not appear in any physically measurable probability. For example, the effective coarse grained Hamiltonian can be obtained as an expansion,

$$\beta\mathcal{H} = \int d^d\mathbf{x} \left[\frac{K}{2}|\nabla\psi|^2 + \frac{t}{2}|\psi|^2 + u|\psi|^4 + \cdots \right]. \tag{II.12}$$

Clearly, eq.(II.12) is equivalent to the Landau–Ginzburg Hamiltonian with $n = 2$ ($\vec{m} \equiv (\psi_{\Re}, \psi_{\Im})$). The superfluid transition is signaled by the onset of a finite value of ψ for $t < 0$. Minimizing the Hamiltonian fixes the magnitude of ψ, but not its phase θ. Now consider a state with a slowly varying phase, i.e. with $\psi(\mathbf{x}) = \bar{\psi}e^{i\theta(\mathbf{x})}$. Inserting this form in the Hamiltonian yields an energy

$$\beta\mathcal{H} = \beta\mathcal{H}_0 + \frac{\bar{K}}{2}\int d^d\mathbf{x}(\nabla\theta)^2, \tag{II.13}$$

where $\bar{K} = K\bar{\psi}^2$. Taking advantage of translational symmetry, Eq.(II.13) can be decomposed into independent modes (in a region of volume V) by setting $\theta(\mathbf{x}) = \sum_q e^{i\mathbf{q}\cdot\mathbf{x}}\theta_{\mathbf{q}}/\sqrt{V}$, as

$$\beta\mathcal{H} = \beta\mathcal{H}_0 + \frac{\bar{K}}{2}\sum_{\mathbf{q}} q^2|\theta(\mathbf{q})|^2. \tag{II.14}$$

Clearly the long wavelength Goldstone modes cost little energy and are easily excited by thermal fluctuations.

Assuming that the amplitude of the order parameter is indeed uniform, the probability of a particular configuration is given by,

$$\mathcal{P}[\theta(\mathbf{x})] \propto \exp\left[-\frac{\bar{K}}{2}\int d^d\mathbf{x}(\nabla\theta)^2\right]. \tag{II.15}$$

Alternatively, in terms of the Fourier components,

$$\mathcal{P}[\theta(\mathbf{q})] \propto \exp\left[-\frac{\bar{K}}{2}\sum_{\mathbf{q}} q^2|\theta(\mathbf{q})|^2\right] \propto \prod_{\mathbf{q}} p(\theta_{\mathbf{q}}). \tag{II.16}$$

Each mode $\theta_{\mathbf{q}}$, is an *independent* random variable with a Gaussian distribution of zero mean, and with [†]

$$\langle\theta_{\mathbf{q}}\theta_{\mathbf{q}'}\rangle = \frac{\delta_{\mathbf{q},-\mathbf{q}'}}{\bar{K}q^2}. \tag{II.17}$$

[†] Note that the Fourier transform of a real field $\theta(\mathbf{x})$, is complex $\theta_{\mathbf{q}} = \theta_{\mathbf{q},\Re} + i\theta_{\mathbf{q},\Im}$. However, the number of fields is not doubled, due to the constraint of $\theta_{-\mathbf{q}} = \theta^*_{\mathbf{q}} = \theta_{\mathbf{q},\Re} - i\theta_{\mathbf{q},\Im}$. A Gaussian translational invariant weight has the generic form

$$\mathcal{P}\left[\{\theta_{\mathbf{q}}\}\right] \propto \prod_{\mathbf{q}} \exp\left[-\frac{K(q)}{2}\theta_{\mathbf{q}}\theta_{-\mathbf{q}}\right] = \prod_{\mathbf{q}>0} \exp\left[-\frac{2K(q)}{2}\left(\theta^2_{\mathbf{q},\Re} + \theta^2_{\mathbf{q},\Im}\right)\right].$$

While the first product is over all $\mathbf{q}$, the second is restricted to half of the space. There are clearly no cross correlations for differing $\mathbf{q}$, and the Gaussian variances are

$$\left\langle\theta^2_{\mathbf{q},\Re}\right\rangle = \left\langle\theta^2_{\mathbf{q},\Im}\right\rangle = \frac{1}{2K(q)},$$

from which we can immediately construct

$$\langle\theta_{\mathbf{q}}\theta_{\mp\mathbf{q}}\rangle = \left\langle\theta^2_{\mathbf{q},\Re}\right\rangle \pm \left\langle\theta^2_{\mathbf{q},\Im}\right\rangle = \frac{1\pm 1}{2K(q)}.$$

From eq.(II.17) we can calculate the correlations in the phase $\theta(\mathbf{x})$ in real space. Clearly $\langle\theta(\mathbf{x})\rangle = 0$ by symmetry, while

$$\langle\theta(\mathbf{x})\theta(\mathbf{x}')\rangle = \frac{1}{V}\sum_{\mathbf{q},\mathbf{q}'} e^{i\mathbf{q}\cdot\mathbf{x}+i\mathbf{q}'\cdot\mathbf{x}'}\,\langle\theta_{\mathbf{q}}\theta_{\mathbf{q}'}\rangle = \frac{1}{V}\sum_{\mathbf{q}}\frac{e^{i\mathbf{q}\cdot(\mathbf{x}-\mathbf{x}')}}{\bar{K}q^2}. \tag{II.18}$$

In the continuum limit, the sum can be replaced by an integral ($\sum_{\mathbf{q}} \mapsto V\int d^d\mathbf{q}/(2\pi)^d$), and

$$\langle\theta(\mathbf{x})\theta(\mathbf{x}')\rangle = \int \frac{d^d\mathbf{q}}{(2\pi)^d}\frac{e^{i\mathbf{q}\cdot(\mathbf{x}-\mathbf{x}')}}{\bar{K}q^2} = -\frac{C_d(\mathbf{x}-\mathbf{x}')}{\bar{K}}. \tag{II.19}$$

The function,

$$C_d(\mathbf{x}) = -\int \frac{d^d\mathbf{q}}{(2\pi)^d}\frac{e^{i\mathbf{q}\cdot\mathbf{x}}}{q^2}, \tag{II.20}$$

is the Coulomb potential due to a unit charge at the origin in a d–dimensional space, since it is the solution to

$$\nabla^2 C_d(\mathbf{x}) = \int \frac{d^d\mathbf{q}}{(2\pi)^d}\,\frac{q^2}{q^2}\,e^{i\mathbf{q}\cdot\mathbf{x}} = \delta^d(\mathbf{x}). \tag{II.21}$$

We can easily find a solution by using Gauss' theorem,

$$\int d^dx\nabla^2 C_d = \oint dS\cdot\nabla C_d \quad .$$

For a spherically symmetric solution, $\nabla C_d = (dC_d/dx)\hat{x}$, and the above equation simplifies to

$$1 = S_d x^{d-1}\frac{dC_d}{dx}, \tag{II.22}$$

where

$$S_d = \frac{2\pi^{d/2}}{(d/2-1)!}, \tag{II.23}$$

is the total solid angle (area of unit sphere) in d dimensions. Hence

$$\frac{dC_d}{dx} = \frac{1}{S_d x^{d-1}}, \quad \Longrightarrow \quad C_d(x) = \frac{x^{2-d}}{(2-d)S_d} + c_0, \tag{II.24}$$

where c_0 is a constant of integration.

The long distance behavior of $C_d(x)$ changes dramatically at $d = 2$, as

$$\lim_{x\to\infty} C_d(x) = \begin{cases} c_0 & d > 2 \\ \dfrac{x^{2-d}}{(2-d)S_d} & d < 2 \\ \dfrac{\ln(x)}{2\pi} & d = 2 \end{cases} \quad . \tag{II.25}$$

The constant of integration can obtained by looking at

$$\langle[\theta(\mathbf{x})-\theta(\mathbf{x}')]^2\rangle = 2\langle\theta(\mathbf{x})^2\rangle - 2\langle\theta(\mathbf{x})\theta(\mathbf{x}')\rangle, \tag{II.26}$$

which goes to zero as $\mathbf{x}\to\mathbf{x}'$. Hence,

$$\langle[\theta(\mathbf{x})-\theta(\mathbf{x}')]^2\rangle = \frac{2\left(|\mathbf{x}-\mathbf{x}'|^{2-d}-a^{2-d}\right)}{\bar{K}(2-d)S_d}, \tag{II.27}$$

where a is of the order of the lattice spacing.

For $d>2$, the phase fluctuations are finite, while they become asymptotically large for $d\leq 2$. Since the phase is bounded by 2π, this implies that long range order in the phase is destroyed. This result becomes more apparent by examining the effect of phase fluctuations on the two point correlation function

$$\langle\psi(\mathbf{x})\psi^*(\mathbf{0})\rangle = \bar{\psi}^2\langle e^{i[\theta(\mathbf{x})-\theta(\mathbf{0})]}\rangle. \tag{II.28}$$

(Since amplitude fluctuations are ignored, we are in fact looking at a *transverse* correlation function.) We shall prove later on that for any collection of Gaussian distributed variables,

$$\langle\exp(\alpha\theta)\rangle = \exp\left(\frac{\alpha^2}{2}\langle\theta^2\rangle\right).$$

Taking this result for granted, we obtain

$$\langle\psi(\mathbf{x})\psi^*(0)\rangle = \bar{\psi}^2\exp\left[-\frac{1}{2}\langle[\theta(\mathbf{x})-\theta(\mathbf{0})]^2\rangle\right] = \bar{\psi}^2\exp\left[-\frac{x^{2-d}-a^{2-d}}{\bar{K}(2-d)S_d}\right], \tag{II.29}$$

and asymptotically

$$\lim_{x\to\infty}\langle\psi(\mathbf{x})\psi^*(\mathbf{0})\rangle = \begin{cases}\bar{\psi}'^2 & \text{for } d>2\\ 0 & \text{for } d\leq 2\end{cases}. \tag{II.30}$$

The saddle point approximation to the order parameter $\bar{\psi}$, was obtained by ignoring fluctuations. The above result indicates that inclusion of phase fluctuations leads to a reduction of order in $d>2$, and its complete destruction in $d\leq 2$.

The above example typifies a more general result known as the *Mermin–Wagner theorem*. The theorem states that there is no spontaneous breaking of a continuous symmetry in systems with short range interactions in dimensions $d\leq 2$. Some corollaries to this theorem are:

(1) The borderline dimensionality of two, known as the *lower critical dimension*, has to be treated carefully. As we shall demonstrate later on in the course, there is in fact a phase transition for the two dimensional superfluid, although there is no true long range order.

(2) There are no Goldstone modes when the broken symmetry is discrete (e.g. for $n=1$). In such cases, long range order is possible down to the lower critical dimension of $d_\ell = 1$.

II.D Scattering and Fluctuations

In addition to bulk thermodynamic experiments, scattering measurements can be used to probe microscopic fluctuations at length scales of the order of the probe wavelength λ. In a typical set up, a beam of wavevector $\mathbf{k}_i$ is incident upon the sample and the scattered intensity is measured at wavevector $\mathbf{k}_s = \mathbf{k}_i + \mathbf{q}$. For *elastic* scattering, $|\mathbf{k}_i| = |\mathbf{k}_s| \equiv k$, and $q \equiv |\mathbf{q}| = 2k \sin\theta$, where θ is the angle between incident and scattered beams. Standard treatments of scattering start with the Fermi Golden Rule, and usually lead to a scattering amplitude of the form

$$A(\mathbf{q}) \propto \langle \mathbf{k}_s \otimes f | \mathcal{U} | \mathbf{k}_i \otimes i \rangle \propto \sigma(\mathbf{q}) \int d^d\mathbf{x} e^{i\mathbf{q}.\mathbf{x}} \rho(\mathbf{x}). \tag{II.31}$$

In the above expression, $|i\rangle$ and $|f\rangle$ refer to the initial and final states of the microscopic scattering element (the atom or ion), $\mathcal{U}$ is the scattering potential that can be decomposed as a sum due to the various scattering elements in the sample. The amplitude has a *local* form factor $\sigma(\mathbf{q})$ describing the scattering from an individual element. For our purposes, the more interesting *global* information is contained in $\rho(\mathbf{q})$, the Fourier transform of the global density of scatterers $\rho(\mathbf{x})$. The appropriate scattering density depends on the nature of the probe. Light scattering senses the actual atomic density, electron scattering measures the charge density, while neutron scattering is usually used to probe the magnetization density. Most such probes actually do not look at a snapshot of the system, but look at time averaged configurations. Thus the observed scattering intensity is

$$S(\mathbf{q}) \propto \langle |A(\mathbf{q})|^2 \rangle \propto \langle |\rho(\mathbf{q})|^2 \rangle. \tag{II.32}$$

Here $\langle \bullet \rangle$ indicates the thermal average of $\bullet$, which can be used in place of the time average in most cases due to ergodicity.

Eq.(II.32) indicates that a uniform density only leads to forward scattering ($\mathbf{q} = \mathbf{0}$), while the long–wavelength fluctuations can be studied by working at small angles or with small k. If scattering is caused by the magnetization density, we can use the Landau–Ginzburg Hamiltonian to compute its intensity. The probability of a particular configuration is given by

$$\mathcal{P}[\vec{m}(\mathbf{x})] \propto \exp\left\{ - \int d^d\mathbf{x} \left[\frac{K}{2} (\nabla m)^2 + \frac{t}{2} m^2 + u m^4 \right] \right\}. \tag{II.33}$$

As discussed earlier, the most probable configuration is *uniform*, with $\vec{m}(\mathbf{x}) = \bar{m}\hat{e}_1$, where $\hat{e}_1$ is a unit vector ($\bar{m}$ is zero for $t > 0$, and equal to $\sqrt{-t/4u}$ for $t < 0$). We can examine small fluctuations around such a configuration by setting

$$\vec{m}(\mathbf{x}) = [\bar{m} + \phi_\ell(\mathbf{x})]\hat{e}_1 + \sum_{\alpha=2}^{n} \phi_{t,\alpha}(\mathbf{x})\hat{e}_\alpha, \tag{II.34}$$

where ϕ_ℓ and ϕ_t refer to *longitudinal* and *transverse* fluctuations respectively. The latter can take place along any of the $n-1$ directions perpendicular to the average magnetization.

After the substitution of eq.(II.34), the terms appearing in the Landau–Ginzburg Hamiltonian can be expanded to second order as

$$\begin{aligned}(\nabla m)^2 &= (\nabla\phi_\ell)^2 + (\nabla\phi_t)^2,\\ m^2 &= \bar{m}^2 + 2\bar{m}\phi_\ell + \phi_\ell^2 + \phi_t^2,\\ m^4 &= \bar{m}^4 + 4\bar{m}^3\phi_\ell + 6\bar{m}^2\phi_\ell^2 + 2\bar{m}^2\phi_t^2 + \mathcal{O}(\phi_\ell^3, \phi_t^3),\end{aligned}$$

resulting in a quadratic energy cost

$$\begin{aligned}\beta\mathcal{H} \equiv -\ln\mathcal{P} =& V\left(\frac{t}{2}\bar{m}^2 + u\bar{m}^4\right) + \int d^d\mathbf{x}\left[\frac{K}{2}(\nabla\phi_\ell)^2 + \frac{t + 12u\bar{m}^2}{2}\phi_\ell^2\right]\\ &+ \int d^d\mathbf{x}\left[\frac{K}{2}(\nabla\phi_t)^2 + \frac{t + 4u\bar{m}^2}{2}\phi_t^2\right] + \mathcal{O}(\phi_\ell^3, \phi_t^3).\end{aligned} \tag{II.35}$$

For uniform distortions, the longitudinal and transverse *restoring potentials* have "spring constants" given by,

$$\frac{K}{\xi_\ell^2} \equiv t + 12u\bar{m}^2 = \left.\frac{\partial^2\Psi(m)}{\partial\phi_\ell^2}\right|_{\bar{m}} = \begin{cases} t & \text{for } t > 0\\ -2t & \text{for } t < 0\end{cases}, \tag{II.36}$$

and

$$\frac{K}{\xi_t^2} \equiv t + \ 4u\bar{m}^2 = \left.\frac{\partial^2\Psi(m)}{\partial\phi_t^2}\right|_{\bar{m}} = \begin{cases} t & \text{for } t > 0\\ 0 & \text{for } t < 0\end{cases}. \tag{II.37}$$

(The physical significance of the length scales ξ_ℓ and ξ_t will soon become apparent.) Note that there is no distinction between longitudinal and transverse components for the paramagnet ($t > 0$). For the ordered magnet in $t < 0$, there is no restoring force for the transverse fluctuations which correspond to the Goldstone modes discussed in the previous section.

Following the change of variables to the Fourier modes, $\phi(\mathbf{x}) = \sum_{\mathbf{q}} \phi_{\mathbf{q}} e^{i\mathbf{q}\cdot\mathbf{x}}/\sqrt{V}$, the probability of a particular fluctuation configuration is given by

$$\mathcal{P}\left[\{\phi_{\ell,\mathbf{q}}; \phi_{t,\mathbf{q}}\}\right] \propto \prod_{\mathbf{q}} \exp\left\{-\frac{K}{2}(q^2 + \xi_\ell^{-2})|\phi_{\ell,\mathbf{q}}|^2\right\} \cdot \exp\left\{-\frac{K}{2}(q^2 + \xi_t^{-2})|\phi_{t,\mathbf{q}}|^2\right\}. \tag{II.38}$$

Clearly each mode behaves as a Gaussian random variable of zero mean, and the two point correlation functions are

$$\langle \phi_{\alpha,\mathbf{q}} \phi_{\beta,\mathbf{q}'} \rangle = \frac{\delta_{\alpha,\beta}\delta_{\mathbf{q},-\mathbf{q}'}}{K(q^2+\xi_\alpha^{-2})}, \tag{II.39}$$

where the indices refer the longitudinal, or any of the transverse components. By using a spin polarized source of neutrons, the relative orientations can be adjusted to probe either the longitudinal or the transverse correlations. The *Lorentzian form*, $S(\mathbf{q}) \propto 1/(q^2+\xi^{-2})$, usually provides an excellent fit to scattering line shapes away from the critical point. Eq.(II.39) indicates that in the ordered phase, longitudinal scattering still gives a Lorentzian form (on top of a delta–function at $\mathbf{q}=\mathbf{0}$ due to the spontaneous magnetization), while transverse scattering always grows as $1/q^2$. The same power law decay is also predicted to hold at the critical point, $t=0$. Actual experimental fits yield a power law of the form

$$S(\mathbf{q}, T=T_c) \propto \frac{1}{q^{2-\eta}}, \tag{II.40}$$

with a small positive value of η.

II.E Correlation Functions and Susceptibilities

We can also examine the extent of fluctuations in real space. The averages $\langle \phi_\alpha(\mathbf{x})\rangle = \langle m_\alpha(\mathbf{x}) - \bar{m}_\alpha\rangle$, are clearly zero, and the *connected correlation function* is

$$\begin{aligned} G^c_{\alpha,\beta}(\mathbf{x},\mathbf{x}') \equiv & \langle (m_\alpha(\mathbf{x})-\bar{m}_\alpha)(m_\beta(\mathbf{x}')-\bar{m}_\beta)\rangle \\ = & \langle \phi_\alpha(\mathbf{x})\phi_\beta(\mathbf{x}')\rangle = \frac{1}{V}\sum_{\mathbf{q},\mathbf{q}'} e^{i\mathbf{q}\cdot\mathbf{x}+i\mathbf{q}'\cdot\mathbf{x}'}\langle \phi_{\alpha,\mathbf{q}}\phi_{\beta,\mathbf{q}'}\rangle. \end{aligned} \tag{II.41}$$

Using eq.(II.39), we obtain

$$G^c_{\alpha,\beta}(\mathbf{x},\mathbf{x}') = \frac{\delta_{\alpha,\beta}}{V}\sum_{\mathbf{q}} \frac{e^{i\mathbf{q}\cdot(\mathbf{x}-\mathbf{x}')}}{K(q^2+\xi_\alpha^{-2})} \equiv -\frac{\delta_{\alpha,\beta}}{K} I_d(\mathbf{x}-\mathbf{x}',\xi_\alpha), \tag{II.42}$$

where in the continuum limit,

$$I_d(\mathbf{x},\xi) = -\int \frac{d^d\mathbf{q}}{(2\pi)^d}\frac{e^{i\mathbf{q}\cdot\mathbf{x}}}{q^2+\xi^{-2}}. \tag{II.43}$$

Alternatively, I_d is the solution to the following differential equation

$$\nabla^2 I_d(x) = \int \frac{d^d\mathbf{q}}{(2\pi)^d}\frac{q^2 e^{i\mathbf{q}\cdot\mathbf{x}}}{q^2+\xi^{-2}} = \int \frac{d^d\mathbf{q}}{(2\pi)^d}\left[1-\frac{\xi^{-2}}{q^2+\xi^{-2}}\right]e^{i\mathbf{q}\cdot\mathbf{x}} = \delta^d(\mathbf{x}) + \frac{I_d(\mathbf{x})}{\xi^2}. \tag{II.44}$$

The solution is spherically symmetric, satisfying

$$\frac{d^2 I_d}{dx^2} + \frac{d-1}{x}\frac{dI_d}{dx} = \frac{I_d}{\xi^2} + \delta^d(\mathbf{x}). \tag{II.45}$$

We can try out a solution that decays exponentially at large distances as

$$I_d(x) \propto \frac{\exp(-x/\xi)}{x^p}. \tag{II.46}$$

(We have anticipated the presence of a subleading power law.) The derivatives of I_d are given by

$$\begin{aligned} \frac{dI_d}{dx} &= -\left(\frac{p}{x} + \frac{1}{\xi}\right) I_d, \\ \frac{d^2 I_d}{dx^2} &= \left(\frac{p(p+1)}{x^2} + \frac{2p}{x\xi} + \frac{1}{\xi^2}\right) I_d. \end{aligned} \tag{II.47}$$

For $x \neq 0$, the requirement that eq.(II.46) satisfies eq.(II.45) gives

$$\frac{p(p+1)}{x^2} + \frac{2p}{x\xi} + \frac{1}{\xi^2} - \frac{p(d-1)}{x^2} - \frac{(d-1)}{x\xi} = \frac{1}{\xi^2}. \tag{II.48}$$

The choice of ξ as the decay length ensures that the constant terms in the above equation cancel. The exponent p is determined by requiring the next largest terms to cancel. For $x \ll \xi$, the $1/x^2$ terms are the next most important; we must set $p(p+1) = p(d-1)$, and $p = d-2$. This is the familiar exponent for Coulomb interactions, and indeed at this length scale the correlations don't feel the presence of ξ, and decay as

$$I_d(x) \simeq C_d(x) = \frac{x^{2-d}}{(2-d)S_d} \qquad (x \ll \xi). \tag{II.49}$$

(Note that a constant term can always be added to the solution to satisfy the limits appropriate to the correlation function under study.) At large distances $x \gg \xi$, the $1/(x\xi)$ term dominates eq.(II.48), and its vanishing implies $p = (d-1)/2$. Matching to eq.(II.49) at $x \approx \xi$ yields

$$I_d(x) \simeq \frac{\xi^{(3-d)/2}}{(2-d)S_d x^{(d-1)/2}} \exp(-x/\xi) \qquad (x \gg \xi). \tag{II.50}$$

The length scale ξ is known as the *correlation length*. From eq.(II.42), we observe that transverse and longitudinal correlations behave differently. Close to the critical point, the longitudinal correlation length (eq.(II.36)) behaves as

$$\xi_\ell = \begin{cases} t^{-1/2}/\sqrt{K} & \text{for } t > 0 \\ (-2t)^{-1/2}/\sqrt{K} & \text{for } t < 0 \end{cases}. \tag{II.51}$$

The singularities can be described by $\xi_\pm \simeq \xi_0 B_\pm |t|^{-\nu_\pm}$, where $\nu_\pm = 1/2$ and $B_+/B_- = \sqrt{2}$ are universal, while $\xi_0 \propto 1/\sqrt{K}$ is not. The transverse correlation length (eq.(II.37)) equals ξ_ℓ for $t > 0$, and is infinite for all $t < 0$.

Eq.(II.49) implies that right at T_c, correlations decay as $1/x^{d-2}$. Actually, the decay exponent is usually indicated by $1/x^{d-2+\eta}$, where η is the same exponent introduced in eq.(II.40). Integrating the connected correlation functions results in bulk susceptibilities. For example, the divergence of the longitudinal susceptibility is also obtained from,

$$\chi_\ell \propto \int d^d\mathbf{x} G^c_\ell(\mathbf{x}) \propto \int_0^{\xi_\ell} \frac{d^d x}{x^{d-2}} \propto \xi_\ell^2 \simeq A_\pm t^{-1}. \tag{II.52}$$

The universal exponents and amplitude ratios are again recovered from the above equation. For $T < T_c$, there is no upper cut-off length for transverse correlations, and the divergence of the transverse susceptibility can be related to the system size L, as

$$\chi_t \propto \int d^d\mathbf{x} G^c_t(\mathbf{x}) \propto \int_0^{L} \frac{d^d x}{x^{d-2}} \propto L^2. \tag{II.53}$$

II.F Comparison to Experiments

The true test of the validity of the approach outlined in previous sections is in its comparison with experiments. A table of exponents, and the appropriate experimental materials is provided below.

Transition Type	Material	α	β	γ	ν
Ferromagnets ($n = 3$)	Fe, Ni	-0.1	0.4	1.3	
Superfluid ($n = 2$)	He^4	0	0.3	1.3	0.7
Liquid-Gas ($n = 1$)	CO_2, Xe	0.1	0.3	1.2	0.7
Ferroelectrics and Superconductors	TGS	0	1/2	1	1/2
Mean–field theory		0	1/2	1	1/2

The exponents are actually known to much better accuracy than indicated in the table. The final row (mean–field theory) refers to the results obtained from the saddle point approximation. They agree only with the experiments on ferroelectric and superconducting materials. The disagreement between the exponents for different values of n suggests that the mean–field results are too universal, and leave out some essential dependence on n (and d). How do we account for these discrepancies? The starting point of the Landau–Ginzburg Hamiltonian is sufficiently general to be trustworthy. The difficulty is in the saddle point method used in the evaluation of its partition function, as will become apparent in the following sections.

II.G Gaussian Integrals

In the previous section, the energy cost of fluctuations was calculated at quadratic order. These fluctuations also modify the saddle point free energy. Before calculating this modification, we take a short (but necessary) mathematical diversion on performing Gaussian integrals.

The simplest Gaussian integral involves one variable ϕ,

$$\mathcal{I}_1 = \int_{-\infty}^{\infty} d\phi \, e^{-\frac{K}{2}\phi^2 + h\phi} = \sqrt{\frac{2\pi}{K}} \, e^{\frac{h^2}{2K}}. \tag{II.54}$$

By taking derivatives of the above expression with respect to h, integrals involving powers of ϕ are generated; e.g.

$$\begin{aligned} \frac{d}{dh}: \qquad & \int_{-\infty}^{\infty} d\phi \; \phi \, e^{-\frac{K}{2}\phi^2 + h\phi} = \sqrt{\frac{2\pi}{K}} e^{\frac{h^2}{2K}} \cdot \frac{h}{K}, \\ \frac{d^2}{dh^2}: \qquad & \int_{-\infty}^{\infty} d\phi \; \phi^2 e^{-\frac{K}{2}\phi^2 + h\phi} = \sqrt{\frac{2\pi}{K}} e^{\frac{h^2}{2K}} \cdot \left[\frac{1}{K} + \frac{h^2}{K^2} \right]. \end{aligned} \tag{II.55}$$

If the integrand represents the probability density of the random variable ϕ, the above integrals imply the moments $\langle \phi \rangle = h/K$, and $\langle \phi^2 \rangle = h^2/K^2 + 1/K$. The corresponding cumulants are $\langle \phi \rangle_c = \langle \phi \rangle = h/K$, and $\langle \phi^2 \rangle_c = \langle \phi^2 \rangle - \langle \phi \rangle^2 = 1/K$. In fact all higher order cumulants of the Gaussian distribution are zero since

$$\left\langle e^{-ik\phi} \right\rangle \equiv \exp\left[\sum_{\ell=1}^{\infty} \frac{(-ik)^\ell}{\ell!} \left\langle \phi^\ell \right\rangle_c \right] = \exp\left[-ikh - \frac{k^2}{2K} \right]. \tag{II.56}$$

Now consider the following Gaussian integral involving N variables,

$$\mathcal{I}_N = \int_{-\infty}^{\infty} \prod_{i=1}^{N} d\phi_i \exp\left[-\sum_{i,j} \frac{K_{i,j}}{2} \phi_i \phi_j + \sum_i h_i \phi_i \right]. \tag{II.57}$$

It can be reduced to a product of N one dimensional integrals by diagonalizing the matrix $\mathbf{K} \equiv K_{i,j}$. Since we need only consider *symmetric matrices* ($K_{i,j} = K_{j,i}$), the eigenvalues are real, and the eigenvectors can be made orthonormal. Let us denote the eigenvectors and eigenvalues of $\mathbf{K}$ by $\hat{q}$ and K_q respectively, i.e. $\mathbf{K}\hat{q} = K_q \hat{q}$. The vectors $\{\hat{q}\}$ form a new coordinate basis in the original N dimensional space. Any point in this space can be represented either by coordinates $\{\phi_i\}$, or $\left\{\tilde{\phi}_q\right\}$ with $\phi_i = \sum_q \tilde{\phi}_q \hat{q}_i$. We can now change

the integration variables from $\{\phi_i\}$ to $\left\{\tilde{\phi}_q\right\}$. The Jacobian associated with this unitary transformation is unity, and

$$\mathcal{I}_N = \prod_{q=1}^{N} \int_{-\infty}^{\infty} d\tilde{\phi}_q \exp\left[-\frac{K_q}{2}\tilde{\phi}_q^2 + \tilde{h}_q\tilde{\phi}_q\right] = \prod_{q=1}^{N} \sqrt{\frac{2\pi}{K_q}} \exp\left[\frac{\tilde{h}_q K_q^{-1}\tilde{h}_q}{2}\right]. \tag{II.58}$$

The final expression can be represented in terms of the original coordinates by using the *inverse* matrix $\mathbf{K^{-1}}$, such that $\mathbf{K^{-1}K} = \mathbf{1}$. Since the determinant of the matrix is independent of the choice of basis, $\det \mathbf{K} = \prod_q K_q$, and

$$\mathcal{I}_N = \sqrt{\frac{(2\pi)^N}{\det \mathbf{K}}} \exp\left[\sum_{i,j} \frac{K^{-1}_{i,j}}{2} h_i h_j\right]. \tag{II.59}$$

Regarding $\{\phi_i\}$ as Gaussian random variable distributed with a joint probability distribution function proportional to the integrand of eq.(II.57), the *joint characteristic function* is given by

$$\left\langle e^{-i\sum_j k_j\phi_j} \right\rangle = \exp\left[-i\sum_{i,j} K^{-1}_{i,j} h_i k_j - \sum_{i,j} \frac{K^{-1}_{i,j}}{2} k_i k_j\right]. \tag{II.60}$$

Moments of the distribution are obtained from derivatives of the characteristic function with respect to k_i, and *cumulants* from derivatives of its logarithm. Hence, eq.(II.60) implies

$$\begin{cases} \langle\phi_i\rangle_c = \sum_j K^{-1}_{i,j} h_j \\ \langle\phi_i\phi_j\rangle_c = K^{-1}_{i,j} \end{cases}. \tag{II.61}$$

Another useful form of eq.(II.60) is

$$\langle \exp(A)\rangle = \exp\left[\langle A\rangle_c + \frac{1}{2}\langle A^2\rangle_c\right], \tag{II.62}$$

where $A = \sum_i a_i\phi_i$ is any linear combination of Gaussian distributed variables. We used this result earlier in computing the order parameter correlations in the presence of phase fluctuations in a superfluid.

Gaussian *functional integrals* are a limiting case of the above many variable integrals. Consider the points i as the sites of a d–dimensional lattice and let the spacing go to zero.

In the continuum limit, $\{\phi_i\}$ go over to a function $\phi(\mathbf{x})$, and the matrix K_{ij} is replaced by a *kernel* $K(\mathbf{x},\mathbf{x}')$. The natural generalization of eq.(II.59) is

$$\begin{aligned}&\int_{-\infty}^{\infty}\mathcal{D}\phi(\mathbf{x})\exp\left[-\int d^d\mathbf{x}d^d\mathbf{x}'\frac{K(\mathbf{x},\mathbf{x}')}{2}\phi(\mathbf{x})\phi(\mathbf{x}')+\int d^d\mathbf{x}h(\mathbf{x})\phi(\mathbf{x})\right]\\&\propto(\det\mathbf{K})^{-1/2}\exp\left[\int d^d\mathbf{x}d^d\mathbf{x}'\frac{K^{-1}(\mathbf{x},\mathbf{x}')}{2}h(\mathbf{x})h(\mathbf{x}')\right],\end{aligned}\tag{II.63}$$

where the inverse kernel $K^{-1}(\mathbf{x},\mathbf{x}')$ satisfies

$$\int d^d\mathbf{x}'K(\mathbf{x},\mathbf{x}')K^{-1}(\mathbf{x}',\mathbf{x}'')=\delta^d(\mathbf{x}-\mathbf{x}'').\tag{II.64}$$

The notation $\mathcal{D}\phi(\mathbf{x})$ is used to denote the functional integral. There is a constant of proportionality, $(2\pi)^{N/2}$, left out of eq.(II.63). Although formally infinite in the continuum limit of $N\to\infty$, it does not effect the averages that are obtained as derivatives of such integrals. In particular, for Gaussian distributed functions, eq.(II.61) generalizes to

$$\begin{cases}\langle\phi(\mathbf{x})\rangle_c=\int d^d\mathbf{x}'K^{-1}(\mathbf{x},\mathbf{x}')h(\mathbf{x}')\\\langle\phi(\mathbf{x})\phi(\mathbf{x}')\rangle_c=K^{-1}(\mathbf{x},\mathbf{x}')\end{cases}.\tag{II.65}$$

In dealing with small fluctuations to the Landau–Ginzburg Hamiltonian, we encountered the quadratic form

$$\int d^d\mathbf{x}[(\nabla\phi)^2+\phi^2/\xi^2]\equiv\int d^d\mathbf{x}d^d\mathbf{x}'\phi(\mathbf{x}')\delta^d(\mathbf{x}-\mathbf{x}')(-\nabla^2+\xi^{-2})\phi(\mathbf{x}),\tag{II.66}$$

which implies the kernel

$$K(\mathbf{x},\mathbf{x}')=K\delta^d(\mathbf{x}-\mathbf{x}')(-\nabla^2+\xi^{-2}).\tag{II.67}$$

Following eq.(II.64), the inverse kernel satisfies

$$K\int d^d\mathbf{x}''\delta^d(\mathbf{x}-\mathbf{x}'')(-\nabla^2+\xi^{-2})K^{-1}(\mathbf{x}''-\mathbf{x}')=\delta^d(\mathbf{x}'-\mathbf{x}),\tag{II.68}$$

which implies the differential equation

$$K(-\nabla^2+\xi^{-2})K^{-1}(\mathbf{x})=\delta^d(\mathbf{x}).\tag{II.69}$$

Comparing with eq.(II.44) implies $K^{-1}(\mathbf{x})=\langle\phi(\mathbf{x})\phi(\mathbf{0})\rangle=-I_d(\mathbf{x})/K$, as obtained before by a less direct method.

II.H Fluctuation Corrections to the Saddle Point

We can now examine how fluctuations around the saddle point solution modify the free energy, and other macroscopic properties. Starting with eq.(II.35), the partition function including small fluctuations is

$$\begin{aligned} Z \approx \exp\left[-V\left(\frac{t}{2}\bar{m}^2 + u\bar{m}^4\right)\right] \int \mathcal{D}\phi_\ell(\mathbf{x}) \exp\left\{-\frac{K}{2}\int d^d\mathbf{x}\left[(\nabla\phi_\ell)^2 + \frac{\phi_\ell^2}{\xi_\ell^2}\right]\right\} \\ \cdot \int \mathcal{D}\phi_t(\mathbf{x}) \exp\left\{-\frac{K}{2}\int d^d\mathbf{x}\left[(\nabla\phi_t)^2 + \frac{\phi_t^2}{\xi_t^2}\right]\right\}. \end{aligned} \tag{II.70}$$

Each of the Gaussian kernels is diagonalized by the Fourier transforms

$$\tilde{\phi}(\mathbf{q}) = \int d^d\mathbf{x}\, \exp\left(-i\mathbf{q}\cdot\mathbf{x}\right)\phi(\mathbf{x})/\sqrt{V},$$

and with corresponding eigenvalues $K(\mathbf{q}) = K(q^2 + \xi^{-2})$. The resulting determinant of $\mathbf{K}$ is a product of such eigenvalues, and hence

$$\ln\det\mathbf{K} = \sum_{\mathbf{q}} \ln K(\mathbf{q}) = V\int \frac{d^d\mathbf{q}}{(2\pi)^d} \ln[K(q^2+\xi^{-2})]. \tag{II.71}$$

The free energy resulting from eq.(II.70) is then given by

$$f = -\frac{\ln Z}{V} = \frac{t\bar{m}^2}{2} + u\bar{m}^4 + \frac{1}{2}\int \frac{d^d\mathbf{q}}{(2\pi)^d}\ln[K(q^2+\xi_\ell^{-2})] + \frac{n-1}{2}\int \frac{d^d\mathbf{q}}{(2\pi)^d}\ln[K(q^2+\xi_t^{-2})]. \tag{II.72}$$

(Note that there are $n-1$ transverse components.) Using the dependance of the correlation lengths on reduced temperature, the singular part of the heat capacity is obtained as

$$C_{\rm singular} \propto -\frac{\partial^2 f}{\partial^2 t} = \begin{cases} 0 + \dfrac{n}{2}\displaystyle\int \frac{d^d\mathbf{q}}{(2\pi)^d}\frac{1}{(Kq^2+t)^2} & \text{for } t > 0 \\ \dfrac{1}{8u} + 2\displaystyle\int \frac{d^d\mathbf{q}}{(2\pi)^d}\frac{1}{(Kq^2-2t)^2} & \text{for } t < 0 \end{cases}. \tag{II.73}$$

The correction terms are proportional to

$$C_F = \frac{1}{K^2}\int \frac{d^d\mathbf{q}}{(2\pi)^d}\frac{1}{(q^2+\xi^{-2})^2}. \tag{II.74}$$

The integral has dimensions of (length)$^{4-d}$, and changes behavior at $d = 4$. For $d > 4$ the integral diverges at large $\mathbf{q}$, and is dominated by the upper cutoff $\Lambda \simeq 1/a$, where a is

the lattice spacing. For $d < 4$, the integral is convergent in both limits. It can be made dimensionless by rescaling $\mathbf{q}$ by ξ^{-1}, and is hence proportional to ξ^{4-d}. Therefore

$$C_F \simeq \frac{1}{K^2} \begin{cases} a^{4-d} & \text{for } d > 4 \\ \xi^{4-d} & \text{for } d < 4 \end{cases} . \tag{II.75}$$

In dimensions $d > 4$, fluctuation corrections to the heat capacity add a constant term to the background on each side of the transition. However, the primary form of the singularity, a discontinuity in C, is not changed. For $d < 4$, the divergence of $\xi \propto t^{-1/2}$, at the transition leads to a correction term from eq.(II.75) which is more important than the original discontinuity. Indeed, the correction term corresponds to an exponent $\alpha = (4-d)/2$. However, this is only the first correction to the saddle point result. The diverge of C_F merely implies that the saddle point conclusions are no longer reliable in dimensions $d \leq 4$, called the *upper critical dimension*. Although we obtained this dimension by looking at the fluctuation corrections to the heat capacity, we would have reached the same conclusion in examining the singular part of any other quantity, such as magnetization or susceptibility. The contributions due to fluctuations always modify the leading singular behavior, and hence the critical exponents, in dimensions $d \leq 4$.

II.I The Ginzburg Criterion

We have thus established the importance of fluctuations, and identified them as the probable reason for the failure of the saddle point approximation to correctly describe the observed exponents. However, as noted in sec.II.G, there are some materials, such as superconductors, in which the experimental results are well fitted to the singular forms predicted by this approximation. Can we quantify why fluctuations are less important in superconductors than in other phase transitions?

Eq.(II.75) indicates that fluctuation corrections become important due to the divergence of the correlation length. Within the saddle point approximation, the correlation length diverges as $\xi \approx \xi_0 |t|^{-1/2}$, where $t = (T_c - T)/T_c$ is the reduced temperature, and $\xi_0 \approx \sqrt{K}$ is a *microscopic* length scale. In principal, ξ_0 can be measured experimentally from fitting scattering line shapes. It has to approximately equal the size of the units that undergo ordering at the phase transition. For the liquid–gas transition, ξ_0 can be estimated as $(v_c)^{1/3}$, where v_c is the critical atomic volume. In superfluids, ξ_0 is approximately the thermal wavelength $\lambda(T)$. Both these estimates are of the order of a few atomic spacings, 1–10Å. On the other hand, the underlying unit for superconductors is a Cooper pair. The

paired electrons are forced apart by their Coulomb repulsion, resulting in a relatively large separation of $\xi_0 \approx 10^3$Å.

The importance of fluctuations can be gauged by comparing the two terms in eq.(II.73); the saddle point discontinuity $\Delta C_{\rm S.P.} \propto 1/u$, and the correction term C_F. Since $K \propto \xi_0^2$, the correction term is proportional to $\xi_0^{-d} t^{-(4-d)/2}$. Thus fluctuations are important provided,

$$\xi_0^{-d} t^{-\frac{4-d}{2}} \gg \Delta C_{\rm S.P.}, \quad \Longrightarrow \quad |t| \ll t_G \simeq \frac{1}{(\xi_0^d \Delta C_{\rm S.P.})^{\frac{2}{4-d}}}. \tag{II.76}$$

The above requirement is known as the *Ginzburg criterion*. Naturally in $d < 4$, it is satisfied sufficiently close to the critical point. However, the resolution of the experiment may not be good enough to get closer than the Ginzburg reduced temperature t_G. If so, the apparent singularities at reduced temperatures $t > t_G$ may show saddle point behavior. It is this apparent discontinuity that then appears in eq.(II.76), and may be used to self–consistently estimate t_G. Clearly, $\Delta C_{\rm S.P.}$ and ξ_0 can both be measured in dimensionless units; ξ_0 in units of atomic size a, and $\Delta C_{\rm S.P.}$ in units of Nk_B. The latter is of the order of unity for most transitions, and thus $t_G \approx \xi_0^{-6}$ in $d = 3$. In cases where ξ_0 is a few atomic spacings, a resolution of $t_G \approx 10^{-1} - 10^{-2}$ will suffice. However, in superconductors with $\xi_0 \approx 10^3 a$, a resolution of $t_G < 10^{-18}$ is necessary to see any fluctuation effects. This is much beyond the ability of current apparatus. The newer ceramic high temperature superconductors have a much smaller coherence length of $\xi_0 \approx 10a$, and they indeed show some effects of fluctuations.

Again, it is worth emphasizing that a similar criterion could have been obtained by examining any other quantity. Fluctuations corrections become important in measurement of a quantity X for $t \ll t_G(X) \simeq A(X)\xi_0^{-2d/(4-d)}$. However, the coefficient $A(X)$ may be different (by one or two orders of magnitude) for different quantities. So, it is in principle possible to observe saddle point behavior in one quantity, while fluctuations are important in another quantity measured at the same resolution. Of course, fluctuations will always become important at sufficiently high resolutions.

A summary of the results obtained so far from the Landau–Ginzburg approach is as follows:

- For dimensions d greater than an upper critical dimension of $d_u = 4$, the saddle point approximation is valid, and singular behavior at the critical point is described by exponents $\alpha = 0$, $\beta = 1/2$, $\gamma = 1$, $\nu = 1/2$, $\cdots$.
- For d less than a lower critical dimensions ($d_\ell = 2$ for continuous symmetry, and $d_\ell = 1$ for discrete symmetry) fluctuations are strong enough to destroy the ordered phase.
- In the intermediate dimensions, $d_\ell \leq d \leq d_u$, fluctuations are strong enough to change the saddle point results, but not sufficiently important to completely destroy order. Unfortunately, or happily, this is the case of interest to us in $d = 3$.

III. The Scaling Hypothesis

III.A The Homogeneity Assumption

In the previous chapters, the singular behavior in the vicinity of a continuous transition was characterized by a set of critical exponents $\{\alpha, \beta, \gamma, \delta, \nu, \eta, \cdots\}$. The saddle–point estimates of these exponents were found to be unreliable due to the importance of fluctuations. Since the various thermodynamic quantities are related, these exponents can not be independent of each other. The goal of this chapter is to discover the relationships between them, and to find the minimum number of independent exponents needed to describe the critical point.

The non-analytical structure is a coexistence line for $t < 0$ and $h = 0$, that terminates at the critical point $t = h = 0$. The various exponents describe the leading singular behavior of a thermodynamic quantity $Q(t, h)$, in the vicinity of this point. A basic quantity in the canonical ensemble is the free energy, which in the saddle–point approximation is given by

$$f(t,h) = \min\left[\frac{t}{2}m^2 + um^4 - h.m\right]_m \propto \begin{cases} -\dfrac{t^2}{u} & \text{for } h = 0,\ t < 0 \\ -\dfrac{h^{4/3}}{u^{1/3}} & \text{for } h \neq 0,\ t = 0 \end{cases} . \qquad \text{(III.1)}$$

The singularities in the free energy can in fact be described by a single *homogeneous* function[†] in t and h, as

$$f(t,h) = |t|^2 g_f\left(h/|t|^{\Delta}\right). \qquad \text{(III.2)}$$

The function g_f only depends on the combination $x \equiv h/|t|^{\Delta}$, where Δ is known as the *gap exponent*. The asymptotic behavior of g_f is easily obtained by comparing eqs.(III.1) and (III.2). The $h = 0$ limit is recovered if $\lim_{x\to 0} g_f(x) \sim 1/u$, while to get the proper power of h, we must set $\lim_{x\to\infty} g_f(x) \sim x^{4/3}/u^{1/3}$. The latter implies $f \sim |t|^2 h^{4/3}/(u^{1/3}|t|^{4\Delta/3})$.

[†] In general, a function $f(x_1, x_2, \cdots)$ is homogeneous if

$$f\left(b^{p_1}x_1, b^{p_2}x_2, \cdots\right) = b^{p_f} f(x_1, x_2, \cdots),$$

for any rescaling factor b. With the proper choice of b one of the arguments can be removed, leading to a scaling forms used in this section.

Since f can have no t dependence along $t = 0$, the gap exponent (corresponding to Eq.(III.1) has the value

$$\Delta = \frac{3}{2} \quad . \tag{III.3}$$

The assumption of homogeneity is that, on going beyond the saddle–point approximation, the singular form of the free energy (and any other thermodynamic quantity) retains the homogeneous form

$$f_{\text{sing.}}(t,h) = |t|^{2-\alpha} g_f\left(h/|t|^{\Delta}\right). \tag{III.4}$$

The actual exponents α and Δ depend on the critical point being considered. The dependence on t is chosen to reproduce the heat capacity singularity at $h = 0$. The singular part of the energy is obtained from (say for $t > 0$)

$$\begin{aligned} E_{\text{sing.}} \sim \frac{\partial f}{\partial t} &\sim (2-\alpha)t^{1-\alpha} g_f\left(h/|t|^{\Delta}\right) - \Delta h t^{1-\alpha-\Delta} g_f'\left(h/|t|^{\Delta}\right) \\ &\sim t^{1-\alpha}\left[(2-\alpha) g_f\left(h/|t|^{\Delta}\right) - \frac{\Delta h}{t^{\Delta}} g_f'\left(h/|t|^{\Delta}\right)\right] \equiv t^{1-\alpha} g_E\left(h/|t|^{\Delta}\right). \end{aligned} \tag{III.5}$$

Thus the derivative of one homogeneous function is another. Similarly, the second derivative takes the form (again for $t > 0$)

$$C_{\text{sing.}} \sim -\frac{\partial^2 f}{\partial t^2} \sim t^{-\alpha} g_C\left(h/|t|^{\Delta}\right), \tag{III.6}$$

reproducing the scaling $C_{\text{sing.}} \sim t^{-\alpha}$, as $h \to 0$.

It may appear that we have the freedom to postulate a more general form

$$C_{\pm}(t,h) = |t|^{-\alpha_{\pm}} g_{\pm}\left(h/|t|^{\Delta_{\pm}}\right), \tag{III.7}$$

with different functions and exponents for $t > 0$ and $t < 0$, that match at $t = 0$. However, this is ruled out by the condition that the free energy is analytic everywhere except on the coexistence line for $h = 0$ and $t < 0$, as proven as follows: Consider a point at $t = 0$ and finite h. By assumption, the function C is perfectly analytic in the vicinity of this point, expandable in a taylor series,

$$C\left(t \ll h^{\Delta}\right) = \mathcal{A}(h) + t\mathcal{B}(h) + \mathcal{O}(t^2). \tag{III.8}$$

Furthermore, the same expansion should be obtained from both C_+ and C_-. But eq.(III.7) leads to the expansions,

$$C_{\pm} = |t|^{-\alpha_{\pm}}\left[A_{\pm}\left(\frac{h}{|t|^{\Delta_{\pm}}}\right)^{p_{\pm}} + B_{\pm}\left(\frac{h}{|t|^{\Delta_{\pm}}}\right)^{q_{\pm}} + \cdots\right], \tag{III.9}$$

where $\{p_\pm, q_\pm\}$ are the leading powers in asymptotic expansions of $g_\pm$ for large arguments, and $\{A_\pm, B_\pm\}$ are the corresponding pre-factors. Matching to the taylor series in eq.(III.8) requires $p_\pm \Delta_\pm = -\alpha_\pm$ and $q_\pm \Delta_\pm = -(1+\alpha_\pm)$, and leads to

$$C_\pm \left(t \ll h^\Delta \right) = A_\pm h^{-\alpha_\pm/\Delta_\pm} + B_\pm h^{-(1+\alpha_\pm)/\Delta_\pm} |t| + \cdots . \tag{III.10}$$

Continuity at $t = 0$ now forces $\alpha_+/\Delta_+ = \alpha_-/\Delta_-$, and $(1+\alpha_+)/\Delta_+ = (1+\alpha_-)/\Delta_-$, which in turn implies

$$\begin{cases} \alpha_+ = \alpha_- \equiv \alpha \\ \Delta_+ = \Delta_- \equiv \Delta \end{cases} . \tag{III.11}$$

Despite using $|t|$ in the postulated scaling form, we can still ensure the analyticity of the function at $t = 0$ for finite h by appropriate choice of parameters, e.g. by setting $B_- = -B_+$ to match Eq.(III.10) to the analytic form in Eq.(III.8). Having established this result, we can be somewhat careless henceforth in replacing $|t|$ in the scaling equations with t. Naturally these arguments apply to any quantity $Q(t, h)$.

Starting from the free energy in eq.(III.4), we can compute the singular parts of other quantities of interest:

- The *magnetization* is obtained from

$$m(t,h) \sim \frac{\partial f}{\partial h} \sim |t|^{2-\alpha-\Delta} g_m \left(h/|t|^\Delta \right) . \tag{III.12}$$

In the limit $x \to 0$, $g_m(x)$ is a constant, and

$$m(t, h=0) \sim |t|^{2-\alpha-\Delta}, \quad \Longrightarrow \quad \beta = 2 - \alpha - \Delta. \tag{III.13}$$

On the other hand, if $x \to \infty$, $g_m(x) \sim x^p$, and

$$m(t=0, h) \sim |t|^{2-\alpha-\Delta} \left(\frac{h}{|t|^\Delta} \right)^p . \tag{III.14}$$

Since this limit is independent of t, we must have $p\Delta = 2 - \alpha - \Delta$. Hence

$$m(t, h=0) \sim h^{(2-\alpha-\Delta)/\Delta}, \quad \Longrightarrow \quad \delta = \Delta/(2-\alpha-\Delta) = \Delta/\beta. \tag{III.15}$$

- Similarly, the *susceptibility* is computed as

$$\chi(t,h) \sim \frac{\partial m}{\partial h} \sim |t|^{2-\alpha-2\Delta} g_\chi(h/|t|^\Delta), \ \Rightarrow \ \chi(t, h=0) \sim |t|^{2-\alpha-2\Delta}, \ \Rightarrow \quad \gamma = 2\Delta - 2 + \alpha. \tag{III.16}$$

Thus, the consequences of the homogeneity assumption are:

(1) The singular parts of all critical quantities $Q(t,h)$, are homogeneous, with the same exponents above and below the transition.

(2) Because of the interconnections via thermodynamic derivatives, the same gap exponent Δ, occurs for all such quantities.

(3) All (bulk) critical exponents can be obtained from only *two* independent ones, e.g. α and Δ.

(4) As a result of the above, there are a number of *exponent identities*. For example, eqs.(III.13), (III.15), and (III.16) imply

$$\begin{aligned} \alpha + 2\beta + \gamma = \alpha + 2(2-\alpha-\Delta) + (2\Delta - 2 + \alpha) = 2 \qquad & \text{(Rushbrooke's Identity)}, \\ \delta - 1 = \frac{\Delta}{2-\alpha-\Delta} - 1 = \frac{2\Delta - 2 + \alpha}{2-\alpha-\Delta} = \frac{\gamma}{\beta} \qquad & \text{(Widom's Identity)}. \end{aligned} \tag{III.17}$$

These identities can be checked against the following table of critical exponents. The first three rows are based on a number of theoretical estimates in $d = 3$; the last row comes from an exact solution in $d = 2$. The exponent identities are completely consistent with these values, as well as with all reliable experimental data.

	α	β	γ	δ	ν	η
$n=1$	0.11	0.32	1.24	4.9	0.63	0.04
$n=2$	-0.01	0.35	1.32	4.7	0.67	0.04
$n=3$	-0.11	0.36	1.39	4.9	0.70	0.04
$n=1$	0	1/8	7/4	15	1	1/4

III.B Divergence of the Correlation Length

The homogeneity assumption relates to the free energy and quantities derived from it. It says nothing about the behavior of correlation functions. An important property of a critical point is the divergence of the correlation length, which is responsible for, and can be deduced from, diverging response functions. In order to obtain an identity involving the exponent ν for the divergence of the correlation length, we replace the homogeneity assumption for the free energy, with the following *two* conditions:

(1) The correlation length ξ has a homogeneous form,

$$\xi(t,h) \sim |t|^{-\nu} g\left(h/|t|^{\Delta}\right). \tag{III.18}$$

(For $t = 0$, ξ diverges as $h^{-\nu_h}$ with $\nu_h = \nu/\Delta$.)

(2) Close to criticality, the correlation length ξ is the most important length in the system, and is *solely* responsible for singular contributions to thermodynamic quantities.

The second condition determines the singular part of the free energy. Since $\ln Z(t,h)$ is *extensive* and *dimensionless*, it must take the form

$$\ln Z = \left(\frac{L}{\xi}\right)^d \times g_s + \left(\frac{L}{a}\right)^d \times g_a \quad , \tag{III.19}$$

where g_s and g_a are non-singular functions of dimensionless parameters (a is an appropriate microscopic length). The singular part of the free energy comes from the first term, and behaves as

$$f_{\text{sing.}}(t,h) \sim \frac{\ln Z}{L^d} \sim \xi^{-d} \sim |t|^{d\nu} g_f\left(h/|t|^{\Delta}\right). \tag{III.20}$$

A simple interpretation of the above result is obtained by dividing the system into units of the size of the correlation length. Each unit is then regarded as an independent random variable, contributing a constant factor to the critical free energy. The number of units grows as $(L/\xi)^d$, leading to eq.(III.19).

The consequences of the above assumptions are:

(1) The homogeneity of $f_{\text{sing.}}(t,h)$ emerges naturally.

(2) We obtain the additional exponent relation

$$2 - \alpha = d\nu \qquad (\text{Joshephson}'\text{s identity}) \quad . \tag{III.21}$$

Identities obtained from the generalized homogeneity assumption involve the space dimension d, and are known as *hyperscaling relations*. The relation between α and ν is consistent with the exponents in the above table. However, it does not agree with the saddle point values, $\alpha = 0$ and $\nu = 1/2$, which are valid for $d > 4$. Any theory of critical behavior must thus account for the validity of this relation in low dimension, and its breakdown for $d > 4$.

III.C Critical Correlation Functions and Self-Similarity

One exponent that has not so far been accounted for is η, describing the decay of correlation functions at criticality. Exactly at the critical point, the correlation length is infinite, and there is no other length scale (except sample size) to cut off the decay of correlation functions. Thus all correlations decay as a power of the separation. As discussed in the previous chapter, the magnetization correlations fall off as

$$G^c_{m,m}(\mathbf{x}) \equiv \langle m(\mathbf{x})m(\mathbf{0})\rangle - \langle m\rangle^2 \sim 1/|\mathbf{x}|^{d-2+\eta}. \tag{III.22}$$

Similarly, we can define an exponent η' for the decay of energy–energy correlations as

$$G^c_{E,E}(\mathbf{x}) = \langle \mathcal{H}(\mathbf{x})\mathcal{H}(\mathbf{0})\rangle - \langle \mathcal{H}\rangle^2 \sim 1/|\mathbf{x}|^{d-2+\eta'}. \tag{III.23}$$

Away from criticality, the power laws are cut off for distances $|\mathbf{x}| \gg \xi$. As the response functions can be obtained from integrating the connected correlation functions, there are additional exponent identities, such as (Fisher's identity)

$$\chi \sim \int d^d\mathbf{x} G^c_{mm}(\mathbf{x}) \sim \int^{\xi} \frac{d^dx}{|x|^{d-2+\eta}} \sim \xi^{2-\eta} \sim |t|^{-\nu(2-\eta)}, \quad \Longrightarrow \quad \gamma = (2-\eta)\nu \quad . \tag{III.24}$$

Similarly, for the heat capacity,

$$C \sim \int d^d\mathbf{x} G^c_{EE}(\mathbf{x}) \sim \int^{\xi} \frac{d^dx}{|x|^{d-2+\eta'}} \sim \xi^{2-\eta'} \sim |t|^{-\nu(2-\eta')}, \quad \Longrightarrow \quad \alpha = (2-\eta')\nu \quad . \tag{III.25}$$

As before, two *independent* exponents are sufficient to describe all singular critical behavior.

An important consequence of these scaling ideas is that the critical system has an additional *dilation symmetry*. Under a change of scale, the critical correlation functions behave as

$$G_{\rm critical}(\lambda\mathbf{x}) = \lambda^p G_{\rm critical}(\mathbf{x}). \tag{III.26}$$

This implies a *scale invariance* or *self–similarity*: if a snapshot of the critical system is blown up by a factor of λ, apart from a change of contrast (multiplication by λ^p), the resulting snapshot is statistically similar to the original one. Such statistical self–similarity is the hallmark of *fractal* geometry. As discussed by Mandelbrot, many naturally occurring forms (clouds, shore-lines, river basins, etc.) exhibit such behavior. The Landau–Ginzburg probability was constructed on the basis of *local* symmetries such as rotation invariance. If we could add to the list of constraints the requirement of *dilation symmetry*, the resulting probability would indeed describe the critical point. Unfortunately, it is not possible to directly see how such a requirement constrains the effective Hamiltonian. One notable exception is in $d = 2$, where dilation symmetry implies conformal invariance, and a lot of information can be obtained by constructing conformally invariant theories. We shall instead prescribe a less direct route of following the effects of the dilation operation on the effective energy; the *renormalization group* procedure.

III.D The Renormalization Group (Conceptual)

Success of the scaling theory in correctly predicting various exponent identities strongly supports the assumption that close to the critical point the correlation length ξ, is the only important length scale, and that microscopic length scales are irrelevant. The critical behavior is dominated by fluctuations that are self–similar up to the scale ξ. The self–similarity is of course only statistical, in that a magnetization configuration is generated with a weight $W[\vec{m}(\mathbf{x})] \propto \exp\{-\beta\mathcal{H}[\vec{m}(\mathbf{x})]\}$. Kadanoff suggested taking advantage of the self–similarity of the fluctuations to gradually eliminate the correlated degrees of freedom at length scales $x \ll \xi$, until one is left with the relatively simple, uncorrelated degrees of freedom at scale ξ. This is achieved through a procedure called the *renormalization group* (RG), whose conceptual foundation is the three steps outlined in this section.

(1) *Coarse Grain:* There is an implicit short distance length scale a, for allowed variations of $\vec{m}(\mathbf{x})$ in the system. This is the lattice spacing for a model of spins, or the coarse graining scale that underlies the Landau–Ginzburg Hamiltonian. In a digital picture of the system, a corresponds to the pixel size. The first step of the RG is to decrease the resolution by changing this minimum scale to ba ($b > 1$). The *coarse–grained* magnetization is then given by

$$\overline{m}_i(\mathbf{x}) = \frac{1}{b^d} \int_{\text{Cell centered at } \mathbf{x}} d^d\mathbf{x}' m_i(\mathbf{x}'). \tag{III.27}$$

(2) *Rescale:* Due to the change in resolution, the coarse grained 'picture' is grainier than the original. The original resolution of a can be restored by decreasing all length scales by a factor of b, i.e. by setting

$$\mathbf{x}_{\text{new}} = \frac{\mathbf{x}_{\text{old}}}{b}. \tag{III.28}$$

(3) *Renormalize:* The variations of fluctuations in the rescaled magnetization profile is in general different from the original, i.e. there is a difference in contrast between the pictures. This can be remedied by introducing a change of contrast by a factor ζ, through defining a *renormalized* magnetization

$$\vec{m}_{\text{new}}(\mathbf{x}_{\text{new}}) = \frac{1}{\zeta b^d} \int_{\text{Cell centered at } b\mathbf{x}_{\text{new}}} d^d\mathbf{x}' \vec{m}(\mathbf{x}'). \tag{III.29}$$

By following these steps, for each configuration $\vec{m}_{\text{old}}(\mathbf{x})$, we generate a renormalized configuration $\vec{m}_{\text{new}}(\mathbf{x})$. Eq.(III.29) can be regarded as a mapping from one set of random variables to another, and can be used to construct the probability distribution, or weight

$W_b[\vec{m}_{\rm new}(\mathbf{x})] \equiv \exp\{-\beta\mathcal{H}_b[\vec{m}_{\rm new}(\mathbf{x})]\}$. Kadanoff's insight was that since on length scales less than ξ, the renormalized configurations are statistically similar to the original ones, they may be distributed by a Hamiltonian $\beta\mathcal{H}_b$ that is also 'close' to the original. In particular, the original Hamiltonian becomes critical by tuning the two parameter t and h to zero, at which point the dominant configurations are similar to those of the rescaled system; the critical Hamiltonian is thus invariant under such rescaling. In the original problem, one moves away from criticality for finite t and h. Kadanoff's assumption is that the corresponding new Hamiltonian is also described by non-zero $t_{\rm new}$ or $h_{\rm new}$.

The assumption that the vicinity of the original and renormalized Hamiltonians to criticality is described by the two parameters t and h greatly simplifies the analysis. The effect of the RG transformation on the probability of configurations is now described by the two parameter mappings $t_{\rm new} \equiv t_b(t_{\rm old}, h_{\rm old})$ and $h_{\rm new} \equiv h_b(t_{\rm old}, h_{\rm old})$. The next assumption is that since the transformation only involves changes at the shortest length scales, it cannot cause any singularities. The renormalized parameters must be *analytic* functions of the original ones, and hence expandable as

$$\begin{cases} t_b(t,h) = A(b)t + B(b)h + \cdots \\ h_b(t,h) = C(b)t + D(b)h + \cdots \end{cases} . \tag{III.30}$$

Note that there are no constant terms in the above Taylor expansions. This expresses the condition that if $\beta\mathcal{H}$ is at its critical point ($t = h = 0$), then $\beta\mathcal{H}_b$ is also at criticality, and $t_{\rm new} = h_{\rm new} = 0$. Furthermore, due to rotational symmetry, under the combined transformation $(m(x) \mapsto -m(x), h \mapsto -h, t \mapsto t)$ the weight of a configuration is unchanged. As this symmetry is preserved by the RG, the coefficients B and C in the above expression must be zero, leading to the further simplifications

$$\begin{cases} t_b(t,h) = A(b)t + \cdots \\ h_b(t,h) = D(b)h + \cdots \end{cases} . \tag{III.31}$$

The remaining coefficients $A(b)$ and $D(b)$ depend on the (arbitrary) rescaling factor b, and trivially $A(1) = D(1) = 1$ for $b = 1$. Since the above transformations can be carried out in sequence, and the net effect of rescalings of b_1 and b_2 is a change of scale by $b_1 b_2$, the RG procedure is sometimes referred to as a *semi-group*. The term applies to the action of RG on the space of configurations: each magnetization profile is mapped uniquely to one at larger scale, but the inverse process is non-unique as some short scale information is lost in the coarse graining. (There is in fact no problem with inverting the

transformation in the space of the parameters of the Hamiltonian.) The dependence of A and D in eqs.(III.31) on b can be deduced from this group property. Since at $b = 1$, $A = D = 1$, and $t(b_1 b_2) \approx A(b_1)A(b_2)t \approx A(b_1 b_2)t$; we must have $A(b) = b^{y_t}$, and similarly $D(b) = b^{y_h}$, yielding

$$\begin{cases} t' \equiv t_b = b^{y_t} t + \cdots \\ h' \equiv h_b = b^{y_h} h + \cdots \end{cases} . \tag{III.32}$$

If $\beta\mathcal{H}_{\rm old}$ is slightly away from criticality, it is described by a large but finite correlation length $\xi_{\rm old}$. After the RG transformation, due to the rescaling in eq.(III.28), the new correlation length is smaller by a factor of b. Hence the renormalized Hamiltonian is less critical, and the RG procedure moves the parameters further away from the origin, i.e. the exponents y_t and y_h must be positive.

- We can now explore some consequences of the assumptions leading to eq.(III.32).

1. *The free energy:* The RG transformation is a many to one map of the original configurations to new ones. Since the weight of a new configuration, $W'([m'])$, is the sum of the weights $W([m])$, of old configurations, the partition function is preserved, i.e.

$$Z = \int DmW([m]) = \int Dm'W'([m']) = Z'. \tag{III.33}$$

Hence $\ln Z = \ln Z'$, and the corresponding free energies are related by

$$Vf(t,h) = V'f(t',h'). \tag{III.34}$$

In d–dimensions, the rescaled volume is smaller by a factor of b^d, and

$$f(t,h) = b^{-d} f(b^{y_t} t, b^{y_t} h), \tag{III.35}$$

where we have made use of the assumption that two free energies are obtained from the *same Hamiltonian* in which only the parameters t and h have changed according to eqs.(III.32). Eq.(III.35) describes a *homogeneous* function of t and h. This is made apparent by choosing a rescaling factor b such that b^{y_t} is a constant, say unity, i.e. $b = t^{-1/y_t}$, leading to

$$f(t,h) = t^{d/y_t} f(1, h/t^{y_h/y_t}) \equiv t^{d/y_t} g_f(h/t^{y_h/y_t}). \tag{III.36}$$

We have thus recovered the scaling form in eq.(III.4), and can identify the exponents as

$$2 - \alpha = d/y_t \qquad , \qquad \Delta = y_h/y_t. \tag{III.37}$$

2. *Correlation length:* All length scales are reduced by a factor of b during the RG transformation. This is also true of the correlation length, $\xi' = \xi/b$, implying

$$\xi(t,h) = b\xi(b^{y_t}t, b^{y_h}h) = t^{-1/y_t}\xi(1, h/t^{y_h/y_t}) \sim t^{-\nu}. \tag{III.38}$$

This identifies $\nu = 1/y_t$, and using eq.(III.37) the hyperscaling identity, $2 - \alpha = d\nu$, is recovered.

3. *Magnetization:* From the homogenous form of the free energy (eq.(III.36)), we can obtain other bulk quantities such as magnetization. Alternatively, from the RG results for Z, V, and h, we may directly conclude

$$m(t,h) = -\frac{1}{V}\frac{\partial \ln Z(t,h)}{\partial h} = -\frac{1}{b^d V'}\frac{\partial \ln Z'(t',h')}{b^{-y_h}\partial h'} = b^{y_h - d} m(b^{y_t}t, b^{y_h}h). \tag{III.39}$$

Choosing $b = t^{-1/y_t}$, we obtain $\beta = (y_h - d)/y_t$, and $\Delta = y_h/y_t$ as before.

It is thus apparent that quite generally, the singular part of any quantity X has a homogeneous form

$$X(t,h) = b^{y_X} X(b^{y_t}t, b^{y_h}h). \tag{III.40}$$

For any conjugate pair of variables, contributing a term $\int d^d\mathbf{x} F \cdot X$, to the Hamiltonian, the *scaling dimensions* are related by $y_X = y_F - d$, where $F' = b^{y_F}F$ under RG.

III.E The Renormalization Group (Formal)

In the previous section we noted that all critical properties can be obtained from the recursion relations in eqs.(III.32). Though conceptually appealing, it is not clear how such a procedure can be formally carried out. In particular, why should the forms of the two Hamiltonians be identical, and why are two parameters t and h sufficient to describe the transformation? In this section we outline a more formal procedure for identifying the effects of the dilation operation on the Hamiltonian. The various steps of the program are as follows:

(1) Start with most general Hamiltonian allowed by symmetries. For example, in the presence of rotational symmetry,

$$\beta\mathcal{H} = \int d^d\mathbf{x} \left[\frac{t}{2}m^2 + um^4 + vm^6 + \cdots + \frac{K}{2}(\nabla m)^2 + \frac{L}{2}(\nabla^2 m)^2 + \cdots \right]. \tag{III.41}$$

A particular system with such symmetry is therefore completely specified by a point in the (infinite–dimensional) parameter space $S \equiv (t, u, v, \cdots, K, L, \cdots)$.

(2) Apply the three steps of renormalization in configuration space: (i) Coarse grain by b; (ii) Rescale, $\mathbf{x}' = \mathbf{x}/b$; and (iii) Renormalize, $m' = m/\zeta$. This defines a change of variables,

$$m'(\mathbf{x}') = \frac{1}{\zeta b^d} \int_{\text{Cell of size } b \text{ centered at } b\mathbf{x}'} d^d\mathbf{x} m(\mathbf{x}). \tag{III.42}$$

Given the probabilities $\mathcal{P}[m(\mathbf{x})] \propto \exp(-\beta\mathcal{H}[m(\mathbf{x})])$, for the original configurations, we can use the above change of variable to construct the corresponding probabilities $\mathcal{P}'[m'(\mathbf{x}')]$, for the new configurations. Naturally this is the most difficult step in the program.

(3) Since rotational symmetry is preserved by the RG procedure, the rescaled Hamiltonian must also be described by a point in the parameter space of eq.(III.41), i.e.

$$\begin{aligned} &\beta\mathcal{H}'[m'(\mathbf{x}')] \equiv \ln \mathcal{P}[m'(\mathbf{x}')] \\ &= f_b + \int d^d\mathbf{x}' \left[\frac{t'}{2} m'^2 + u' m'^4 + v' m'^6 + \cdots + \frac{K'}{2} (\nabla m')^2 + \frac{L'}{2} (\nabla^2 m')^2 + \cdots \right]. \end{aligned} \tag{III.43}$$

The renormalized parameters are functions of the original ones, i.e. $t' = t_b(t, u, ...)$; $u' = u_b(t, u, ...)$, etc., defining a mapping $S' = \Re_b S$ in parameter space.

(4) The operation $\Re_b$ describes the effects of dilation on the Hamiltonian of the system. Hamiltonians that describe statistically self–similar configurations must thus correspond to *fixed points* S^*, such that $\Re_b S^* = S^*$. Since the correlation length, a function of Hamiltonian parameters, is reduced by b under the RG operation (i.e. $\xi(S) = b\xi(\Re_b S)$), the correlation length at a fixed point must be zero or infinity. Fixed points with $\xi^* = 0$ describe independent fluctuations at each point and correspond to complete disorder (infinite temperature), or complete order (zero temperature). A fixed point with $\xi^* = \infty$ describes a critical point ($T = T_c$).

(5) Eqs.(III.32) represent a simplified case in which the parameter space is two dimensional. The point $t = h = 0$ is a fixed point, and the lowest order terms in these equations describe the behavior in its neighborhood. In general, we can study the stability of a fixed point by *linearizing* the recursion relations in its vicinity: Under RG, a point $S^* + \delta S$ is transformed to

$$S^*_\alpha + \delta S'_\alpha = S^*_\alpha + (\Re^L_b)_{\alpha\beta} \delta S_\beta + \cdots, \qquad \text{where} \qquad (\Re^L_b)_{\alpha\beta} \equiv \left. \frac{\partial S'_\alpha}{\partial S_\beta} \right|_{S^*}. \tag{III.44}$$

We now diagonalize the matrix $(\Re_b^L)_{\alpha\beta}$ to get the eigenvectors $\mathcal{O}_i$, and corresponding eigenvalues $\lambda(b)_i$. Because of the group property[†],

$$\Re_b^L \Re_{b'}^L \mathcal{O}_i = \lambda(b)_i \lambda(b')_i \mathcal{O}_i = \Re_{bb'}^L \mathcal{O}_i = \lambda(bb')_i \mathcal{O}_i. \tag{III.45}$$

Together with the condition $\lambda(1)_i = 1$, the above equation implies

$$\lambda(b)_i = b^{y_i}. \tag{III.46}$$

The vectors $\mathcal{O}_i$ are called scaling directions associated with the fixed point S^*, and y_i are the corresponding *anomalous dimensions*. Any Hamiltonian in the vicinity of the fixed point is described by a point $S = S^* + \Sigma_i g_i \mathcal{O}_i$. The renormalized Hamiltonian has to interaction parameters $S' = S^* + \Sigma_i g_i b^{y_i} \mathcal{O}_i$. The following terminology is used to classify the eigen-operators:

- If $y_i > 0$, g_i *increases* under scaling, and $\mathcal{O}_i$ is a *relevant operator*.
- If $y_i < 0$, g_i *decreases* under scaling, and $\mathcal{O}_i$ is an *irrelevant operator*.
- If $y_i = 0$, g_i is called a *marginal operator*, and higher order terms are necessary to track its behavior.

The subspace spanned by the irrelevant operators is the *basin of attraction* of the fixed point S^*. Since ξ always decreases under RG, and $\xi(S^*) = \infty$; then ξ is also infinite for any point on the basin of attraction of S^*. For a general point in the vicinity of S^*, the correlation length satisfies

$$\xi(g_1, g_2, \cdots) = b\xi(b^{y_1} g_1, b^{y_2} g_2, \cdots). \tag{III.47}$$

For a sufficiently large b, all the irrelevant operators scale to zero. The leading singularities of ξ are then determined by the remaining set of *relevant* operators. In particular if the operators are indexed in order of decreasing dimensions, we can choose b such that $b^{y_1} g_1 = 1$. In this case, eq.(III.47) implies

$$\xi(g_1, g_2, \cdots) = g_1^{-1/y_1} f(g_2/g_1^{y_2/y_1}, \cdots). \tag{III.48}$$

[†] The group property $\Re_b^L \Re_{b'}^L = \Re_{bb'}^L = \Re_{b'}^L \Re_b^L$, also implies that the linearized matrices for different b commute. It is thus possible to diagonalize them simultaneously, implying that the eigenvectors $\{\mathcal{O}_i\}$ are independent of b.

We have thus obtained an exponent $\nu_1 = 1/y_1$, for the divergence of ξ, and a generalized set of gap exponents $\Delta_\alpha = y_\alpha/y_1$, associated with g_α.

Let us imagine that the fixed point S^* describes the critical point of the magnet in eq.(III.41) at zero magnetic field. As the temperature, or some other control parameter, is changed, the coefficients of the Hamiltonian are altered, and the point S moves along a trajectory in parameter space. Except for a single point (at the critical temperature) the magnet has a finite correlation length. This can be achieved if the trajectory taken by the point S intersects the basis of attraction of S^* only at one point. To achieve this, the basin of attraction must have co-dimension one, i.e. the fixed point S^* must have one and only one relevant operator. This provides an explanation of *universality*, in that the very many microscopic details of the system make up the huge space of irrelevant operators comprising the basin of attraction. In the presence of a magnetic field, two system parameters must be adjusted to reach the critical point ($T = T_c$ and $h = 0$). Thus the magnetic field corresponds to an additional relevant operator at S^*. Again, other 'odd' interactions, such as $\{m^3, m^5, \cdots\}$ should not lead to any other relevant operators.

Although the formal procedure outlined in this section is quite rigorous, it suffers from some quite obvious shortcomings: How do we actually implement the RG transformations of step (2) analytically? There are an infinite number of interactions allowed by symmetry, and hence the space of parameters S, is inconveniently large. How do we know a priori that there are fixed points for the RG transformation; that $\Re_b$ can be linearized; that relevant operators are few, etc.? Following the initial formulation of RG by Kadanoff, there was a period of uncertainty until Wilson showed how these steps can be implemented (at least perturbatively) in the Landau–Ginzburg model.

III.F The Gaussian Model (Direct solution)

The RG approach will be applied to the *Gaussian model* in the next section. For the sake of later comparison, here we provide the direct solution of this problem. The Gaussian model is obtained by keeping only the quadratic terms in the Landau–Ginzburg expansion. The resulting partition function is

$$Z = \int \mathcal{D}\vec{m}(\mathbf{x}) \exp\left\{ - \int d^d\mathbf{x} \left[\frac{t}{2} m^2 + \frac{K}{2} (\nabla m)^2 + \frac{L}{2} (\nabla^2 m)^2 + \cdots - \vec{h} \cdot \vec{m} \right] \right\}. \quad \text{(III.49)}$$

Clearly the model is well defined only for $t \geq 0$, since there is no m^4 term to insure its stability for $t < 0$. The partition function still has a singularity at $t = 0$, and we can regard this as representing approaching a phase transition from the disordered side.

The quadratic form is easily evaluated by the usual rules of Gaussian integration. The kernel is first diagonalized by the Fourier modes: The allowed $\mathbf{q}$ values are discretized in a finite system of size L, with spacing of $2\pi/L$. The largest $\mathbf{q}$ are limited by the lattice spacing, and confined to a *Brillouin Zone* whose shape is determined by the underlying lattice. We shall in fact use a slightly different normalization for the Fourier modes, and keep careful track of the volume factors, by setting

$$\begin{cases} \vec{m}(\mathbf{q}) = \int d^d\mathbf{x} e^{i\mathbf{q}\cdot\mathbf{x}} \vec{m}(\mathbf{x}) \\ \vec{m}(\mathbf{x}) = \sum_{\mathbf{q}} \dfrac{e^{-i\mathbf{q}\cdot\mathbf{x}}}{V} \vec{m}(\mathbf{q}) = \int \dfrac{d^d\mathbf{q}}{(2\pi)^d} e^{-i\mathbf{q}\cdot\mathbf{x}} \vec{m}(\mathbf{q}) \end{cases} . \quad \text{(III.50)}$$

(We should really use a different symbol, such as $\tilde{m}_i(\mathbf{q})$ to indicate the Fourier modes. For the sake of brevity we use the same symbol, but explicitly include the argument $\mathbf{q}$ as the indicator of the Frourier transformed function.) The last transformation applies to the infinite size limit ($L \to \infty$), and V is the system volume.

In reexpressing the Hamiltonian in terms of Fourier modes, we encounter expressions such as

$$\int d^d\mathbf{x} m(\mathbf{x})^2 = \int d^d\mathbf{x} \sum\nolimits_{\mathbf{q},\mathbf{q}'} \frac{e^{-i(\mathbf{q}+\mathbf{q}')\cdot\mathbf{x}}}{V^2} \vec{m}(\mathbf{q}) \cdot \vec{m}(\mathbf{q}') = \sum\nolimits_{\mathbf{q}} \frac{\vec{m}(\mathbf{q}) \cdot \vec{m}(-\mathbf{q})}{V}. \quad \text{(III.51)}$$

The last expression follows from the vanishing of the integral over $\mathbf{x}$ unless $\mathbf{q} + \mathbf{q}' = \mathbf{0}$, in which case it equals the system volume. Similar manipulations leads to the Hamiltonian

$$\beta\mathcal{H} = \sum_{\mathbf{q}} \left(\frac{t + Kq^2 + Lq^4 + \cdots}{2V} \right) |m(\mathbf{q})|^2 - \vec{h} \cdot \vec{m}(\mathbf{q} = \mathbf{0}). \quad \text{(III.52)}$$

With the choice of the normalization in eq.(III.50), the Jacobian of the transformation to Fourier modes is $1/\sqrt{V}$ per mode, and the partition function equals

$$Z = \prod_{\mathbf{q}} V^{-n/2} \int d\vec{m}(\mathbf{q}) \exp\left[-\frac{t + Kq^2 + Lq^4 + \cdots}{2V} |m(\mathbf{q})|^2 + \vec{h} \cdot \vec{m}(\mathbf{q} = 0) \right]. \quad \text{(III.53)}$$

The integral for $\mathbf{q} = \mathbf{0}$ is

$$Z_0 = V^{-n/2} \int_{-\infty}^{\infty} d\vec{m}(\mathbf{0}) \exp\left[-\frac{t}{2V} |m(\mathbf{0})|^2 + \vec{h} \cdot \vec{m}(\mathbf{0}) \right] = \left(\frac{2\pi}{t} \right)^{n/2} \exp\left[\frac{Vh^2}{2t} \right]. \quad \text{(III.54)}$$

After performing the integrations for $\mathbf{q} \neq \mathbf{0}$, we obtain

$$Z = \exp\left[\frac{Vh^2}{2t} \right] \prod_{\mathbf{q}} \left(\frac{2\pi}{t + Kq^2 + Lq^4 + \cdots} \right)^{n/2}. \quad \text{(III.55)}$$

The total number of modes N, equals the number of original lattice points. Apart from a constant factor resulting from $(2\pi)^{nN/2}$, the free energy is

$$f(t,h) = -\frac{\ln Z}{V} = \frac{n}{2} \int_{B.Z.} \frac{d^d\mathbf{q}}{(2\pi)^d} \ln\left(t + Kq^2 + Lq^4 + \cdots \right) - \frac{h^2}{2t}. \quad \text{(III.56)}$$

The integral in eq.(III.56) is over the Brillouin zone, which for a hypercubic lattice of spacing a, is a cube of side $2\pi/a$ centered on the origin. However, we expect the singularities to originate from the long wavelength modes close to $\mathbf{q} = \mathbf{0}$. The contributions from the vicinity of the Brillouin zone edge are clearly analytic, since the logarithm can be simply expanded in powers of t for a finite q^2. Thus to simplify the extraction of the singular behavior as $t \to 0$, we approximate the shape of the Brillouin zone by a hypershpere of radius $\Lambda \approx \pi/a$. The spherical symmetry of the integrand then allows us to write

$$f_{\text{sing.}}(t,h) = \frac{n}{2} K_d \int_0^{\Lambda} dq q^{d-1} \ln\left(t + Kq^2 + Lq^4 + \cdots \right) - \frac{h^2}{2t}, \quad \text{(III.57)}$$

where $K_d \equiv S_d/(2\pi)^d$, and S_d is the d-dimensional solid angle. The leading dependence of the integral on t can be extracted after rescaling q by a factor of $\sqrt{t/K}$, to

$$f_{\text{sing.}}(t,h) = \frac{n}{2} K_d \left(\frac{t}{K} \right)^{d/2} \int_0^{\Lambda\sqrt{K}/\sqrt{t}} dx x^{d-1} \left[\ln t + \ln\left(1 + x^2 + Ltx^4/K^2 + \cdots \right) \right] - \frac{h^2}{2t}. \quad \text{(III.58)}$$

Ignoring analytic contributions in t, the leading singular dependence of the free energy can be written as

$$f_{\rm sing.}(t,h) = -t^{d/2}\left[A + \frac{h^2}{2t^{1+d/2}}\right] \equiv t^{2-\alpha} g_f(h/t^{\Delta}). \tag{III.59}$$

Note that the higher order gradients, i.e. terms proportional to $L, \cdots$, do not effect the singular behavior in eq.(III.59). On approaching the point $h = 0$ for $t = 0^+$, the singular part of the free energy is described by a homogeneous scaling form, with exponents

$$\alpha_+ = 2 - d/2 \qquad , \qquad \Delta = 1/2 + d/4. \tag{III.60}$$

Since the ordered phase for $t < 0$ is not stable, the exponent β is undefined. The susceptibility $\chi \propto \partial^2 f/\partial h^2 \propto 1/t$, however, diverges with the exponent $\gamma_+ = 1$.

III.G The Gaussian Model (Renormalization Group)

The RG of the Gaussian model is most conveniently performed in terms of the Fourier modes. The goal is to evaluate the partition function

$$Z \sim \int \mathcal{D}\vec{m}(\mathbf{q}) \exp\left[-\int_0^{\Lambda} \frac{d^d\mathbf{q}}{(2\pi)^d}\left(\frac{t + Kq^2 + Lq^4 + \cdots}{2}\right)|m(\mathbf{q})|^2 + \vec{h}\cdot\vec{m}(\mathbf{0})\right], \tag{III.61}$$

indirectly via the three steps of RG. Note that the Brillouin zone is approximated by a hypersphere of radius Λ.

1. *Coarse-Grain:* Eliminating fluctuations at scales $a < x < ba$; is similar to removing Fourier modes with wavenumbers $\Lambda/b < q < \Lambda$. We thus break up the momenta into two subsets,

$$\{\vec{m}(\mathbf{q})\} = \{\vec{\sigma}(\mathbf{q}^>)\} \oplus \{\tilde{\vec{m}}(\mathbf{q}^<)\}, \tag{III.62}$$

and write

$$Z = \int \mathcal{D}\tilde{\vec{m}}(\mathbf{q}^<) \int \mathcal{D}\vec{\sigma}(\mathbf{q}^>) e^{-\beta\mathcal{H}[\tilde{\vec{m}},\vec{\sigma}]}. \tag{III.63}$$

Since the two sets of modes are decoupled in the Gaussian model, the integration is trivial, and

$$\begin{aligned} Z \sim & \exp\left[-\frac{n}{2}V\int_{\Lambda/b}^{\Lambda}\frac{d^d\mathbf{q}}{(2\pi)^d}\ln(t + Kq^2 + Lq^4 + \cdots)\right] \times \\ & \int \mathcal{D}\tilde{\vec{m}}(\mathbf{q}^<) \exp\left[-\int_0^{\Lambda/b}\frac{d^d\mathbf{q}}{(2\pi)^d}\left(\frac{t + Kq^2 + Lq^4 + \cdots}{2}\right)|\tilde{m}(\mathbf{q})|^2 + \vec{h}\cdot\tilde{\vec{m}}(\mathbf{0})\right]. \end{aligned} \tag{III.64}$$

2. *Rescale:* The partition function for the modes $\tilde{\vec{m}}(\mathbf{q}^<)$ is similar to the original, except that the upper cut–off has decreased to Λ/b, reflecting the coarsening in resolution. The rescaling $\mathbf{x}' = \mathbf{x}/b$ in real space, is equivalent to $\mathbf{q}' = b\mathbf{q}$ in *momentum space*, and restores the cut-off to its original value. The rescaled partition function is

$$Z = e^{-V\delta f_b(t)} \times \int \mathcal{D}\tilde{\vec{m}}(\mathbf{q}') \exp\left[- \int_0^\Lambda \frac{d^d\mathbf{q}'}{(2\pi)^d} b^{-d} \left(\frac{t + Kb^{-2}q'^2 + Lb^{-4}q'^4 + \cdots}{2} \right) |\tilde{m}(\mathbf{q}')|^2 + \vec{h} \cdot \tilde{\vec{m}}(\mathbf{0}) \right] . \tag{III.65}$$

3. *Renormalize:* The final step of RG in real space is the renormalization of magnetization, $\vec{m}'(\mathbf{x}') = \tilde{\vec{m}}(\mathbf{x}')/\zeta$. Alternatively, we can renormalize the Fourier modes according to $\vec{m}'(\mathbf{q}') = \tilde{\vec{m}}(\mathbf{q}')/z$, resulting in

$$Z = e^{-V\delta f_b(t)} \times \int \mathcal{D}\vec{m}'(\mathbf{q}') \exp\left[- \int_0^\Lambda \frac{d^d\mathbf{q}'}{(2\pi)^d} b^{-d} z^2 \left(\frac{t + Kb^{-2}q'^2 + Lb^{-4}q'^4 + \cdots}{2} \right) |m'(\mathbf{q}')|^2 + z\vec{h} \cdot \vec{m}'(\mathbf{0}) \right] . \tag{III.66}$$

(Note that the factors ζ and z, for rescalings of magnetization in real and Fourier space, are different.)

Eq.(III.66) indicates the renormalized modes are distributed according to a Gaussian Hamiltonian, with renormalized parameters,

$$\begin{cases} t' = z^2 b^{-d} t \\ h' = zh \\ K' = z^2 b^{-d-2} K \\ L' = z^2 b^{-d-4} L \\ \quad \cdots \end{cases} . \tag{III.67}$$

The singular point $t = h = 0$ is mapped onto itself as expected. To make the fluctuations scale invariant at this point, we must ensure that the remaining Hamiltonian, stays fixed. This is achieved by the choice of $z = b^{1+d/2}$, which sets $K' = K$, and makes the remaining parameters $L, \cdots$ scale to zero. Away from criticality, the two relevant directions now scale as

$$\begin{cases} t' = b^2 t \\ h' = b^{1+d/2} h \end{cases} , \quad \Longrightarrow \quad \begin{cases} y_t = 2 \\ y_h = 1 + d/2 \end{cases} . \tag{III.68}$$

Using the results of sec.(III.D), we can identify the critical exponents,

$$\nu = 1/y_t = 1/2,$$

$$\Delta = \frac{y_h}{y_t} = \frac{1+d/2}{2} = \frac{1}{2} + \frac{d}{4},$$

$$\alpha = 2 - d\nu = 2 - d/2,$$

in agreement with the direct solution in the previous section.

The fixed point Hamiltonian ($t^* = h^* = L^* = \cdots = 0$), in *real space* is

$$\beta\mathcal{H}^* = \frac{K}{2}\int_a d^d\mathbf{x}(\nabla m)^2. \tag{III.69}$$

(The subscript a is placed on the integral as a reminder of the implicit short distance cut–off.) Under a simple rescaling $\mathbf{x} \mapsto \mathbf{x}'$, and $\vec{m}(\mathbf{x}) \mapsto \zeta\vec{m}'(\mathbf{x}')$; $K \mapsto K' = b^{d-2}\zeta^2 K$. Scale invariance is achieved with the choice $\zeta = b^{1-d/2}$. Forgetting the coarse–graining step, a general power of $\vec{m}(\mathbf{x})$, added as a small perturbation to $(\beta\mathcal{H})^*$, behaves as

$$\beta\mathcal{H}^* + u_n\int d^d\mathbf{x} m^n \quad \mapsto \quad \beta\mathcal{H}^* + u_n b^d\zeta^n\int d^d\mathbf{x}' m'^n, \tag{III.70}$$

suggesting that such perturbations scale as

$$u_n' = b^d b^{n(\frac{2-d}{2})}u_n, \quad \Longrightarrow \quad y_n = n - d\left(\frac{n}{2} - 1\right). \tag{III.71}$$

The values $y_1 = 1 + d/2$, and $y_2 = 2$, reproduce the exponents for y_h and y_t in eq.(III.68). The operators with higher powers are less relevant. The next most important operator in a system with spherical symmetry is $y_4 = 4 - d$, which is irrelevant for $d > 4$ but relevant for $d < 4$; $y_6 = 6 - 2d$ is relevant only for $d < 3$. Indeed the majority of operators are irrelevant at the Gaussian fixed point for $d > 2$.

IV. Perturbative Renormalization Group

IV.A Expectation Values in the Gaussian Model

Can we treat the Landau–Ginzburg Hamiltonian, as a perturbation to the Gaussian model? In particular, for zero magnetic field, we shall examine

$$\beta\mathcal{H} = \beta\mathcal{H}_0 + \mathcal{U} \equiv \int d^d\mathbf{x} \left[\frac{t}{2} m^2 + \frac{K}{2}(\nabla m)^2 + \frac{L}{2}(\nabla^2 m)^2 + \cdots \right] + u \int d^d\mathbf{x} m^4 + \cdots . \quad \text{(IV.1)}$$

The *unperturbed* Gaussian Hamiltonian can be decomposed into independent Fourier modes, as

$$\beta\mathcal{H}_0 = \frac{1}{V} \sum_{\mathbf{q}} \frac{t + Kq^2 + Lq^4 + \cdots}{2} |m(\mathbf{q})|^2 \equiv \int \frac{d^d\mathbf{q}}{(2\pi)^d} \frac{t + Kq^2 + Lq^4 + \cdots}{2} |m(\mathbf{q})|^2 . \quad \text{(IV.2)}$$

The *interaction* mixes up the normal modes, and

$$\begin{aligned} \mathcal{U} &= u \int d^d\mathbf{x} m(\mathbf{x})^4 + \cdots \\ &= u \int d^d\mathbf{x} \int \frac{d^d\mathbf{q}_1 d^d\mathbf{q}_2 d^d\mathbf{q}_3 d^d\mathbf{q}_4}{(2\pi)^{4d}} e^{-i\mathbf{x}\cdot(\mathbf{q}_1+\mathbf{q}_2+\mathbf{q}_3+\mathbf{q}_4)} m_\alpha(\mathbf{q}_1) m_\alpha(\mathbf{q}_2) m_\beta(\mathbf{q}_3) m_\beta(\mathbf{q}_4) \\ &\quad + \cdots , \end{aligned} \quad \text{(IV.3)}$$

where summation over α and β is implicit. The integral over $\mathbf{x}$ sets $\mathbf{q}_1 + \mathbf{q}_2 + \mathbf{q}_3 + \mathbf{q}_4 = \mathbf{0}$, and

$$\mathcal{U} = u \int \frac{d^d\mathbf{q}_1 d^d\mathbf{q}_2 d^d\mathbf{q}_3}{(2\pi)^{3d}} m_\alpha(\mathbf{q}_1) m_\alpha(\mathbf{q}_2) m_\beta(\mathbf{q}_3) m_\beta(-\mathbf{q}_1 - \mathbf{q}_2 - \mathbf{q}_3) + \cdots . \quad \text{(IV.4)}$$

From the variance of the Gaussian weights, the two–point expectation values in a finite sized system with discretized modes are easily obtained as

$$\langle m_\alpha(\mathbf{q})\, m_\beta(\mathbf{q}') \rangle_0 = \frac{\delta_{\mathbf{q},-\mathbf{q}'}\, \delta_{\alpha,\beta}\, V}{t + Kq^2 + Lq^4 + \cdots} . \quad \text{(IV.5)}$$

In the limit of infinite size, the spectrum becomes continuous, and eq.(IV.5) goes over to

$$\langle m_\alpha(\mathbf{q})\, m_\beta(\mathbf{q}') \rangle_0 = \frac{\delta_{\alpha,\beta} (2\pi)^d \delta^d(\mathbf{q} + \mathbf{q}')}{t + Kq^2 + Lq^4 + \cdots} . \quad \text{(IV.6)}$$

The subscript 0 is used to indicate that the expectation values are taken with respect to the unperturbed (Gaussian) Hamiltonian. Expectation values involving any product of m's can be obtained starting from the identity

$$\left\langle \exp\left[\sum_i a_i m_i\right]\right\rangle_0 = \exp\left[\sum_{i,j}\frac{a_i a_j}{2}\langle m_i m_j\rangle_0\right], \tag{IV.7}$$

which is valid for any set of Gaussian distributed variables $\{m_i\}$. (This is easily seen by 'completing the square.') Expanding both sides of the equation in powers of $\{a_i\}$ leads to

$$\begin{aligned}&1 + a_i\langle m_i\rangle_0 + \frac{a_i a_j}{2}\langle m_i m_j\rangle_0 + \frac{a_i a_j a_k}{6}\langle m_i m_j m_k\rangle_0 + \frac{a_i a_j a_k a_l}{24}\langle m_i m_j m_k m_k\rangle_0 + \cdots = \\ &1 + \frac{a_i a_j}{2}\langle m_i m_j\rangle_0 + \frac{a_i a_j a_k a_l}{24}\left(\langle m_i m_j\rangle_0\langle m_k m_l\rangle_0 + \langle m_i m_k\rangle_0\langle m_j m_l\rangle_0 + \langle m_i m_k\rangle_0\langle m_j m_l\rangle_0\right) \\ &\quad + \cdots.\end{aligned} \tag{IV.8}$$

Matching powers of $\{a_i\}$ on the two sides of the above equation gives

$$\left\langle \prod_{i=1}^{\ell} m_i\right\rangle_0 = \begin{cases} 0 & \text{for } \ell \text{ odd} \\ \text{sum over all pairwise contractions} & \text{for } \ell \text{ even}\end{cases}. \tag{IV.9}$$

This result is known as *Wick's theorem*; and for example,

$$\langle m_i m_j m_k m_l\rangle_0 = \langle m_i m_j\rangle_0\langle m_k m_l\rangle_0 + \langle m_i m_k\rangle_0\langle m_j m_l\rangle_0 + \langle m_i m_k\rangle_0\langle m_j m_l\rangle_0\,.$$

IV.B Expectation values in Perturbation Theory

In the presence of an interaction $\mathcal{U}$, the expectation value of any operator $\mathcal{O}$, is computed perturbatively as follows:

$$\begin{aligned}\langle\mathcal{O}\rangle =& \frac{\int \mathcal{D}\vec{m}\,\mathcal{O}e^{-\beta\mathcal{H}_0-\mathcal{U}}}{\int \mathcal{D}\vec{m}\,e^{-\beta\mathcal{H}_0-\mathcal{U}}} = \frac{\int \mathcal{D}\vec{m}\,e^{-\beta\mathcal{H}_0}\mathcal{O}[1-\mathcal{U}+\mathcal{U}^2/2-\cdots]}{\int \mathcal{D}\vec{m}\,e^{-\beta\mathcal{H}_0}[1-\mathcal{U}+\mathcal{U}^2/2-\cdots]} \\ =& \frac{Z_0[\langle\mathcal{O}\rangle_0 - \langle\mathcal{O}\mathcal{U}\rangle_0 + \langle\mathcal{O}\mathcal{U}^2\rangle_0/2-\cdots]}{Z_0[1-\langle\mathcal{U}\rangle_0+\langle\mathcal{U}^2\rangle_0/2-\cdots]}.\end{aligned} \tag{IV.10}$$

Inverting the denominator by an expansion in powers of $\mathcal{U}$ gives

$$\begin{aligned}\langle\mathcal{O}\rangle =& \left[\langle\mathcal{O}\rangle_0 - \langle\mathcal{O}\mathcal{U}\rangle_0 + \frac{1}{2}\langle\mathcal{O}\mathcal{U}^2\rangle_0 - \cdots\right]\left[1+\langle\mathcal{U}\rangle_0 + \langle\mathcal{U}\rangle_0^2 - \frac{1}{2}\langle\mathcal{U}^2\rangle_0 - \cdots\right] \\ =& \langle\mathcal{O}\rangle_0 - \left(\langle\mathcal{O}\mathcal{U}\rangle_0 - \langle\mathcal{O}\rangle_0\langle\mathcal{U}\rangle_0\right) + \frac{1}{2}\left(\langle\mathcal{O}\mathcal{U}^2\rangle_0 - 2\langle\mathcal{O}\mathcal{U}\rangle_0\langle\mathcal{U}\rangle_0 + 2\langle\mathcal{O}\rangle_0\langle\mathcal{U}\rangle_0^2 - \langle\mathcal{O}\rangle_0\langle\mathcal{U}^2\rangle_0\right) \\ &+ \cdots \equiv \sum_{n=0}^{\infty}\frac{(-1)^n}{n!}\langle\mathcal{O}\mathcal{U}^n\rangle_0^c\,.\end{aligned} \tag{IV.11}$$

The *connected averages* are defined as the combination of unperturbed expectation values appearing at various orders in the expansion. Their significance will become apparent in diagrammatic representations, and from the following example.

Let us calculate the two point correlation function of the Landau–Ginzburg model to first order in the parameter u. [In view of their expected irrelevance, we shall ignore higher order interactions, and also only keep the lowest order Gaussian terms.] Substituting eq.(IV.4) into eq.(IV.11) yields

$$\begin{aligned}\langle m_\alpha(\mathbf{q})\, m_\beta(\mathbf{q}')\rangle = \langle m_\alpha(\mathbf{q})\, m_\beta(\mathbf{q}')\rangle_0 - u \int \frac{d^d\mathbf{q}_1 d^d\mathbf{q}_2 d^d\mathbf{q}_3}{(2\pi)^{3d}} \\ [\langle m_\alpha(\mathbf{q})\, m_\beta(\mathbf{q}') m_i(\mathbf{q}_1) m_i(\mathbf{q}_2) m_j(\mathbf{q}_3) m_j(-\mathbf{q}_1-\mathbf{q}_2-\mathbf{q}_3)\rangle_0 - \\ \langle m_\alpha(\mathbf{q})\, m_\beta(\mathbf{q}')\rangle_0 \langle m_i(\mathbf{q}_1) m_i(\mathbf{q}_2) m_j(\mathbf{q}_3) m_j(-\mathbf{q}_1-\mathbf{q}_2-\mathbf{q}_3)\rangle_0] + \mathcal{O}(u^2).\end{aligned} \tag{IV.12}$$

To calculate $\langle \mathcal{O}\mathcal{U}\rangle_0$ we need the unperturbed expectation value of the product of six m's. This can be evaluated using eq.(IV.9) as the sum of all pair-wise contractions, 15 in all. Three contractions are obtained by first pairing m_α to m_β, and then the remaining four m's in $\mathcal{U}$. Clearly these contractions cancel exactly with corresponding ones in $\langle\mathcal{O}\rangle_0\langle\mathcal{U}\rangle_0$. The only surviving terms involve contractions that connect $\mathcal{O}$ to $\mathcal{U}$. This cancellation persists at all orders, and $\langle \mathcal{O}\mathcal{U}^n\rangle_0^c$ contains only terms in which all $n+1$ operators are connected by contractions. The remaining 12 pairings in $\langle\mathcal{O}\mathcal{U}\rangle_0$ fall into two classes:

(i) 4 pairings involve contracting m_α and m_β to m's with the same index, e.g.

$$\begin{aligned}\langle m_\alpha(\mathbf{q})\, m_i(\mathbf{q}_1)\rangle_0 \langle m_\beta(\mathbf{q}')\, m_i(\mathbf{q}_2)\rangle_0 \langle m_j(\mathbf{q}_3)\, m_j(-\mathbf{q}_1-\mathbf{q}_2-\mathbf{q}_3)\rangle_0 \\ = \frac{\delta_{\alpha i}\,\delta_{\beta i}\,\delta_{jj}\,(2\pi)^{3d}\,\delta^d(\mathbf{q}+\mathbf{q}_1)\,\delta^d(\mathbf{q}'+\mathbf{q}_2)\,\delta^d(\mathbf{q}_1+\mathbf{q}_2)}{(t+Kq^2)\,(t+Kq'^2)\,(t+Kq_3^2)},\end{aligned} \tag{IV.13}$$

where we have used eq.(IV.6). After summing over i and j, and integrating over $\mathbf{q}_1$, $\mathbf{q}_2$, and $\mathbf{q}_3$, such terms make a contribution

$$-4u \frac{n\delta_{\alpha\beta}\,(2\pi)^d\,\delta^d\,(\mathbf{q}+\mathbf{q}')}{(t+Kq^2)^2} \int \frac{d^d\mathbf{q}_3}{(2\pi)^d} \frac{1}{t+Kq_3^2}. \tag{IV.14}$$

(ii) 8 pairings involve contracting m_α and m_β to m's with different indices, e.g.

$$\begin{aligned}\langle m_\alpha(\mathbf{q})\, m_i(\mathbf{q}_1)\rangle_0 \langle m_\beta(\mathbf{q}')\, m_j(\mathbf{q}_3)\rangle_0 \langle m_i(\mathbf{q}_2)\, m_j(-\mathbf{q}_1-\mathbf{q}_2-\mathbf{q}_3)\rangle_0 \\ = \frac{\delta_{\alpha i}\,\delta_{\beta j}\,\delta_{ij}\,(2\pi)^{3d}\,\delta^d(\mathbf{q}+\mathbf{q}_1)\,\delta^d(\mathbf{q}'+\mathbf{q}_3)\,\delta^d(\mathbf{q}_1+\mathbf{q}_3)}{(t+Kq^2)\,(t+Kq'^2)\,(t+Kq_2^2)}.\end{aligned} \tag{IV.15}$$

Summing over all indices, and integrating over the momenta leads to an overall contribution of

$$-8u \frac{\delta_{\alpha\beta}\,(2\pi)^d\,\delta^d\,(\mathbf{q}+\mathbf{q}')}{(t+Kq^2)^2} \int \frac{d^d\mathbf{q}_2}{(2\pi)^d} \frac{1}{t+Kq_2^2}. \tag{IV.16}$$

Adding up both contributions, we obtain

$$\langle m_\alpha(\mathbf{q})\, m_\beta(\mathbf{q}')\rangle = \frac{\delta_{\alpha\beta}\,(2\pi)^d\,\delta^d\,(\mathbf{q}+\mathbf{q}')}{t+Kq^2} \left[1 - \frac{4u(n+2)}{t+Kq^2} \int \frac{d^d\mathbf{k}}{(2\pi)^d} \frac{1}{t+Kk^2} + \mathcal{O}(u^2)\right]. \tag{IV.17}$$

IV.C Diagrammatic Representation of Perturbation Theory

The calculations become more involved at higher orders in perturbation theory. A diagrammatic representation can be introduced to help keep track of all possible contractions. To calculate the ℓ–point expectation value $\langle \prod_{i=1}^{\ell} m_{\alpha_i}(\mathbf{q}_i) \rangle$, at $p^{\rm th}$ order in u, proceed according to the following rules:

(1) Draw ℓ *external points* labelled by $(\mathbf{q}_i, \alpha_i)$ corresponding to the coordinates of the required correlation function. Draw p *vertices* with 4 legs each, labelled by *internal* momenta and indices, e.g. $\{(\mathbf{k}_1, i), (\mathbf{k}_2, i), (\mathbf{k}_3, j), (\mathbf{k}_4, j)\}$. Since the four legs are not equivalent, the four point vertex is indicated by two solid branches joined by a dotted line. (The extension to higher order interactions is straightforward.)

(2) Each point of the graph now corresponds to one factor of $m_{\alpha_i}(\mathbf{q}_i)$, and the unperturbed average of the product is computed by Wick's theorem. This is implemented by joining all external and internal points *pairwise*, by lines connecting one point to another, in all topologically distinct ways (see #5 below).

(3) The algebraic value of each such graph is obtained as follows: **(i)** A line joining a pair of points represents the two point average[†]; e.g. a connection $(\mathbf{q}, \alpha) \longleftrightarrow (\mathbf{q}', \beta)$, contributes $\delta_{\alpha\alpha'}(2\pi)^d \delta^d(\mathbf{q} + \mathbf{q}')/(t + Kq^2)$; **(ii)** A vertex is represented by a term such as $u(2\pi)^d \delta^d(\mathbf{k}_1 + \mathbf{k}_2 + \mathbf{k}_3 + \mathbf{k}_4)$ (the delta-function insures that momentum is conserved).

(4) Integrate over the $4p$ internal momenta $\{\mathbf{k}_i\}$, and sum over the $2p$ internal indices. Note that each closed loop produces a factor of $\delta_{ii} = n$ at this stage.

(5) There is a numerical factor of

$$\frac{(-1)^p}{p!} \times \text{number of different pairings leading to the same topology.}$$

The first contribution comes from the expansion of the exponential; the second merely states that graphs related by symmetry give the same result, and can be calculated once.

(6) When calculating cumulants, only fully connected diagrams (without disjoint pieces) need to be included. This is a tremendous simplification.

[†] Because of its original formulation in quantum field theory, the line joining two points is usually called a *propagator*. In this context, the line represents the world-line of a particle in time, while the perturbation $\mathcal{U}$ is an 'interaction' between particles. For the same reason, the Fourier index is called a 'momentum.'

IV.D Susceptibility

It is no accident that the correction term in eq.(IV.17) is similar in form to the unperturbed value. This is because the form of the two point correlation function is constrained by symmetries, as can be seen from

$$\langle m_\alpha(\mathbf{q})\, m_\beta(\mathbf{q}')\rangle = \int d^d\mathbf{x} \int d^d\mathbf{x}' e^{i\mathbf{q}\cdot\mathbf{x}+i\mathbf{q}'\cdot\mathbf{x}'} \langle m_\alpha(\mathbf{x})\, m_\beta(\mathbf{x}')\rangle. \tag{IV.18}$$

The two point correlation function in real space must satisfy translation and rotation symmetry (in the high temperature phase), and $\langle m_\alpha(\mathbf{x})\, m_\beta(\mathbf{x}')\rangle = \delta_{\alpha\beta}\langle m_1(\mathbf{x}-\mathbf{x}')\, m_1(\mathbf{0})\rangle$. Transforming to center of mass and relative coordinates, the above integral becomes,

$$\begin{aligned}
&\langle m_\alpha(\mathbf{q})\, m_\beta(\mathbf{q}')\rangle = \\
&\int d^d\left(\frac{\mathbf{x}+\mathbf{x}'}{2}\right) d^d\left(\mathbf{x}-\mathbf{x}'\right) e^{i(\mathbf{q}+\mathbf{q}')\cdot(\mathbf{x}+\mathbf{x}')/2} e^{i(\mathbf{x}-\mathbf{x}')\cdot(\mathbf{q}-\mathbf{q}')/2} \delta_{\alpha\beta}\langle m_1(\mathbf{x}-\mathbf{x}')\, m_1(\mathbf{0})\rangle \\
&\qquad\qquad \equiv (2\pi)^d \delta^d(\mathbf{q}+\mathbf{q}')\delta_{\alpha\beta} S(q),
\end{aligned} \tag{IV.19}$$

where

$$S(q) = \left\langle |m_1(\mathbf{q})|^2 \right\rangle = \int d^d\mathbf{x} e^{i\mathbf{q}\cdot\mathbf{x}} \langle m_1(\mathbf{x}-\mathbf{x}')\, m_1(\mathbf{0})\rangle, \tag{IV.20}$$

is the quantity observed in scattering experiments (sec.II.D).

From eq.(IV.17) we obtain

$$S(q) = \frac{1}{t+Kq^2}\left[1 - \frac{4u\,(n+2)}{t+Kq^2}\int \frac{d^d\mathbf{k}}{(2\pi)^d}\frac{1}{t+Kk^2} + \mathcal{O}(u^2)\right]. \tag{IV.21}$$

It is useful to examine the expansion of the inverse quantity

$$S(q)^{-1} = t + Kq^2 + 4u(n+2)\int \frac{d^d\mathbf{k}}{(2\pi)^d}\frac{1}{t+Kk^2} + \mathcal{O}(u^2). \tag{IV.22}$$

In the high temperature phase, eq.(IV.20) indicates that the $q \to 0$ limit of S(q) is just the magnetic susceptibility χ. For this reason, $S(q)$ is sometimes denoted by $\chi(q)$. From eq.(IV.22), the inverse susceptibility is given by

$$\chi^{-1}(t) = t + 4u(n+2)\int \frac{d^d\mathbf{k}}{(2\pi)^d}\frac{1}{t+Kk^2} + \mathcal{O}(u^2). \tag{IV.23}$$

The susceptibility no longer diverges at $t = 0$, since

$$\chi^{-1}(0) = 4u(n+2)\int \frac{d^d\mathbf{k}}{(2\pi)^d}\frac{1}{Kk^2} = \frac{4(n+2)u}{K}\frac{S_d}{(2\pi)^d}\int_0^\Lambda dk\, k^{d-3} = \frac{4(n+2)u}{K}K_d\left(\frac{\Lambda^{d-2}}{d-2}\right), \tag{IV.24}$$

is a finite number. This is because in the presence of u the critical temperature is reduced to a negative value. The modified critical point is obtained by requiring $\chi^{-1}(t_c) = 0$, and hence from eq.(IV.23), to order of u,

$$t_c = -4u(n+2)\int \frac{d^d\mathbf{k}}{(2\pi)^d}\frac{1}{t_c + Kk^2} \approx -\frac{4u(n+2)K_d\Lambda^{d-2}}{(d-2)K} < 0. \tag{IV.25}$$

How does the perturbed susceptibility diverge at the shifted critical point? From eq.(IV.23),

$$\begin{aligned}\chi^{-1}(t) - \chi^{-1}(t_c) &= t - t_c + 4u(n+2)\int \frac{d^d\mathbf{k}}{(2\pi)^d}\left(\frac{1}{t+Kk^2} - \frac{1}{t_c+Kk^2}\right) \\ &= (t-t_c)\left[1 - \frac{4u(n+2)}{K^2}\int \frac{d^d\mathbf{k}}{(2\pi)^d}\frac{1}{k^2(k^2+(t-t_c)/K)} + \mathcal{O}(u^2)\right].\end{aligned} \tag{IV.26}$$

(In going from the first equation to the second, we have changed the position of t_c from one denominator to another. Since $t_c = \mathcal{O}(u)$, the corrections to such change only appear at $\mathcal{O}(u^2)$.) The final integral has dimensions of $\left[k^{d-4}\right]$. For $d > 4$ it is dominated by the largest momenta and scales as $K_d\Lambda^{d-4}$. For $2 < d < 4$, the integral is convergent at both limits. Its magnitude is therefore set by the momentum scale $\xi^{-1} = \sqrt{(t-t_c)/K}$, which can be used to make the integrand dimensionless. Hence, in these dimensions,

$$\chi^{-1}(t) = (t-t_c)\left[1 - \frac{4u(n+2)}{K^2}c\left(\frac{K}{t-t_c}\right)^{2-d/2} + \mathcal{O}(u^2)\right], \tag{IV.27}$$

where c is a constant. For $d < 4$, the correction term at the order of u diverges at the phase transition, masking the unperturbed singularity of χ with $\gamma = 1$. Thus the perturbation series is inherently inapplicable for describing the divergence of susceptibility in $d < 4$. The same situation applies in calculating any other quantity perturbatively. Although, we start by treating u as the perturbation parameter, it is important to realize that it is not dimensionless; u/K^2 has dimensions of (length)$^{d-4}$. The perturbation series for any quantity then takes the form $X(t,u) = X_0(t)[1 + f(ua^{4-d}/K^2, u\xi^{4-d}/K^2)]$, where f is a power series. The two length scales a and ξ are available to construct dimensionless variables. Since ξ diverges close to the critical point, there is an inherent failure of the perturbation series. The effective (dimensionless) perturbation parameter diverges at t_c and is not small.

IV.E Perturbative RG (First Order)

The last section demonstrated how various expectation values associated with the Landau–Ginzburg Hamiltonian can be calculated perturbatively in powers of u. However, the perturbative series is inherently divergent close to the critical point and cannot be used to characterize critical behavior in dimensions $d \leq 4$. Wilson showed that it is possible to combine perturbative and renormalization group approaches into a systematic method for calculating critical exponents. Accordingly, we shall extend the RG calculation of Gaussian model in sec.III.G to the Landau–Ginzburg Hamiltonian, by treating $\mathcal{U} = u \int d^d\mathbf{x} m^4$ as a perturbation.

1. *Coarse Grain:* This is the most difficult step of the RG procedure. As before, subdivide the fluctuations into two components as,

$$\vec{m}(\mathbf{q}) = \begin{cases} \tilde{\vec{m}}(\mathbf{q}) & \text{for } 0 < q < \Lambda/b \\ \\ \vec{\sigma}(\mathbf{q}) & \text{for } \Lambda/b < q < \Lambda \end{cases} . \tag{IV.28}$$

In the partition function,

$$Z = \int \mathcal{D}\tilde{\vec{m}}(\mathbf{q}) \mathcal{D}\vec{\sigma}(\mathbf{q}) \exp\left\{ - \int_0^\Lambda \frac{d^d\mathbf{q}}{(2\pi)^d} \left(\frac{t + Kq^2}{2} \right) \left(|\tilde{m}(\mathbf{q})|^2 + |\sigma(\mathbf{q})|^2 \right) - \mathcal{U}[\tilde{\vec{m}}(\mathbf{q}), \vec{\sigma}(\mathbf{q})] \right\}, \tag{IV.29}$$

the two sets of modes are mixed by the operator $\mathcal{U}$. Formally, the result of integrating out $\{\vec{\sigma}(\mathbf{q})\}$ can be written as

$$\begin{aligned} Z = & \int \mathcal{D}\tilde{\vec{m}}(\mathbf{q}) \exp\left\{ - \int_0^{\Lambda/b} \frac{d^d\mathbf{q}}{(2\pi)^d} \left(\frac{t + Kq^2}{2} \right) |\tilde{m}(\mathbf{q})|^2 \right\} \times \\ & \exp\left\{ - \frac{nV}{2} \int_{\Lambda/b}^\Lambda \frac{d^d\mathbf{q}}{(2\pi)^d} \ln\left(t + Kq^2 \right) \right\} \left\langle e^{-\mathcal{U}[\tilde{m}, \vec{\sigma}]} \right\rangle_\sigma \equiv \int \mathcal{D}\tilde{\vec{m}}(\mathbf{q}) e^{-\beta \tilde{\mathcal{H}}[\tilde{m}]}. \end{aligned} \tag{IV.30}$$

Here we have defined the partial averages

$$\langle \mathcal{O} \rangle_\sigma \equiv \int \frac{\mathcal{D}\vec{\sigma}(\mathbf{q})}{Z_\sigma} \mathcal{O} \exp\left[- \int_{\Lambda/b}^\Lambda \frac{d^d\mathbf{q}}{(2\pi)^d} \left(\frac{t + Kq^2}{2} \right) |\sigma(\mathbf{q})|^2 \right], \tag{IV.31}$$

with $Z_\sigma = \int \mathcal{D}\vec{\sigma}(\mathbf{q}) \exp\{-\beta \mathcal{H}_0[\vec{\sigma}]\}$, being the *Gaussian* partition function associated with the short wavelength fluctuations. From eq.(IV.30), we obtain

$$\beta \tilde{\mathcal{H}}[\tilde{\vec{m}}] = V \delta f_b^0 + \int_0^{\Lambda/b} \frac{d^d\mathbf{q}}{(2\pi)^d} \left(\frac{t + Kq^2}{2} \right) |\tilde{m}(\mathbf{q})|^2 - \ln \left\langle e^{-\mathcal{U}[\tilde{\vec{m}}, \vec{\sigma}]} \right\rangle_\sigma . \tag{IV.32}$$

The final expression can be calculated perturbatively as,

$$\ln\left\langle e^{-\mathcal{U}}\right\rangle_\sigma = -\left\langle \mathcal{U}\right\rangle_\sigma + \frac{1}{2}\left(\left\langle \mathcal{U}^2\right\rangle_\sigma - \left\langle \mathcal{U}\right\rangle_\sigma^2\right) + \cdots + \frac{(-1)^\ell}{\ell!}\times \ell^{\rm th}\text{ cumulant of }\mathcal{U} + \cdots . \quad \text{(IV.33)}$$

The cumulants can be computed using the rules set in the previous sections. For example, at the first order we need to compute

$$\begin{array}{l}\left\langle \mathcal{U}\left[\tilde{\vec{m}},\vec{\sigma}\right]\right\rangle_\sigma = u\displaystyle\int \frac{d^d\mathbf{q}_1 d^d\mathbf{q}_2 d^d\mathbf{q}_3 d^d\mathbf{q}_4}{(2\pi)^{4d}}(2\pi)^d\delta^d(\mathbf{q}_1+\mathbf{q}_2+\mathbf{q}_3+\mathbf{q}_4) \\ \left\langle\left[\tilde{\vec{m}}(\mathbf{q}_1)+\vec{\sigma}(\mathbf{q}_1)\right]\cdot\left[\tilde{\vec{m}}(\mathbf{q}_2)+\vec{\sigma}(\mathbf{q}_2)\right]\ \left[\tilde{\vec{m}}(\mathbf{q}_3)+\vec{\sigma}(\mathbf{q}_3)\right]\cdot\left[\tilde{\vec{m}}(\mathbf{q}_4)+\vec{\sigma}(\mathbf{q}_4)\right]\right\rangle_\sigma\end{array} . \quad \text{(IV.34)}$$

The following types of terms result from expanding the product:

$$\begin{array}{lll}[1] & 1 & \left\langle \tilde{\vec{m}}(\mathbf{q}_1)\cdot\tilde{\vec{m}}(\mathbf{q}_2)\,\tilde{\vec{m}}(\mathbf{q}_3)\cdot\tilde{\vec{m}}(\mathbf{q}_4)\right\rangle_\sigma \\ [2] & 4 & \left\langle \vec{\sigma}(\mathbf{q}_1)\cdot\tilde{\vec{m}}(\mathbf{q}_2)\,\tilde{\vec{m}}(\mathbf{q}_3)\cdot\tilde{\vec{m}}(\mathbf{q}_4)\right\rangle_\sigma \\ [3] & 2 & \left\langle \vec{\sigma}(\mathbf{q}_1)\cdot\vec{\sigma}(\mathbf{q}_2)\,\tilde{\vec{m}}(\mathbf{q}_3)\cdot\tilde{\vec{m}}(\mathbf{q}_4)\right\rangle_\sigma \\ [4] & 4 & \left\langle \vec{\sigma}(\mathbf{q}_1)\cdot\tilde{\vec{m}}(\mathbf{q}_2)\,\vec{\sigma}(\mathbf{q}_3)\cdot\tilde{\vec{m}}(\mathbf{q}_4)\right\rangle_\sigma \\ [5] & 4 & \left\langle \vec{\sigma}(\mathbf{q}_1)\cdot\vec{\sigma}(\mathbf{q}_2)\,\vec{\sigma}(\mathbf{q}_3)\cdot\tilde{\vec{m}}(\mathbf{q}_4)\right\rangle_\sigma \\ [6] & 1 & \left\langle \vec{\sigma}(\mathbf{q}_1)\cdot\vec{\sigma}(\mathbf{q}_2)\,\vec{\sigma}(\mathbf{q}_3)\cdot\vec{\sigma}(\mathbf{q}_4)\right\rangle_\sigma\end{array} . \quad \text{(IV.35)}$$

The second element in each line is the number of terms with the a given 'symmetry'. The total of these coefficients is $2^4 = 16$. Since the averages $\langle\mathcal{O}\rangle_\sigma$, involve only the short wavelength fluctuations, only contractions with $\vec{\sigma}$ appear. The resulting internal momenta are integrated from Λ/b to Λ.

Term [1] has no $\vec{\sigma}$ factors and evaluates to $\mathcal{U}[\tilde{\vec{m}}]$. The second and fifth terms involve an odd number of $\vec{\sigma}$s and their average is zero. Term [3] has one contraction and evaluates to

$$\begin{array}{l}-u\times 2\displaystyle\int \frac{d^d\mathbf{q}_1\cdots d^d\mathbf{q}_4}{(2\pi)^{4d}}(2\pi)^d\delta^d(\mathbf{q}_1+\cdots+\mathbf{q}_4)\frac{\delta_{jj}(2\pi)^d\delta^d(\mathbf{q}_1+\mathbf{q}_2)}{t+Kq_1^2}\tilde{\vec{m}}(\mathbf{q}_3)\cdot\tilde{\vec{m}}(\mathbf{q}_4) = \\ -2nu\displaystyle\int_0^{\Lambda/b}\frac{d^d\mathbf{q}}{(2\pi)^d}|\tilde{m}(\mathbf{q})|^2\int_{\Lambda/b}^{\Lambda}\frac{d^d\mathbf{k}}{(2\pi)^d}\frac{1}{t+Kk^2}.\end{array} \quad \text{(IV.36)}$$

Term [4] also has one contraction but there is no closed loop (the factor δ_{jj}) and hence no factor of n. The various contractions of 4 $\vec{\sigma}$ in term [6] lead to a number of terms with

no dependence on $\tilde{\vec{m}}$. We shall denote the sum of these terms by $uV\delta f_b^1$. Summing up all terms, the coarse grained Hamiltonian at order of u is given by

$$\begin{aligned}\beta\tilde{\mathcal{H}}[\tilde{\vec{m}}] =& V\left(\delta f_b^0 + u\delta f_b^1\right) + \int_0^{\Lambda/b} \frac{d^d\mathbf{q}}{(2\pi)^d}\left(\frac{\tilde{t}+Kq^2}{2}\right)|\tilde{m}(\mathbf{q})|^2 \\ &+ u\int_0^{\Lambda/b} \frac{d^d\mathbf{q}_1 d^d\mathbf{q}_2 d^d\mathbf{q}_3}{(2\pi)^{3d}}\tilde{\vec{m}}(\mathbf{q}_1)\cdot\tilde{\vec{m}}(\mathbf{q}_2)\tilde{\vec{m}}(\mathbf{q}_3)\cdot\tilde{\vec{m}}(-\mathbf{q}_1-\mathbf{q}_2-\mathbf{q}_3)\end{aligned} \quad , \tag{IV.37}$$

where

$$\tilde{t} = t + 4u(n+2)\int_{\Lambda/b}^{\Lambda}\frac{d^d\mathbf{k}}{(2\pi)^d}\frac{1}{t+Kk^2}. \tag{IV.38}$$

The coarse grained Hamiltonian is thus described by the same 3 parameters t, K, and u. The other two parameters in the coarse grained Hamiltonian are unchanged, i.e.

$$\tilde{K} = K, \quad \text{and} \quad \tilde{u} = u. \tag{IV.39}$$

2. *Rescale* by setting $\mathbf{q} = b^{-1}\mathbf{q}'$, and

3. *Renormalize*, $\tilde{\vec{m}} = z\vec{m}'$, to get

$$\begin{aligned}(\beta\mathcal{H})'[m'] =& V\left(\delta f_b^0 + u\delta f_b^1\right) + \int_0^{\Lambda}\frac{d^d\mathbf{q}'}{(2\pi)^d}b^{-d}z^2\left(\frac{\tilde{t}+Kb^{-2}q'^2}{2}\right)|m'(\mathbf{q}')|^2 \\ &+ uz^4b^{-3d}\int_0^{\Lambda}\frac{d^d\mathbf{q}_1' d^d\mathbf{q}_2' d^d\mathbf{q}_3'}{(2\pi)^{3d}}\vec{m}'(\mathbf{q}_1')\cdot\vec{m}'(\mathbf{q}_2')\,\vec{m}'(\mathbf{q}_3')\cdot\vec{m}'(-\mathbf{q}_1'-\mathbf{q}_2'-\mathbf{q}_3')\end{aligned} \quad . \tag{IV.40}$$

The renormalized Hamiltonian is characterized by the triplet of interactions (t', K', u'), such that

$$t' = b^{-d}z^2\tilde{t}, \quad K' = b^{-d-2}z^2K, \quad u' = b^{-3d}z^4u. \tag{IV.41}$$

As in the Gaussian model there is a fixed point at $t^* = u^* = 0$, provided that we set $z = b^{1+\frac{d}{2}}$, such that $K' = K$. The recursion relations for t and u in the vicinity of this point are given by

$$\begin{cases} t_b' = b^2\left[t + 4u(n+2)\displaystyle\int_{\Lambda/b}^{\Lambda}\frac{d^d\mathbf{k}}{(2\pi)^d}\frac{1}{t+Kk^2}\right] \\ u_b' = b^{4-d}u \end{cases} \quad . \tag{IV.42}$$

While the recursion relation for u at this order is identical to that obtained by dimensional analysis; the one for t is different. It is common to convert the discrete recursion relations to continuous differential equations by setting $b = e^{\ell}$, such that for an infinitesimal $\delta\ell$,

$$t_b' \equiv t(b) = t(1+\delta\ell) = t + \delta\ell\frac{dt}{d\ell} + \mathcal{O}(\delta\ell^2) \quad , \quad u_b' \equiv u(b) = u + \delta\ell\frac{du}{d\ell} + \mathcal{O}(\delta\ell^2).$$

Expanding eqs.(IV.42) to order of $\delta\ell$, gives

$$\begin{cases} t + \delta\ell \dfrac{dt}{d\ell} = (1 + 2\delta\ell)\left(t + 4u(n+2)\dfrac{S_d}{(2\pi)^d}\dfrac{1}{t + K\Lambda^2}\Lambda^d\delta\ell\right) \\ u + \delta\ell\dfrac{du}{d\ell} = (1 + (4-d)\delta\ell)\, u \end{cases} . \tag{IV.43}$$

The differential equations governing the evolution of t and u under rescaling are then

$$\begin{cases} \dfrac{dt}{d\ell} = 2t + \dfrac{4u(n+2)K_d\Lambda^d}{t + K\Lambda^2} \\ \dfrac{du}{d\ell} = (4-d)u \end{cases} . \tag{IV.44}$$

The recursion relation for u is easily integrated to give $u(\ell) = u_0 e^{(4-d)\ell} = u_0 b^{(4-d)}$.

The recursion relations can be linearized in the vicinity of the fixed point $t^* = u^* = 0$, by setting $t = t^* + \delta t$ and $u = u^* + \delta u$, as

$$\frac{d}{d\ell}\begin{pmatrix} \delta t \\ \delta u \end{pmatrix} = \begin{pmatrix} 2 & \frac{4(n+2)K_d\Lambda^{d-2}}{K} \\ 0 & 4-d \end{pmatrix}\begin{pmatrix} \delta t \\ \delta u \end{pmatrix} \tag{IV.45}$$

In the differential form of the recursion relations, the eigenvalues of the matrix determine the relevance of operators. Since the above matrix has zero elements on one side, its eigenvalues are the diagonal elements, and as in the Gaussian model we can identify $y_t = 2$, and $y_u = 4 - d$. The results at this order are identical to those obtained from dimensional analysis on the Gaussian model. The only difference is in the eigen–directions. The exponent $y_t = 2$ is still associated with $u = 0$, while $y_u = 4 - d$ is actually associated with the direction $t = -4u(n+2)K_d\Lambda^{d-2}/K$. This agrees with the shift in the transition temperature calculated to order of u from the susceptibility.

For $d > 4$ the Gaussian fixed point has only one unstable direction associated with y_t. It thus correctly describes the phase transition. For $d < 4$ it has two relevant directions and is unstable. Unfortunately, the recursion relations have no other fixed point at this order and it appears that we have learned little from the perturbative RG. However, since we are dealing with an alternating series we can *anticipate* that the recursion relations at the next order are modified to

$$\begin{cases} \dfrac{dt}{d\ell} = 2t + \dfrac{4u(n+2)K_d\Lambda^d}{t + K\Lambda^2} - Au^2 \\ \dfrac{du}{d\ell} = (4-d)u - Bu^2 \end{cases} , \tag{IV.46}$$

with A and B positive. There is now an additional fixed point at $u^* = (4-d)/B$ for $d < 4$. For a systematic perturbation theory we need to keep the parameter u small. Thus the new fixed point can be explored systematically only for small $\epsilon = 4 - d$; we are led to consider an expansion in the dimension of space in the vicinity of $d = 4$! For a calculation valid at $\mathcal{O}(\epsilon)$ we have to keep track of terms of second order in the recursion relation for u, but only to first order in that of t. It is thus unnecessary to calculate the term A in the above recursion relation.

IV.F Perturbative RG (Second Order)

The coarse grained Hamiltonian at second order in $\mathcal{U}$ is

$$\beta\tilde{\mathcal{H}}[\tilde{\vec{m}}] = V\delta f_b^0 + \int_0^{\Lambda/b} \frac{d^d\mathbf{q}}{(2\pi)^d}\left(\frac{t+Kq^2}{2}\right)|\tilde{m}(\mathbf{q})|^2 + \langle\mathcal{U}\rangle_\sigma - \frac{1}{2}\left(\langle\mathcal{U}^2\rangle_\sigma - \langle\mathcal{U}\rangle_\sigma^2\right) + O(\mathcal{U}^3). \tag{IV.47}$$

To calculate $\left(\langle\mathcal{U}^2\rangle_\sigma - \langle\mathcal{U}\rangle_\sigma^2\right)$ we need to consider all possible decompositions of two $\mathcal{U}$s into $\tilde{\vec{m}}$ and $\vec{\sigma}$ as in eq.(IV.34). Since each $\mathcal{U}$ can be broken up into 6 types of terms as in eq.(IV.35), there are 36 such possibilities for two $\mathcal{U}$s which can be arranged in a 6×6 table. Many of the elements of this table are either zero, or can be neglected at this stage, due to a number of considerations:

(i) All the 11 terms involving at least one factor of type [1] are zero because they cannot be contracted into a *connected* piece, and the disconnected elements cancel in calculating the cumulant.

(ii) An additional 12 terms (such as $[2]\times[3]$) involve an *odd* number of $\vec{\sigma}$s and are zero due to their *parity*.

(iii) Two terms, $[2]\times[5]$ and $[5]\times[2]$, involve a vertex where two $\vec{\sigma}$s are contracted together, leaving a $\tilde{\vec{m}}(\mathbf{q}^<)$ and a $\vec{\sigma}(\mathbf{q}^>)$. This configuration is not allowed by the δ–function which ensures momentum conservation for the vertex, as by construction $\mathbf{q}^> + \mathbf{q}^< \neq \mathbf{0}$.

(iv) Terms $[3]\times[6]$, $[4]\times[6]$ and their partners by exchange have two factors of $\tilde{\vec{m}}$. They involve *two loop* integrations, and appear as corrections to the coefficient $\tilde{t}$. We shall denote their net effect by A, which as noted earlier does not need to be known precisely at this order.

(v) The term $[5]\times[5]$ also involves two factors of $\tilde{\vec{m}}$, while $[2]\times[2]$ includes 6 such factors. The latter is important as it indicates that the space of parameters *is not closed* at this order. Even if initially zero, a term proportional to m^6 is generated under RG. In fact, considerations of momentum conservation indicate that both these terms are zero for $\mathbf{q}=0$, and are thus contributions to q^2m^2 and q^2m^6. We shall comment on their effect later on.

(vi) The contributions resulting from $[6]\times[6]$ are constants, and will be collectively denoted by $u^2V\delta f_b^2$.

(vii) The terms [3] × [3], [3] × [4], [4] × [3], and [4] × [4] contribute to $\tilde{\vec{m}}^4$. For example, [3] × [3] results in

$$\begin{aligned}
&\frac{u^2}{2}\times 2\times 2\times 2\int_0^{\Lambda/b}\frac{d^d\mathbf{q}_1\cdots d^d\mathbf{q}_4}{(2\pi)^{4d}}\int_{\Lambda/b}^{\Lambda}\frac{d^d\mathbf{k}_1 d^d\mathbf{k}_2 d^d\mathbf{k}_1' d^d\mathbf{k}_2'}{(2\pi)^{4d}}\\
&\quad\times(2\pi)^{2d}\delta^d(\mathbf{q}_1+\mathbf{q}_2+\mathbf{k}_1+\mathbf{k}_2)\delta^d(\mathbf{k}_1+\mathbf{k}_2+\mathbf{q}_3+\mathbf{q}_4)\\
&\quad\times\frac{\delta_{\alpha\alpha'}(2\pi)^d\delta^d(\mathbf{k}_1+\mathbf{k}_1')}{t+Kk_1^{2'}}\frac{\delta_{\alpha\alpha'}(2\pi)^d\delta^d(\mathbf{k}_2+\mathbf{k}_2')}{t+Kk_2^{2'}}\tilde{\vec{m}}(\mathbf{q}_1)\cdot\tilde{\vec{m}}(\mathbf{q}_2)\tilde{\vec{m}}(\mathbf{q}_3)\cdot\tilde{\vec{m}}(\mathbf{q}_4)=\\
&4nu^2\int_0^{\Lambda/b}\frac{d^d\mathbf{q}_1\cdots d^d\mathbf{q}_4}{(2\pi)^{4d}}(2\pi)^d\delta^d(\mathbf{q}_1+\mathbf{q}_2+\mathbf{q}_3+\mathbf{q}_4)\tilde{\vec{m}}(\mathbf{q}_1)\cdot\tilde{\vec{m}}(\mathbf{q}_2)\tilde{\vec{m}}(\mathbf{q}_3)\cdot\tilde{\vec{m}}(\mathbf{q}_4)\\
&\quad\times\int\frac{d^d\mathbf{k}}{(2\pi)^d}\frac{1}{(t+Kk^2)\,(t+K(\mathbf{q}_1+\mathbf{q}_2-\mathbf{k})^2)}.
\end{aligned}\tag{IV.48}$$

The contractions from terms [3] × [4], [4] × [3], and [4] × [4] lead to similar expressions with prefactors of 8, 8, and 16 respectively. Apart from the dependence on $\mathbf{q}_1$ and $\mathbf{q}_2$, the final result has the form of $\mathcal{U}[\tilde{\vec{m}}]$. In fact the last integral can be expanded as

$$f(\mathbf{q}_1+\mathbf{q}_2)=\int\frac{d^d\mathbf{k}}{(2\pi)^d}\frac{1}{(t+Kk^2)^2}\left[1-\frac{2K\mathbf{k}\cdot(\mathbf{q}_1+\mathbf{q}_2)-K(\mathbf{q}_1+\mathbf{q}_2)^2}{(t+Kk^2)}+\cdots\right].\tag{IV.49}$$

After fourier transforming back to real space we find in addition to m^4, such terms as $m^2(\nabla m)^2, m^2\nabla^2 m^2,\cdots$.

Putting all contributions together, the coarse grained Hamiltonian at order of u^2 takes the form

$$\begin{aligned}
\beta\tilde{\mathcal{H}}&=V\left(\delta f_b^0+u\delta f_b^1+u^2\delta f_b^2\right)\\
&+\int_0^{\Lambda/b}\frac{d^d\mathbf{q}}{(2\pi)^d}|\tilde{m}(\mathbf{q})|^2\left[\frac{t+Kq^2}{2}+2u(n+2)\int_{\Lambda/b}^{\Lambda}\frac{d^d\mathbf{k}}{(2\pi)^d}\frac{1}{t+Kk^2}-\frac{u^2}{2}A(t,K,q^2)\right]\\
&+\int_0^{\Lambda/b}\frac{d^d\mathbf{q}_1\cdots d^d\mathbf{q}_4}{(2\pi)^{4d}}\tilde{\vec{m}}(\mathbf{q}_1)\cdot\tilde{\vec{m}}(\mathbf{q}_2)\tilde{\vec{m}}(\mathbf{q}_3)\cdot\tilde{\vec{m}}(\mathbf{q}_4)\\
&\times\left[u-\frac{u^2}{2}(8n+64)\int_{\Lambda/b}^{\Lambda}\frac{d^d\mathbf{k}}{(2\pi)^d}\frac{1}{(t+Kk^2)^2}+\mathcal{O}(u^2q^2)\right]+\mathcal{O}(u^2\tilde{m}^6q^2,\cdots)+\mathcal{O}(u^3).
\end{aligned}\tag{IV.50}$$

IV.G The ϵ–Expansion

The parameter space (K,t,u) is no longer closed at this order; several new interactions proportional to m^2, m^4, and m^6, all consistent with symmetries of the problem, appear in

the coarse grained Hamiltonian at second order in u. Ignoring these interactions for the time being, the coarse grained parameters are given by

$$\begin{cases} \tilde{K} = K - u^2 A''(0) \\ \tilde{t} = t + 4(n+2)\ u\ \displaystyle\int_{\Lambda/b}^{\Lambda} \frac{d^d\mathbf{k}}{(2\pi)^d}\, \frac{1}{t + Kk^2} - u^2 A(0) \\ \tilde{u} = u - 4(n+8)u^2 \displaystyle\int_{\Lambda/b}^{\Lambda} \frac{d^d\mathbf{k}}{(2\pi)^d}\, \frac{1}{(t + Kk^2)^2} \end{cases} , \tag{IV.51}$$

where $A(0)$ and $A''(0)$ correspond to the first two terms in the expansion of $A(t, K, q^2)$ in eq.(IV.50) in powers of q.

After the *rescaling* $\mathbf{q} = b^{-1}\mathbf{q}'$, and *renormalization* $\tilde{\vec{m}} = z\vec{m}'$, steps of the RG procedure, we obtain

$$K' = b^{-d-2} z^2 \tilde{K}, \qquad t' = b^{-d} z^2 \tilde{t}, \qquad u' = b^{-3d} z^4 \tilde{u}. \tag{IV.52}$$

As before, the renormalization parameter z is chosen such that $K' = K$, leading to

$$z^2 = \frac{b^{d+2}}{(1 - u^2 A''(0)/K)} = b^{d+2} \left(1 + O(u^2)\right). \tag{IV.53}$$

The value of z does depend on the fixed point position u^*. But as u^* is of the order of ϵ, $z = b^{1+\frac{d}{2}+\mathcal{O}(\epsilon^2)}$, is not changed at the lowest order. Using this value of z, and following the previous steps for constructing differential recursion relations, we obtain

$$\begin{cases} \dfrac{dt}{d\ell} = 2t + \dfrac{4u(n+2)K_d\Lambda^d}{t + K\Lambda^2} - A(t, K, \Lambda)u^2 \\ \dfrac{du}{d\ell} = (4-d)u - \dfrac{4(n+8)K_d\Lambda^d}{(t + K\Lambda^2)^2} u^2 \end{cases} . \tag{IV.54}$$

The fixed points are obtained from $dt/d\ell = du/d\ell = 0$. In addition to the Gaussian fixed point at $u^* = t^* = 0$, discussed in the previous section, there is now a non-trivial fixed point located at

$$\begin{cases} u^* = \dfrac{(t^* + K\Lambda^2)^2}{4(n+8)K_d\Lambda^d}\,\epsilon = \dfrac{K^2}{4(n+8)K_4}\,\epsilon + \mathcal{O}(\epsilon^2) \\ t^* = -\dfrac{2u^*(n+2)K_d\Lambda^d}{t^* + K\Lambda^2} = -\dfrac{(n+2)}{2(n+8)} K\Lambda^2\,\epsilon + \mathcal{O}(\epsilon^2) \end{cases} . \tag{IV.55}$$

The above expressions have been further simplified by systematically keeping terms to first order in $\epsilon = 4 - d$.

Linearizing the recursion relations in the vicinity of the fixed point results in

$$\frac{d}{d\ell}\begin{pmatrix}\delta t\\ \delta u\end{pmatrix}=\begin{pmatrix}2-\frac{4(n+2)K_d\Lambda^d}{(t^*+K\Lambda^2)^2}u^*-A'u^{*2} & \frac{4(n+2)K_d\Lambda^d}{t^*+K\Lambda^2}-2Au^*\\ \frac{8(n+8)K_d\Lambda^d}{(t^*+K\Lambda^2)^3}u^{*2} & \epsilon-\frac{8(n+8)K_d\Lambda^d}{(t^*+K\Lambda^2)^2}u^*\end{pmatrix}\begin{pmatrix}\delta t\\ \delta u\end{pmatrix}. \qquad \text{(IV.56)}$$

At the Gaussian fixed point, $t^*=u^*=0$, eq.(IV.45) is reproduced. At the new fixed point of eqs.(IV.55),

$$\frac{d}{d\ell}\begin{pmatrix}\delta t\\ \delta u\end{pmatrix}=\begin{pmatrix}2-\frac{4(n+2)K_4\Lambda^4}{K^2\Lambda^4}\frac{K^2\epsilon}{4(n+8)K_4} & \cdots\cdots\\ \mathcal{O}(\epsilon^2) & \epsilon-\frac{8(n+8)K_4\Lambda^4}{K^2\Lambda^4}\frac{K^2\epsilon}{4(n+8)K_4}\end{pmatrix}\begin{pmatrix}\delta t\\ \delta u\end{pmatrix}. \qquad \text{(IV.57)}$$

We have not explicitly calculated the top element of the second column as it is not necessary for calculating the eigenvalues. This is because the lower element of the first column is zero to order of ϵ. Hence the eigenvalues are determined by the diagonal elements alone. The first eigenvalue is positive, controlling the instability of the fixed point,

$$y_t=2-\frac{(n+2)}{(n+8)}\,\epsilon+\mathcal{O}(\epsilon^2). \qquad \text{(IV.58)}$$

The second eigenvalue,

$$y_u=-\epsilon+\mathcal{O}(\epsilon^2), \qquad \text{(IV.59)}$$

is negative for $d<4$. The new fixed point thus has co-dimension of one and can describe the phase transition in these dimensions. It is quite satisfying that while various intermediate results, such as the position of the fixed point depend on such microscopic parameters as K and Λ, the final eigenvalues are pure numbers, only depending on n and $d=4-\epsilon$. These eigenvalues characterize the *universality classes* of rotational symmetry breaking in $d<4$. (Long range interaction may lead to new universality classes.)

The divergence of the correlation length, $\xi\sim(\delta t)^{-\nu}$, is controlled by the exponent

$$\nu=\frac{1}{y_t}=\left\{2\left[1-\frac{(n+2)}{2(n+8)}\,\epsilon\right]\right\}^{-1}=\frac{1}{2}+\frac{1}{4}\,\frac{n+2}{n+8}\,\epsilon+\mathcal{O}(\epsilon^2). \qquad \text{(IV.60)}$$

The singular part of the free energy scales as, $f\sim(\delta t)^{2-\alpha}$, and the heat capacity diverges with the exponent

$$\alpha=2-d\nu=2-\frac{(4-\epsilon)}{2}\left[1+\frac{1}{2}\,\frac{n+2}{n+8}\,\epsilon\right]=\frac{4-n}{2(n+8)}\,\epsilon+\mathcal{O}(\epsilon^2). \qquad \text{(IV.61)}$$

To complete the calculation of critical exponents, we need the eigenvalue associated with the (relevant) symmetry breaking field h. This is easily found by adding a term $-\vec{h}\cdot$

$\int d^d\mathbf{x}\vec{m}(\mathbf{x}) = -\vec{h}\cdot\vec{m}(\mathbf{q}=\mathbf{0})$ to the Hamiltonian. This term is not effected by coarse graining or rescaling, and after the renormalization step changes to $-z\vec{h}\cdot\vec{m}'(\mathbf{q}'=\mathbf{0})$, implying

$$h' = zh = b^{1+\frac{d}{2}}h, \quad \Longrightarrow \quad y_h = 1+\frac{d}{2}+\mathcal{O}(\epsilon^2) = 3-\frac{\epsilon}{2}+\mathcal{O}(\epsilon^2). \tag{IV.62}$$

The vanishing of magnetization as $T \to T_c^-$, is controlled by the exponent

$$\begin{aligned}\beta = \frac{d-y_h}{y_t} &= \left(\frac{4-\epsilon}{2}-1\right)\times\frac{1}{2}\left(1+\frac{n+2}{2(n+8)}\,\epsilon+\mathcal{O}(\epsilon^2)\right)\\ &= \frac{1}{2}-\frac{3}{2(n+8)}\,\epsilon+\mathcal{O}(\epsilon^2),\end{aligned} \tag{IV.63}$$

while the susceptibility diverges as $\chi \sim (\delta t)^{-\gamma}$, with

$$\gamma = \frac{2y_h-d}{y_t} = 2\times\frac{1}{2}\left(1+\frac{n+2}{2(n+8)}\,\epsilon\right) = 1+\frac{n+2}{2(n+8)}\,\epsilon+O(\epsilon^2). \tag{IV.64}$$

Using the above results, we can estimate various exponents as a function of d and n. For example, for $n=1$, by setting $\epsilon = 1$ or 2 in eqs.(IV.60) and (IV.63) we obtain the values $\nu(1)\approx 0.58$, $\nu(2)\approx 0.67$, and $\beta(1)\approx 0.33$, $\beta(2)\approx 0.17$. The best estimates of these exponents in $d=3$ are $\nu\approx 0.63$, and $\beta\approx 0.32$. In $d=2$ the exact values are known to be $\nu = 1$ and $\beta = 0.125$. The estimates for β are quite good, while those for ν are less reliable. It is important to note that in all cases these estimates are an improvement over the mean field (saddle point) values. Since the expansion is around four dimensions, the results are more reliable in $d=3$ than in $d=2$. In any case, they correctly describe the decrease of β with lowering dimension, and the increase of ν. They also correctly describe the trends with varying n at a fixed d as indicated by the following table of exponents $\alpha(n)$.

	$n=1$	$n=2$	$n=3$	$n=4$
$\mathcal{O}(\epsilon)$ at $\epsilon=1$	0.17	0.11	0.06	0
Experiments in $d=3$	0.11	-0.01	-0.12	–

Although the sign of α is incorrectly predicted at this order for $n=2$ and 3, the decrease of α with increasing n is correctly described.

IV.H Irrelevance of other interactions

The fixed point Hamiltonian at $\mathcal{O}(\epsilon)$ (from eqs.(IV.55)) has only three terms

$$\beta\mathcal{H}^* = \frac{K}{2}\int_\Lambda d^d\mathbf{x}\left[(\nabla m)^2 - \frac{(n+2)}{(n+8)}\,\epsilon\Lambda^2 m^2 + \frac{\epsilon\Lambda^{-\epsilon}}{2(n+8)}\,\frac{K}{K_4}m^4\right], \tag{IV.65}$$

and explicitly depends on the imposed cutoff $\Lambda \sim 1/a$ (unlike the exponents). However, as described in section III.E, the starting point for RG must be the most general Hamiltonian consistent with symmetries. We also discovered that even if some of these terms are left out of the original Hamiltonian, they are generated under coarse graining. At second order in u, terms proportional to m^6 were generated; higher powers of m will appear at higher orders in u.

Let us focus on a rotatationally symmetric Hamiltonian for $\vec{h} = 0$. We can incorporate all terms consistent with this symmetry in a perturbative RG by setting $\beta\mathcal{H} = \beta\mathcal{H}_0 + \mathcal{U}$, where

$$\beta\mathcal{H}_0 = \int d^d\mathbf{x}\left[\frac{t}{2}m^2 + \frac{K}{2}(\nabla m)^2 + \frac{L}{2}(\nabla^2 m)^2 + \cdots\right], \tag{IV.66}$$

includes all quadratic (Gaussian terms), while the remaining higher order terms are placed in the perturbation

$$\mathcal{U} = \int d^d\mathbf{x}\left[um^4 + vm^2(\nabla m)^2 + \cdots + u_6 m^6 + \cdots + u_8 m^8 + \cdots\right]. \tag{IV.67}$$

After coarse graining, and steps (ii) and (iii) of RG in real space, $\mathbf{x} = b\mathbf{x}'$ and $\tilde{\vec{m}} = \zeta\vec{m}'$, the renormalized weight depends on the parameters

$$\begin{cases} t \mapsto & b^d\zeta^2\tilde{t} = b^2\tilde{t} \\ K \mapsto & b^{d-2}\zeta^2\tilde{K} = K \\ L \mapsto & b^{d-4}\zeta^2\tilde{L} = b^{-2}\tilde{L} \\ & \vdots \\ u \mapsto & b^d\zeta^4\tilde{u} = b^{4-d}\tilde{u} \\ v \mapsto & b^{d-2}\zeta^4\tilde{v} = b^{2-d}\tilde{v} \\ & \vdots \\ u_6 \mapsto & b^d\zeta^6\tilde{u_6} = b^{6-2d}\tilde{u_6} \\ u_8 \mapsto & b^d\zeta^8\tilde{u_8} = b^{8-3d}\tilde{u_8} \\ & \vdots \end{cases} . \tag{IV.68}$$

The second set of equalities are obtained by choosing $\zeta^2 = b^{2-d}K/\tilde{K} = b^{2-d}[1 + \mathcal{O}(u^2, uv, v^2, \cdots)]$, such that $K' = K$. By choosing an infinitesimal rescaling, the recursion relations take the differential forms

$$\begin{cases} \dfrac{dt}{d\ell} = 2t + \mathcal{O}(u, v, u_6, u_8, \cdots) \\ \dfrac{dK}{d\ell} = 0 \\ \dfrac{dL}{d\ell} = -2L + \mathcal{O}(u^2, uv, v^2, \cdots) \\ \quad \vdots \\ \dfrac{du}{d\ell} = \epsilon u - Bu^2 + \mathcal{O}(uv, v^2, \cdots) \\ \dfrac{dv}{d\ell} = (-2+\epsilon)v + \mathcal{O}(u^2, uv, v^2, \cdots) \\ \quad \vdots \\ \dfrac{du_6}{d\ell} = (-2+2\epsilon)u_6 + \mathcal{O}(u^3, u_6^2, \cdots) \\ \dfrac{du_8}{d\ell} = (-4+3\epsilon)u_8 + \mathcal{O}(u^3, u^2u_6, \cdots) \\ \quad \vdots \end{cases} . \tag{IV.69}$$

These recursion relations describe two fixed points:

(i) The Gaussian fixed point, $t^* = L^* = u^* = v^* = \cdots = 0$, and $K \neq 0$, has eigenvalues

$$y_t^0 = 2,\ y_L^0 = -2,\ \cdots,\ y_u^0 = +\epsilon,\ y_v^0 = -2+\epsilon,\ \cdots,\ y_6^0 = -2+2\epsilon,\ y_8^0 = -4+3\epsilon,\ \cdots. \tag{IV.70}$$

(ii) Setting eqs.(IV.69) to zero, a non-trivial fixed point is located at

$$t^* \sim u^* \sim \mathcal{O}(\epsilon), \quad L^* \sim v^* \sim \cdots \sim \mathcal{O}(\epsilon^2), \quad u_6^* \sim \cdots \sim \mathcal{O}(\epsilon^3), \quad \cdots. \tag{IV.71}$$

The stability of this fixed point is determined by the matrix,

$$\frac{d}{d\ell}\begin{pmatrix} \delta t \\ \delta L \\ \vdots \\ \delta u \\ \delta v \\ \vdots \end{pmatrix} = \begin{pmatrix} 2-\mathcal{O}(u^*) & \mathcal{O}(\epsilon) & \cdots & \mathcal{O}(1) & \mathcal{O}(1) & \cdots \\ \mathcal{O}(\epsilon^2) & -2+\mathcal{O}(\epsilon) & & & & \\ \vdots & & \ddots & & & \\ \mathcal{O}(\epsilon^2) & \mathcal{O}(\epsilon) & & & & \\ \mathcal{O}(\epsilon^2) & \mathcal{O}(\epsilon) & & & & \\ \vdots & & & & & \end{pmatrix}\begin{pmatrix} \delta t \\ \delta L \\ \vdots \\ \delta u \\ \delta v \\ \vdots \end{pmatrix}. \tag{IV.72}$$

Note that as $\epsilon \to 0$, the non-trivial fixed part, its eigenvalues and eigendirections continuously go over to the Gaussian fixed points. Hence the eigenvalues can only be corrected by order of ϵ, and eq.(IV.70) is modified to

$$\begin{aligned} y_t = 2 - \frac{n+2}{n+8}\epsilon + \mathcal{O}(\epsilon^2), \qquad y_L = -2 + \mathcal{O}(\epsilon), \cdots, \\ y_u = -\epsilon + \mathcal{O}(\epsilon^2),\, y_v = -2 + \mathcal{O}(\epsilon), \cdots, y_6 = -2 + \mathcal{O}(\epsilon),\, y_8 = -4 + \mathcal{O}(\epsilon), \cdots. \end{aligned} \tag{IV.73}$$

While the eigenvalues are still labelled with the coefficients of the various terms in the Landau–Ginzburg expansion, we must remember that the actual eigendirections are now rotated away from the axes of this parameter space, although their largest projection is still parallel to the corresponding axis.

Whereas the Gaussian fixed point has two relevant directions in $d < 4$, the generalized $O(n)$ fixed point has only one relevant direction corresponding to y_t. At least perturbatively, this fixed point has a basin of attraction of co-dimension one, and thus describes the phase transition. The original concept of Kadanoff is thus explicitly realized and the universality of exponents is traced to the irrelevance (at least perturbatively) of the multitude of other possible interactions. The perturbative approach does not exclude the existence of other fixed points at finite values of these parameter. The uniqueness of the critical exponents observed so far for each universality class, and their proximity to the values calculated from the ϵ–expansion, suggests that postulating such *non-perturbative* fixed points is unnecessary.

IV.I Comments on the ϵ-Expansion

The perturbative implementation of RG for the Landau–Ginzburg Hamiltonian was achieved by K.G. Wilson in the early 1970s; the ϵ–expansion was developed jointly with M.E. Fisher. This led to a flurry of activity in the topic which still continues. Wilson was awarded the Nobel prize in 1982. Historical details can be found in his Nobel lecture reprinted in Rev. Mod. Phys. **55**, 583 (1983). A few comments on the ϵ–expansion are in order at this stage.

1. *Higher orders, and convergence of the series:* Calculating the exponents to $\mathcal{O}(\epsilon)^2$ and beyond, by going to order of $\mathcal{U}^3$ and higher, is quite complicated as we have to keep track of many more interactions. It is in fact quite unappealing that the intermediate steps of the RG explicitly keep track of the cutoff scale Λ, while the final exponents must be independent of it. In fact there are a number of field theoretical RG schemes (dimensional

regularization, summing leading divergences, etc.) that avoid many of these difficulties. These methods are harder to visualize and will not be described here. All higher order calculations are currently performed using one of these schemes. It is sometimes (but not always) possible to prove that these approaches are consistent with each other, and can be carried out to all orders. In principle, the problem of evaluating critical exponents in $d = 3$ is now solved: simple computations lead to approximate results, while more refined calculations should provide better answers. The situation is somewhat like finding the energy levels of a He atom which can not be done exactly, but which may be obtained with sufficient accuracy using various approximation methods.

To estimate how reliable the exponents are, we need some information on the convergence of the series. The ϵ expansion has been carried out to the fifth order, and the results for the exponent γ, for $n = 1$ at $d = 3$, are

$$\begin{aligned} \gamma &= 1 + 0.167\epsilon + 0.077\epsilon^2 - 0.049\epsilon^3 + 0.180\epsilon^4 - 0.415\epsilon^5 \\ 1.2385 \pm 0.0025 &= 1.000, \quad 1.167, \quad 1.244, \quad 1.195, \quad 1.375, \quad 0.96 \end{aligned} \quad . \tag{IV.74}$$

The second line compares the values obtained at different orders by substituting $\epsilon = 1$, with the best estimate of $\gamma \approx 1.2385$ in $d = 3$. Note that the elements of the series have alternating signs. The truncated series evaluated at $\epsilon = 1$ improves up to third order, beyond which it starts to oscillate, and deviates from the left hand side. These are characteristics of an *asymptotic series*. It can be proved that for large p, the coefficients in the expansion of most quantities scale as $|f_p| \sim cp!a^{-p}$. As a result, the ϵ-expansion series is *non-convergent*, but can be evaluated by the *Borel summation* method, using the identity, $\int_0^\infty dx\, x^p e^{-x} = p!$, as

$$f(\epsilon) = \sum_p f_p \epsilon^p = \sum_p f_p \epsilon^p \frac{1}{p!} \int_0^\infty dx\, x^p e^{-x} = \int_0^\infty dx e^{-x} \sum_p \frac{f_p (\epsilon x)^p}{p!}. \tag{IV.75}$$

The final summation (which is convergent) results in a function of x which can be integrated to give $f(\epsilon)$. Very good estimates of exponents in $d = 3$, such as the one for γ quoted above, are obtained by this summation method. There is no indication of any singularity in the exponents up to $\epsilon = 2$, corresponding to the lower critical dimension $d = 2$.

2. *The* $1/n$ *expansion:* The fixed point position,

$$u^* = \frac{(t^* + K\Lambda^2)^2 (4 - d)}{4(n + 8) K_d \Lambda^d},$$

vanishes as $n \to \infty$. This suggests that a controlled $1/n$ expansion of the critical exponents is also possible. Indeed such an expansion can be developed by a number of methods, such as a saddle point expansion that takes advantage of the exponential dependence of the Hamiltonian on n, or by an exact resummation of the perturbation series. Eq.(IV.58) in this limit gives,

$$y_t = \lim_{n\to\infty} \left[2 - \frac{n+2}{n-8}(4-d) \right] = d - 2, \quad \Longrightarrow \quad \nu = \frac{1}{d-2}. \tag{IV.76}$$

This result is exact in dimensions $4 < d < 2$. Above four dimensions the mean field value of $1/2$ is recovered, while for $d < 2$ there is no order.

V. Position Space Renormalization Group

V.A Lattice Models

While Wilson's perturbative RG provides a systematic approach to probing critical properties, carrying out the ϵ-expansion to high orders is quite cumbersome. Models defined on a discrete lattice provide a number of alternative computational routes that can complement the perturbative RG approach. Because of universality, we expect that all models with appropriate microscopic symmetries and range of interactions, no matter how simplified, lead to the same critical exponents. Lattice models are convenient for visualization, computer simulation, and series expansion purposes. We shall thus describe models in which an appropriate "spin" degree of freedom is placed on each site of a lattice, and the spins are subject to simple interaction energies. While such models are formulated in terms of explicit 'microscopic' degrees of freedom, depending on their degree of complexity, they may or may not provide a more accurate description of a specific material than the Landau–Ginzburg model. The point is that universality dictates that both descriptions describe the same *macroscopic* physics, and the choice of continuum or discrete models is a matter of computational convenience. Some commonly used lattice models are described here:

1. *The Ising Model* is the simplest and most widely applied paradigm in statistical mechanics. At each site i of a lattice, there is a spin σ_i which takes the two values of $+1$ or -1. Each state may correspond to one of two species in a binary mixture, or to empty and occupied cells in a lattice approximation to an interacting gas. The simplest possible *short range* interaction involves only neighboring spins, and is described by a Hamiltonian

$$\mathcal{H} = \sum_{<i,j>} \hat{B}(\sigma_i, \sigma_j), \tag{V.1}$$

where the notation $< i, j >$ is commonly used to indicate the sum over all *nearest neighbor* pairs on the lattice. Since $\sigma_i^2 = 1$, the most general interaction between two spins is

$$\hat{B}(\sigma, \sigma') = -\hat{g} - \frac{\hat{h}}{z}(\sigma + \sigma') - J\sigma\sigma'. \tag{V.2}$$

For N spins, there are 2^N possible *micro-states*, and the (Gibbs) partition function is

$$Z = \sum_{\{\sigma_i\}} e^{-\beta\mathcal{H}} = \sum_{\{\sigma_i\}} \exp\left[K \sum_{<i,j>} \sigma_i\sigma_j + h\sum_i \sigma_i + g \right], \tag{V.3}$$

where we have set $K = \beta J$, $h = \beta\hat{h}$, and $g = \beta\hat{g}$ ($\beta = 1/k_B T$, and z is the number of bonds per site, i.e. the coordination number of the lattice). For $h = 0$ at $T = 0$, the ground state has a two fold degeneracy with all spins pointing up or down ($K > 0$). This order is destroyed at a critical $K_c = J/k_B T_c$ with a phase transition to a disordered state. The field h breaks the *up–down symmetry* and removes the phase transition. The parameter g merely shifts the origin of energy, and has no effect on the relative weights of microstates, or the macroscopic properties.

All the following models can be regarded as generalizations of the Ising model.

2. *The $O(n)$ model:* Each lattice site is now occupied by an n-component *unit* vector, i.e

$$S_i \equiv (S_i^1, S_i^2, \cdots, S_i^n), \quad \text{with} \quad \sum_{\alpha=1}^{n} (S_i^\alpha)^2 = 1. \tag{V.4}$$

A nearest–neighbor interaction can be written as

$$\mathcal{H} = -J \sum_{<i,j>} \vec{S}_i \cdot \vec{S}_j - \hat{\vec{h}} \cdot \sum_i \vec{S}_i. \tag{V.5}$$

In fact, the most general interaction consistent with spherical symmetry is $f(\vec{S}_i \cdot \vec{S}_j)$ for an arbitrary function f. Similarly, the *rotational symmetry* can be broken by a number of "fields" such as $\sum_i (\vec{h}_p \cdot \vec{S}_i)^p$. Specific cases are the Ising model ($n = 1$), the *XY model* ($n = 2$), and the *Heisenberg model* ($n = 3$).

3. *The Potts model:* Each site of the lattice is occupied by a q-valued spin $S_i \equiv 1, 2, \cdots, q$. The interactions between the spins are described by the Hamiltonian

$$\mathcal{H} = -J \sum_{<i,j>} \delta_{S_i, S_j} - \hat{h} \sum_i \delta_{S_i, 1}. \tag{V.6}$$

The field h now breaks the *permutation symmetry* amongst the q-states. The Ising model is recovered for $q = 2$, since $\delta_{\sigma,\sigma'} = (1 + \sigma\sigma')/2$. The 3 state Potts model can for example describe the distortion of a cube along one of its faces. Potts models with $q > 2$ represent new universality classes not covered by the $O(n)$ model. Actually, the transitions for $q \geq 4$ in $d = 2$, and $q > 3$ in $d = 3$ are discontinuous.

4. *Spin s-models:* The spin at each site takes the $2s + 1$ values, $s_i = -s, -s + 1, \cdots, +s$. A general nearest–neighbor Hamiltonian is

$$\mathcal{H} = \sum_{<i,j>} \left(J_1 s_i s_j + J_2 (s_i s_j)^2 + \cdots + J_{2s} (s_i s_j)^{2s} \right) - \hat{h} \sum_i s_i. \tag{V.7}$$

The Ising model corresponds to $s = 1/2$, while $s = 1$ is known as the Blume–Emery–Griffith (BEG) model. It describes a mixture of non-magnetic ($s = 0$), and magnetic ($s = \pm 1$) elements. This model exhibits a tricritical point separating continuous and discontinuous transitions. However, since the ordered phase breaks an up–down symmetry, the phase transition belongs to the Ising universality class for all values of s.

Some of the computational tools employed in the study of discrete models are:

1. *Position space renormalizations:* These are implementations of Kadanoff's RG scheme on lattice models. Some approximation is usually necessary to keep the space of interactions tractable. Most such approximations are uncontrolled; a number of them will be discussed here.

2. *Series expansions:* Low-temperature expansions start with the ordered ground state and examine the lowest energy excitations around it. High temperatures expansions begin with the collection of non-interacting spins at infinite temperature and include the interactions between spins perturbatively. Critical behavior is then extracted from the singularities of such series.

3. *Exact solutions* can be obtained for a very limited subset of lattice models. These include one dimensional chains which will be solved by the transfer matrix method in recitations, and the two dimensional Ising model as described later in the course.

4. *Monte-Carlo simulations:* The aim of such methods is to generate configurations of spins that are distributed with the correct Boltzmann weight $\exp(-\beta\mathcal{H})$. There are a number of methods, most notably the Metropolis algorithm, for achieving this aim. Various expectation values and correlation functions are then directly computed from these configurations. With the continuing increase of computer power, numerical simulations have become increasingly popular. Limitations of the method are due to the size of systems that can be studied, and the amount of time needed to ensure that the correctly weighted configurations are generated. There is an extensive literature on numerical simulations which will not be further discussed in this course.

V.B Exact treatment in $d = 1$

An exact RG treatment can be carried out for the Ising model with nearest neighbor interactions (eq.(V.1)) in one dimension. The basic idea is to find a transformation that reduces the number of degrees of freedom by a factor b, while preserving the partition function, i.e.

$$Z = \sum_{\{\sigma_i | i=1,\cdots,N\}} e^{-\beta \mathcal{H}[\sigma_i]} = \sum_{\left\{\sigma'_{i'} | i'=1,\cdots,N/b\right\}} e^{-\beta \mathcal{H}'[\sigma'_{i'}]}. \tag{V.8}$$

There are many mappings $\{\sigma_i\} \mapsto \{\sigma'_{i'}\}$, that satisfy this condition. The choice of the transformation is therefore guided by the simplicity of the resulting RG. With $b = 2$, for example, one possible choice is to group pairs of neighboring spins and define the renormalized spin as their average. This *majority rule*, $\sigma'_i = (\sigma_{2i-1} + \sigma_{2i})/2$, is in fact not very convenient as the new spin has three possible values $(0, \pm 1)$ while the original spins are two valued. We can remove the ambiguity by assigning one of the two spins, e.g. σ_{2i-1}, the role of tie–breaker whenever the sum is zero. In this case the transformation is simply $\sigma'_i = \sigma_{2i-1}$. Such an RG procedure effectively removes the even numbered spins, $s_i = \sigma_{2i}$ and is usually called a *decimation*. Note that since $\sigma' = \pm 1$ as in the original model, no renormalization factor ζ, is necessary in this case. Since the interaction is over adjacent neighbors, the partition function can be written as

$$Z = \sum_{\{\sigma_i\}} \exp\left[\sum_{i=1}^{N} B(\sigma_i, \sigma_{i+1})\right] = \sum_{\left\{\sigma'_i\right\}} \sum_{\{s_i\}}^{N/2} \exp\left[\sum_{i=1}^{N/2} \left[B(\sigma'_i, s_i) + B(s_i, \sigma'_{i+1})\right]\right]. \tag{V.9}$$

Summing over the decimated spins, $\{s_i\}$, leads to

$$e^{-\beta \mathcal{H}'[\sigma'_i]} \equiv \prod_{i=1}^{N/2} \left[\sum_{s_i=\pm 1} e^{\left[B(\sigma'_i, s_i) + B(s_i, \sigma'_{i+1})\right]}\right] \equiv e^{\sum_{i=1}^{N/2} B'(\sigma'_i, \sigma'_{i+1})}, \tag{V.10}$$

where following eq.(V.2),

$$B(\sigma_1, \sigma_2) = g + \frac{h}{2}(\sigma_1 + \sigma_2) + K\sigma_1\sigma_2, \tag{V.11}$$

and

$$B'(\sigma'_1, \sigma'_2) = g' + \frac{h'}{2}(\sigma'_1 + \sigma'_2) + K'\sigma'_1\sigma'_2, \tag{V.12}$$

are the most general interaction forms for Ising spins.

Following eq.(V.10), the renormalized interactions are obtained from

$$\begin{aligned} R(\sigma_1', \sigma_2') &\equiv \exp\left[K'\sigma_1'\sigma_2' + \frac{h'}{2}(\sigma_1' + \sigma_2') + g'\right] \\ &= \sum_{s_1=\pm 1} \exp\left[Ks_1(\sigma_1' + \sigma_2') + \frac{h}{2}(\sigma_1' + \sigma_2') + hs_1 + 2g\right]. \end{aligned} \tag{V.13}$$

To solve for the renormalized interactions it is convenient to set

$$\begin{cases} x = e^K, & y = e^h, & z = e^g \\ x' = e^{K'}, & y' = e^{h'}, & z' = e^{g'} \end{cases}. \tag{V.14}$$

The four possible configurations of the bond are

$$\begin{cases} R(+,+) = x'y'z' = z^2 y(x^2 y + x^{-2}y^{-1}) \\ R(-,-) = x'y'^{-1}z' = z^2 y^{-1}(x^{-2}y + x^2 y^{-1}) \\ R(+,-) = x'^{-1}z' = z^2(y + y^{-1}) \\ R(-,+) = x'^{-1}z' = z^2(y + y^{-1}) \end{cases}. \tag{V.15}$$

The last two equations are identical, resulting in three equations in three unknowns, with the solutions,

$$\begin{cases} z'^4 = z^8(x^2 y + x^{-2}y^{-1})(x^{-2}y + x^2 y^{-1})(y + y^{-1})^2 \\ y'^2 = y^2 \dfrac{x^2 y + x^{-2}y^{-1}}{x^{-2}y + x^2 y^{-1}} \\ x'^4 = \dfrac{(x^2 y + x^{-2}y^{-1})(x^{-2}y + x^2 y^{-1})}{(y + y^{-1})^2} \end{cases}. \tag{V.16}$$

Taking the logarithms, we find recursion relations of the form

$$\begin{cases} g' = 2g + \delta g(K,h) \\ h' = h + \delta h(K,h) \\ K' = K'(K,h) \end{cases}. \tag{V.17}$$

The parameter g is just an additive constant to the Hamiltonian. It does not effect the probabilities and hence does not appear in the recursion relations for K and h. $\delta g(K,h)$ is the contribution of the decimated spins to the overall free energy.

1. *Fixed points:* The $h = 0$ subspace is closed by symmetry, and it can be checked that for $y = 1$ eqs.(V.16) imply $y' = 1$, and

$$e^{4K'} = \left(\frac{e^{2K} + e^{-2K}}{2}\right)^2, \qquad \Longrightarrow \qquad K' = \frac{1}{2}\ln\cosh 2K. \tag{V.18}$$

The recursion relation for K has the following fixed points:

(a) An infinite temperature fixed point at $K^* = 0$, which is the *sink* for the disordered phase. If K is small, $K' \approx \ln(1 + 4K^2/2)/2 \approx K^2$, is even smaller, indicating that this is a *stable* fixed point with zero correlation length.

(b) A zero temperature fixed point at $K^* \to \infty$, describing the ordered phase. For a large but finite K, the renormalized interaction $K' \approx \ln\left(e^{2K}/2\right)/2 \approx K - \ln 2/2$, is somewhat smaller. This fixed point is thus unstable with an infinite correlation length.

Clearly any finite interaction renormalizes to zero, indicating that the one dimensional chain is always disordered at sufficiently long length scales. The absence of any other fixed point is apparent by noting that the recursion relation eq.(V.18) can alternatively be written as $\tanh K' = (\tanh K)^2$.

2. *Flow diagrams* indicate that in the presence of a field h, all flows terminate on a line of fixed points with $K^* = 0$ and arbitrary h^*. These fixed points describe *independent* spins and all have zero correlation length. The flows originate from the fixed point at $K^* = h^* = 0$ which has two unstable directions in the (K, h) parameter space.

3. *Linearizing* the recursion relations around this fixed point ($x \to \infty$) yields,

$$\begin{cases} x'^4 \approx x^4/4 \\ y'^2 \approx y^4 \end{cases}, \qquad \Longrightarrow \qquad \begin{cases} e^{-K'} = \sqrt{2}e^{-K} \\ h' = 2h \end{cases}. \tag{V.19}$$

We can thus regard e^{-K} and h as scaling fields. Since $\xi' = \xi/2$, the correlation length in the vicinity of the fixed point satisfies the homogeneous form ($b = 2$)

$$\begin{aligned} \xi\left(e^{-K}, h\right) &= 2\xi\left(\sqrt{2}e^{-K}, 2h\right) \\ &= 2^\ell \xi\left(2^{\ell/2}e^{-K}, 2^\ell h\right). \end{aligned} \tag{V.20}$$

The second equation is obtained by repeating the RG procedure ℓ times. Choosing ℓ such that $2^{\ell/2}e^{-K} \approx 1$, we obtain the scaling form

$$\xi\left(e^{-K}, h\right) = e^{2K} g_\xi\left(he^{2K}\right). \tag{V.21}$$

The correlation length diverges on approaching $T = 0$ for $h = 0$. However, its divergence is not a power law of temperature. There is thus an ambiguity in identifying the exponent ν related to the choice of the measure of vicinity to $T = 0$ ($1/K$ or e^{-K}).

The hyperscaling assumption states that the singular part of the free energy in d dimensions is proportional to ξ^{-d}. Hence we expect

$$f_{\text{sing.}}(K,h) \propto \xi^{-1} = e^{-2K} g_f\left(he^{2K}\right). \tag{V.22}$$

At zero field, the magnetization is always zero, while the susceptibility behaves as

$$\chi(K) \sim \left.\frac{\partial^2 f}{\partial^2 h}\right|_{h=0} \sim e^{2K}. \tag{V.23}$$

On approaching zero temperature, the divergence of the susceptibility is proportional to that of the correlation length. Using the general forms, $\langle s_i, s_{i+x}\rangle \sim e^{-x/\xi}/x^{d-2+\eta}$, and $\chi \sim \int d^d\mathbf{x} < s_0 s_{\mathbf{x}} >_c \sim \xi^{2-\eta}$, we conclude that $\eta = 1$.

The one dimensional Ising model can be solved exactly by a *transfer matrix method* which will be described in more detail in the recitations. The results of the direct solution are in full agreement with those of the RG. The transfer matrix approach can be applied to any one dimensional chain with nearest neighbor interactions, since the partition function can be written as

$$Z = \sum_{\{s_i\}} \exp\left[\sum_{i=1}^{N} B(s_i, s_{i+1})\right] = \sum_{\{s_i\}} \prod_{i=1}^{N} e^{B(s_i, s_{i+1})}. \tag{V.24}$$

Defining a *transfer matrix*,

$$\langle s_i|T|s_j\rangle = e^{B(s_i,s_j)}, \tag{V.25}$$

and with *periodic boundary conditions*, we obtain

$$Z = \text{tr}\left[T^N\right] \approx \lambda_{\max}^N. \tag{V.26}$$

Note that for $N \to \infty$, the trace is dominated by the largest eigenvalue $\lambda_{\max}$. *Frobenius's theorem* states that for any finite matrix with finite positive elements, the largest eigenvalue is always non-degenerate. This implies that $\lambda_{\max}$ and Z are analytic functions of the parameters appearing in B, and that one dimensional models can exhibit singularities (and hence a phase transition) only at zero temperature (when some matrix elements become infinite). The transfer matrix method also provides an alternative RG scheme for all such one dimensional chains. For decimation by a factor b, we can use $Z = \text{tr}\left[\left(T^b\right)^{N/b}\right]$ to construct the rescaled bond energy as

$$e^{B(s'_i,s'_j)} \equiv \left\langle s'_i|T'|s'_j\right\rangle = \left\langle s'_i|T^b|s'_j\right\rangle. \tag{V.27}$$

V.C The Niemeijer–van Leeuwen Cumulant Approximation

Unfortunately, the decimation procedure cannot be performed exactly in higher dimensions. For example, the square lattice can be divided into two sublattices. For an RG with $b = \sqrt{2}$, we can start by decimating the spins on one sublattice. The interactions between the four spins surrounding each decimated spin are obtained by generalizing eq.(V.13). If initially $h = g = 0$, we obtain

$$R(\sigma_1', \sigma_2', \sigma_3', \sigma_4') = \sum_{s=\pm 1} e^{Ks(\sigma_1'+\sigma_2'+\sigma_3'+\sigma_4')} = 2\cosh\left[K(\sigma_1' + \sigma_2' + \sigma_3' + \sigma_4')\right]. \qquad \text{(V.28)}$$

Clearly the four spins appear symmetrically in the above expression, and hence are subject to the same two body interaction. This implies that new interactions along the diagonals of the renormalized lattice are also generated, and the nearest neighbor form of the original Hamiltonian is not preserved. There is also a four point interaction, and

$$R = \exp\left[g' + K'(\sigma_1'\sigma_2' + \sigma_2'\sigma_3' + \sigma_3'\sigma_4' + \sigma_4'\sigma_1' + \sigma_1'\sigma_3' + \sigma_2'\sigma_4') + K_4'\sigma_1'\sigma_2'\sigma_3'\sigma_4'\right]. \qquad \text{(V.29)}$$

The number (and range) of new interactions increases with each RG step, and some truncating approximation is necessary. Two such schemes are described in the following sections.

One of the earliest approaches was developed by Niemeijer and van Leeuwen (NvL) for treating the Ising model on a *triangular lattice*, subject to the usual nearest neighbor Hamiltonian $-\beta\mathcal{H} = K\sum_{\langle ij\rangle}\sigma_i\sigma_j$. The original lattice sites are grouped into *cells* of three spins (e.g. in alternating up pointing triangles). Labelling the three spins in cell α as $\{\sigma_\alpha^1, \sigma_\alpha^2, \sigma_\alpha^3\}$, we can use a *majority rule* to define the renormalized cell spin as

$$\sigma_\alpha' = \text{sign}\left[\sigma_\alpha^1 + \sigma_\alpha^2 + \sigma_\alpha^3\right]. \qquad \text{(V.30)}$$

(There is no ambiguity in the rule for any odd number of sites, and the renormalized spin is two–valued.) The renormalized interactions corresponding to the above map are obtained from the constrained sum

$$e^{-\beta\mathcal{H}'[\sigma_\alpha']} = \sum_{\{\sigma_\alpha^i \mapsto \sigma_\alpha'\}}{}' e^{-\beta\mathcal{H}[\sigma_\alpha^i]} \quad . \qquad \text{(V.31)}$$

To truncate the number of interactions in the renormalized Hamiltonian, NvL introduced a perturbative scheme by setting $\beta\mathcal{H} = \beta\mathcal{H}_0 + \mathcal{U}$. The unperturbed Hamiltonian

$$-\beta\mathcal{H}_0 = K\sum_{\alpha}\left(\sigma_\alpha^1\sigma_\alpha^2 + \sigma_\alpha^2\sigma_\alpha^3 + \sigma_\alpha^3\sigma_\alpha^1\right), \tag{V.32}$$

involves only *intra–cell interactions*. Since the cells are decoupled, this part of the Hamiltonian can be treated exactly. The remaining *inter–cell interactions* are treated as a perturbation

$$-\mathcal{U} = K\sum_{<\alpha,\beta>}\left(\sigma_\beta^{(1)}\sigma_\alpha^{(2)} + \sigma_\beta^{(1)}\sigma_\alpha^{(3)}\right). \tag{V.33}$$

The sum is over all neighboring cells, each connected by two bonds. (The actual spins involved depend on the relative orientations of the cells.) Eq.(V.31) is now evaluated perturbatively as

$$e^{-\beta\mathcal{H}'[\sigma'_\alpha]} = {\sum_{\{\sigma_\alpha^i \mapsto \sigma'_\alpha\}}}' e^{-\beta\mathcal{H}_0[\sigma_\alpha^i]}\left[1 - \mathcal{U} + \frac{\mathcal{U}^2}{2} - \cdots\right]. \tag{V.34}$$

The renormalized Hamiltonian is given by the cumulant series

$$\beta\mathcal{H}'[\sigma'_\alpha] = -\ln Z_0[\sigma'_\alpha] + \langle\mathcal{U}\rangle_0 - \frac{1}{2}\left(\langle\mathcal{U}^2\rangle_0 - \langle\mathcal{U}\rangle_0^2\right) + \mathcal{O}(\mathcal{U}^3), \tag{V.35}$$

where $\langle\rangle_0$ refers to the expectation values with respect to $\beta\mathcal{H}_0$, with the restriction of fixed $[\sigma'_\alpha]$, and Z_0 is the corresponding partition function.

To proceed, we construct a table of all possible configurations of spins within a cell, their renormalized value, and contribution to the cell energy:

σ'_α	σ_α^1	σ_α^2	σ_α^3	$\exp\left[-\beta\mathcal{H}_0\right]$
$+$	$+$	$+$	$+$	e^{3K}
$+$	$-$	$+$	$+$	e^{-K}
$+$	$+$	$-$	$+$	e^{-K}
$+$	$+$	$+$	$-$	e^{-K}
$-$	$-$	$-$	$-$	e^{3K}
$-$	$+$	$-$	$-$	e^{-K}
$-$	$-$	$+$	$-$	e^{-K}
$-$	$-$	$-$	$+$	e^{-K}

The restricted partition function is the product of contributions from the independent cells,

$$Z_0[\sigma'_\alpha] = \prod_\alpha \left[{\sum_{\{\sigma^i_\alpha \mapsto \sigma'_\alpha\}}}' e^{K(\sigma^1_\alpha\sigma^2_\alpha + \sigma^2_\alpha\sigma^3_\alpha + \sigma^3_\alpha\sigma^1_\alpha)} \right] = \left(e^{3K} + 3e^{-K}\right)^{N/3}. \tag{V.36}$$

It is *independent* of $[\sigma'_\alpha]$, thus contributing an additive constant to the Hamiltonian. The first cumulant of the interaction is

$$-\langle \mathcal{U} \rangle_0 = K \sum_{<\alpha,\beta>} \left[\left\langle \sigma^1_\beta \right\rangle_0 \left\langle \sigma^2_\alpha \right\rangle_0 + \left\langle \sigma^1_\beta \right\rangle_0 \left\langle \sigma^3_\alpha \right\rangle_0 \right] = 2K \sum_{<\alpha,\beta>} \left\langle \sigma^i_\alpha \right\rangle_0 \left\langle \sigma^j_\beta \right\rangle_0, \tag{V.37}$$

where we have taken advantage of the equivalence of the three spins in each cell. Using the table, we can evaluate the restricted average of site spins as

$$\left\langle \sigma^i_\alpha \right\rangle_0 = \left\{ \begin{array}{ll} \dfrac{+e^{3K} - e^{-K} + 2e^{-K}}{e^{3K} + 3e^{-K}} & \text{for} \quad \sigma'_\alpha = +1 \\ \dfrac{-e^{3K} + e^{-K} - 2e^{-K}}{e^{3K} + 3e^{-K}} & \text{for} \quad \sigma'_\alpha = -1 \end{array} \right\} \equiv \frac{e^{3K} + e^{-K}}{e^{3K} + 3e^{-K}} \, \sigma'_\alpha \, . \tag{V.38}$$

Substituting in eq.(V.37) leads to

$$-\beta \mathcal{H}'[\sigma'_\alpha] = \frac{N}{3} \ln\left(e^{3K} + 3e^{-K}\right) + 2K \left(\frac{e^{3K} + e^{-K}}{e^{3K} + 3e^{-K}} \right)^2 \sum_{\langle \alpha\beta \rangle} \sigma'_\alpha \sigma'_\beta + \mathcal{O}(\mathcal{U}^2). \tag{V.39}$$

At this order, the renormalized Hamiltonian involves only nearest neighbor interactions, with the recursion relation

$$K' = 2K \left(\frac{e^{3K} + e^{-K}}{e^{3K} + 3e^{-K}} \right)^2 . \tag{V.40}$$

1. Eq.(V.40) has the following *fixed points:*

(a) The high temperature sink at $K^* = 0$. If $K \ll 1$, $K' \approx 2K(2/4)^2 = K/2 < K$, i.e. this fixed point is *stable*, and has zero correlation length.

(b) The low temperature sink at $K^* = \infty$. If $K \gg 1$, then $K' \approx 2K > K$, i.e. unlike the one dimensional case, this fixed point is also stable with zero correlation length.

(c) Since both of the above fixed points are unstable, there must be at least one stable fixed point at finite $K' = K = K^*$. From eq.(V.40), the fixed point position satisfies

$$\frac{1}{\sqrt{2}} = \frac{e^{3K^*} + e^{-K^*}}{e^{3K^*} + 3e^{-K^*}}, \quad \Longrightarrow \quad \sqrt{2}e^{4K^*} + \sqrt{2} = e^{4K^*} + 3. \tag{V.41}$$

The fixed point value

$$K^* = \frac{1}{4}\ln\left(\frac{3-\sqrt{2}}{\sqrt{2}-1}\right) \approx 0.3356, \tag{V.42}$$

can be compared to the exactly known value of 0.2747 for the triangular lattice.

2. Linearizing the recursion relation around the non-trivial fixed point yields,

$$\left.\frac{\partial K'}{\partial K}\right|_{K^*} = 2\left(\frac{e^{4K^*}+1}{e^{4K^*}+3}\right)^2 + 32K^* e^{4K^*}\frac{(e^{4K^*}+1)}{(e^{4K^*}+3)^3} \approx 1.624. \tag{V.43}$$

The fixed point is indeed unstable as required by the continuity of flows. This RG scheme removes 1/3 of the degrees of freedom, and corresponds to $b = \sqrt{3}$. The thermal eigenvalue is thus obtained as

$$b^{y_t} = \left.\frac{\partial K'}{\partial K}\right|_{K^*}, \quad \Longrightarrow \quad y_t \approx \frac{\ln(1.624)}{\ln(\sqrt{3})} \approx 0.883. \tag{V.44}$$

This can be compared to the exactly known value of $y_t = 1$, for the two dimensional Ising model. It is certainly better than the mean-field (Gaussian) estimate of $y_t = 2$. From this eigenvalue we can estimate the exponents

$$\nu = 1/y_t \approx 1.13 \quad (1), \quad \text{and} \quad \alpha = 2 - 2/y_t = -0.26 \quad (0),$$

where the exact values are given in the brackets.

3. To complete the calculation of exponents, we need the *magnetic eigenvalue* y_h, obtained after adding a magnetic field to the Hamiltonian, i.e. from

$$\beta\mathcal{H} = \beta\mathcal{H}_0 + \mathcal{U} - h\sum_i \sigma_\alpha^i \quad . \tag{V.45}$$

Since the fixed point occurs for $h^* = 0$, the added term can also be treated perturbatively, and to the lowest order

$$\beta\mathcal{H}' = \beta\mathcal{H}_0 + \langle\mathcal{U}\rangle_0 - h\sum_\alpha \left\langle(\sigma_\alpha^1 + \sigma_\alpha^2 + \sigma_\alpha^3)\right\rangle_0, \tag{V.46}$$

where the spins are grouped according to their cells. Using eq.(V.38),

$$\beta\mathcal{H}' = \ln Z_0 + K'\sum_{<\alpha,\beta>}\sigma'_\alpha\sigma'_\beta - 3h\sum_\alpha\left(\frac{e^{3K}+e^{-K}}{e^{3K}+3e^{-K}}\right)\sigma'_\alpha, \tag{V.47}$$

thus identifying the renormalized magnetic field as

$$h' = 3h \left(\frac{e^{3K} + e^{-K}}{e^{3K} + 3e^{-K}} \right). \tag{V.48}$$

In the vicinity of the unstable fixed point

$$b^{y_h} = \left. \frac{\partial h'}{\partial h} \right|_{K^*} = 3 \, \frac{e^{4K^*} + 1}{e^{4K^*} + 3} = \frac{3}{\sqrt{2}}, \tag{V.49}$$

and

$$y_h = \frac{\ln\left(3/\sqrt{2}\right)}{\ln\left(\sqrt{3}\right)} \approx 1.37. \tag{V.50}$$

This is lower than the exact value of $y_h = 1.875$. (The Gaussian value of $y_h = 2$ is closer to the correct result in this case.)

4. NvL carried out the approach to the second order in $\mathcal{U}$. At this order two additional interactions over further neighbor spins are generated. The recursion relations in this three parameter space have a non-trivial fixed point with one unstable direction. The resulting eigenvalue of $y_t = 1.053$, is tantalizingly close to the exact value of 1, but this agreement is probably accidental.

V.D The Migdal–Kadanoff Bond Moving Approximation

Consider a $b = 2$ RG for the Ising model on a square lattice, in which every other spin along each lattice direction is decimated. As noted earlier, such decimation generates new interactions between the remaining spins. One way of overcoming this difficulty is to simply remove the bonds not connected to the retained spins. The renormalized spins are then connected to their nearest neighbors by two successive bonds. Clearly after decimation, the renormalized bond is given by the recursion relation in eq.(V.18), characteristic of a one dimensional chain. The approximation of simply removing the unwanted bonds weakens the system to the extent that it behaves one dimensionally. This is remedied by using the unwanted bonds to strengthen those that are left behind. The spins that are retained are now connected by a pair of double bonds (of strength $2K$), and the decimation leads to

$$K' = \frac{1}{2} \ln \cosh(2 \times 2K) \, . \tag{V.51}$$

1. Fixed points of this recursion relation are located at

(a) $K^* = 0$: For $K \ll 1$, $K' \approx \ln(1 + 8K^2)/2 \approx 4K^2 \ll K$, i.e. this fixed point is stable.

(b) $K^* \to \infty$: For $K \gg 1$, $K' \approx \ln(e^{4K}/2)/2 \approx 2K \gg K$, indicating that the low temperature sink is also stable.

(c) The domains of attractions of the above sinks are separated by a third fixed point at

$$e^{2K^*} = \frac{e^{4K^*} + e^{-4K^*}}{2}, \quad \Longrightarrow \quad K^* \approx 0.305, \tag{V.52}$$

which can be compared with the exact value of $K_c \approx 0.441$.

2. Linearizing eq.(V.51) near the fixed point gives

$$b^{y_t} = \left.\frac{\partial K'}{\partial K}\right|_{K^*} = 2\tanh 4K^* \approx 1.6786, \quad \Longrightarrow \quad y_t \approx 0.747, \tag{V.53}$$

compared to the exact value of $y_t = 1$.

The bond moving procedure can be extended to *higher dimensions*. For a hypercubic lattice in d-dimensions, the bond moving step strengthens each bond by a factor of 2^{d-1}. After decimation, the recursion relation is

$$K' = \frac{1}{2}\ln\cosh\left[2 \times 2^{d-1}K\right]. \tag{V.54}$$

The high and low temperature sinks at $K^* = 0$ and $K^* \to \infty$, are stable, since

$$K \ll 1, \quad \Longrightarrow \quad K' \approx \frac{1}{2}\ln(1 + 2^{2d-1}K^2) \approx 2^{2(d-1)}K^2 \ll K, \tag{V.55}$$

and

$$K \gg 1, \quad \Longrightarrow \quad K' \approx \frac{1}{2}\ln\frac{e^{2^d K}}{2} \approx 2^{d-1}K \gg K. \tag{V.56}$$

(Note that the above result correctly identifies the lower critical dimension of the Ising model, in that the low temperature sink is stable only for $d > 1$.) The intervening fixed point has an eigenvalue

$$2^{y_t} = \left.\frac{\partial K'}{\partial K}\right|_{K^*} = 2^{d-1}\tanh\left(2^d K^*\right). \tag{V.57}$$

The resulting values of $K^* \approx 0.065$ and $y_t \approx 0.934$ for $d = 3$, can be compared with the known values of $K_c \approx 0.222$ and $y_t \approx 1.59$ on a cubic lattice. Clearly the approximation gets worse at higher dimensions. (It fails to identify an upper critical dimension, and as $d \to \infty$, $K^* \to 2^{2(1-d)}$ and $y_t \to 1$.)

The Migdal–Kadanoff scheme can also be applied to more general spin systems. For a one dimensional model described by the set of interactions $\{K\}$, the transfer matrix method in eq.(V.27) gives the recursion relations as

$$T'_b(\{K'\}) = T(\{K\})^b.$$

For a d-dimensional lattice, the bond moving step strengthens each bond by a factor of b^{d-1}, and the generalized Migdal–Kadanoff recursion relations are

$$T'_b(\{K'\}) = T(\{b^{d-1}K\})^b. \tag{V.58}$$

The above equations can be used as a quick way of estimating phase diagrams and exponents. The procedure is exact in $d = 1$, and does progressively worse in higher dimensions. It thus compliments mean–field (saddle point) approaches that are more reliable in higher dimensions. Unfortunately, it is not possible to develop a systematic scheme to improve upon its results. The RG procedure also allows evaluation of free energies, heat capacities, and other thermodynamic functions. One possible worry is that the approximations used to construct RG schemes may result in unphysical behavior, e.g. negative values of response functions C and χ. In fact most of these recursion relations (e.g. eq.(V.58)) are exact on *hierarchical* (Berker) lattices. The realizability of such lattices ensures that there are no unphysical consequences of the recursion relations.

VI. Series Expansions

VI.A Low-temperature expansions

Lattice models can also be studied by series expansions. Such expansions start with certain exactly solvable limits, and typically represent perturbations around such limits by graphs on the lattice. High temperature expansions are described in the next section. Here we describe the *low temperature* expansion for the Ising model with a Hamiltonian $-\beta\mathcal{H} = K\sum_{\langle i,j\rangle}\sigma_i\sigma_j$, on a d-dimensional hypercubic lattice. The ground state with $K = \beta J > 0$ is ferromagnetic, e.g. with $\sigma_i = +1$ for all spins. A series expansion for the partition function is obtained by including low energy excitations around this state. The lowest energy excitation is a single overturned spin. Any of N sites can be chosen for this excitation, which has an energy cost of $2K \times 2d$, with respect to the ground state. The next lowest energy excitation corresponds to a dimer of negative spins with energy cost of $2K \times (4d-2)$, and a multiplicity of $N \times d$ (there are d possible orientations for the dimer). The first few terms in the expansion give

$$Z = 2e^{NdK}\left[1 + Ne^{-4dK} + dNe^{-4(2d-1)K} + \frac{N(N-2d-1)}{2}e^{-8dK} + \cdots\right]. \qquad \text{(VI.1)}$$

The fourth term comes from flipping two disjoint single spins. The zeroth order term comes from the ground state, which has a two fold degeneracy. The overall factor of 2 is insignificant in the $N \to \infty$ limit, and

$$Z \simeq e^{NdK} \sum_{\text{droplets of } \ominus \text{ spins}} e^{-2K\times \text{ boundary of droplet}}. \qquad \text{(VI.2)}$$

The free energy per site is obtained from the series,

$$\begin{aligned} -\beta f = \frac{\ln Z}{N} &= dK + \frac{1}{N}\ln\left[1 + Ne^{-4dK} + dNe^{-4(2d-1)K} + \frac{N(N-2d-1)}{2}e^{-8dK} + \cdots\right] \\ &= dK + e^{-4dK} + de^{-4(2d-1)K} - \frac{(2d+1)}{2}e^{-8dK} + \cdots. \end{aligned} \qquad \text{(VI.3)}$$

Note that there is an explicit cancellation of the term proportional to N^2 in the expansion for Z. Such higher N dependances result from *disconnected* diagrams with several disjoint

droplets. Extensivity of the free energy ensures that these terms are cancelled by products of connected graphs. The energy per site is then obtained from

$$\begin{aligned}\frac{E}{N} &= -\frac{\partial}{\partial\beta}\left(\frac{\ln Z}{N}\right) = -J\frac{\partial}{\partial K}\left(\frac{\ln Z}{N}\right) \\ &= -J\left[d - 4de^{-4dK} - 4d(2d-1)e^{-4(2d-1)K} + 4d(2d+1)e^{-8dK} + \cdots\right],\end{aligned} \tag{VI.4}$$

and the heat capacity is proportional to

$$\begin{aligned}\frac{C}{Nk_B} =& \frac{1}{Nk_B}\frac{\partial E}{\partial T} = -\frac{K^2}{NJ}\frac{\partial E}{\partial K} \\ =& K^2\left[16d^2e^{-4dK} + 16d(2d-1)^2e^{-4(2d-1)K} - 32d^2(2d+1)e^{-8dK} + \cdots\right].\end{aligned} \tag{VI.5}$$

Can such series be used to extract the critical coupling K_c, and more importantly, the singularities associated with the disordering transition? Suppose that we have identified a number of terms in a series $C = \sum_{\ell=0}^{\infty} a_\ell u^\ell$. From the expected divergence of the heat capacity, we expect an asymptotic expansion of the form

$$C \simeq A\left(1 - \frac{u}{u_c}\right)^{-\alpha} = A\left[1 + \frac{\alpha}{u_c}u + \frac{\alpha(\alpha+1)}{2!u_c^2}u^2 + \cdots + \frac{\alpha(\alpha+1)\cdots(\alpha+\ell-1)}{\ell!u_c^\ell}u^\ell\cdots\right]. \tag{VI.6}$$

The above singular form is characterized by the three parameters A, u_c, and α. We can try to extract these parameters from the calculated coefficients in the series by requiring that they match at large ℓ, i.e. by fitting the ratio of successive terms to

$$\frac{a_\ell}{a_{\ell-1}} \simeq \left(\frac{\alpha+\ell-1}{\ell u_c}\right) = u_c^{-1}\left(1 + \frac{\alpha-1}{\ell}\right). \tag{VI.7}$$

Thus a plot of $a_\ell/a_{\ell-1}$ versus $1/\ell$ should be a straight line with intercept u_c^{-1}, and slope $u_c^{-1}(\alpha-1)$. Note, however, that adding a finite sum $\sum_{\ell=0}^{\ell_m} d_\ell u^\ell$ does not change the asymptotic singular form, but essentially renders the first ℓ_m terms useless in determining α and u_c^{-1}. There is thus no a priori guarantee that such a fitting procedure will succeed with a finite number of coefficients. In practice, this procedure works very well and very good estimates of critical exponents in $d = 3$ (e.g. $\alpha = 0.105 \pm 0.007$) are obtained in this way by including a rather large number of terms.

The three terms calculated for the heat capacity in eq.(VI.5) have different signs, unlike those of eq.(VI.6). As this continues at higher orders in e^{-K}, the ratio fitting procedure described above cannot be used directly. The alternation of signs usually signifies singularities in the *complex* $z = e^{-K}$ plane, closer to the origin than the critical point of

interest at real $z_c = e^{-K_c}$. If it is possible to construct a mapping $u(z)$ on the complex plane such that the spurious singularities are pushed further away than $u_c = u(z_c)$, then the ratio method can be used. In the case of low temperature series, the choice of $u = \tanh K$ achieves this goal. (As we shall demonstrate shortly, $\tanh K$ is also the natural variable for the high temperature expansion.) Quite sophisticated methods, such as *Padé approximants*, have been developed for analyzing the singular behavior of series.

Low temperature expansions can be similarly constructed for other *discrete* spin systems, such as the Potts model. For *continuous* spins, the low energy excitations are Goldstone modes, and the perturbation series cannot be represented in terms of lattice graphs. The low temperature description in this case starts with the Gaussian treatment of the Goldstone modes. Further terms in the series involve interactions between such modes, and a corresponding calculation will be performed later on.

VI.B High-temperature Expansions

High temperature expansions work equally well for discrete and continuous spin systems. The basic idea is to start with *independent* spins, and expand the partition function in powers of $\beta = (k_B T)^{-1}$, i.e.

$$Z = \mathrm{tr}\left(e^{-\beta\mathcal{H}}\right) = \mathrm{tr}\left[1 - \beta\mathcal{H} + \frac{\beta^2\mathcal{H}^2}{2} - \cdots\right], \tag{VI.8}$$

and

$$\frac{\ln Z}{N} = \frac{\ln Z_0}{N} - \beta\frac{\langle\mathcal{H}\rangle_0}{N} + \frac{\beta^2}{2}\frac{\langle\mathcal{H}^2\rangle_0 - \langle\mathcal{H}\rangle_0^2}{N} - \cdots. \tag{VI.9}$$

The averages $\langle\rangle_0$ are calculated over non-interacting spins. For the Ising model, it is more convenient to organize the expansion in powers of $\tanh K$ as follows. Since $(\sigma_i\sigma_j)^2 = 1$, the Boltzmann factor for each bond can be written as

$$e^{K\sigma_i\sigma_j} = \frac{e^K + e^{-K}}{2} + \frac{e^K - e^{-K}}{2}\sigma_i\sigma_j = \cosh K\,(1 + t\sigma_i\sigma_j)\,, \tag{VI.10}$$

where $t \equiv \tanh K$ is a good high temperature expansion parameter. Applying this transformation to each bond of the lattice results in

$$Z = \sum_{\{\sigma_i\}} e^{K\sum_{\langle i,j\rangle}\sigma_i\sigma_j} = (\cosh K)^{\text{number of bonds}} \sum_{\{\sigma_i\}}\prod_{\langle i,j\rangle}(1 + t\sigma_i\sigma_j). \tag{VI.11}$$

For N_b bonds on the lattice, the above product generates 2^{N_b} terms, which can be represented diagrammatically by drawing a line connecting sites i and j for each factor of $t\sigma_i\sigma_j$. Note that there can at most be one such line for each lattice bond, which is either empty or occupied. This is a major simplification, resulting from the use of t, rather than K, as the expansion parameter. Each site now obtains a factor of $\sigma_i^{p_i}$, where p_i is the number of occupied bonds emanating from i. Summing over the two possible values $\sigma_i = \pm 1$, gives a factor of 2 if p_i is even, and 0 is p_i is odd. Thus, the only graphs that survive the sum have an even number of lines passing through each site. The resulting graphs are collections of closed paths on the lattice, and

$$Z = 2^N \times (\cosh K)^{N_b} \sum_{\text{All closed graphs}} t^{\text{ number of bonds in the graph}}. \tag{VI.12}$$

For a d-dimensional hypercubic lattice, the smallest closed graph is a square of 4 bonds which has $d(d-1)/2$ possible orientations. As the next graph has 6 bonds,

$$Z = 2^N (\cosh K)^{dN} \left[1 + \frac{d(d-1)N}{2}\, t^4 + d(d-1)(2d-3)\, t^6 + \cdots\right], \tag{VI.13}$$

and

$$\frac{\ln Z}{N} = \ln 2 + d \ln\cosh K + \frac{d(d-1)}{2}\, t^4 + \cdots. \tag{VI.14}$$

In the following sections, we shall employ high temperature expansions not as a numerical tool, but to establish the following: (a) Exact solution of the Ising model in $d = 1$. (b) The duality relating models at low and high temperatures. (c) The validity of the Gaussian model in high dimensions. (d) Exact solution of the Ising model in $d = 2$.

VI.C Exact Solution of the One Dimensional Ising Model

The graphical method provides a rapid way of solving the Ising model at zero field in $d = 1$. We can compare and contrast the solutions on chains with open and closed (periodic) boundary conditions.

1. *An open chain* of N sites has $N_b = N - 1$ bonds. It is impossible to draw any closed graphs on such a lattice, and hence

$$Z = 2^N \cosh K^{N-1} \times 1, \quad \Longrightarrow \quad \frac{\ln Z}{N} = \ln[2\cosh K] - \frac{\ln[\cosh K]}{N}. \tag{VI.15}$$

The same method can also be used to calculate the correlation function $\langle \sigma_m \sigma_n \rangle$, since

$$\langle \sigma_m \sigma_n \rangle = \frac{1}{Z} \sum_{\{\sigma_i\}} e^{K \sum_{\langle i,j \rangle} \sigma_i \sigma_j} \sigma_m \sigma_n = \frac{2^N (\cosh K)^{N-1}}{Z} \sum_{\{\sigma_i\}} \sigma_m \sigma_n \prod_{\langle i,j \rangle} (1 + t \sigma_i \sigma_j). \tag{VI.16}$$

The terms in the numerator involve an additional factor of $\sigma_m \sigma_n$. To get a finite value after summing over $\sigma_m = \pm 1$ and $\sigma_n = \pm 1$, we have to examine graphs with an odd number of bonds emanating from these *external* sites. The only such graph for the open chain is one that directly connects these two sites, and results in

$$\langle \sigma_m \sigma_n \rangle = t^{|m-n|} = e^{-|m-n|/\xi}, \quad \text{with} \quad \xi = -\frac{1}{\ln \tanh K}. \tag{VI.17}$$

These results are in agreement with the RG conclusions of sec.V.B; the correlation length diverges as e^{2K} for $K \to \infty$, and there is no power law modifying the exponential decay of correlations.

2. *A closed chain* has the same number of sites and bonds, N. It is now possible to draw a closed graph that circles the whole chain, and

$$\begin{aligned} Z = (2 \cosh K)^N \left[1 + t^N\right] &= 2^N \left(\cosh K^N + \sinh K^N\right), \\ \Longrightarrow \qquad \frac{\ln Z}{N} &= \ln(2 \cosh K) + \frac{\ln\left[1 + t^N\right]}{N}. \end{aligned} \tag{VI.18}$$

The difference between the free energies of closed and open chains vanishes in the thermodynamic limit. The correction to the extensive free energy, $N \ln(2 \cosh K)$, is of the order of $1/N$ for the open chain, and can be regarded as the surface free energy. There is no such correction for the closed chain, which has no boundaries; there is instead an exponential term t^N. The correlation function can again be calculated from eq.(VI.16). There are two paths connecting the points m and n, and

$$\langle \sigma_m \sigma_n \rangle = \frac{t^{|m-n|} + t^{N-|m-n|}}{1 + t^N}. \tag{VI.19}$$

Note that the final answer is symmetric with respect to the two ways of measuring the distance between the two sites m and n.

VI.D Self–Duality in the Two Dimensional Ising Model

Kramers and Wannier discovered a hidden symmetry that relates the properties of the Ising model on the square lattice at low and high temperatures. One way of obtaining this symmetry is to compare the high and low temperature series expansions of the problem. The low temperature expansion has the form

$$\begin{aligned} Z =& e^{2NK}\left[1+Ne^{-4\times 2K}+2Ne^{-6\times 2K}+\cdots\right] \\ =& e^{2NK}\sum_{\text{Islands of }(-)\text{ spins}} e^{-2K\times\text{perimeter of island}} \quad . \end{aligned} \tag{VI.20}$$

The high temperature series is

$$\begin{aligned} Z =& 2^N\cosh K^{2N}\left[1+N\tanh K^4+2N\tanh K^6+\cdots\right] \\ =& 2^N\cosh K^{2N}\sum_{\text{graphs with 2 or 4 lines per site}} \tanh K^{\,\text{length of graph}} \quad . \end{aligned} \tag{VI.21}$$

As the boundary of any island of spins serves as an acceptable graph (and vice versa), there is a one to one correspondence between the two series. Defining a function g to indicate the logarithm of the above series, the free energy is given by

$$\frac{\ln Z}{N} = 2K + g\left(e^{-2K}\right) = \ln 2 + 2\ln\cosh K + g\left(\tanh K\right). \tag{VI.22}$$

The arguments of g in the above equation are related by the *duality* condition

$$e^{-2\tilde{K}} \leftrightarrow \tanh K, \qquad \Longrightarrow \qquad \tilde{K} = D(K) \equiv -\frac{1}{2}\ln\tanh K\,. \tag{VI.23}$$

The function g (which contains the singular part of the free energy) must have a special symmetry that relates its values for dual arguments. (For example the function $f(x) = x/(1+x^2)$ equals $f(x^{-1})$, establishing a duality between the arguments at x and x^{-1}.) Eq.(VI.23) has the following properties:

1. Low temperatures are mapped to high temperatures, and vice versa.

2. The mapping connects *pairs* of points since $D(D(K)) = K$. This condition is established by using trigonometric identities to show that

$$\begin{aligned} \sinh 2K =& 2\sinh K\cosh K = 2\tanh K\cosh^2 K \\ =& \frac{2\tanh K}{1-\tanh^2 K} = \frac{2e^{-2\tilde{K}}}{1-e^{-4\tilde{K}}} = \frac{2}{e^{2\tilde{K}}-e^{-2\tilde{K}}} = \frac{1}{\sinh 2\tilde{K}}. \end{aligned} \tag{VI.24}$$

Hence, the dual interactions are symmetrically related by

$$\sinh 2K \cdot \sinh 2\tilde{K} = 1 \quad . \tag{VI.25}$$

3. If the function $g(K)$ is singular at a point K_c, it must also be singular at $\tilde{K}_c$. Since the free energy is expected to be analytic everywhere except at the transition, the critical model must be *self dual*. At the self dual point

$$e^{-2K_c} = \tanh K_c = \frac{1 - e^{-2K_c}}{1 + e^{-2K_c}},$$

which leads to the quadratic equation,

$$e^{-4K_c} + 2e^{-K_c} - 1 = 0, \qquad \Longrightarrow \qquad e^{-2K_c} = -1 \pm \sqrt{2} \quad .$$

Only the positive solution is acceptable, and

$$K_c = -\frac{1}{2}\ln\left(\sqrt{2} - 1\right) = \frac{1}{2}\ln\left(\sqrt{2} + 1\right) = 0.441\cdots. \tag{VI.26}$$

4. As will be explored in the next section and problem sets, it is possible to obtain dual partners for many other spin systems, such as the Potts model, the XY model, etc. While such mappings place useful constraints on the shape of phase boundaries, they generally provide no information on critical exponents. (The self–duality of many two dimensional models does restrict the ratio of critical amplitudes to unity.)

VI.E Dual of the Three Dimensional Ising model

We can attempt to follow the same procedure to search for the dual of the Ising model on a simple cubic lattice. The low temperature series is

$$\begin{aligned} Z =& e^{3NK}\left[1 + Ne^{-2K\times 6} + 3Ne^{-2K\times 10} + \cdots\right] \\ =& e^{3NK} \sum_{\text{Islands of } (-) \text{ spins}} e^{-2K\times \text{area of island's boundary}}. \end{aligned} \tag{VI.27}$$

By contrast, the high temperature series takes the form

$$\begin{aligned} Z =& 2^N \cosh K^{3N}\left[1 + 3N\tanh K^4 + 18N\tanh K^6 + \cdots\right] \\ =& 2^N \cosh K^{3N} \sum_{\text{graphs with 2, 4, or 6 lines per site}} \tanh K^{\text{number of lines}} \quad . \end{aligned} \tag{VI.28}$$

Clearly the two sums are different, and the $3d$ Ising model is not dual to itself. Is there any other Hamiltonian whose high temperature series reproduces the low temperature terms for the $3d$ Ising model? To construct such a model note that:

1. The low temperature terms have the form $e^{-2K\times\text{area}}$, and the area is the sum of faces covered on the cubic lattice. Thus *plaquettes* must replace bonds as the building blocks of the required high temperature series.

2. How should these plaquettes be joined together? The number of bonds next to a site can be anywhere from 3 to 12 while there are only two or four faces adjacent to each bond. This suggests 'glueing' the plaquettes together by placing spins $\tilde{\sigma}_i = \pm 1$, on the *bonds* of the lattice.

3. By analogy to the Ising model, we can construct a partition function,

$$\tilde{Z} = \sum_{\{\tilde{\sigma}_P^i = \pm 1\}} \prod_{\text{plaquettes } P} (1 + \tanh \tilde{K} \tilde{\sigma}_P^1 \tilde{\sigma}_P^2 \tilde{\sigma}_P^3 \tilde{\sigma}_P^4) \propto \sum_{\{\tilde{\sigma}_i\}} e^{\tilde{K} \sum_P \tilde{\sigma}_P^1 \tilde{\sigma}_P^2 \tilde{\sigma}_P^3 \tilde{\sigma}_P^4}, \qquad \text{(VI.29)}$$

where $\tilde{\sigma}_P^i$ are used to denote the 4 dual spins around each plaquette, and $\tilde{K}$ is given by eq.(VI.23). This partition function describes a system dual to the original $3d$ Ising model, in the sense of reproducing its low temperature series. (Some reflection demonstrates that the low temperature expansion of the above partition function reproduces the high temperature expansion of the Ising model.)

Eq.(VI.29) describes a Z_2 *lattice gauge theory.* The general rules for constructing such theories in all dimensions are: **(i)** Place Ising spins $\tilde{\sigma}_i = \pm 1$, on the *bonds* of the lattice. **(ii)** The Hamiltonian is $-\beta\mathcal{H} = K \sum_{\text{all plaquettes}} \prod \tilde{\sigma}_P^i$. In addition to the *global* Ising symmetry, $\tilde{\sigma}_i \to -\tilde{\sigma}_i$, the Hamiltonian has a *local* (gauge) symmetry. To observe this symmetry, select any site and change the signs of spins on all bonds emanating from it. As in each of the faces adjacent to the chosen site two bond spins change sign, their product, and hence the overall energy, is not changed.

There is a rigorous proof (*Elitzur's theorem*) that there can be no spontaneous symmetry breaking for Hamiltonians with a *local* symmetry. The essence of the proof is that even in the presence of a symmetry breaking field h, the energy cost of flipping a spin is finite ($6h$ for the gauge theory on the cubic lattice). Hence the expectation value of spin changes continuously as $h \to 0$. (By contrast, the energy cost of a spin flip in the Ising model grows as Nh.) This theorem presents us with the following paradox: Since the three dimensional Ising model undergoes a phase transition, there must be a singularity in its

partition function, and also that of its dual. How can there be a singularity in the partition function of the three dimensional gauge theory if it does not undergo a spontaneous symmetry breaking?

To resolve this contradiction, Wegner suggested the possibility of a phase transition without a local order parameter. The two phases are then distinguished by the asymptotic behavior of correlation functions. The appropriate correlation function must be invariant under the local gauge transformation. For example, the *Wilson loop* is constructed by selecting a closed path of bonds S, on the lattice and examining

$$C_S = \langle \text{Product of } \tilde{\sigma} \text{ around the loop} \rangle = \left\langle \prod_{i \in S} \tilde{\sigma}_i \right\rangle . \tag{VI.30}$$

As any gauge transformation changes the signs of two bonds on the loop, their product is unaffected and C_S is gauge invariant. Since the Hamiltonian encourages spins of the same sign, this expectation value is always positive. Let us examine the asymptotic dependence of C_S on the shape of the loop at high and low temperatures. In a high temperature expansion, the correlation function is obtained as a sum of all graphs constructed from plaquettes with S as a boundary. Each plaquette contributes a factor of $\tanh \tilde{K}$, and

$$\begin{aligned} C_S =& \frac{1}{Z} \sum_{\{\tilde{\sigma}_i\}} \prod_{i \in S} \tilde{\sigma}_i \quad e^{K \sum_P \tilde{\sigma}_P^1 \tilde{\sigma}_P^2 \tilde{\sigma}_P^3 \tilde{\sigma}_P^4} \\ =& \left(\tanh \tilde{K} \right)^{\text{Area of } S} \left[1 + \mathcal{O}\left(\tanh \tilde{K}^2 \right) \right] \approx \exp \left[-f \left(\tanh \tilde{K} \right) \times \text{Area of } S \right] . \end{aligned} \tag{VI.31}$$

The low temperature expansion starts with the lowest energy configuration. There are in fact $\mathcal{N}_G = 2^N$ such ground states related by gauge transformations. The N_P plaquette interactions are satisfied in the ground states, and excitations involve creating unsatisfied plaquettes. Since C_S is gauge independent, it is sufficient to look at one of the ground states, e.g. the one with $\tilde{\sigma}_i = +1$ for all i. Flipping the sign of any of the $3N$ bonds creates an excitation of energy $8\tilde{K}$ with respect to the ground state. Denoting the number of bonds on the perimeter of the Wilson loop by P_S, we obtain

$$\begin{aligned} C_S =& \frac{\mathcal{N}_G}{\mathcal{N}_G} \cdot \frac{e^{\tilde{K} N_P} \left[1 + (3N - P_S) e^{-2\tilde{K} \times 4} (+1) + (-1) P_S e^{-2\tilde{K} \times 4} + \cdots \right]}{e^{\tilde{K} N_P} \left[1 + 3N e^{-2\tilde{K} \times 4} + \cdots \right]} \\ =& 1 - 2P_S e^{-8\tilde{K}} + \cdots \approx \exp \left[-2e^{-8\tilde{K}} P_S + \cdots \right] . \end{aligned} \tag{VI.32}$$

The asymptotic decay of C_S is thus different at high and low temperatures. At high temperatures, the decay is controlled by the *area* of the loop, while at low temperatures it depends on its *length*. The phase transition marks the change from one type of decay to the other, and by duality has the same singularities in free energy as the Ising model.

The prototype of gauge theories in physics is quantum electrodynamics (QED), with the action

$$S = \int d^4\mathbf{x} \left[\bar{\psi} \left(-i\partial\!\!\!/ + eA\!\!\!/ + m \right) \psi + \frac{1}{4} \left(\partial_\mu A_\nu - \partial_\nu A_\mu \right)^2 \right]. \tag{VI.33}$$

The spinor ψ is the Dirac field for the electron, and the 4–vector A describes the electromagnetic potential. The phase of ψ is not observable, and the action is invariant under the gauge symmetry $\psi \mapsto e^{ie\phi}\psi$, and $A_\mu \mapsto A_\mu - \partial_\mu \phi$, for any $\phi(\mathbf{x})$. The Z_2 lattice gauge theory can be regarded as the Ising analog of QED with the bond spins playing the role of the electromagnetic field. We can introduce a 'matter' field by placing spins $s_i = \pm 1$, on the *sites* of the lattice. The two fields are coupled by the Hamiltonian,

$$-\beta\mathcal{H} = J \sum_{\langle i,j \rangle} s_i \, \tilde{\sigma}_{ij} \, s_j + K \sum_P \tilde{\sigma}_P^1 \tilde{\sigma}_P^2 \tilde{\sigma}_P^3 \tilde{\sigma}_P^4, \tag{VI.34}$$

where $\tilde{\sigma}_{ij}$ is the spin on the bond joining i and j. The Hamiltonian has the gauge symmetry $s_i \mapsto (-1)s_i$, and $\tilde{\sigma}_{i,\mu} \mapsto -\tilde{\sigma}_{i,\mu}$, for all bonds emanating from any site i.

Regarding one of the lattice directions as time, a Wilson loop is obtained by creating two particles at a distance x, propagating them for a time t, and then removing them. The probability of such an event is roughly given by $C_s \sim e^{-U(x)t}$, where $U(x)$ is the interaction between the two particles. In the high temperature phase, C_S decays with the area of the loop, suggesting $U(x)t = f(\tanh \tilde{K})|x|t$. The resulting potential $U(x) = f(\tanh \tilde{K})|x|$, is like a *string* that connects the particles together. This is also the potential that describes the confinement of quarks at large distances in quantum chromodynamics. The decay with the length of the loop at low temperatures implies $U(x)t \approx g(e^{-8\tilde{K}})(|x| + t)$. For $t \gg |x|$ the potential is a constant and the force vanishes. (This *asymptotic freedom* describes the behavior of quarks at short distances.) The phase transition implies a change in the nature of interactions between particles mediated by the gauge field.

VI.F Summing over Phantom Loops

The high temperature series can be *approximately* summed so as to reproduce the Gaussian model. This correspondence provides a better understanding of why Gaussian behavior is applicable in high dimensions, and also prepares the way for the exact summation of the series in two dimensions in the next section. The high temperature series for the partition function of the Ising model on a d–dimensional hypercubic lattice is obtained from

$$Z = \sum_{\{\sigma_i\}} e^{K \sum_{\langle ij \rangle} \sigma_i \sigma_j} = 2^N \cosh^{dN} K \times S, \tag{VI.35}$$

where S is the sum over all allowed graphs on the lattice, each weighted by $t \equiv \tanh K$ raised to the power of the number of bonds in the graph. The allowed graphs have an even number of bonds per site. The simplest graphs have the topology of a single closed loop. There are also graphs composed of *disconnected* closed loops. Keeping in mind the cumulant expansion, we can set

$$\Xi = \text{sum over contribution of all graphs with one loop}, \tag{VI.36}$$

and introduce another sum,

$$\begin{aligned} S' = \exp(\Xi) =& 1 + \Xi + \frac{1}{2}(\Xi)^2 + \frac{1}{6}(\Xi)^3 + \cdots \\ =& 1 + (1 \text{ loop graphs}) + (2 \text{ loop graphs}) + (3 \text{ loop graphs}) + \cdots . \end{aligned} \tag{VI.37}$$

Despite their similarities, the sums S and S' are not identical: There are ambiguities associated with loops that intersect at a single site, which will be discussed more fully in the next section. More importantly, S' includes additional graphs where a particular bond contributes more than once, while in the original sum S, each lattice bond contributes a factor of 1 or t. This arises because after raising Ξ to a power ℓ, a particular bond may contribute up to ℓ times for a factor of t^ℓ. In the spirit of the approximation that includes multiple appearances of a bond, we shall allow additional closed paths in Ξ, in which a particular bond is traversed more than once in completing the loop. Qualitatively, S is the partition function of a gas of *self–avoiding* polymer loops with a monomer fugacity of t. The self–avoiding constraint is left out in the partition function S', which thus corresponds to a gas of *phantom* polymer loops, which may pass through each other with impunity.

Loops of various shapes can be constructed from closed random walks on the lattice, and the corresponding free energy of phantom loops is

$$\begin{aligned}\ln S' =& \sum \text{all closed random walks on the lattice} \times t^{\text{length of walk}} \\ =& N \sum_{\ell} \frac{t^{\ell}}{\ell} \,(\text{number of closed walks of } \ell \text{ steps starting and ending at } \mathbf{0}).\end{aligned} \tag{VI.38}$$

Note that extensivity is guaranteed since (up to boundary effects) the same loop can be started from any point on the lattice. The overall factor of $1/\ell$ accounts for the ℓ possible starting points for a loop of length ℓ.

A *transfer matrix* method can be used to count all possible (phantom) random walks on the lattice. Let us introduce a set of $N \times N$ matrices,

$$\langle \mathbf{i}|W(\ell)|\mathbf{j}\rangle \equiv \text{number of walks from } \mathbf{j} \text{ to } \mathbf{i} \text{ in } \ell \text{ steps}, \tag{VI.39}$$

in terms of which eq.(VI.38) becomes

$$\frac{\ln S'}{N} = \frac{1}{2} \sum_{\ell} \frac{t^{\ell}}{\ell} \langle \mathbf{0}|W(\ell)|\mathbf{0}\rangle. \tag{VI.40}$$

The additional factor of 2 arises since the same loop can be traversed by two random walks moving in opposite directions. Similarly, the spin–spin correlation function

$$\langle \sigma(\mathbf{0})\sigma(\mathbf{r})\rangle = \frac{1}{Z} \sum_{\{\sigma_i\}} \sigma(\mathbf{0})\sigma(\mathbf{r}) \prod_{\langle ij\rangle} (1 + t\sigma_i\sigma_j), \tag{VI.41}$$

is related to the sum over all paths connecting the points $\mathbf{0}$ and $\mathbf{r}$ on the lattice. In addition to the simple paths that directly connect the two points, there are *disconnected* graphs that contain additional closed loops. In the same approximation of allowing all intersections between paths, the partition function S' can be factored out of the numerator and denominator of eq.(VI.41), and

$$\langle \sigma(\mathbf{0})\sigma(\mathbf{r}\rangle \approx \sum_{\ell} t^{\ell} \langle \mathbf{r}|W(\ell)|\mathbf{0}\rangle \,. \tag{VI.42}$$

The counting of phantom paths on a lattice is easily accomplished by taking advantage of their *Markovian* property. This is the property that each step of a random walk proceeds from its last location and is independent of its previous steps. Hence, the number of walks can be calculated *recursively*. First, note that the any walk from $\mathbf{0}$ to $\mathbf{r}$ in ℓ steps can be

accomplished as a walk from $\mathbf{0}$ to some other point $\mathbf{r}'$ in $\ell-1$ steps, followed by a single step from $\mathbf{r}'$ to $\mathbf{r}$. Summing over all possible locations of the intermediate point leads to

$$\begin{aligned}\langle \mathbf{r}|W(\ell)|\mathbf{0}\rangle &= \sum_{\mathbf{r}'} \langle \mathbf{r}|W(1)|\mathbf{r}'\rangle \times \langle \mathbf{r}'|W(\ell-1)|\mathbf{0}\rangle \\ &= \langle \mathbf{r}|TW(\ell-1)|\mathbf{0}\rangle\,,\end{aligned} \tag{VI.43}$$

where the sum corresponds to the product of two matrices, and we have defined $T \equiv W(1)$. The recursion process can be continued and

$$W(\ell) = TW(\ell-1) = T^2W(\ell-2)^2 = \cdots = T^\ell. \tag{VI.44}$$

Thus all lattice random walks are generated by the *transfer matrix* T, whose elements are

$$\langle \mathbf{r}|T|\mathbf{r}'\rangle = \begin{cases} 1 & \text{if } \mathbf{r} \text{ and } \mathbf{r}' \text{ are nearest neighbors} \\ 0 & \text{otherwise} \end{cases}. \tag{VI.45}$$

(It is also called the *adjacency*, or *connectivity* matrix.) For example in $d=2$,

$$\langle x,y|T|x',y'\rangle = \delta_{y,y'}\left(\delta_{x,x'+1}+\delta_{x,x'-1}\right) + \delta_{x,x'}\left(\delta_{y,y'+1}+\delta_{y,y'-1}\right), \tag{VI.46}$$

and successive actions of T on a walker starting at the origin $|x,y>=\delta_{x,0}\delta_{y,0}$, generate the patterns

$$\begin{matrix}0&0&0\\0&1&0\\0&0&0\end{matrix} \xrightarrow{T} \begin{matrix}0&1&0\\1&0&1\\0&1&0\end{matrix} \xrightarrow{T} \begin{matrix}0&0&1&0&0\\0&2&0&2&0\\1&0&4&0&1\\0&2&0&2&0\\0&0&1&0&0\end{matrix} \xrightarrow{T} \cdots.$$

The value at each site is the number of walks ending at that point after ℓ steps.

Various properties of random walks can be deduced from diagonalizing the matrix T. Due to the translational symmetry of the lattice, this is achieved in the Fourier basis $\langle \mathbf{r}|\mathbf{q}\rangle = e^{i\mathbf{q}\cdot\mathbf{r}}/\sqrt{N}$. For example in $d=2$, starting from eq(VI.46), it can be checked that

$$\begin{aligned}\langle x,y|T|q_x,q_y\rangle &= \sum_{x',y'} \langle x,y|T|x',y'\rangle \langle x',y'|q_x,q_y\rangle \\ &= \frac{1}{\sqrt{N}}\left[e^{iq_y y}\left(e^{iq_x(x+1)}+e^{iq_x(x-1)}\right)+e^{iq_x x}\left(e^{iq_y(y+1)}+e^{iq_y(y-1)}\right)\right] \\ &= \frac{1}{\sqrt{N}}e^{i(q_x x+q_y y)}\left[2\cos q_x + 2\cos q_y\right] = T(q_x,q_y)\langle x,y|q_x,q_y\rangle\,.\end{aligned} \tag{VI.47}$$

The generalized eigenvalue for a d–dimensional hypercubic lattice is

$$T(\mathbf{q}) = 2\sum_{\alpha=1}^{d} \cos q_\alpha \,. \tag{VI.48}$$

The correlation function in eq.(VI.42) is now evaluated as

$$\begin{aligned}\langle\sigma(\mathbf{r})\sigma(\mathbf{0})\rangle \approx& \sum_{\ell}^{\infty} t^\ell \,\langle \mathbf{r}|W(\ell)|\mathbf{0}\rangle = \sum_{\ell}^{\infty} \big\langle \mathbf{r}|(tT)^\ell|\mathbf{0}\big\rangle \\ =& \left\langle \mathbf{r}\left|\frac{1}{1-tT}\right|\mathbf{0}\right\rangle = \sum_{\mathbf{q}} \langle \mathbf{r}|\mathbf{q}\rangle \,\frac{1}{1-tT(\mathbf{q})}\,\langle \mathbf{q}|\mathbf{0}\rangle \\ =& N\int \frac{d^d\mathbf{q}}{(2\pi)^d}\,\frac{e^{i\mathbf{q}\cdot\mathbf{r}}}{N}\,\frac{1}{1-2t\sum_{\alpha=1}^{d}\cos q_\alpha} = \int \frac{d^d\mathbf{q}}{(2\pi)^d}\,\frac{e^{i\mathbf{q}\cdot\mathbf{r}}}{1-2t\sum_\alpha \cos q_\alpha}\,.\end{aligned} \tag{VI.49}$$

For $t \to 0$, the shortest path costs least energy and $\langle\sigma(\mathbf{0})\sigma(\mathbf{r})\rangle \sim t^{|\mathbf{r}|}$. As t increases, larger paths dominate the sum because they are more numerous (i.e. entropically favored). Eventually, there is a singularity for $1 - tT(\mathbf{0}) = 0$, i.e. at $2d \times t_c = 1$, when arbitrarily long paths become important. For $t < t_c$, the partition function is dominated by small loops, and a polymer connecting two far away points is stretched by its line tension. When the fugacity exceeds t_c, the line tension vanishes and loops of arbitrary size are generated. Clearly the neglect of intersections (which stabilizes the system at a finite density) is no longer justified in this limit. This transition is the manifestation of Ising ordering in the language of paths representing the high temperature series. On approaching the transition from the high temperature side, the sums are dominated by very long paths. Accordingly, the denominator of eq.(VI.49) can be expanded for small $\mathbf{q}$ as

$$1 - tT(\mathbf{q}) = 1 - 2t\sum_{\alpha=1}^{d}\cos q_\alpha \simeq (1-2dt) + tq^2 + \mathcal{O}(q^4) \approx t_c(\xi^{-2} + q^2 + \mathcal{O}(q^4)), \tag{VI.50}$$

where

$$\xi \equiv \left(\frac{1-2dt}{t_c}\right)^{-1/2}. \tag{VI.51}$$

The resulting correlation functions, $\langle\sigma(\mathbf{0})\sigma(\mathbf{r})\rangle \propto \int \frac{d^d\mathbf{q}}{(2\pi)^d} e^{i\mathbf{q}\cdot\mathbf{r}}/(q^2+\xi^{-2})$, are identical to those obtained from the Gaussian model, and

$$\langle\sigma(\mathbf{0})\sigma(\mathbf{r})\rangle \propto \begin{cases} \dfrac{1}{r^{d-2}} & \text{for } r < \xi \qquad (\eta = 0) \\ \dfrac{e^{-r/\xi}}{r^{(d-1)/2}} & \text{for } r > \xi \end{cases}. \tag{VI.52}$$

The correlation length in eq.(VI.51) diverges as $\xi \sim (t_c - t)^{-1/2}$, i.e. with the Gaussian exponent of $\nu = 1/2$.

We can also calculate the free energy in eq.(VI.40) as

$$\begin{aligned}\frac{\ln S'}{N} =& \frac{1}{2}\sum_{\ell}^{\infty}\frac{t^\ell}{\ell}\langle \mathbf{0}|W(\ell)|\mathbf{0}\rangle = \frac{1}{2}\left\langle \mathbf{0}\left|\frac{t^\ell T^\ell}{\ell}\right|\mathbf{0}\right\rangle \\ =& -\frac{1}{2}\langle \mathbf{0}|\ln(1-tT)|\mathbf{0}\rangle = -\frac{N}{2}\int\frac{d^d\mathbf{q}}{(2\pi)^d}\langle \mathbf{0}|\mathbf{q}\rangle \ln\left(1-tT(\mathbf{q})\right)\langle \mathbf{q}|\mathbf{0}\rangle \\ =& -\frac{1}{2}\int\frac{d^d\mathbf{q}}{(2\pi)^d}\ln\left(1-2t\sum_{\alpha=1}^{d}\cos q_\alpha\right).\end{aligned} \tag{VI.53}$$

In the vicinity of the critical point at $t_c = 1/(2d)$, the argument of the logarithm is proportional to $(q^2+\xi^{-2})$ from eq.(VI.50). This is precisely as in the Gaussian model, and as discussed earlier the singular part of the free energy scales as

$$f_{\rm sing} \propto \xi^{-d} \propto (t_c - t)^{d/2}. \tag{VI.54}$$

The singular part of the heat capacity, obtained after taking two derivatives, is governed by the exponent $\alpha = 2 - d/2$. Note that in evaluating the sums appearing in eqs.(VI.49) and (VI.53), the lower limit for ℓ is not treated very carefully. The series in eq.(VI.49) is assumed to start from $\ell = 0$, and that of eq.(VI.53) from $\ell = 1$. In fact the first few terms of both series may be zero because the number of steps is not sufficient to reach $\mathbf{0}$ from $\mathbf{r}$, or to from a closed loop. This is not a serious omission, in that the *singular* behavior of a series is not effected by its first few terms. Treating the first few terms properly can only add analytic corrections to the singular forms calculated in eqs.(VI.49) and (VI.53).

The equivalence of these results to the Gaussian model is a manifestation of field–particle duality. In a field theoretical description, (imaginary) time appears as an additional dimension, and the two point correlations describe the probability of propagating a particle from one point in space–time to another. In a wave description, this probability is calculated by evolving the wave function using the Schrödinger equation. Alternatively, the probability can be calculated as the sum over all (Feynman) paths connecting the two points, each path weighted with the correct action. The second sum is similar to the above calculation of $\langle \sigma(\mathbf{r})\sigma(\mathbf{0})\rangle$.

This approach provides an interesting geometrical interpretation of the phase transition. The establishment of long range order implies that all parts of the system have selected the same state. This information is carried by the bonds connecting nearest

neighbors, and can be passed from the origin to a point $\mathbf{r}$, through all paths connecting these two points. The fugacity t is a measure of the reliability of information transfer between neighboring sites. Along a one dimensional chain, unless $t = 1$, the transferred information decays at large distances and it is impossible to establish long range order. In higher dimensions there are many more paths, and by accumulating the information from all paths it is possible to establish order at $t_c < 1$. Since the number of paths of length ℓ grows as $(2d)^\ell$ while their information content decays as t^ℓ, the transition occurs at $t_c = 1/(2d)$. (A better approximation is obtained by including some of the constraints by noting that the random walk cannot back track. In this case the number of walks grows as $(2d-1)^\ell$.) The total information from paths of length ℓ is weighted by $(2dt)^\ell$, and decays exponentially for $t < t_c$. The characteristic path length, $\overline{\ell} = -1/\ln(2dt)$, diverges as $(t_c - t)^{-1}$ on approaching the transition. For paths of size $\ell \ll \overline{\ell}$ there is very good information transfer. Such paths execute random walks on the lattice and cover a distance $\xi \approx \overline{\ell}^{\,1/2}$. The divergence of ν with an exponent of $1/2$ is thus a consequence of the random walk nature of the paths.

Why does the classical picture fail for $d \leq 4$? Let us focus on the dominant paths close to the phase transition. Is it justified to ignore the intersections of such paths? Random walks can be regarded as geometrical entities of fractal (Hausdorf) dimension $d_f = 2$. This follows from the general definition of dimension relating the mass and extent of an object by $M \propto R^{d_f}$, and the observation that the size of a random walk ($R \propto \xi$) is the square root of its length ($M \propto \ell$). Two geometrical entities of dimensions d_1 and d_2 will generally intersect in d–dimensional space if $d_1 + d_2 \geq d$. Thus our random walkers are unlikely to intersect in $d \geq d_u = 2+2 = 4$, and the above (Gaussian) results obtained by neglecting the intersections are asymptotically valid. Below the upper critical dimension of 4, random walks have frequent encounters and their intersections must be treated correctly. The diagrams obtained in the perturbative calculation of the propagator with um^4 correspond precisely to taking into account the intersections of paths. (Each factor of u corresponds to one intersection.) It is now clear that the constraint of self-avoidance will swell the paths beyond their random walk size leading to an increase in the exponent ν. Below the transition the length of paths grows without bound and the self–avoiding constraint is necessary to ensure the stability of the system.

The loop expansion is easily generalized to n-component spins. The only difference is that each closed loop now contributes a factor of n. In the phantom limit, where intersections are ignored, the free energy (eq.(VI.53)) is simply multiplied by n, while the

correlation function is left unchanged (precisely as in the Gaussian model). Corrections due to intersections, which modify critical behavior in $d < 4$, now depend on n. For example, in correcting the two point correlation function, we have to subtract contributions from the self-intersection of the random walk, as well as from contacts with loops (which have a fugacity of n). The correspondence with the perturbative series of the propagator with a nonlinearity $u(\vec{m} \cdot \vec{m})^2$, is again apparent.

VI.G Exact free energy of the Square Lattice Ising model

As indicated in eq.(VI.35), the Ising partition function is related to a sum S, over collections of paths on the lattice. The allowed graphs for a square lattice have 2 or 4 bonds per site. Each bond can appear only once in each graph, contributing a factor of $t \equiv \tanh K$. While it is tempting to replace S with the exactly calculable sum S', of all phantom loops of random walks on the lattice, this leads to an overestimation of S. The differences between the two sums arise from intersections of random walks, and can be divided into two categories:

(a) There is an over-counting of graphs which intersect at a *site*, i.e. with 4 bonds through a point. Consider a graph composed of two loops meeting at a site. Since a walker entering the intersection has three choices, this graph can be represented by *three distinct random walks*. One choice leads to two disconnected loops; the other two are single loops with or without a self–crossing in the walker's path.

(b) The independent random walkers in S' may go through a particular lattice *bond* more than once.

Including these constraints amounts to introducing interactions between paths. The resulting interacting random walkers are non–Markovian, as each step is no longer independent of previous ones and of other walkers. While such interacting walks are not in general amenable to exact treatment, in two dimensions an interesting topological property allows us to make the following assertion:

$$S = \sum \text{collections of loops of random walks } \textit{with no } \text{U } \textit{turns} \times t^{\text{number of bonds}} \times (-1)^{\text{number of crossings}}. \tag{VI.55}$$

The negative signs for same terms reduce the overestimate and render the exact sum.

Proof: We shall deal in turn with the two problems mentioned above.

(a) Consider a graph with many intersections and focus on a particular one. A walker must enter and leave such an intersection twice. This can be done in three ways only one of which involves the path of the walker crossing itself (when the walker proceeds straight through the intersection). This configuration carries an additional factor of (-1) according to eq.(VI.55). Thus, independent of other crossings, these three configurations sum up to contribute a factor of 1. By repeating this reasoning at each intersection, we see that the over-counting problem is removed and the sum over all possible ways of tracing the graph leads to the correct factor of one.

(b) Consider a bond that is crossed by two walkers (or twice by the same walker). We can imagine the bond as an avenue with two sides. For each configuration in which the two paths enter and leave on the same side of the avenue, there is another one in which the paths go to the opposite side. The latter involves a crossing of paths and hence carries a minus sign with respect to the former. The two possibilities thus cancel out! The reasoning can be generalized to multiple passes through any bond. The only exception is when the doubled bond is created as a result of a U–turn. This is why such backward steps are explicitly excluded from eq.(VI.55).

Let us label random walkers with no U–turns, and weighted by $(-1)^{\text{number of crossings}}$, as RW*s. Then as in eq.(VI.37) the terms in S can be organized as

$$\begin{aligned} S &= \sum(\text{RW}^*\text{s with 1 loop}) + \sum(\text{RW}^*\text{s with 2 loops}) + \sum(\text{RW}^*\text{s with 3 loops}) + \cdots \\ &= \exp\left[\sum(\text{RW}^*\text{s with 1 loop})\right]. \end{aligned} \tag{VI.56}$$

The exponentiation of the sum is justified, since the only interaction between RW*s is the sign related to their crossings. As two RW* loops always cross an even number of times, this is equivalent to no interaction at all. Using eq.(VI.35), the full Ising free energy is calculated as

$$\ln Z = N \ln 2 + 2N \ln\cosh K + \sum \left(\text{RW}^*\text{s with 1 loop} \times t^{\#\text{ of bonds}}\right). \tag{VI.57}$$

Organizing the sum in terms of the number of bonds, and taking advantage of the translational symmetry of the lattice (up to corrections due to boundaries),

$$\frac{\ln Z}{N} = \ln\left(2\cosh^2 K\right) + \sum_{\ell}^{\infty} \frac{t^\ell}{\ell} \langle \mathbf{0}|W^*(\ell)|\mathbf{0}\rangle, \tag{VI.58}$$

where

$$\begin{aligned} \langle \mathbf{0}|W^*(\ell)|\mathbf{0}\rangle =& \text{number of closed loops of } \ell \text{ steps, with no U turns, from } \mathbf{0} \text{ to } \mathbf{0} \\ & \times (-1)^{\#\text{ of crossings}}. \end{aligned} \tag{VI.59}$$

The absence of U–turns, a local constraint, does not complicate the counting of loops. On the other hand, the number of crossings is a function of the complete configuration of the loop and is a non–Markovian property. Fortunately, in two dimensions it is possible to obtain the *parity* of the number of crossings from local considerations. The first step is to

construct the loops from *directed* random walks, indicated by placing an arrow along the direction that the path is traversed. Since any loop can be traversed in two directions,

$$\langle \mathbf{0}|W^*(\ell)|\mathbf{0}\rangle = \frac{1}{2}\sum \textit{directed RW}^* \text{ loops of } \ell \text{ steps, no U turns, from } \mathbf{0} \text{ to } \mathbf{0} \times (-1)^{n_c}, \tag{VI.60}$$

where n_c is the number of self–crossings of the loop. We can now take advantage of the following topological result:

Whitney's Theorem: The number of self–crossings of a planar loop is related to the total angle Θ, through which the tangent vector turns in going around the loop by

$$(n_c)_{\text{mod } 2} = \left(1 + \frac{\Theta}{2\pi}\right)_{\text{mod } 2}. \tag{VI.61}$$

This theorem can be checked by a few examples. A single loop corresponds to $\Theta = \pm 2\pi$, while a single intersection results in $\Theta = 0$.

Since the total angle Θ, is the sum of the angles through which the walker turns at each step, the parity of crossings can be obtained using *local* information alone as

$$(-1)^{n_c} = e^{i\pi n_c} = \exp\left[i\pi\left(1 + \frac{\Theta}{2\pi}\right)\right] = -e^{\frac{i}{2}\sum_{j=1}^{\ell}\theta_j}, \tag{VI.62}$$

where θ_j is the angle through which the walker turns on the j^{th} step, leading to

$$\begin{aligned}\langle \mathbf{0}|W^*(\ell)|\mathbf{0}\rangle = -\frac{1}{2}\sum \textit{directed RW}^* \text{ loops of } \ell \text{ steps, with no U turns, from } \mathbf{0} \text{ to } \mathbf{0} \\ \times \exp\left(\frac{1}{2}\sum \text{ local change of angle by the tangent vector}\right).\end{aligned} \tag{VI.63}$$

The angle turned can be calculated at each site, if we keep track of the directions of arrival and departure of the path. To this end, we introduce a label μ for the 4 directions *going out* of each site, e.g. $\mu = 1$ for right, $\mu = 2$ for up, $\mu = 3$ for left, and $\mu = 4$ for down. We next introduce a set of $4N \times 4N$ matrices generalizing eq.(VI.39) as

$$\begin{aligned}\langle x_2 y_2, \mu_2|W^*(\ell)|x_1 y_1, \mu_1\rangle = \sum \text{directed random walks of } \ell \text{ steps, with no U turns,} \\ \text{departing } (x_1, y_1) \text{ along } \mu_1, \text{ proceeding along } \mu_2 \text{ after reaching } (x_2, y_2) \times e^{\frac{i}{2}\sum_{j=1}^{\ell}\theta_j}.\end{aligned} \tag{VI.64}$$

Thus μ_2 specifies a direction taken *after* the walker reaches its destination. It serves to exclude some paths (arriving along -μ_2), and leads to an additional phase. As in eq.(VI.43), due to their Markovian property, these matrices can be calculated recursively as

$$\begin{aligned}
&\langle x_2 y_2, \mu_2 | W^*(\ell) | x_1 y_1, \mu_1 \rangle \\
&\qquad = \sum_{x'y',\mu'} \langle x_2 y_2, \mu_2 | T^* | x'y', \mu' \rangle \, \langle x'y', \mu' | W^*(\ell - 1) | x_1 y_1, \mu_1 \rangle \\
&\qquad = \langle x_2 y_2, \mu_2 | T^* W^*(\ell - 1) | x_1 y_1, \mu_1 \rangle = \left\langle x_2 y_2, \mu_2 | T^{*\ell} | x_1 y_1, \mu_1 \right\rangle ,
\end{aligned} \tag{VI.65}$$

where $T^* \equiv W^*(1)$ describes one step of the walk. The direction of arrival uniquely determines the nearest neighbor from which the walker departed, and the angle between the two directions fixes the phase of the matrix element. We can thus generalize eq.(VI.46) to a 4×4 matrix that keeps track of both connectivity and phase between pairs of sites. The steps taken can be represented diagrammatically as

$$T = \left[\begin{array}{cccc} \rightarrow\!\rightarrow & \rightarrow\!\uparrow & \rightarrow\!\leftarrow & \rightarrow\!\downarrow \\ \uparrow\!\rightarrow & \uparrow\!\uparrow & \uparrow\!\leftarrow & \uparrow\!\downarrow \\ \leftarrow\!\rightarrow & \leftarrow\!\uparrow & \leftarrow\!\leftarrow & \leftarrow\!\downarrow \\ \downarrow\!\rightarrow & \downarrow\!\uparrow & \downarrow\!\leftarrow & \downarrow\!\downarrow \end{array} \right] , \tag{VI.66}$$

and correspond to the matrix

$$\langle x'y'|T^*|xy\rangle = \left[\begin{array}{cccc} \langle x', y'|x+1, y\rangle & \langle x', y'|x+1, y\rangle\, e^{\frac{i\pi}{4}} & 0 & \langle x', y'|x+1, y\rangle\, e^{-\frac{i\pi}{4}} \\ \langle x', y'|x, y+1\rangle\, e^{-\frac{i\pi}{4}} & \langle x', y'|x, y+1\rangle & \langle x', y'|x, y+1\rangle\, e^{\frac{i\pi}{4}} & 0 \\ 0 & \langle x', y'|x-1, y\rangle\, e^{-\frac{i\pi}{4}} & \langle x', y'|x-1, y\rangle & \langle x', y'|x-1, y\rangle\, e^{\frac{i\pi}{4}} \\ \langle x', y'|x, y-1\rangle\, e^{\frac{i\pi}{4}} & 0 & \langle x', y'|x, y-1\rangle\, e^{-\frac{i\pi}{4}} & \langle x', y'|x, y-1\rangle \end{array} \right] , \tag{VI.67}$$

where $< x, y|x', y' > \equiv \delta_{x,x'}\delta_{y,y'}$.

Because of its translational symmetry, the $4N \times 4N$ matrix takes a *block diagonal* form in the Fourier basis, $\langle xy|q_x q_y\rangle = e^{i(q_x x + q_y y)}/\sqrt{N}$, i.e.

$$\sum_{xy} \langle x'y', \mu'|T^*|xy, \mu\rangle \, \langle xy|q_x q_y\rangle = \langle \mu'|T^*(\mathbf{q})|\mu\rangle \, \langle x'y'|q_x q_y\rangle \, . \tag{VI.68}$$

Each 4×4 block is labelled by a wavevector $\mathbf{q} = (q_x, q_y)$, and takes the form

$$T^*(\mathbf{q}) = \left[\begin{array}{cccc} e^{-iq_x} & e^{-i(q_x - \frac{\pi}{4})} & 0 & e^{-i(q_x + \frac{\pi}{4})} \\ e^{-i(q_y + \frac{\pi}{4})} & e^{-iq_y} & e^{-i(q_y - \frac{\pi}{4})} & 0 \\ 0 & e^{i(q_x - \frac{\pi}{4})} & e^{iq_x} & e^{i(q_x + \frac{\pi}{4})} \\ e^{i(q_y + \frac{\pi}{4})} & 0 & e^{i(q_y - \frac{\pi}{4})} & e^{iq_y} \end{array} \right] . \tag{VI.69}$$

To ensure that a path that starts at the origin completes a loop properly, the final arrival direction at the origin must coincide with the original one. Summing over all 4 such directions, the total number of such loops is obtained from

$$\langle \mathbf{0}|W^*(\ell)|\mathbf{0}\rangle = \sum_{\mu=1}^{4} \langle 00,\mu|T^{*\ell}|00,\mu\rangle = \frac{1}{N}\sum_{xy,\mu} \langle xy,\mu|T^{*\ell}|xy,\mu\rangle = \frac{1}{N}\,\mathrm{tr}\left(T^{*\ell}\right). \quad \text{(VI.70)}$$

Using eq.(VI.58), the free energy is calculated as

$$\begin{aligned}\frac{\ln Z}{N} &= \ln\left(2\cosh^2 K\right) - \frac{1}{2}\sum_{\ell}\frac{t^\ell}{\ell}\,\langle \mathbf{0}|W^*(\ell)|\mathbf{0}\rangle = \ln\left(2\cosh^2 K\right) - \frac{1}{2N}\,\mathrm{tr}\left[\sum_{\ell}\frac{T^{*\ell}t^\ell}{\ell}\right] \\ &= \ln\left(2\cosh^2 K\right) + \frac{1}{2N}\,\mathrm{tr}\ln\left(1-tT^*\right) \\ &= \ln\left(2\cosh^2 K\right) + \frac{1}{2N}\sum_{\mathbf{q}}\mathrm{tr}\ln\left(1-tT^*(\mathbf{q})\right).\end{aligned} \quad \text{(VI.71)}$$

But for any matrix M with eigenvalues $\{\lambda_\alpha\}$,

$$\mathrm{tr}\ln M = \sum_\alpha \ln\lambda_\alpha = \ln\prod_\alpha \lambda_\alpha = \ln\det M.$$

Converting the sum over $\mathbf{q}$ in eq.(VI.71) to an integral leads to

$$\begin{aligned}\frac{\ln Z}{N} &= \ln\left(2\cosh^2 K\right) + \\ &\frac{1}{2}\int\frac{d^2\mathbf{q}}{(2\pi)^2}\ln\left\{\det\begin{vmatrix} 1-te^{-iq_x} & -te^{-i(q_x-\frac{\pi}{4})} & 0 & -te^{-i(q_x+\frac{\pi}{4})} \\ -te^{-i(q_y+\frac{\pi}{4})} & 1-te^{-iq_y} & -te^{-i(q_y-\frac{\pi}{4})} & 0 \\ 0 & -te^{i(q_x-\frac{\pi}{4})} & 1-te^{iq_x} & -te^{i(q_x+\frac{\pi}{4})} \\ -te^{i(q_y+\frac{\pi}{4})} & 0 & -te^{i(q_y-\frac{\pi}{4})} & 1-te^{iq_y}\end{vmatrix}\right\}.\end{aligned} \quad \text{(VI.72)}$$

Evaluation of the above determinant is straightforward, and the final result is

$$\frac{\ln Z}{N} = \ln\left(2\cosh^2 K\right) + \frac{1}{2}\int\frac{d^2\mathbf{q}}{(2\pi)^2}\ln\left[\left(1+t^2\right)^2 - 2t\left(1-t^2\right)\left(\cos q_x+\cos q_y\right)\right]. \quad \text{(VI.73)}$$

Taking advantage of trigonometric identities, the result can be simplified to

$$\frac{\ln Z}{N} = \ln 2 + \frac{1}{2}\int_{-\pi}^{\pi}\frac{dq_x dq_y}{(2\pi)^2}\ln\left[\cosh^2(2K) - \sinh(2K)\left(\cos q_x+\cos q_y\right)\right]. \quad \text{(VI.74)}$$

While it is possible to obtain a closed form expression by performing the integrals exactly, the final expression involves a hypergeometric function, and is not any more illuminating.

VI.H Critical behavior of the two-dimensional Ising model

To understand the singularity in the free energy of the two dimensional Ising model in eq.(VI.73), we start with the simpler expression obtained by the unrestricted sum over phantom loops in sec.VI.F. Specializing eq.(VI.53) to $d = 2$,

$$f_G = \ln\left(2\cosh^2 K\right) - \frac{1}{2}\int \frac{dq_x dq_y}{(2\pi)^2} \ln\left[1 - 2t\left(\cos q_x + \cos q_y\right)\right]. \tag{VI.75}$$

Apart from the argument of the logarithm, this expression is similar to the exact result. Is it possible that such similar functional forms lead to distinct singular behaviors? The singularity results from the vanishing of the argument of the logarithm at $t_c = 1/4$. In the vicinity of this point we make an expansion as in eq.(VI.50),

$$A_G(t, \mathbf{q}) = (1 - 4t) + tq^2 + \mathcal{O}(q^4) \approx t_c\left(q^2 + 4\frac{\delta t}{t_c}\right), \tag{VI.76}$$

where $\delta t = t_c - t$. The singular part of eq.(VI.75) can be obtained by focusing of the behavior of the integrand as $\mathbf{q} \to \mathbf{0}$, and replacing the square Brillouin zone for the range of the integral with a circle of radius $\Lambda \approx 2\pi$,

$$\begin{aligned} f_{\text{sing.}} &= -\frac{1}{2}\int_0^\Lambda \frac{2\pi q dq}{4\pi^2} \ln\left(q^2 + 4\frac{\delta t}{t_c}\right) \\ &= -\frac{1}{8\pi}\left[\left(q^2 + 4\frac{\delta t}{t_c}\right)\ln\left(\frac{q^2 + 4\delta t/t_c}{e}\right)\right]_0^\Lambda. \end{aligned} \tag{VI.77}$$

Only the expression evaluated at $q = 0$ is singular, and

$$f_{\text{sing.}} = \frac{1}{2\pi}\left(\frac{\delta t}{t_c}\right)\ln\left(\frac{\delta t}{t_c}\right). \tag{VI.78}$$

The resulting heat capacity, $C_G \propto \partial^2 f_G/\partial^2 t$, diverges as $1/\delta t$. Since eq.(VI.75) is not valid for $t > t_c$, we cannot obtain the behavior of heat capacity on the low temperature side.

For the exact result of eq.(VI.73), the argument of the logarithm is

$$A^*(t, \mathbf{q}) = \left(1 + t^2\right)^2 - 2t\left(1 - t^2\right)\left(\cos q_x + \cos q_y\right). \tag{VI.79}$$

The minimum value of this expression, for $\mathbf{q} = \mathbf{0}$, is

$$A^*(t, \mathbf{0}) = \left(1 + t_c^2\right)^2 - 4t_c\left(1 - t_c^2\right) = \left(1 - t_c^2\right)^2 + 4t_c^2 - 4t_c\left(1 - t_c^2\right) = \left(1 - t_c^2 - 2t_c\right)^2. \tag{VI.80}$$

Since this expression (and hence the argument of the logarithm) is always non–negative, the integral exists for all values of t. As required, unlike eq.(VI.75), the exact result is valid at *all* temperatures. There is a singularity when the argument vanishes for

$$t_c^2 + 2t_c - 1 = 0, \qquad \Longrightarrow \qquad t_c = -1 \pm \sqrt{2}. \tag{VI.81}$$

The positive solution describes a ferromagnet, and leads to a value of $K_c = \ln\left(\sqrt{2}+1\right)/2$, in agreement with the duality arguments of sec.VI.D. Setting $\delta t = t - t_c$, and expanding eq.(VI.79) in the vicinity of $\mathbf{q} \to 0$ gives

$$\begin{aligned} A^*(t,\mathbf{q}) \approx & \left[(-2t_c - 2)\delta t\right]^2 + t_c(1-t_c^2)q^2 + \cdots \\ \approx & 2t_c^2 \left[q^2 + 4\left(\frac{\delta t}{t_c}\right)^2 \right]. \end{aligned} \tag{VI.82}$$

The important difference from eq.(VI.76) is that $(\delta t/t_c)$ appears at quadratic order. Following the steps in eqs.(VI.77) and (VI.78), the singular part of the free energy is

$$\begin{aligned} \left.\frac{\ln Z}{N}\right|_{\text{sing.}} = & \frac{1}{2}\int_0^\Lambda \frac{2\pi q dq}{4\pi^2} \ln\left[q^2 + 4\left(\frac{\delta t}{t_c}\right)^2 \right] \\ = & \frac{1}{8\pi}\left[\left(q^2 + 4\left(\frac{\delta t}{t_c}\right)^2 \right) \ln\left(\frac{q^2 + 4(\delta t/t_c)^2}{e} \right) \right]_0^\Lambda \\ = & -\frac{1}{\pi}\left(\frac{\delta t}{t_c}\right)^2 \ln\left|\frac{\delta t}{t_c}\right| + \text{analytic terms}. \end{aligned} \tag{VI.83}$$

The heat capacity is obtained by taking two derivatives and diverges as $C(\delta t)_{\text{sing.}} = A_\pm \ln|\delta t|$. The logarithmic singularity corresponds to the limit $\alpha = 0$; the peak is symmetric, characterized by the amplitude ratio $A_+/A_- = 1$.

The exact partition function of the Ising model on the square lattice was originally calculated by Lars Onsager in 1944 (Phys. Rev. **65**, page 117). Onsager used a $2^L \times 2^L$ transfer matrix to study a lattice of width L. He then identified various symmetries of this matrix which allowed him to diagonalize it and obtain the largest eigenvalue as a function of L. For any finite L, this eigenvalue is non-degenerate as required by Frobenius's theorem. In the limit $L \to \infty$, the top two eigenvalues become degenerate at K_c. The result in this limit naturally coincides with eq.(VI.74). Onsager's paper is quite long and complicated, and regarded as a *tour de force* of mathematical physics. A somewhat streamlined version of this solution was developed by B. Kaufman (Phys. Rev. **76**, 1232 (1949)) and is

more or less reproduced in chapter 15 of Huang. This exact solution, for the first time, demonstrated that critical behavior at a phase transition can in fact be quite different from predictions of Landau (mean–field) theory. It took almost three decades to reconcile the two results by the renormalization group.

The graphical method presented in this section was originally developed by Kac and Ward (Phys. Rev. **88**, 1332 (1952)). The main ingredient of the derivation is the result that the correct accounting of the paths can be achieved by including a factor of (-1) for each intersection. (This conjecture by Feynman is proved in S. Sherman, J. Math. Phys. **1**, 202 (1960).) The change of sign is reminiscent of the exchange factor between fermions. Indeed, Schultz, Mattis, and Lieb (Rev. Mod. Phys. **36**, 856 (1964)) describe how the Onsager transfer matrix can be regarded as a Hamiltonian for the evolution of non-interacting fermions in one dimension. The Pauli exclusion principle prevents intersections of the world-lines of these fermions in two dimensional space-time.

In addition to the partition function, the correlation functions $\langle \sigma_{\mathbf{i}} \sigma_{\mathbf{j}} \rangle$ can also be calculated by summing over paths (see Itzykson and Drouffe, *Statistical field theory: 1*). Since the combination $q^2 + 4(\delta t/t_c)^2$ in eq.(VI.82) describes the behavior of these random walks, we expect a correlation length $\xi \sim |t_c/\delta t|$, i.e. diverging with an exponent $\nu = 1$ on both sides of the phase transition with an amplitude ratio of unity. The exponents α and ν are related by the hyperscaling identity $\alpha = 2 - 2\nu$. The critical correlations at t_c are more subtle and decay as $\langle \sigma_{\mathbf{i}} \sigma_j \rangle_c \sim 1/|\mathbf{i} - \mathbf{j}|^\eta$, with $\eta = 1/4$. Integrating the correlation functions yields the susceptibility, which diverges as $\chi_\pm \simeq C_\pm |\delta t|^{-\gamma}$, with $\gamma = 7/4$, and $C_+/C_- = 1$. A rather simple expression for the zero field magnetization,

$$m = \left(1 - \sinh^{-4}(2K)\right)^{1/8}, \tag{VI.84}$$

was presented without proof by Onsager. A rather difficult derivation of this result was finally given by C.N. Yang (Phys. Rev. **85**, 808 (1952)). The exponent $\beta = 1/8$ satisfies the required exponent identities.

VII. Continuous Spins at Low Temperatures

VII.A The non-linear σ-model

Previously we considered low temperature expansions for *discrete* spins (Ising, Potts, etc.), in which the low energy excitations are droplets of incorrect spin in a uniform background selected by broken symmetry. These excitations occur at small scales, and are easily described by graphs on the lattice. By contrast, for *continuous* spins, the lowest energy excitations are long-wavelength Goldstone modes, as discussed in section II.C. The thermal excitation of these modes destroys the long-range order in dimensions $d \leq 2$. For d close to 2, the critical temperature must be small, making low temperature expansions a viable tool for the study of critical phenomena. As we shall demonstrate next, such an approach requires keeping track of the interactions between Goldstone modes.

Consider unit n-component spins on the sites of a lattice, i.e.

$$\vec{s}\,(\mathbf{i}) = (s_1, s_2, \cdots, s_n), \quad \text{with} \quad |\vec{s}\,(\mathbf{i})|^2 = s_1^2 + \cdots + s_n^2 = 1. \tag{VII.1}$$

The usual nearest neighbor Hamiltonian can be written as

$$-\beta\mathcal{H} = K \sum_{\langle \mathbf{ij} \rangle} \vec{s}\,(\mathbf{i}) \cdot \vec{s}\,(\mathbf{j}) = K \sum_{\langle \mathbf{ij} \rangle} \left(1 - \frac{(\vec{s}\,(\mathbf{i}) - \vec{s}\,(\mathbf{j}))^2}{2} \right). \tag{VII.2}$$

At low temperatures, the fluctuations between neighboring spins are small and the difference in eq.(VII.2) can be replaced by a gradient. Assuming a unit lattice spacing,

$$-\beta\mathcal{H} = -\beta E_0 - \frac{K}{2} \int d^d\mathbf{x} \left(\nabla \vec{s}\,(\mathbf{x}) \right)^2, \tag{VII.3}$$

where the discrete index $\mathbf{i}$ has been replaced by a continuous vector $\mathbf{x} \in \Re^d$. A cutoff of $\Lambda \approx \pi$ is thus implicit in eq.(VII.3). Ignoring the ground state energy, the partition function is

$$Z = \int \mathcal{D} \left[\vec{s}\,(\mathbf{x}) \delta \left(s(\mathbf{x})^2 - 1 \right) \right] e^{-\frac{K}{2} \int d^d\mathbf{x} (\nabla \vec{s})^2}. \tag{VII.4}$$

A possible ground state configuration is $\vec{s}\,(\mathbf{x}) = (0, \cdots, 1)$. There are $n-1$ Goldstone modes describing the transverse fluctuations. To examine the effects of these fluctuations close to zero temperature, set

$$\vec{s}\,(\mathbf{x}) = (\pi_1(\mathbf{x}), \cdots, \pi_{n-1}(\mathbf{x}), \sigma(\mathbf{x})) \equiv (\vec{\pi}\,(\mathbf{x}), \sigma(\mathbf{x})), \tag{VII.5}$$

where $\vec{\pi}\,(\mathbf{x})$ is an $n-1$ component vector. The unit length of the spin fixes $\sigma(\mathbf{x})$ in terms of $\vec{\pi}\,(\mathbf{x})$. For each degree of freedom

$$\begin{aligned}\int d\vec{s}\,\delta(s^2-1) &= \int_{-\infty}^{\infty} d\vec{\pi}\,d\sigma\delta\left(\pi^2+\sigma^2-1\right)\\ &= \int_{-\infty}^{\infty} d\vec{\pi}\,d\sigma\delta\left[\left(\sigma-\sqrt{1-\pi^2}\right)\left(\sigma+\sqrt{1-\pi^2}\right)\right] = \int_{-\infty}^{\infty}\frac{d\vec{\pi}}{2\sqrt{1-\pi^2}}\ ,\end{aligned} \tag{VII.6}$$

where we have used the identity $\delta(ax)=\delta(x)/|a|$. Using this result, the partition function in eq.(VII.4) can be written as

$$\begin{aligned}Z &\propto \int \frac{\mathcal{D}\vec{\pi}\,(\mathbf{x})}{\sqrt{1-\pi(\mathbf{x})^2}}\,e^{-\frac{K}{2}\int d^d\mathbf{x}\left[(\nabla\vec{\pi}\,)^2+\left(\nabla\sqrt{1-\pi^2}\right)^2\right]}\\ &= \int \mathcal{D}\vec{\pi}\,(\mathbf{x})\exp\left\{-\int d^d\mathbf{x}\left[\frac{K}{2}(\nabla\vec{\pi}\,)^2+\frac{K}{2}\left(\nabla\sqrt{1-\pi^2}\right)^2+\frac{\rho}{2}\ln(1-\pi^2)\right]\right\}.\end{aligned} \tag{VII.7}$$

In going from the lattice to the continuum, we have introduced a density $\rho=N/V=1/a^d$ of lattice points. For unit lattice spacing $\rho=1$, but for the purpose of renormalization we shall keep an arbitrary ρ. Whereas the original Hamiltonian was quite simple, the one describing the Goldstone modes $\vec{\pi}\,(\mathbf{x})$, is rather complicated. In selecting a particular ground state, the rotational symmetry was broken. The nonlinear terms in eq.(VII.7) ensure that this symmetry is properly reflected when considering only $\vec{\pi}$.

We can expand the nonlinear terms for the effective Hamiltonian in powers of $\vec{\pi}\,(\mathbf{x})$, resulting in a series

$$\beta\mathcal{H}[\vec{\pi}\,(\mathbf{x})] = \beta\mathcal{H}_0+\mathcal{U}_1+\mathcal{U}_2+\cdots, \tag{VII.8}$$

where

$$\beta\mathcal{H}_0 = \frac{K}{2}\int d^d\mathbf{x}(\nabla\vec{\pi}\,)^2, \tag{VII.9}$$

describes independent Goldstone modes, while

$$\mathcal{U}_1 = \int d^d\mathbf{x}\left[\frac{K}{2}(\vec{\pi}\cdot\nabla\vec{\pi}\,)^2-\frac{\rho}{2}\pi^2\right], \tag{VII.10}$$

is the first order perturbation when the terms in the series are organized according to powers of $T=1/K$. Since we expect fluctuations $\langle\pi^2\rangle\propto T$, $\beta\mathcal{H}_0$ is order of one, the two

terms in $\mathcal{U}_1$ are order of T; remaining terms are order of T^2 and higher. In the language of Fourier modes,

$$\begin{aligned}\beta\mathcal{H}_0 =& \frac{K}{2}\int \frac{d^d\mathbf{q}}{(2\pi)^d}\, q^2\, |\vec{\pi}\,(\mathbf{q})|^2,\\ \mathcal{U}_1 =& -\frac{K}{2}\int \frac{d^d\mathbf{q}_1\, d^d\mathbf{q}_2\, d^d\mathbf{q}_3}{(2\pi)^{3d}}\pi_\alpha(\mathbf{q}_1)\,\pi_\alpha(\mathbf{q}_2)\,\pi_\beta(\mathbf{q}_3)\,\pi_\beta(-\mathbf{q}_1-\mathbf{q}_2-\mathbf{q}_3)\,(\mathbf{q}_1\cdot\mathbf{q}_3)\\ & -\frac{\rho}{2}\int \frac{d^d\mathbf{q}}{(2\pi)^d}\,|\vec{\pi}\,(\mathbf{q})|^2.\end{aligned} \tag{VII.11}$$

For the non-interacting (quadratic) theory, the correlation functions of the Goldstone modes are

$$\langle \pi_\alpha(\mathbf{q})\pi_\beta(\mathbf{q}')\rangle_0 = \frac{\delta_{\alpha,\beta}(2\pi)^d\delta^d(\mathbf{q}+\mathbf{q}')}{Kq^2}. \tag{VII.12}$$

The resulting fluctuations in real space behave as

$$\left\langle \pi(\mathbf{x})^2\right\rangle_0 = \int \frac{d^d\mathbf{q}}{(2\pi)^d}\left\langle|\vec{\pi}\,(\mathbf{q})|^2\right\rangle_0 = \frac{(n-1)}{K}\int_{1/L}^{1/a}\frac{d^d\mathbf{q}}{(2\pi)^d}\,\frac{1}{q^2} = \frac{(n-1)}{K}\,\frac{K_d\left(a^{2-d}-L^{2-d}\right)}{(d-2)}. \tag{VII.13}$$

For $d>2$ the fluctuations are indeed proportional to T. However, for $d\leq 2$ they diverge as $L\to\infty$. This is a consequence of the Mermin–Wagner theorem on the absence of long range order in $d\leq 2$. Polyakov (1975) argued that this implies a critical temperature $T_c\sim\mathcal{O}(d-2)$ for such systems, and that an RG expansion in powers of T may provide a systematic way to explore critical behavior close to two dimensions.

To construct a perturbative RG, consider a spherical Brillouin zone of radius Λ, and divide the modes as $\vec{\pi}\,(\mathbf{q}) = \vec{\pi}^{\,<}(\mathbf{q}) + \vec{\pi}^{\,>}(\mathbf{q})$. The modes $\vec{\pi}^{\,<}$ involve momenta $0<|\mathbf{q}|<\Lambda/b$, while we shall integrate over the short wavelength fluctuations $\vec{\pi}^{\,>}$ with momenta in the shell $\Lambda/b<|\mathbf{q}|<\Lambda$. To order of T, the coarse–grained Hamiltonian is given by

$$\beta\tilde{\mathcal{H}}\left[\vec{\pi}^{\,<}\right] = V\delta f_b^0 + \beta\mathcal{H}_0\left[\vec{\pi}^{\,<}\right] + \left\langle \mathcal{U}_1\left[\vec{\pi}^{\,<}+\vec{\pi}^{\,>}\right]\right\rangle_0^> + \mathcal{O}(T^2), \tag{VII.14}$$

where $\langle\ \rangle_0^>$ indicates averaging over $\vec{\pi}^{\,>}$. The term proportional to ρ in eq.(VII.11) results in two contributions, one is a constant addition to free energy (from $\left\langle(\pi^>)^2\right\rangle$), and the other is simply $\rho(\pi^<)^2$. (The cross terms proportional to $\vec{\pi}^{\,<}\cdot\vec{\pi}^{\,>}$ vanish by symmetry.) The quartic part of $\mathcal{U}_1$ generates 16 terms. Nontrivial contributions arise from products of two $\vec{\pi}^{\,<}$ and two $\vec{\pi}^{\,>}$. There are three types of such contributions; the first has the form

$$\begin{aligned}\langle \mathcal{U}_1^a\rangle_0^> = 2\times\frac{-K}{2}\int \frac{d^d\mathbf{q}_1\, d^d\mathbf{q}_2\, d^d\mathbf{q}_3}{(2\pi)^{3d}}(\mathbf{q}_1\cdot\mathbf{q}_3)\\ \left\langle\pi_\alpha^>(\mathbf{q}_1)\pi_\alpha^>(\mathbf{q}_2)\right\rangle_0^>\,\pi_\beta^<(\mathbf{q}_3)\pi_\beta^<(-\mathbf{q}_1-\mathbf{q}_2-\mathbf{q}_3).\end{aligned} \tag{VII.15}$$

The integral over the shell momentum $\mathbf{q}_1$ is odd and this contribution is zero. (Two similar vanishing terms arise from contractions with different indices α and β.) The next term is a renormalization of ρ, arising from

$$\begin{aligned}\left\langle \mathcal{U}_1^b \right\rangle_0^> =& -\frac{K}{2}\int \frac{d^d\mathbf{q}_1\, d^d\mathbf{q}_2\, d^d\mathbf{q}_3}{(2\pi)^{3d}}(\mathbf{q}_1\cdot\mathbf{q}_3) \\ & \left\langle \pi_\alpha^>(\mathbf{q}_1)\pi_\beta^>(\mathbf{q}_3)\right\rangle_0^> \pi_\alpha^<(\mathbf{q}_2)\pi_\beta^<(-\mathbf{q}_1-\mathbf{q}_2-\mathbf{q}_3) \\ =& \frac{K}{2}\int_0^{\Lambda/b}\frac{d^d\mathbf{q}}{(2\pi)^d}|\vec{\pi}^{\,<}(\mathbf{q})|^2 \times \int_{\Lambda/b}^{\Lambda}\frac{d^d\mathbf{k}}{(2\pi)^d}\frac{k^2}{Kk^2} \\ =& \frac{\rho}{2}\int_0^{\Lambda/b}\frac{d^d\mathbf{q}}{(2\pi)^d}|\vec{\pi}^{\,<}(\mathbf{q})|^2 \times \left(1-b^{-d}\right).\end{aligned} \tag{VII.16}$$

(Note that in general $\rho = N/V = \int_0^\Lambda d^d\mathbf{q}/(2\pi)^d$.) Finally, a renormalization of K is obtained from

$$\begin{aligned}\langle \mathcal{U}_1^c\rangle_0^> =& -\frac{K}{2}\int \frac{d^d\mathbf{q}_1\, d^d\mathbf{q}_2\, d^d\mathbf{q}_3}{(2\pi)^{3d}}(\mathbf{q}_1\cdot\mathbf{q}_3) \\ & \left\langle \pi_\alpha^>(\mathbf{q}_2)\pi_\beta^>(-\mathbf{q}_1-\mathbf{q}_2-\mathbf{q}_3)\right\rangle_0^> \pi_\alpha^<(\mathbf{q}_1)\pi_\beta^<(\mathbf{q}_3) \\ =& \frac{K}{2}\int_0^{\Lambda/b}\frac{d^d\mathbf{q}}{(2\pi)^d}\, q^2|\vec{\pi}^{\,<}(\mathbf{q})|^2 \times \frac{I_d(b)}{K},\end{aligned} \tag{VII.17}$$

where

$$I_d(b) \equiv \int_{\Lambda/b}^{\Lambda}\frac{d^d\mathbf{k}}{(2\pi)^d}\,\frac{1}{k^2} = \frac{K_d\Lambda^{d-2}\left(1-b^{2-d}\right)}{(d-2)}. \tag{VII.18}$$

The coarse–grained Hamiltonian in eq.(VII.14) now equals

$$\begin{aligned}\beta\tilde{\mathcal{H}}\left[\vec{\pi}^{\,<}\right] =& V\delta f_b^0 + V\delta f_b^1 + \frac{K}{2}\left(1+\frac{I_d(b)}{K}\right)\int_0^{\Lambda/b}\frac{d^d\mathbf{q}}{(2\pi)^d}\, q^2|\vec{\pi}^{\,<}(\mathbf{q})|^2 \\ & + \frac{K}{2}\int \frac{d^d\mathbf{q}_1\, d^d\mathbf{q}_2\, d^d\mathbf{q}_3}{(2\pi)^{3d}}\pi_\alpha^<(\mathbf{q}_1)\,\pi_\alpha^<(\mathbf{q}_2)\,\pi_\beta^<(\mathbf{q}_3)\,\pi_\beta^<(-\mathbf{q}_1-\mathbf{q}_2-\mathbf{q}_3)\,(\mathbf{q}_1\cdot\mathbf{q}_3) \\ & - \frac{\rho}{2}\int_0^{\Lambda/b}\frac{d^d\mathbf{q}}{(2\pi)^d}|\vec{\pi}^{\,<}(\mathbf{q})|^2 \times \left[1-\left(1-b^{-d}\right)\right] + \mathcal{O}(T^2).\end{aligned} \tag{VII.19}$$

The most important consequence of coarse graining is the change of the elastic coefficient K to

$$\tilde{K} = K\left(1+\frac{I_d(b)}{K}\right). \tag{VII.20}$$

After rescaling, $\mathbf{x}' = \mathbf{x}/b$, and renormalizing, $\vec{\pi}\,'(\mathbf{x}) = \vec{\pi}^{\,<}(\mathbf{x})/\zeta$, we obtain the renormalized Hamiltonian in real space as

$$\begin{aligned} -\beta\mathcal{H}' = &- V\delta f_b^0 - V\delta f_b^1 - \frac{\tilde{K}b^{d-2}\zeta^2}{2}\int d^d\mathbf{x}'(\nabla'\pi')^2 \\ &-\frac{Kb^{d-2}\zeta^4}{2}\int d^d\mathbf{x}'\,(\vec{\pi}\,'(\mathbf{x}')\nabla\vec{\pi}\,'(\mathbf{x}'))^2 + \frac{\rho\zeta^2}{2}\int d^d\mathbf{x}'\,\pi'(\mathbf{x}')^2 + \mathcal{O}(T^2). \end{aligned} \tag{VII.21}$$

The easiest method for obtaining the rescaling factor ζ, is to take advantage of the rotational symmetry of spins. After averaging over the short wavelength modes, the spin is

$$\begin{aligned} \left\langle \tilde{\vec{s}} \right\rangle_0^> &= \left\langle \left(\pi_1^< + \pi_1^>, \cdots, \sqrt{1-(\vec{\pi}^{\,<}+\vec{\pi}^{\,>})^2} \right) \right\rangle_0^> \\ &= \left(\pi_1^<, \cdots, 1 - \frac{(\vec{\pi}^{\,<})^2}{2} - \left\langle \frac{(\vec{\pi}^{\,>})^2}{2} \right\rangle_0^> + \cdots \right) \\ &= \left(1 - \left\langle \frac{(\vec{\pi}^{\,>})^2}{2} \right\rangle_0^> + \mathcal{O}(T^2) \right) \left(\pi_1^<, \cdots, \sqrt{1-(\vec{\pi}^{\,<})^2} \right). \end{aligned} \tag{VII.22}$$

We thus identify

$$\zeta = 1 - \left\langle \frac{(\vec{\pi}^{\,>})^2}{2} \right\rangle_0^> + \mathcal{O}(T^2) = 1 - \frac{(n-1)}{2}\,\frac{I_d(b)}{K} + \mathcal{O}(T^2), \tag{VII.23}$$

as the length of the coarse-grained spin. The renormalized coupling constant in eq.(VII.21) is now obtained from

$$\begin{aligned} K' &= b^{d-2}\zeta^2\tilde{K} \\ &= b^{d-2}\left[1 - \frac{n-1}{2K}I_d(b)\right]^2 K\left[1 + \frac{1}{K}I_d(b)\right] \\ &= b^{d-2}K\left[1 - \frac{n-2}{K}I_d(b) + \mathcal{O}\left(\frac{1}{K^2}\right)\right]. \end{aligned} \tag{VII.24}$$

For infinitesimal rescaling, $b = (1+\delta\ell)$, the shell integral results in

$$I_d(b) = K_d\Lambda^{d-2}\delta\ell. \tag{VII.25}$$

The differential recursion relation corresponding to eq.(VII.24) is thus

$$\frac{dK}{d\ell} = (d-2)K - (n-2)K_d\Lambda^{d-2}. \tag{VII.26}$$

Alternatively, the scaling of temperature $T = K^{-1}$, is

$$\frac{dT}{d\ell} = -\frac{1}{K^2}\frac{dK}{d\ell} = -(d-2)T + (n-2)K_d\Lambda^{d-2}T^2. \tag{VII.27}$$

It may appear that we should also keep track of the evolution of the coefficients of the two terms in $\mathcal{U}_1$ under RG. In fact, spherical symmetry ensures that the coefficient of the quartic term is precisely the same as K at all orders. The apparent difference between the two is of order of $\mathcal{O}(T^2)$, and will vanish when all terms at this order are included. The coefficient of the second order term in $\mathcal{U}_1$ merely tracks the density of points and also has trivial renormalization.

The behavior of temperature under RG changes drastically at $d = 2$. For $d < 2$, the linear flow is away from zero, indicating that the ordered phase is unstable and there is no broken symmetry. For $d > 2$, small T flows back to zero, indicating that the ordered phase is stable. The flows for $d = 2$ are controlled by the second ordered term which changes sign at $n = 2$. For $n > 2$ the flow is towards high temperatures, indicating that Heisenberg and higher spin models are disordered. The situation for $n = 2$ is ambiguous, and it can in fact be shown that $dT/d\ell$ is zero to all orders. This special case will be discussed in more detail in the next section. For $d > 2$ and $n > 2$, there is a phase transition at the fixed point,

$$T^* = \frac{\epsilon}{(n-2)K_d\Lambda^{d-2}} = \frac{2\pi\epsilon}{(n-2)} + \mathcal{O}(\epsilon^2), \tag{VII.28}$$

where $\epsilon = d - 2$ is used as a small parameter. The recursion relation at order of ϵ is

$$\frac{dT}{d\ell} = -\epsilon T + \frac{(n-2)}{2\pi}T^2. \tag{VII.29}$$

Stability of the fixed point is determined by the linearized recursion relation

$$\left.\frac{d\delta T}{d\ell}\right|_{T^*} = \left[-\epsilon + \frac{(n-2)}{\pi}T^*\right]\delta T = \left[-\epsilon + 2\epsilon\right]\delta T = \epsilon\delta T, \qquad \Longrightarrow \qquad y_t = \epsilon \quad . \tag{VII.30}$$

The thermal eigenvalue, and the resulting exponents $\nu = 1/\epsilon$, and $\alpha = 2-(2+\epsilon)/\epsilon \approx -2/\epsilon$, are independent of n at this order.

The magnetic eigenvalue can be obtained by adding a term $-\vec{h}\cdot\int d^d\mathbf{x}\,\vec{s}\,(\mathbf{x})$, to the Hamiltonian. Under the action of RG, $h' = b^d\zeta h \equiv b^{y_h}h$, with

$$b^{y_h} = b^d\left[1 - \frac{n-1}{2K}I_d(b)\right]. \tag{VII.31}$$

For an infinitesimal rescaling

$$1 + y_h \delta\ell = (1 + d\delta\ell)\left(1 - \frac{n-1}{2} T^* K_d \Lambda^{d-2} \delta\ell\right), \tag{VII.32}$$

leading to

$$y_h = d - \frac{n-1}{2(n-2)}\epsilon = 1 + \frac{n-3}{2(n-2)}\epsilon + \mathcal{O}(\epsilon^2), \tag{VII.33}$$

which does depend on n. Using exponent identities, we find

$$\eta = 2 + d - 2y_h = \frac{\epsilon}{n-2}. \tag{VII.34}$$

The exponent η is zero at the lowest order in a $4 - d$ expansion, but appears at first order in the vicinity of two dimensions. The actual values of the exponents calculated at this order are not very satisfactory.

VII.B Topological Defects in the XY model

As stated in the previous section, thermal excitation of Goldstone modes destroys spontaneous order in two dimensional models with a broken continuous symmetry. The RG study of the non-linear σ-model confirms that the transition temperature of n-component spins vanishes as $T^* = 2\pi\epsilon/(n-2)$ for $\epsilon = (d-2) \to 0$. However, the same RG procedure appears to suggest a different behavior for $n = 2$. The first indication of unusual behavior for the two dimensional XY model ($n = 2$), appeared in an analysis of high temperature series by Stanley and Kaplan in 1966. The series results strongly suggested the divergence of susceptibility at a finite temperature, seemingly in contradiction with the absence of symmetry breaking. It was indeed this contradiction that led Wigner to explore the possibility of a phase transition without symmetry breaking. The Z_2 lattice gauge theory, discussed in sec.VI.E as the dual of the three dimensional Ising model, realizes such a possibility. The two phases of the Z_2 gauge theory are characterized by different functional forms for the decay of an appropriate correlation function (the Wilson loop). We can similarly examine the asymptotic behavior of the spin-spin correlation functions of the XY model at high and low temperatures.

A high temperature expansion for the correlation function for the XY model on a lattice is constructed from

$$\begin{aligned}\langle \vec{s}_{\mathbf{0}} \cdot \vec{s}_{\mathbf{r}} \rangle = \langle \cos(\theta_{\mathbf{0}} - \theta_{\mathbf{r}}) \rangle &= \frac{1}{Z} \prod_{i=1}^{N} \left(\int_0^{2\pi} \frac{d\theta_i}{2\pi} \right) \cos\left(\theta_{\mathbf{0}} - \theta_{\mathbf{r}}\right) e^{K \sum_{<i,j>} \cos(\theta_i - \theta_j)} \\ &= \frac{1}{Z} \prod_{i=1}^{N} \left(\int_0^{2\pi} \frac{d\theta_i}{2\pi} \right) \cos\left(\theta_{\mathbf{0}} - \theta_{\mathbf{r}}\right) \prod_{<i,j>} \left[1 + K \cos\left(\theta_i - \theta_j\right) + \mathcal{O}\left(K^2\right) \right].\end{aligned} \tag{VII.35}$$

The expansion for the partition function is similar, except for the absence of the factor $\cos(\theta_{\mathbf{0}} - \theta_{\mathbf{r}})$. To the lowest order in K, each bond on the lattice contributes either a factor of one, or $K\cos(\theta_i - \theta_j)$. Since,

$$\int_0^{2\pi} \frac{d\theta_1}{2\pi} \cos\left(\theta_1 - \theta_2\right) = 0, \tag{VII.36}$$

any graph with a single bond emanating from an *internal* site vanishes. For the numerator of eq.(VII.35) to be non-zero, there must be bonds originating from the *external* points at $\mathbf{0}$ and $\mathbf{r}$. Integrating over an *internal* point with two bonds leads to

$$\int_0^{2\pi} \frac{d\theta_2}{2\pi} \cos\left(\theta_1 - \theta_2\right) \cos\left(\theta_2 - \theta_3\right) = \frac{1}{2} \cos\left(\theta_1 - \theta_3\right). \tag{VII.37}$$

The first graph that contributes to eq.(VII.35) is the shortest path (of length r) connecting the points $\mathbf{0}$ and $\mathbf{r}$. Since integrating over the end points gives

$$\int_0^{2\pi} \frac{d\theta_{\mathbf{0}} d\theta_{\mathbf{r}}}{(2\pi)^2} \cos\left(\theta_{\mathbf{0}} - \theta_{\mathbf{r}}\right)^2 = \frac{1}{2}, \tag{VII.38}$$

each bond along the path contributes $(K/2)$. (In constructing graphs for the partition function, there is an additional factor of 2 for every loop.) Thus to lowest order

$$\langle \vec{s}_{\mathbf{0}} \cdot \vec{s}_{\mathbf{r}} \rangle \approx \left(\frac{K}{2}\right)^r = e^{-r/\xi}, \qquad \text{with} \qquad \xi \approx \frac{1}{\ln\left(2/K\right)}, \tag{VII.39}$$

and the disordered high temperature phase is characterized by an exponential decay of correlations. (This is clearly quite generic in all spin systems.)

At low temperatures, the cost of small fluctuations around the ground state is obtained by a quadratic expansion, which gives $K \int d^d\mathbf{x} (\nabla\theta)^2/2$ in the continuum limit. The standard rules of Gaussian integration yield,

$$\langle \vec{s}_{\mathbf{0}} \cdot \vec{s}_{\mathbf{r}} \rangle = \left\langle \Re e^{i(\theta_{\mathbf{0}} - \theta_{\mathbf{r}})} \right\rangle = \Re \exp\left[-\frac{1}{2} \left\langle \left(\theta_{\mathbf{0}} - \theta_{\mathbf{r}}\right)^2 \right\rangle \right]. \tag{VII.40}$$

In two dimensions, the Gaussian fluctuations grow as

$$\frac{1}{2} \left\langle \left(\theta_{\mathbf{0}} - \theta_{\mathbf{r}}\right)^2 \right\rangle = \frac{1}{2\pi K} \ln\left(\frac{r}{a}\right), \tag{VII.41}$$

where a is a short distance cut-off (of the order of the lattice spacing). Hence, at low temperatures,

$$\langle \vec{s}_{\mathbf{0}} \cdot \vec{s}_{\mathbf{r}} \rangle \approx \left(\frac{a}{r}\right)^{\frac{1}{2\pi K}}, \tag{VII.42}$$

i.e. the decay of correlations is *algebraic* rather than *exponential*. A power law decay of correlations implies self–similarity (no correlation length), and is usually associated with a critical point. Here it arises from the logarithmic growth of angular fluctuations, which is specific to two dimensions.

The distinct asymptotic decays of correlations at high and low temperatures allows for the possibility of a finite temperature phase transition separating the two regimes. However, the arguments put forward above are not specific to the XY model. Any continuous spin model will exhibit exponential decay of correlations at high temperature, and a power law decay in a low temperature Gaussian approximation. To show that the Gaussian behavior persists at finite temperatures, we must prove that it is not modified by the

additional terms in the gradient expansion. Quartic terms, such as $\int d^d\mathbf{x}(\nabla\theta)^4$, generate interactions between the Goldstone modes. The *relevance* of these interactions was probed in the previous section using the non-linear σ-model. The zero temperature fixed point in $d = 2$ is unstable for all $n > 2$, but apparently stable for $n = 2$. (There is only one branch of Goldstone modes for $n = 2$. It is the interactions between different branches of these modes for $n > 2$ that leads to instability towards high temperature behavior.) The low temperature phase of the XY model is said to posses *quasi–long range order*, as opposed to *true long range order* that accompanies a finite magnetization.

What is the mechanism for the disordering of the quasi–long range ordered phase? As the RG study suggests that higher order terms in the gradient expansion are not relevant, we must search for other operators. The gradient expansion describes the energy cost of *small* deformations around the ground state, and applies to configurations that can be continuously deformed to the uniformly ordered state. Kosterlitz and Thouless (1973) suggested that the disordering is caused by *topological defects* that can not be regarded as simple deformations of the ground state. Since the angle describing the orientation of a spin is undefined up to an integer multiple of 2π, it is possible to construct spin configurations for which in going around a closed path the angle rotates by $2\pi n$. The integer n is the *topological charge* enclosed by the path. Because of the discrete nature of this charge, it is impossible to continuously deform to the uniformly ordered state in which the charge is zero. (More generally, topological defects arise in any model with a compact group describing the order parameter.)

The elementary defect, or *vortex*, has unit charge. In completing a circle centered on the defect the orientation of the spin changes by $\pm 2\pi$. If the radius r, of the circle is sufficiently large, the variations in angle will be small and the lattice structure can be ignored. By symmetry, $\nabla\theta$ has a uniform magnitude, and points along the circle (i.e. perpendicular to the radial vector). The magnitude of the distortion is obtained from

$$\oint \nabla\theta \cdot d\vec{s} = \frac{d\theta}{ds}(2\pi r) = 2\pi n, \qquad \Longrightarrow \qquad \frac{d\theta}{ds} = \frac{n}{r}. \tag{VII.43}$$

Since $\nabla\theta$ is a radial vector, it can be written as

$$\nabla\theta = n\left(-\frac{y}{r^2}, +\frac{x}{r^2}, 0\right) = -\frac{n}{r}\hat{r} \times \hat{z} = -n\nabla \times (\hat{z}\ln r)\,. \tag{VII.44}$$

Here, $\hat{r}$ and $\hat{z}$ are unit vectors respectively in the plane and perpendicular to it, and $\vec{a} \times \vec{b}$ indicates the cross product of the two vectors. This (continuum) approximation fails close to the center (core) of the vortex, where the lattice structure is important.

The energy cost of a single vortex of charge n has contributions from the core region, as well as from the relatively uniform distortions away from the center. The distinction between regions inside and outside the core is arbitrary, and for simplicity, we shall use a circle of radius a to distinguish the two, i.e.

$$\begin{aligned}\beta\mathcal{E}_n =&\beta\mathcal{E}_n^0(a) + \frac{K}{2}\int_a d^2\mathbf{x}(\nabla\theta)^2 \\ =&\beta\mathcal{E}_n^0(a) + \frac{K}{2}\int_a^L (2\pi r dr)\left(\frac{n}{r}\right)^2 = \beta\mathcal{E}_n^0(a) + \pi K n^2 \ln\left(\frac{L}{a}\right).\end{aligned} \tag{VII.45}$$

The dominant part of the energy comes from the region outside the core, and diverges with the size of the system, L. The large energy cost of defects prevents their spontaneous formation close to zero temperature. The partition function for a configuration with a single vortex is

$$Z_1(n) \approx \left(\frac{L}{a}\right)^2 \exp\left[-\beta\mathcal{E}_n^0(a) - \pi K n^2 \ln\left(\frac{L}{a}\right)\right] = y_n^0(a)\left(\frac{L}{a}\right)^{2-\pi K n^2}, \tag{VII.46}$$

where $(L/a)^2$ results from the *configurational entropy* of possible vortex locations in an area of size L^2. The entropy and energy of a vortex both grow as $\ln L$, and the free energy is dominated by one or the other. At low temperatures (large K) energy dominates and Z_1, a measure of the weight of configurations with a single vortex, vanishes. At high enough temperatures, $K < K_n = 2/(\pi n^2)$, the entropy contribution is large enough to favor spontaneous formation of vortices. On increasing temperature, the first vortices to appear correspond to $n = \pm 1$ at $K_c = 2/\pi$. Beyond this point there are many vortices in the system, and eq.(VII.46) is no longer useful.

The coupling $K_c = 2/\pi$ is a *lower bound* for the stability of the system to topological defects. This is because pairs (dipoles) of defects may appear at larger couplings. Consider a pair of charges ± 1 at a separation d. The distortions far away from the dipole center, $r \gg d$, can be obtained by superposing those of the individual vortices, and

$$\nabla\theta = \nabla\theta_+ + \nabla\theta_- \approx \vec{d}\cdot\nabla\left(\frac{\hat{r}\times\hat{z}}{r}\right), \tag{VII.47}$$

decays as d/r^2. Integrating this distortion leads to a *finite* energy, and hence dipoles appear with the appropriate Boltzmann weight at any temperature. The low temperature phase should thus be visualized as a gas of tightly bound dipoles. The number (and size) of dipoles increases with temperature, and the high temperature state is a plasma of unbound

vortices. The distinction between the two regimes can be studied by examining a typical net topological charge, $Q(\ell)$, in a large area of dimension $\ell \gg a$. The average charge in always zero, while fluctuations in the low temperature phase are due to the dipoles straddling the parameter, i.e. $\left\langle Q(\ell)^2 \right\rangle \propto \ell$. In the high temperature state, charges of either sign can appear without restriction and $\left\langle Q(\ell)^2 \right\rangle \propto \ell^2$. (Note the similarity to the distinct behaviors of the Wilson loop in the high and low temperature phases of the Z_2 gauge theory.)

To describe the transition between the two regimes, we need to properly account for the interactions between vortices. The distortion field $\vec{u} \equiv \nabla\theta$, in the presence of a collection of vortices is similar to the velocity of a fluid. In the absence of vorticity, the flow is *potential*, i.e. $\vec{u} = \vec{u}_0 = \nabla\phi$, and $\nabla \times \vec{u}_0 = 0$. The topological charge can be related to $\nabla \times \vec{u}$ by noting that for any closed path,

$$\oint \vec{u} \cdot d\vec{s} = \int (d^2\mathbf{x}\, \hat{z}) \cdot \nabla \times \vec{u} \quad , \tag{VII.48}$$

where the second integral is over the area enclosed by the path. Since the left hand side is an integer multiple of 2π, we can set

$$\nabla \times \vec{u} = 2\pi \hat{z} \sum_i n_i\, \delta^2(\mathbf{x} - \mathbf{x}_i), \tag{VII.49}$$

describing a collection of vortices of charge $\{n_i\}$ at locations $\{\mathbf{x}_i\}$. The solution to eq.(VII.49) can be obtained by setting $\vec{u} = \vec{u}_0 - \nabla \times (\hat{z}\psi)$, leading to

$$\nabla \times \vec{u} = \hat{z}\nabla^2\psi, \qquad \Longrightarrow \qquad \nabla^2\psi = 2\pi \sum_i n_i\, \delta^2(\mathbf{x} - \mathbf{x}_i). \tag{VII.50}$$

Thus ψ behaves like the potential due to a set of charges $\{2\pi n_i\}$. The solution,

$$\psi(\mathbf{x}) = \sum_i n_i\, \ln\left(|\mathbf{x} - \mathbf{x}_i|\right), \tag{VII.51}$$

is simply a superposition of the potentials as in eq.(VII.44).

Any two dimensional distortion can thus be written as

$$\vec{u} = \vec{u}_0 + \vec{u}_1 = \nabla\phi - \nabla \times (\hat{z}\psi), \tag{VII.52}$$

and the corresponding "kinetic energy", $\beta\mathcal{H} = K \int d^2\mathbf{x}\, |\vec{u}|^2/2$, decomposed as

$$\beta\mathcal{H} = \int d^2\mathbf{x} \left[(\nabla\phi)^2 - 2\nabla\phi \cdot \nabla \times (\hat{z}\psi) + (\nabla \times \hat{z}\psi)^2 \right]. \tag{VII.53}$$

The second term vanishes, since following an integration by parts,

$$-\int d^2\mathbf{x}\,\nabla\phi\cdot\nabla\times(\hat{z}\psi)=\int d^2\mathbf{x}\,\phi\nabla\cdot(\nabla\times\hat{z}\psi)\,, \tag{VII.54}$$

and $\nabla\cdot\nabla\times\vec{u}=0$ for any vector. The third term in eq.(VII.53) can be simplified by noting that $\nabla\psi=(\partial_x\psi,\partial_y\psi,0)$, and $\nabla\times(\hat{z}\psi)=(-\partial_y\psi,\partial_x\psi,0)$, are orthogonal vectors of equal length. Hence

$$\beta\mathcal{H}_1\equiv\frac{K}{2}\int d^2\mathbf{x}\,(\nabla\times\hat{z}\psi)^2=\frac{K}{2}\int d^2\mathbf{x}\,(\nabla\psi)^2=-\frac{K}{2}\int d^2\mathbf{x}\,\psi\nabla^2\psi, \tag{VII.55}$$

where the second identity follows an integration by parts. Equations (VII.50) and (VII.51) now result in

$$\begin{aligned}\beta\mathcal{H}_1=&-\frac{K}{2}\int d^2\mathbf{x}\,\left(\sum_i n_i\,\ln\left(|\mathbf{x}-\mathbf{x}_i|\right)\right)\left(2\pi\sum_j n_j\,\delta^2(\mathbf{x}-\mathbf{x}_j)\right)\\ =&-2\pi^2K\sum_{i,j}n_in_j\,C(\mathbf{x}_i-\mathbf{x}_j),\end{aligned} \tag{VII.56}$$

where $C(\mathbf{x})=\ln(|\mathbf{x}|)/2\pi$ is the two dimensional Coulomb potential. There is a difficulty with the above result for $i=j$ due to the divergence of the logarithm at small arguments. This is a consequence of the breakdown of the continuum treatment at short distances. The self-interaction of a vortex is simply its core energy $\beta\mathcal{E}^0_n$, and

$$\beta\mathcal{H}_1=\sum_i\beta\mathcal{E}^0_{n_i}-4\pi^2K\sum_{i<j}n_in_jC(\mathbf{x}_i-\mathbf{x}_j). \tag{VII.57}$$

The configuration space of the XY model close to zero temperature can thus be partitioned into different topological segments. The degrees of freedom in each segment are the charges $\{n_i\}$, and locations $\{\mathbf{x}_i\}$, of the *vortices*, in addition to the field $\phi(\mathbf{x})$ describing *spin waves*. The partition function of the model can thus be approximated as

$$\begin{aligned}Z=&\prod_i\int_0^{2\pi}\frac{d\theta_i}{2\pi}\,\exp\left[K\sum_{<i,j>}\cos(\theta_i-\theta_j)\right]\\ \propto&\int\mathcal{D}\phi(\mathbf{x})\,e^{-\frac{K}{2}\int d^2\mathbf{x}\,(\nabla\phi)^2}\sum_{\{n_i\}}\int d^2\mathbf{x}_i\,e^{-\sum_i\beta\mathcal{E}^0_{n_i}+4\pi^2K\sum_{i<j}n_in_jC(\mathbf{x}_i-\mathbf{x}_j)}\\ \equiv&\,Z_{\rm s.w.}Z_Q\quad,\end{aligned} \tag{VII.58}$$

where $Z_{\rm s.w.}$ is the Gaussian partition function of spin waves, and Z_Q is the contribution of vortices. The latter describes a grand canonical gas of charged particles, interacting via the two dimensional Coulomb interaction. In calculating the Hamiltonian $\beta\mathcal{H}_1$ in eq.(VII.55), we performed an integration by parts. The surface integral that was ignored in the process in fact grows with system size as $(\sum_i n_i)\ln L$. Thus only configurations that are overall neutral are included in calculating Z_Q. We further simplify the problem by considering only the elementary excitations with $n_i = \pm 1$, which are most likely at low temperatures due to their lower energy. Setting $y_0 \equiv \exp\left[-\beta\mathcal{E}^0_{\pm 1}\right]$,

$$Z_Q = \sum_{N=0}^{\infty} y_0^N \int \prod_{i=1}^{N} d^2\mathbf{x}_i \, \exp\left[4\pi^2 K \sum_{i<j} q_i q_j C(\mathbf{x}_i - \mathbf{x}_j)\right], \tag{VII.59}$$

where $q_i = \pm 1$, and $\sum_i q_i = 0$.

VII.C Renormalization Group for the Coulomb Gas

The two partition functions in eq.(VII.58) are independent and can be calculated separately. As the Gaussian partition function is analytic, any phase transitions of the XY model must originate in the Coulomb gas. As briefly discussed earlier, in the low temperature phase the charges appear only in the small density of tightly bound dipole pairs. The dipoles dissociate in the high temperature phase, forming a plasma. The two phases can be distinguished by examining the interaction between two *external* test charges at a large separation X. In the absence of any *internal* charges (for $y_0 = 0$) in the medium, the two particles interact by the *bare* Coulomb interaction $C(X)$. A finite density of internal charges for small y_0 partially screens the external charges, and reduces the interaction between the test charges to $C(X)/\varepsilon$, where ε is an effective *dielectric* constant. There is an *insulator to metal* transition at sufficiently large y_0. In the metallic (plasma) phase, the external charges are completely screened and their effective interaction decays exponentially.

To quantify the above picture, we shall compute the effective interaction between two *external* charges at $\mathbf{x}$ and $\mathbf{x}'$, perturbatively in the fugacity y_0. To lowest order, we need to include configurations with two *internal* charges (at $\mathbf{y}$ and $\mathbf{y}'$), and

$$\begin{aligned} e^{-\beta\mathcal{V}(\mathbf{x}-\mathbf{x}')} &= e^{-4\pi^2 KC(\mathbf{x}-\mathbf{x}')}\times \\ &\frac{\left[1+y_0^2\int d^2\mathbf{y}d^2\mathbf{y}'\, e^{-4\pi^2 KC(\mathbf{y}-\mathbf{y}')+4\pi^2 K\left[C(\mathbf{x}-\mathbf{y})-C(\mathbf{x}-\mathbf{y}')-C(\mathbf{y}'-\mathbf{x})+C(\mathbf{x}'-\mathbf{y}')\right]}+\mathcal{O}(y_0^4)\right]}{\left[1+y_0^2\int d^2\mathbf{y}d^2\mathbf{y}'\, e^{-4\pi^2 KC(\mathbf{y}-\mathbf{y}')}+\mathcal{O}(y_0^4)\right]} \\ &= e^{-4\pi^2 KC(\mathbf{x}-\mathbf{x}')}\left[1+y_0^2\int d^2\mathbf{y}d^2\mathbf{y}'\, e^{-4\pi^2 KC(\mathbf{y}-\mathbf{y}')}\left(e^{4\pi^2 KD(\mathbf{x},\mathbf{x}';\mathbf{y},\mathbf{y}')}-1\right)+\mathcal{O}(y_0^4)\right], \end{aligned} \tag{VII.60}$$

where $D(\mathbf{x},\mathbf{x}';\mathbf{y},\mathbf{y}')$ is the interaction *between* the internal and external dipoles. The direct interaction between internal charges tends to keep the separation $\mathbf{r}=\mathbf{y}'-\mathbf{y}$ small. Using the center of mass $\mathbf{R}=(\mathbf{y}+\mathbf{y}')/2$, we can change variables to $\mathbf{y}=\mathbf{R}-\mathbf{r}/2$ and $\mathbf{y}'=\mathbf{R}+\mathbf{r}/2$, and expand the dipole–dipole interaction for small $\mathbf{r}$ as

$$\begin{aligned} D\left(\mathbf{x},\mathbf{x}';\mathbf{y},\mathbf{y}'\right) =& C\left(\mathbf{x}-\mathbf{R}+\frac{\mathbf{r}}{2}\right)-C\left(\mathbf{x}-\mathbf{R}-\frac{\mathbf{r}}{2}\right)-C\left(\mathbf{x}'-\mathbf{R}+\frac{\mathbf{r}}{2}\right)+C\left(\mathbf{x}'-\mathbf{R}-\frac{\mathbf{r}}{2}\right) \\ =& -\mathbf{r}\cdot\nabla_{\mathbf{R}}C(\mathbf{x}-\mathbf{R})+\mathbf{r}\cdot\nabla_{\mathbf{R}}C(\mathbf{x}'-\mathbf{R})+\mathcal{O}(r^3). \end{aligned} \tag{VII.61}$$

To the same order

$$\begin{aligned} e^{4\pi^2 KD(\mathbf{x},\mathbf{x}';\mathbf{y},\mathbf{y}')}-1 =& -4\pi^2 K\mathbf{r}\cdot\nabla_{\mathbf{R}}\left(C(\mathbf{x}-\mathbf{R})-C(\mathbf{x}'-\mathbf{R})\right) \\ &+8\pi^4K^2\left[\mathbf{r}\cdot\nabla_{\mathbf{R}}\left(C(\mathbf{x}-\mathbf{R})-C(\mathbf{x}'-\mathbf{R})\right)\right]^2+\mathcal{O}(r^3). \end{aligned} \tag{VII.62}$$

After the change of variables $\int d^2\mathbf{y}d^2\mathbf{y}' \to \int d^2\mathbf{r}d^2\mathbf{R}$, the effective interaction becomes

$$e^{-\beta\mathcal{V}(\mathbf{x}-\mathbf{x}')} = e^{-4\pi^2 KC(\mathbf{x}-\mathbf{x}')}\Bigg\{\Bigg[1 + y_0^2\int d^2\mathbf{r}d^2\mathbf{R}\, e^{-4\pi^2 KC(\mathbf{r})}\times$$
$$\Big(-4\pi^2 K\mathbf{r}\cdot\nabla_{\mathbf{R}}\left(C(\mathbf{x}-\mathbf{R}) - C(\mathbf{x}'-\mathbf{R})\right) + 8\pi^4K^2\left[\mathbf{r}\cdot\nabla_{\mathbf{R}}\left(C(\mathbf{x}-\mathbf{R}) - C(\mathbf{x}'-\mathbf{R})\right)\right]^2$$
$$+\mathcal{O}(r^3)\Big) + \mathcal{O}(y_0^4)\Bigg]\Bigg\}. \tag{VII.63}$$

Following the angular integrations in $d^2\mathbf{r}$, the term linear in $\mathbf{r}$ vanishes, while the angular average of $(\mathbf{r}\cdot\nabla_{\mathbf{R}}C)^2$ is $r^2|\nabla_{\mathbf{R}}C|^2/2$. Hence eq.(VII.63) simplifies to

$$e^{-\beta\mathcal{V}(\mathbf{x}-\mathbf{x}')} = e^{-4\pi^2 KC(\mathbf{x}-\mathbf{x}')}\times$$
$$\left[1 + y_0^2\int(2\pi r dr)e^{-4\pi^2 KC(r)}8\pi^4K^2\,\frac{r^2}{2}\int d^2\mathbf{R}\big(\nabla_{\mathbf{R}}\left(C(\mathbf{x}-\mathbf{R}) - C(\mathbf{x}'-\mathbf{R})\right)\big)^2 + \mathcal{O}(r^4)\right]. \tag{VII.64}$$

The remaining integral can be evaluated by parts,

$$\begin{aligned}
&\int d^2\mathbf{R}\,\left[\nabla_{\mathbf{R}}\left(C(\mathbf{x}-\mathbf{R}) - C(\mathbf{x}'-\mathbf{R})\right)\right]^2\\
&= -\int d^2\mathbf{R}\,\left(C(\mathbf{x}-\mathbf{R}) - C(\mathbf{x}'-\mathbf{R})\right)\left(\nabla^2C(\mathbf{x}-\mathbf{R}) - \nabla^2C(\mathbf{x}'-\mathbf{R})\right)\\
&= -\int d^2\mathbf{R}\,\left(C(\mathbf{x}-\mathbf{R}) - C(\mathbf{x}'-\mathbf{R})\right)\left(\delta^2(\mathbf{x}-\mathbf{R}) - \delta^2(\mathbf{x}'-\mathbf{R})\right)\\
&= 2C(\mathbf{x}-\mathbf{x}') - 2C(0).
\end{aligned} \tag{VII.65}$$

The short distance divergence can again be absorbed into a proper cutoff with $C(x) \to \ln(x/a)/2\pi$, and

$$e^{-\beta\mathcal{V}(\mathbf{x}-\mathbf{x}')} = e^{-4\pi^2 KC(\mathbf{x}-\mathbf{x}')}\left[1 + 16\pi^5K^2y_0^2C(\mathbf{x}-\mathbf{x}')\int drr^3e^{-2\pi K\ln(r/a)} + \mathcal{O}(y_0^4)\right]. \tag{VII.66}$$

The second order term can be exponentiated to give an effective interaction $\beta\mathcal{V}(\mathbf{x}-\mathbf{x}') \equiv 4\pi^2K_{\rm eff}C(\mathbf{x}-\mathbf{x}')$, with

$$K_{\rm eff} = K - 4\pi^3K^2y_0^2a^{2\pi K}\int_a^\infty drr^{3-2\pi K} + \mathcal{O}(y_0^4). \tag{VII.67}$$

We have thus evaluated the dielectric constant of the medium, $\varepsilon = K/K_{\rm eff}$, perturbatively to order of y_0^2. However, the perturbative correction is small only as long as the integral in r converges at large r. The breakdown of the perturbation theory for

$K < K_c = 2/\pi$, occurs precisely at the point where the free energy of an isolated vortex changes sign. This breakdown of perturbation theory is reminiscent of that encountered in the Landau–Ginzburg model for $d < 4$. Using the experience gained from that problem, we shall reorganize the perturbation series into a renormalization group for the parameters K and y_0.

To construct an RG for the Coulomb gas, note that the partition function for the system in eq.(VII.59), involves two parameters (K, y_0), and has an implicit cutoff a, related to the minimum separation between vortices. As discussed earlier, the distinction between regions inside and outside the core of a vortex are arbitrary. Increasing the core size to ba modifies not only the core energy, hence y_0, but also the interaction parameter K. The latter is a consequence of the change in the dielectric properties of the medium due to dipoles of separations between a and ba. The change in fugacity is obtained from eq.(VII.46) by changing a to ba as

$$\tilde{y_0}(ba) = b^{2-\pi K} y_0(a) \quad . \tag{VII.68}$$

The modified Coulomb interaction due to dipoles of all size is given in eq.(VII.67). (The perturbative calculation at order of y_0^2 incorporates only dipoles.) From dipoles in the size range, a to ba, we obtain a contribution

$$\tilde{K} = K \left[1 - (2\pi^2 K) \int_a^{ba} (2\pi r dr) \left(y_0^2 e^{-4\pi^2 K C(r)} \right) r^2 \right], \tag{VII.69}$$

where the terms are grouped so as to make the similarity to standard computations of the dielectric constant apparent. (The probability of creating a dipole is multiplied by its polarizability; the role of $\beta = (k_B T)^{-1}$ is played by $2\pi^2 K$.)

By choosing an infinitesimal $b = e^{\ell} \approx 1 + \ell$, eq.(VII.69) is converted to

$$\frac{dK}{d\ell} = -4\pi^3 K^2 a^4 y_0^2 + \mathcal{O}(y_0^4) \quad . \tag{VII.70}$$

Including the fugacity, the recursion relations are

$$\begin{cases} \dfrac{dK^{-1}}{d\ell} = 4\pi^3 a^4 y_0^2 + \mathcal{O}(y_0^4) \\ \dfrac{dy_0}{d\ell} = (2 - \pi K) y_0 + \mathcal{O}(y_0^3) \end{cases} , \tag{VII.71}$$

originally obtained by Kosterlitz in 1975. While $dK^{-1}/d\ell \geq 0$, the recursion relation for y_0 changes sign at $K_c^{-1} = \pi/2$. At smaller values of K^{-1} (high temperatures) y_0 is relevant,

while at lower temperatures it is irrelevant. Thus the RG flows separate the parameter space into two regions. At low temperatures and small y_0, flows terminate on a *fixed line* at $y_0 = 0$ and $K_{\rm eff} \geq 2/\pi$. This is the insulating phase in which only dipoles of finite size occur. (Hence the vanishing of y_0 under coarse graining.) The strength of the effective Coulomb interaction is given by the point on the fixed line that the flows terminate on. Flows not terminating on the fixed line asymptote to larger values of K^{-1} and y_0, where perturbation theory breaks down. This is the signal of the high temperature phase with an abundance of vortices.

The critical trajectory that separates the two regions of the phase diagram flows to a fixed point at $(K_c^{-1} = \pi/2, y_0 = 0)$. To find the critical behavior at the transition, expand the recursion relations in the vicinity of this point by setting $x = K^{-1} - \pi/2$, and $y = y_0 a^2$. To lowest order, eqs.(VII.71) simplify to

$$\begin{cases} \dfrac{dx}{d\ell} = 4\pi^3 y^2 + \mathcal{O}(xy^2, y^4) \\ \dfrac{dy}{d\ell} = \dfrac{4}{\pi} xy + \mathcal{O}(x^2 y, y^3) \end{cases} . \tag{VII.72}$$

The recursion relations are inherently *nonlinear* in the vicinity of the fixed point. This is quite different from the linear recursion relations that we have encountered so far, and the resulting critical behavior is non-standard. First note that eqs.(VII.72) imply

$$\frac{dx^2}{d\ell} = 8\pi^3 y^2 x = \pi^4 \frac{dy^2}{d\ell}, \quad \Rightarrow \quad \frac{d}{d\ell}\left(x^2 - \pi^4 y^2\right) = 0, \quad \Rightarrow \quad x^2 - \pi^4 y^2 = c. \tag{VII.73}$$

The RG flows thus proceed along hyperbolas characterized by different values of c. For $c > 0$, the focus of the hyperbola is along the y-axis, and the flows proceed to $(x, y) \to \infty$. The hyperbolas with $c < 0$ have foci along the x-axis, and have two branches in the half plane, $y \geq 0$: the branches for $x < 0$ flow to the fixed line, while those in the $x > 0$ quadrant flow to infinity. The critical trajectory separating flows to zero and infinite y corresponds to $c = 0$, i.e. $x_c = -\pi^2 y_c$. Therefore, a small but finite fugacity y_0 reduces the critical temperature to $K_c^{-1} = \pi/2 - \pi^2 y_0 a^2 + \mathcal{O}(y_0^2)$.

In terms of the original XY model, the low temperature phase is characterized by a line of fixed points with $K_{\rm eff} = \lim_{\ell\to\infty} K(\ell) \geq 2/\pi$. There is no correlation length at a fixed point, and indeed the correlations in this phase decay as a power law, $\langle \cos(\theta_{\mathbf{r}} - \cos\theta_{\mathbf{0}})\rangle \sim 1/r^{\eta}$, with $\eta = 1/(2\pi K_{\rm eff}) \leq 1/4$. Since the parameter c is negative in the low temperature phase, and vanishes at the critical point, we can set it to $c = -b^2(T_c - T)$ close to the transition. In other words, the trajectory of initial points tracks a line $(x_0(T), y_0(T))$.

The resulting $c = x_0^2 - \pi^4 y_0^2 \propto (T_c - T)$ is a linear measure of the vicinity to the phase transition. Under renormalization, such trajectories flow to a fixed point at $y = 0$, and $x = -b\sqrt{T_c - T}$. Thus in the vicinity of transition, the effective interaction parameter

$$K_{\rm eff} = \frac{2}{\pi} - \frac{4}{\pi^2} \lim_{\ell \to \infty} x(\ell) = \frac{2}{\pi} + \frac{4b}{\pi^2}\sqrt{T_c - T}, \tag{VII.74}$$

has a square root singularity.

The *stiffness* $K_{\rm eff}$, can be measured in experiments on superfluid films. In the superfluid phase, the order parameter is the condensate wavefunction $\psi(\mathbf{x}) = \Psi e^{i\theta}$. Variations in the phase θ, lead to a superfluid kinetic energy,

$$\mathcal{H} = \int d^d\mathbf{x}\, \psi^* \left(-\frac{\hbar^2\nabla^2}{2m}\right)\psi = \frac{\hbar^2\Psi^2}{2m}\int d^d\mathbf{x}(\nabla\theta)^2, \tag{VII.75}$$

where m is the particle (helium 4) mass. The corresponding XY model has a stiffness $K = \hbar^2\rho_s/(2mk_BT)$, where $\rho_s = \Psi^2$ is the superfluid density. The density ρ_s is measured by examining the changes in the inertia of a torsional oscillator; the superfluid fraction, $\rho_s m$, experiences no friction and does not oscillate. Bishop and Reppy (1978) examined ρ_s for a variety of superfluid films (of different thickness, helium 3 concentration, etc.) wrapped around a torsional cylinder. They constructed the effective stiffness K as a function of temperature, and found that for all films it undergoes a *universal jump* of $2/\pi$ at the transition. The behavior of K for $T < T_c$ was consistent with a square root singularity.

Correlations decay exponentially in the high temperature phase. How does the correlation length ξ, diverge at T_c? The parameter $c = x^2 - \pi^4 y^2 = b^2(T - T_c)$ is now positive all along the hyperbolic trajectory. The recursion relation for x,

$$\frac{dx}{d\ell} = 4\pi^3 y^2 = \frac{4}{\pi}\left(x^2 + b^2(T - T_c)\right), \tag{VII.76}$$

can be integrated to give

$$\frac{dx}{x^2 + b^2(T - T_c)} = \frac{4}{\pi}d\ell, \quad \Longrightarrow \quad \frac{1}{b\sqrt{T - T_c}}\arctan\left(\frac{x}{b\sqrt{T - T_c}}\right) = \frac{4}{\pi}\ell\,. \tag{VII.77}$$

The contribution of the initial point to the left hand side of the above equation can be left out if $x_0 \propto (T - T_c) \ll 1$. The integration has to be stopped when $x(\ell) \sim y(\ell) \sim 1$, since

the perturbative calculation is no longer valid beyond this point. This occurs for a value of

$$\ell^* \approx \frac{\pi}{4b\sqrt{T-T_c}}\,\frac{\pi}{2}, \tag{VII.78}$$

where we have used $\arctan(1/b\sqrt{T-T_c}) \approx \arctan(\infty) = \pi/2$. The resulting correlation length is

$$\xi \approx a e^{\ell^*} \approx a \exp\left(\frac{\pi^2}{8b\sqrt{T-T_c}}\right). \tag{VII.79}$$

Unlike any of the transitions encountered so far, the divergence of the correlation length is not through a power law. This is a consequence of the nonlinear nature of the recursion relations in the vicinity of the fixed point.

Vortices occur in bound pairs for distances smaller than ξ, while there can be an excess of vortices of one sign or the other at larger separations. The interactions between vortices at large distances can be obtained from the Debye-Hückel theory of polyelectrolytes. According to this theory the free charges screen each other leading to a screened Coulomb interaction, $\exp(-r/\xi)C(r)$. On approaching the transition from the high temperature side, the singular part of the free energy,

$$f_{\text{sing.}} \propto \xi^{-2} \propto \exp\left(-\frac{\pi^2}{4b\sqrt{T-T_c}}\right), \tag{VII.80}$$

has only an *essential singularity*. All derivatives of this function are finite at T_c. Thus the predicted heat capacity is quite smooth at the transition. Numerical results based on the RG equations (Berker and Nelson) indicate a smooth maximum in the heat capacity at a temperature higher than T_c, corresponding to the point at which the majority of dipoles unbind.

The Kosterlitz-Thouless picture of vortex unbinding has found numerous applications in two dimensional systems such as superconducting and superfluid films, thin liquid crystals, Josephson junction arrays, electrons on the surface of helium films, etc. Perhaps more importantly, the general idea of topological defects has had much impact in understanding the behavior of many systems. The theory of two dimensional melting developed in the next section is one such example.

VII.D Two Dimensional Solids

The transition from a liquid to solid involves the breaking of translational symmetry. Here we shall examine the types of order that are present in a two dimensional solid. The destruction of such order upon melting is discussed next.

(a) A low temperature treatment of the problem starts with the perfect solid at $T = 0$. The equilibrium configuration of atoms forms a lattice, $\mathbf{r}_0(m,n) = m\mathbf{e_1} + n\mathbf{e_2}$, where $\mathbf{e_1}$ and $\mathbf{e_2}$ are basis vectors, and $\{m,n\}$ are integers. At finite temperatures, the atoms fluctuate away from their equilibrium position, moving to

$$\mathbf{r}(m,n) = \mathbf{r}_0(m,n) + \mathbf{u}(m,n). \tag{VII.81}$$

The low temperature distortions do not vary substantially over nearby atoms, enabling us to define a coarse-grained *distortion field* $\mathbf{u}(\mathbf{x})$, where $\mathbf{x} \equiv (x_1, x_2)$ is treated as continuous, with an implicit short distance cutoff of the lattice spacing a. The distortion $\mathbf{u}$, is the analog of the angle θ, is the XY model.

(b) Due to translational symmetry, the energy depends only on the *strain matrix*,

$$u_{ij}(\mathbf{x}) = \frac{1}{2}\left(\partial_i u_j + \partial_j u_i\right), \qquad \Longrightarrow \qquad u_{ij}(\mathbf{q}) = \frac{i}{2}\left(q_i u_j + q_j u_i\right). \tag{VII.82}$$

The elastic energy must respect the symmetries of the underlying lattice. For simplicity, we shall consider the triangular lattice whose elastic energy is fully isotropic, i.e. invariant under all rotations (see Landau and Lifshitz, *Theory of Elasticity*). In terms of the *Lamé coefficients* λ and μ,

$$\begin{aligned}\beta\mathcal{H} =& \frac{1}{2}\int d^2\mathbf{x}\left[2\mu u_{ij}u_{ij} + \lambda u_{ii}u_{jj}\right] \\ =& \frac{1}{2}\int \frac{d^2\mathbf{q}}{(2\pi)^2}\left[\mu q^2 u^2 + (\mu+\lambda)(\mathbf{q}\cdot\mathbf{u})^2\right].\end{aligned} \tag{VII.83}$$

The rotational invariance of energy is ensured by the implicit sum over the indices (i,j) in the above expression. In the Fourier representation, the energy depends on the quantities q^2, $|\mathbf{u}|^2$, and $(\mathbf{q}\cdot\mathbf{u})^2$ which are clearly independent of rotations. For other lattices, there are more elastic coefficients, since the energy should only be invariant under lattice rotations. For example, the symmetry of a square lattice permits a term proportional to $\left(q_x^2 u_x^2 + q_y^2 u_y^2\right)$.

(c) The Goldstone modes associated with the broken translational symmetry are *phonons*, the normal modes of vibrations. Equation (VII.83) supports two types of normal modes:

(i) *Transverse modes* with $\mathbf{q} \perp \mathbf{u}$, have energy

$$\beta\mathcal{H}_T = \frac{\mu}{2}\int \frac{d^2\mathbf{q}}{(2\pi)^2}\, q^2 u_T^2\,, \qquad \Longrightarrow \qquad \left\langle |u_T(\mathbf{q})|^2 \right\rangle = \frac{1}{\mu q^2}. \tag{VII.84}$$

(ii) *Longitudinal modes* with $\mathbf{q} \parallel \mathbf{u}$, with energy

$$\beta\mathcal{H}_L = \frac{2\mu+\lambda}{2}\int \frac{d^2\mathbf{q}}{(2\pi)^2}\, q^2 u_L^2\,, \qquad \Longrightarrow \qquad \left\langle |u_L(\mathbf{q})|^2 \right\rangle = \frac{1}{(2\mu+\lambda)q^2}. \tag{VII.85}$$

Combining the above results, we find that a general correlation function is given by

$$\langle u_i(\mathbf{q}) u_j(\mathbf{q}')\rangle = \frac{(2\pi)^2\delta^2(\mathbf{q}+\mathbf{q}')}{\mu q^2}\left[\delta_{ij} - \frac{\mu+\lambda}{2\mu+\lambda}\,\frac{q_i q_j}{q^2}\right]. \tag{VII.86}$$

The extent of fluctuations in position space is given by

$$\begin{aligned}\left\langle [\mathbf{u}(\mathbf{x})-\mathbf{u}(\mathbf{0})]^2 \right\rangle =& \int \frac{d^2\mathbf{q}}{(2\pi)^2}\,\frac{2-2\cos(\mathbf{q}\cdot\mathbf{x})}{\mu q^2}\,\left[\delta_{ii} - \frac{\mu+\lambda}{2\mu+\lambda}\,\frac{q_i q_i}{q^2}\right] \\ =& \frac{3\mu+\lambda}{\mu(2\mu+\lambda)}\,\frac{\ln(|\mathbf{x}|/a)}{\pi}.\end{aligned} \tag{VII.87}$$

The unbounded growth of fluctuations with $|\mathbf{x}|$ indicates the destruction of long-range translational order in two dimensions. A similar calculation in higher dimensions results in a *finite* maximum extent of fluctuations proportional to temperature. The *Lindeman criterion* identifies the melting point heuristically as the temperature for which these thermal fluctuations reach a fraction (roughly 0.1) of the perfect lattice spacing. According to this criterion, the two dimensional solid melts at any finite temperature. This is of coarse another manifestation of the general absence of true long-range order in two dimension. Is some form of quasi-long-range order, similar to the XY model possible in this case?

(d) The *order parameter* describing broken translational symmetry is $\rho_{\mathbf{G}}(\mathbf{x}) = e^{i\mathbf{G}\cdot\mathbf{r}(\mathbf{x})}$, where $\mathbf{G}$ is any *reciprocal lattice* vector. Since $\mathbf{G}\cdot\mathbf{r}_0$ is an integer multiple of 2π by definition, $\rho_{\mathbf{G}} = 1$ at zero temperature. Due to fluctuations $\langle\rho_{\mathbf{G}}(\mathbf{x})\rangle = \left\langle e^{i\mathbf{G}\cdot\mathbf{u}(\mathbf{x})}\right\rangle$, decreases at finite temperatures, and its correlations decay as

$$\begin{aligned}\langle\rho_{\mathbf{G}}(\mathbf{x})\rho^*_{\mathbf{G}}(\mathbf{0})\rangle =& \left\langle e^{i\mathbf{G}\cdot(\mathbf{u}(\mathbf{x})-\mathbf{u}(\mathbf{0}))}\right\rangle \\ =& \exp\left(-\frac{G_\alpha G_\beta}{2}\,\langle(u_\alpha(\mathbf{x})-u_\alpha(\mathbf{0}))(u_\beta(\mathbf{x})-u_\beta(\mathbf{0}))\rangle\right) \\ =& \exp\left\{-\frac{G_\alpha G_\beta}{2}\int\frac{d^2\mathbf{q}\,d^2\mathbf{q}'}{(2\pi)^2}\left(e^{i\mathbf{q}\cdot\mathbf{x}}-1\right)\left(e^{i\mathbf{q}'\cdot\mathbf{x}}-1\right)\langle u_\alpha(\mathbf{q})u_\beta(\mathbf{q}')\rangle\right\} \\ =& \exp\left\{-\frac{1}{2}\int\frac{d^2\mathbf{q}}{(2\pi)^2}\,\frac{2-2\cos\mathbf{q}\cdot\mathbf{x}}{q^2}\,\left(\frac{G^2}{\mu}-\frac{\mu+\lambda}{\mu(2\mu+\lambda)}\,\frac{(\mathbf{G}\cdot\mathbf{q})^2}{q^2}\right)\right\} \\ \approx& \exp\left\{-\frac{G^2(3\mu+\lambda)}{2\mu(2\mu+\lambda)}\,\frac{\ln(|\mathbf{x}|/a)}{2\pi}\right\} = \left(\frac{a}{|\mathbf{x}|}\right)^{\eta_G}.\end{aligned} \tag{VII.88}$$

The integration over $\mathbf{q}$ is performed after replacing $(\mathbf{G}\cdot\mathbf{q})^2$ with the angular average of $G^2q^2/2$. This is not strictly correct because of the presence of the term $\cos\mathbf{q}\cdot\mathbf{x}$ which breaks the rotational symmetry. Nevertheless, this approximation captures the correct asymptotic growth of the integral. Correlations thus decay algebraically with a power

$$\eta_G = \frac{G^2(3\mu+\lambda)}{4\pi\mu(2\mu+\lambda)}. \tag{VII.89}$$

The translational correlations are measured in diffraction experiments. The scattering amplitude is the Fourier transform of $\rho_{\mathbf{q}}$, and the scattered intensity at a wave-vector $\mathbf{q}$ is proportional to the structure factor

$$\begin{aligned} S(\mathbf{q}) = \left\langle |A(\mathbf{q})|^2 \right\rangle &= \left\langle \left| \sum_{m,n} e^{i\mathbf{q}\cdot\mathbf{r}(m,n)} \right|^2 \right\rangle = N \sum_{m,n} \left\langle e^{i\mathbf{q}\cdot(\mathbf{r}(m,n)-\mathbf{r}(0,0))} \right\rangle \\ &= N \sum_{m,n} e^{i\mathbf{q}\cdot(\mathbf{r}_0(m,n)-\mathbf{r}_0(0,0))} \left\langle e^{i\mathbf{q}\cdot(\mathbf{u}(\mathbf{x})-\mathbf{u}(\mathbf{0}))} \right\rangle, \end{aligned} \tag{VII.90}$$

where N is the total number of particles. At zero temperature, the structure factor is a set of delta-functions (Bragg peaks) at the reciprocal lattice vectors. Even at finite temperature the sum is zero due to varying phases, unless $\mathbf{q}$ is in the vicinity of a lattice vector $\mathbf{G}$. We can then replace the sum with an integral, and

$$S(\mathbf{q}) \approx N \sum_{\mathbf{G}} \int d^2\mathbf{x} e^{i(\mathbf{q}-\mathbf{G})\cdot\mathbf{x}} \left(\frac{a}{|\mathbf{x}|}\right)^{\eta_{\mathbf{G}}} \approx N \sum_{\mathbf{G}} \frac{1}{|\mathbf{q}-\mathbf{G}|^{2-\eta_{\mathbf{G}}}}. \tag{VII.91}$$

The Bragg peaks are now replaced by power law singularities. The strength of the divergence decreases with temperature and increasing $|\mathbf{G}|$. The peaks corresponding to sufficiently large $|\mathbf{G}|$ are no longer visible, and gradually more of them disappear on increasing temperature. In three dimensions, the structure factor is still a set of delta-functions, but with magnitudes diminished by the so called *Debye-Waller* factor of $\exp\left(-\frac{G^2}{12\pi a}\,\frac{5\mu+2\lambda}{\mu(2\mu+\lambda)}\right)$.

(e) The crystal phase is also characterized by a broken rotational symmetry. We can define an *orientational order parameter* $\Psi(\mathbf{x}) = e^{6i\theta(\mathbf{x})}$, where $\theta(\mathbf{x})$ is the angle between local lattice bonds and a reference axis. (The factor of 6 results from the equivalence of the 6 possible directions on the triangular lattice. The appropriate choice for a square lattice is $e^{4i\theta(\mathbf{x})}$.) The order parameter has unit magnitude at $T=0$, and is expected to decrease due to fluctuations at finite temperature. The distortion $\mathbf{u}(\mathbf{x})$ leads to a change in bond angle given by

$$\theta(\mathbf{x}) = -\frac{1}{2}\left(\frac{\partial u_y}{\partial x} - \frac{\partial u_x}{\partial y}\right) = -\frac{1}{2}\hat{z}\cdot\nabla\times\mathbf{u}. \tag{VII.92}$$

The decay of orientational fluctuations is now calculated from

$$\begin{aligned}
\langle \Psi(\mathbf{x})\Psi^*(0)\rangle &= \left\langle e^{i6(\theta(\mathbf{x})-\theta(\mathbf{0}))}\right\rangle \\
&= \exp\left[-\frac{6^2}{2}\,\frac{1}{4}\left\langle [\nabla\times\mathbf{u}(\mathbf{x})-\nabla\times\mathbf{u}(\mathbf{0})]^2\right\rangle\right] \\
&= \exp\left\{-\frac{9}{2}\int \frac{d^2\mathbf{q}\,d^2\mathbf{q}'}{(2\pi)^4}\,(e^{i\mathbf{q}\cdot\mathbf{x}}-1)(e^{i\mathbf{q}'\cdot\mathbf{x}}-1)\,\varepsilon_{ijk}\varepsilon_{ij'k'}q_jq'_{j'}\;\langle u_k(\mathbf{q})u_{k'}(\mathbf{q}')\rangle\right\} \\
&= \exp\left\{-\frac{9}{2}\int \frac{d^2\mathbf{q}}{(2\pi)^2}\,(2-2\cos\mathbf{q}\cdot\mathbf{x})\left(q^2\left\langle|u(\mathbf{q})|^2\right\rangle-\left\langle(\mathbf{q}\cdot\mathbf{u})^2\right\rangle\right)\right\} \\
&= \exp\left\{-\frac{9}{2\mu}\int \frac{d^2\mathbf{q}}{(2\pi)^2}\,(2-2\cos\mathbf{q}\cdot\mathbf{x})\right\} \approx \exp\left(-\frac{9}{a^2\mu}\right).
\end{aligned} \tag{VII.93}$$

(Note that $\int d^2\mathbf{q}/(2\pi)^2$ is the density $n = N/L^2 = 1/a^2$.) The final result is *independent* of $\mathbf{x}$ at large distances, and asymptotes to a constant that decays exponentially with temperature (since $\mu \propto 1/T$). The two dimensional solid is thus characterized by quasi-long-range translational order, and true long-range orientational order.

VII.E Two Dimensional Melting

There are qualitative similarities between the melting of a two dimensional solid and the disordering of the XY spin system. Expanding on the work of Kosterlitz and Thouless, Halperin and Nelson, and independently, Young, developed a theory of two dimensional melting. The resulting, so called KTHNY theory, is briefly sketched here.

(a) The topological defects of a solid are *dislocations*. A single dislocation corresponds to an extra half lattice plane, and is characterized by performing a *Burger's circuit:* The circuit is a series of steps from site to site that on a perfect lattice returns to the starting point (e.g. 5 steps to the right, 4 down, followed by 5 left, and 4 up on a square lattice.) If the circuit encloses a region with dislocations, it will fail to close. The difference between the initial and final sites of the circuit defines $\mathbf{b}$, the *Burger's vector* of the dislocation. This closure failure is allowed, since the distortion field $\mathbf{u}(\mathbf{x})$, is defined only up to a lattice vector. In the continuum limit this degeneracy is described by

$$\oint \nabla u_\alpha \, d\mathbf{s} = b^\alpha. \tag{VII.94}$$

Thus each component of the distortion field behaves like the angle $\theta(\mathbf{x})$ is the XY model. Using this analogy, the distortion field due to a collection of dislocations $\{\mathbf{b}_i\}$, at locations $\{\mathbf{x}_i\}$, has a singular part

$$\nabla \tilde{u}^*_\alpha = -\nabla \times \left(\hat{z} \sum_i \frac{b^\alpha_i}{2\pi} \ln |\mathbf{x} - \mathbf{x}_i| \right). \tag{VII.95}$$

While $\tilde{u}^*_\alpha$ correctly describes the singularities due to the presence of vortices, it is not a local equilibrium configuration, i.e. not a solution to $2\mu\tilde{u}_{\alpha\beta} + \lambda\delta_{\alpha\beta}\tilde{u}_{\gamma\gamma} = 0$. Allowing the particles to equilibrate in the presence of the dislocations leads to a solution $\tilde{u}_\alpha$, which differs from $\tilde{u}^*_\alpha$ only by a regular part. The total strain field can now decomposed as $u_{\alpha\beta} = \phi_{\alpha\beta} + \tilde{u}_{\alpha\beta}$, where $\tilde{u}_{\alpha\beta}$ results from dislocations, and $\phi_{\alpha\beta}$ is the contribution of phonons. After substituting this form in the elastic energy $\beta\mathcal{H} = \int d^2\mathbf{x} \left[2\mu u_{\alpha\beta}u_{\alpha\beta} + \lambda u_{\alpha\alpha}u_{\beta\beta}\right]/2$, manipulations similar to the XY model lead to $\beta\mathcal{H} = \beta\mathcal{H}_0 + \beta\mathcal{H}_1$, where

$$\beta\mathcal{H}_0 = \frac{1}{2}\int d^2\mathbf{x} \left[2\mu\phi_{\alpha\beta}\phi_{\alpha\beta} + \lambda\phi_{\alpha\alpha}\phi_{\beta\beta}\right], \tag{VII.96}$$

and

$$\beta\mathcal{H}_1 = -\bar{K}\sum_{i<j} b^\alpha_i b^\beta_j C_{\alpha\beta}(\mathbf{x}_i - \mathbf{x}_j) - \sum_i \ln[y_0(\mathbf{b}_i)]. \tag{VII.97}$$

The dislocations behave as a grand-canonical gas of particles with vector charges $\{\mathbf{b}_i\}$. The fugacity y_0 comes from the core energy of each dislocation. The charges interact via a vectorial generalization of the Coulomb interaction,

$$C_{\alpha\beta}(\mathbf{x}) = \frac{1}{2\pi}\left[\delta_{\alpha\beta}\ln\left(\frac{|\mathbf{x}|}{a}\right) - \frac{x_\alpha x_\beta}{x^2}\right]. \tag{VII.98}$$

The strength of the interaction in eq.(VII.97) is $\bar{K}a^2 = 2\mu(\mu+\lambda)/(2\mu+\lambda)$. Implicit in the above derivation is an overall neutrality condition, $\sum_i \mathbf{b}_i = \mathbf{0}$.

The bare interaction between dislocations is screened by other dislocations in the medium. The effective strength can be calculated perturbatively and diverges for $\pi\bar{K}a^2 < 2$. This signals the unbinding of paired neutral dislocations. Under coarse graining, the parameters of the theory evolve as

$$\begin{cases} \dfrac{d\bar{K}^{-1}}{d\ell} = Ay^2 + By^3, \\ \dfrac{dy_0}{d\ell} = \left(2 - \pi\bar{K}\right) y + Dy^2, \end{cases} \tag{VII.99}$$

where A, B, and D are constants. In contrast to the XY model, additional terms appear at order of y_0^3. This is because in a scalar Coulomb gas the only neutral configurations have an even number of particles. For dislocations on a triangular lattice, it is possible to construct a neutral configuration from three dislocations at 120° angles.

The low temperature phase maps onto a line of fixed points characterized by renormalized Lamé coefficients, μ_R and λ_R, and $y_0^* = 0$. At high temperatures y_0 and $\bar{K}$ both diverge, indicating the vanishing of the shear modulus μ_R, and a finite correlation length ξ. On approaching the transition from the low temperature side, the effective shear modulus undergoes a discontinuous jump, with a singular behavior, $\mu_R \simeq \mu_c + c(T_c - T)^{\bar{\nu}}$. The correlation length diverges from the high temperature side as $\xi \simeq a \exp\left(c'/(T - T_c)^{\bar{\nu}}\right)$. Due to the cubic terms appearing in eqs.(VII.99), the value of $\bar{\nu} = 0.36963\cdots$ is different from the 1/2 that appears in the XY model, indicating a difference between transitions in vector and scalar Coulomb universality classes.

(b) Does the vanishing of the shear modulus imply that the high temperature phase with unbound dislocations is a liquid? As discussed earlier, the crystalline phase has both translational and orientational order. A distortion $\mathbf{u}(\mathbf{x})$ results in a rotation in bond angles according to eq.(VII.92). The net rotation due to a collection of dislocations is

$$\tilde{\theta}(\mathbf{x}) = -\frac{1}{2}\hat{z}\cdot\nabla\times\tilde{u} = \frac{1}{2\pi}\sum_i \frac{\mathbf{b}_i\cdot(\mathbf{x}-\mathbf{x}_i)}{|\mathbf{x}-\mathbf{x}_i|^2}. \tag{VII.100}$$

In terms of a continuum dislocation density $\mathbf{b}(\mathbf{x}) = \sum_i \mathbf{b}_i\delta^2(\mathbf{x}-\mathbf{x}_i)$,

$$\tilde{\theta}(\mathbf{x}) = \frac{1}{2\pi}\int d^2\mathbf{x}'\,\frac{\mathbf{b}(\mathbf{x}')\cdot(\mathbf{x}-\mathbf{x}')}{|\mathbf{x}-\mathbf{x}'|^2}. \tag{VII.101}$$

Alternatively, in Fourier space,

$$\tilde{\theta}(\mathbf{q}) = \int d^2\mathbf{x}d^2\mathbf{x}'e^{i\mathbf{q}\cdot\mathbf{x}}\frac{b(\mathbf{x}')\cdot(\mathbf{x}-\mathbf{x}')}{2\pi|\mathbf{x}-\mathbf{x}'|^2} = i\,\frac{\mathbf{b}(\mathbf{q})\cdot\mathbf{q}}{q^2}. \tag{VII.102}$$

The angular fluctuations are thus related to correlations in dislocation density via

$$\left\langle|\tilde{\theta}(\mathbf{q})|^2\right\rangle = \frac{q_\alpha q_\beta}{q^4}\left\langle b^\alpha(\mathbf{q})b^\beta(\mathbf{q})\right\rangle, \tag{VII.103}$$

where

$$\left\langle b^\alpha(\mathbf{q})b^\beta(\mathbf{q})\right\rangle = \int d^2\mathbf{x}\,e^{i\mathbf{q}\cdot\mathbf{x}}\left\langle b^\alpha(\mathbf{x})b^\beta(\mathbf{0})\right\rangle. \tag{VII.104}$$

After the dislocations are unbound for $T > T_c$, they interact via a screened Coulomb interaction, and

$$\lim_{|\mathbf{x}|\to\infty} \left\langle b^\alpha(\mathbf{x}) b^\beta(\mathbf{0}) \right\rangle \propto \delta_{\alpha\beta} e^{-|\mathbf{x}|/\xi}, \quad \Longrightarrow \quad \lim_{\mathbf{q}\to\mathbf{0}} \left\langle b^\alpha(\mathbf{q}) b^\beta(\mathbf{q}) \right\rangle \propto \delta_{\alpha\beta} \xi^2. \tag{VII.105}$$

Substituting into eq.(VII.103) leads to

$$\lim_{\mathbf{q}\to\mathbf{0}} \left\langle |\tilde{\theta}(\mathbf{q})|^2 \right\rangle \propto \frac{\xi^2}{q^2}. \tag{VII.106}$$

(In the low temperature phase, the neutrality of the charges at a large scale $|\mathbf{q}|^{-1}$ requires the vanishing of $\mathbf{b}(\mathbf{q})$ as $\mathbf{q} \to \mathbf{0}$, and $\lim_{\mathbf{q}\to\mathbf{0}} \left\langle b^\alpha(\mathbf{q}) b^\beta(\mathbf{q}) \right\rangle \propto q_\alpha q_\beta$, leading to a finite $\langle |\tilde{\theta}(\mathbf{q})|^2 \rangle$.)

Eq.(VII.106) implies that after the unbinding of dislocations the orientational fluctuations are still correlated. In fact such correlations would result from a Hamiltonian

$$\beta\mathcal{H} = \frac{K_A}{2} \int d^2\mathbf{x} \, (\nabla\theta)^2, \qquad \text{with} \qquad K_A \propto \xi^2. \tag{VII.107}$$

The angular stiffness K_A is known as the Frank constant. The bond angle order correlations now decay as

$$\langle \Psi(\mathbf{x}) \Psi^*(\mathbf{0}) \rangle = e^{-\frac{36}{2} \left\langle \left[\tilde{\theta}(\mathbf{x}) - \tilde{\theta}(\mathbf{0})\right]^2 \right\rangle} = \left(\frac{a}{|\mathbf{x}|} \right)^{-\eta_\Psi}, \tag{VII.108}$$

with $\eta_\Psi = 18/(\pi K_A)$. The quasi-long-range decay of orientational fluctuations leads to the appearance of a six fold intensity modulation in the diffraction pattern. The dislocations are thus not effective in completely destroying order, and their unbinding leads to the appearance of an orientationally ordered phase known as a *hexatic*. The stiffness of the hexatic phase diverges at the transition to a solid according to eq.(VII.107).

(c) Orientational order disappears at a higher temperature due to the unbinding of a new set of topological defects known as *disclinations*. These are very similar to the vortices in the XY model, except that since the bond angle is defined only up to $2\pi/6$, they satisfy

$$\oint \nabla\theta \cdot d\vec{s} = \frac{2\pi}{6}. \tag{VII.109}$$

The energy cost of a disclination grows with system size as $\mathcal{E}_1 = \pi K_A \ln(L/a)/36$. Considering the entropy of $2\ln(L/a)$, we find a disclination unbinding transition for $K_A < 72/\pi$. This transition is in the universality class of the scalar Coulomb gas. The resulting high

temperature phase has neither orientational or translational order and is a conventional liquid.

This scenario predicts that the melting of a two dimensional solid proceeds through an intermediate hexatic phase. In fact, computer simulations suggest that simple two dimensional solids, e.g. particles interacting via Lennard-Jones potentials, undergo a direct first order melting transition as in three dimensions. More complicated molecular systems in three dimensions, e.g. long polymers, are known to have intermediate liquid crystal phases. Liquid crystals have order intermediate between solid and fluid and are three dimensional analogs of the hexatic phase. Thin films made up of a few mono-layers of liquid crystals are the best candidates for examining the KTHNY melting scenario.

VIII. Dissipative Dynamics

VIII.A Brownian Motion of a Particle

Observations under a microscope indicate that a dust particle in a liquid drop undergoes a random jittery motion. This is because of the random impacts of the much smaller fluid particles. The theory of such (*Brownian*) motion was developed by Einstein in 1905 and starts with the equation of motion for the particle. The displacement $\vec{x}(t)$, of a particle of mass m is governed by,

$$m\,\ddot{\vec{x}} = -\frac{\dot{\vec{x}}}{\mu} - \frac{\partial \mathcal{V}}{\partial \vec{x}} + \vec{f}_{\rm random}(t). \tag{VIII.1}$$

The three forces acting on the particle are:

(i) A friction force due to the viscosity of the fluid. For a spherical particle of radius R, the mobility in the low Reynolds number limit is given by $\mu = (6\pi\bar{\eta}R)^{-1}$, where $\bar{\eta}$ is the specific viscosity.

(ii) The force due to the external potential $\mathcal{V}(\vec{x})$, e.g. gravity.

(iii) A random force of zero mean due to the impacts of fluid particles.

The viscous term usually dominates the inertial one (i.e. the motion is overdamped), and we shall henceforth ignore the acceleration term. Eq.(VIII.1) now reduces to a *Langevin equation*,

$$\dot{\vec{x}} = \vec{v}(\vec{x}) + \vec{\eta}(t), \tag{VIII.2}$$

where $\vec{v}(\vec{x}) = -\mu\partial\mathcal{V}/\partial\vec{x}$ is the *deterministic* velocity. The *stochastic* velocity, $\vec{\eta}(t) = \mu\vec{f}_{\rm random}(t)$, has zero mean,

$$\langle \vec{\eta}(t) \rangle = 0. \tag{VIII.3}$$

It is usually assumed that the probability distribution for the noise in velocity is Gaussian, i.e.

$$\mathcal{P}\left[\vec{\eta}(t)\right] \propto \exp\left[-\int d\tau\, \frac{\eta(\tau)^2}{4D}\right]. \tag{VIII.4}$$

Note that different components of the noise, and at different times, are independent, and the covariance is

$$\langle \eta_\alpha(t)\eta_\beta(t')\rangle = 2D\delta_{\alpha,\beta}\delta(t-t'). \tag{VIII.5}$$

The parameter D is related to *diffusion* of particles in the fluid. In the absence of any potential, $\mathcal{V}(\vec{x}) = 0$, the position of a particle at time t is given by

$$\vec{x}(t) = \vec{x}(0) + \int_0^t d\tau \vec{\eta}(\tau).$$

Clearly the separation $\vec{x}(t) - \vec{x}(0)$ which is the sum of random Gaussian variables is itself Gaussian distributed with mean zero, and a varaince

$$\left\langle (\vec{x}(t) - \vec{x}(0))^2 \right\rangle = \int_0^t d\tau_1 d\tau_2 \left\langle \vec{\eta}(\tau_1) \cdot \vec{\eta}(\tau_2) \right\rangle = 3 \times 2Dt.$$

For an ensemble of particles released at $\vec{x}(t) = 0$, i.e. with $\mathcal{P}(\vec{x}, t = 0) = \delta^3(\vec{x})$, the particles at time t are distributed according to

$$\mathcal{P}(\vec{x}, t) = \left(\frac{1}{\sqrt{4\pi D t}} \right)^{3/2} \exp\left[-\frac{x^2}{4Dt} \right],$$

which is the solution to the diffusion equation

$$\frac{\partial \mathcal{P}}{\partial t} = D \nabla^2 \mathcal{P}.$$

A simple example is provided by a particle connected to a Hookian spring, with $\mathcal{V}(\vec{x}) = Kx^2/2$. The deterministic velocity is now $\vec{v}(\vec{x}) = -\mu K \vec{x}$, and the Langevin equation, $\dot{\vec{x}} = -\mu K \vec{x} + \vec{\eta}(t)$, can be rearranged as

$$\frac{d}{dt}\left[e^{\mu K t} \vec{x}(t) \right] = e^{\mu K t} \vec{\eta}(t). \tag{VIII.6}$$

Integrating the equation from 0 to t yields

$$e^{\mu K t} \vec{x}(t) - \vec{x}(0) = \int_0^t d\tau e^{\mu K \tau} \vec{\eta}(\tau), \tag{VIII.7}$$

and

$$\vec{x}(t) = \vec{x}(0) e^{-\mu K t} + \int_0^t d\tau e^{-\mu K (t-\tau)} \vec{\eta}(\tau). \tag{VIII.8}$$

Averaging over the noise indicates that the mean position,

$$\langle \vec{x}(t) \rangle = \vec{x}(0) e^{-\mu K t}, \tag{VIII.9}$$

decays with a characteristic *relaxation time*, $\tau = 1/(\mu K)$. Fluctuations around the mean behave as

$$\begin{aligned}\left\langle \left(\vec{x}(t) - \langle\vec{x}(t)\rangle\right)^2 \right\rangle =& \int_0^t d\tau_1 d\tau_2 e^{-\mu K(2t-\tau_1-\tau_2)} \overbrace{\langle\vec{\eta}(\tau_1)\cdot\vec{\eta}(\tau_2)\rangle}^{2D\delta(\tau_1-\tau_2)\times 3} \\ =& 6D\int_0^t d\tau e^{-2\mu K(t-\tau)} \\ =& \frac{3D}{\mu K}\left[1-e^{-2\mu K t}\right] \quad \stackrel{t\to\infty}{\longrightarrow} \quad \frac{3D}{\mu K}.\end{aligned} \tag{VIII.10}$$

However, once the dust particle reaches equilibrium with the fluid at a temperature T, its probability distribution must satisfy the normalized Boltzmann weight

$$\mathcal{P}_{\rm eq.}(\vec{x}) = \left(\frac{K}{2\pi k_B T}\right)^{3/2} \exp\left[-\frac{Kx^2}{2k_B T}\right], \tag{VIII.11}$$

yielding $\langle x^2\rangle = 3k_B T/K$. Since the dynamics is expected to bring the particle to equilibrium with the fluid at temperature T, eq.(VIII.10) implies the condition

$$D = k_B T \mu\,. \tag{VIII.12}$$

This is the Einstein relation connecting the *fluctuations* of noise to the *dissipation* in the medium.

Clearly the Langevin equation at long times reproduces the correct mean and variance for a particle in equilibrium at a temperature T in the potential $\mathcal{V}(\vec{x}) = Kx^2/2$, provided that eq.(VIII.12) is satisfied. Can we show that the whole probability distribution evolves to the Boltzmann weight for any potential? Let $\mathcal{P}(\vec{x},t) \equiv \langle\vec{x}|\mathcal{P}(t)|0\rangle$ denote the probability density of finding the particle at $\vec{x}$ at time t, given that it was at 0 at $t=0$. This probability can be constructed recursively by noting that a particle found at $\vec{x}$ at time $t+\epsilon$ must have arrived from some other point $\vec{x}\,'$ at t. Adding up all such probabilities yields

$$\mathcal{P}(\vec{x},t+\epsilon) = \int d^3\vec{x}\,'\,\mathcal{P}(\vec{x}\,',t)\,\langle\vec{x}|T_\epsilon|\vec{x}\,'\rangle, \tag{VIII.13}$$

where $\langle\vec{x}|T_\epsilon|\vec{x}\,'\rangle \equiv \langle\vec{x}|\mathcal{P}(\epsilon)|\vec{x}\,'\rangle$ is the transition probability. For $\epsilon \ll 1$,

$$\vec{x} = \vec{x}\,' + \vec{v}\,(\vec{x}\,')\epsilon + \vec{\eta}_\epsilon \quad , \tag{VIII.14}$$

where $\vec{\eta}_\epsilon = \int_t^{t+\epsilon} d\tau \vec{\eta}(\tau)$. Clearly, $\langle \vec{\eta}_\epsilon \rangle = 0$, and $\langle \eta_\epsilon^2 \rangle = 2D\epsilon \times 3$, and following eq.(VIII.4),

$$p(\vec{\eta}_\epsilon) = \left(\frac{1}{4\pi D\epsilon}\right)^{3/2} \exp\left[-\frac{\eta_\epsilon^2}{4D\epsilon}\right]. \tag{VIII.15}$$

The transition rate is simply the probability of finding a noise of the right magnitude according to eq.(VIII.14), and

$$\begin{aligned} \langle \vec{x} \,|T(\epsilon)|\vec{x}\,' \rangle = p(\eta_\epsilon) &= \left(\frac{1}{4\pi D\epsilon}\right)^{3/2} \exp\left[-\frac{(\vec{x}-\vec{x}\,'-\epsilon\vec{v}(\vec{x}\,'))^2}{4D\epsilon}\right] \\ &= \left(\frac{1}{4\pi D\epsilon}\right)^{3/2} \exp\left[-\epsilon\,\frac{\left(\dot{\vec{x}}-\vec{v}(\vec{x})\right)^2}{4D}\right]. \end{aligned} \tag{VIII.16}$$

By subdividing the time interval t, into infinitesimal segments of size ϵ, repeated application of the above evolution operator yields

$$\begin{aligned} \mathcal{P}(\vec{x},t) &= \left\langle \vec{x} \,\middle|T(\epsilon)^{t/\epsilon}\middle|\, 0 \right\rangle \\ &= \int_{(0,0)}^{(\vec{x},t)} \frac{\mathcal{D}\vec{x}(\tau)}{\mathcal{N}} \exp\left[-\int_0^t d\tau \frac{\left(\dot{\vec{x}}-\vec{v}(\vec{x})\right)^2}{4D}\right]. \end{aligned} \tag{VIII.17}$$

The integral is over all paths connecting the initial and final points; each path's weight is related to its deviation from the classical trajectory, $\dot{\vec{x}} = \vec{v}(\vec{x})$. The recursion relation (eq.(VIII.13)),

$$\mathcal{P}(\vec{x},t) = \int d^3\vec{x}\,' \left(\frac{1}{4\pi D\epsilon}\right)^{3/2} \exp\left[-\frac{(\vec{x}-\vec{x}\,'-\epsilon\vec{v}(\vec{x}\,'))^2}{4D\epsilon}\right] \mathcal{P}(\vec{x}\,',t-\epsilon), \tag{VIII.18}$$

can be simplified by the change of variables,

$$\begin{aligned} \vec{y} =& \vec{x}\,' + \epsilon\vec{v}(\vec{x}\,') - \vec{x} \quad \Longrightarrow \\ d^3\vec{y} =& d^3\vec{x}\,'\left(1+\epsilon\nabla\cdot\vec{v}(\vec{x}')\right) = d^3\vec{x}\,'\left(1+\epsilon\nabla\cdot\vec{v}(\vec{x})+\mathcal{O}(\epsilon^2)\right). \end{aligned} \tag{VIII.19}$$

Keeping only terms at order of ϵ, we obtain

$$\begin{aligned} \mathcal{P}(\vec{x},t) =& \left[1-\epsilon\nabla\cdot\vec{v}(\vec{x})\right] \int d^3\vec{y} \left(\frac{1}{4\pi D\epsilon}\right)^{3/2} e^{-\frac{y^2}{4D\epsilon}}\ \mathcal{P}(\vec{x}+\vec{y}-\epsilon\vec{v}(\vec{x}),t-\epsilon) \\ =& \left[1-\epsilon\nabla\cdot\vec{v}(\vec{x})\right] \int d^3\vec{y} \left(\frac{1}{4\pi D\epsilon}\right)^{3/2} e^{-\frac{y^2}{4D\epsilon}} \times \\ & \left[\mathcal{P}(\vec{x},t) + (\vec{y}-\epsilon\vec{v}(\vec{x}))\cdot\nabla\mathcal{P} + \frac{y_i y_j - 2\epsilon y_i v_j + \epsilon^2 v_i v_j}{2}\nabla_i\nabla_j\mathcal{P} - \epsilon\frac{\partial\mathcal{P}}{\partial t} + \mathcal{O}(\epsilon^2)\right] \\ =& \left[1-\epsilon\nabla\cdot\vec{v}(\vec{x})\right]\left[\mathcal{P} - \epsilon\vec{v}\cdot\nabla + \epsilon D\nabla^2\mathcal{P} - \epsilon\frac{\partial\mathcal{P}}{\partial t} + \mathcal{O}(\epsilon^2)\right]. \end{aligned} \tag{VIII.20}$$

Equating terms at order of ϵ leads to the *Fokker-Planck equation*,

$$\frac{\partial \mathcal{P}}{\partial t} + \nabla \cdot \vec{J} = 0, \qquad \text{with} \qquad \vec{J} = \vec{v}\,\mathcal{P} - D\nabla\mathcal{P} \quad . \tag{VIII.21}$$

The Fokker-Planck equation is simply the statement of conservation of probability. The probability current has a deterministic component $\vec{v}\,\mathcal{P}$, and a stochastic part $-D\nabla\mathcal{P}$. A *stationary distribution*, $\partial\mathcal{P}/\partial t = 0$, is obtained if the net current vanishes. It is now easy to check that the Boltzmann weight, $\mathcal{P}_{\rm eq.}(\vec{x}) \propto \exp[-\mathcal{V}(\vec{x})/k_BT]$, with $\nabla\mathcal{P}_{\rm eq.} = \vec{v}\,\mathcal{P}_{\rm eq.}/(\mu k_BT)$, leads to a stationary state as long as the fluctuation–dissipation condition in eq.(VIII.12) is satisfied.

VIII.B Equilibrium Dynamics of a Field

The next step is to generalize the Langevin formalism to a collection of degrees of freedom, most conveniently described by a continuous field. Let us consider the order parameter field $\vec{m}(\mathbf{x},t)$ of a magnet. In equilibrium, the probability to find a coarse-grained configuration of the magnetization field is governed by the Boltzmann weight of the Landau-Ginzburg Hamiltonian

$$\mathcal{H}\left[\vec{m}\right] = \int d^d\mathbf{x} \left[\frac{r}{2}m^2 + um^4 + \frac{K}{2}\left(\nabla m\right)^2 + \cdots\right]. \tag{VIII.22}$$

(To avoid confusion with time, the coefficient of the quadratic term is changed from t to r.) Clearly the above energy functional contains no kinetic terms, and should be regarded as the analog of the potential energy $\mathcal{V}(\vec{x})$ employed in the previous section. To construct a Langevin equation governing the dynamics of the field $\vec{m}(\mathbf{x})$, we first calculate the analogous *force* on each field element from the variations of this potential energy. The *functional derivative* of eq.(VIII.22) yields

$$F_i(\mathbf{x}) = -\frac{\delta\mathcal{H}[\vec{m}]}{\delta m_i(\mathbf{x})} = -rm_i - 4um_i|\vec{m}|^2 + K\nabla^2 m_i. \tag{VIII.23}$$

The straightforward analog of eq.(VIII.2) is

$$\frac{\partial m_i(\mathbf{x},t)}{\partial t} = \mu F_i(\mathbf{x}) + \eta_i(\mathbf{x},t), \tag{VIII.24}$$

with a random velocity, $\vec{\eta}$, such that

$$\langle\eta_i(\mathbf{x},t)\rangle = 0, \qquad \text{and} \qquad \langle\eta_i(\mathbf{x},t)\eta_j(\mathbf{x}',t')\rangle = 2D\delta_{ij}\delta(\mathbf{x}-\mathbf{x}')\delta(t-t'). \tag{VIII.25}$$

The resulting Langevin equation,

$$\frac{\partial\vec{m}(\mathbf{x},t)}{\partial t} = -\mu r\vec{m} - 4\mu u m^2\vec{m} + \mu K\nabla^2\vec{m} + \vec{\eta}(\mathbf{x},t), \tag{VIII.26}$$

is known as the *time dependent Landau-Ginzburg equation*. Because of the nonlinear term $m^2\vec{m}$, it is not possible to integrate this equation exactly. To gain some insight into its behavior we start with the disordered phase of the model which is well described by the *Gaussian weight* with $u = 0$. The resulting linear equation is then easily solved by examining the Fourier components,

$$\vec{m}(\mathbf{q},t) = \int d^d\mathbf{x}\, e^{i\mathbf{q}\cdot\mathbf{x}}\vec{m}(\mathbf{x},t), \tag{VIII.27}$$

which evolve according to

$$\frac{\partial \vec{m}(\mathbf{q},t)}{\partial t} = -\mu(r + Kq^2)\ \vec{m}(\mathbf{q},t) + \vec{\eta}(\mathbf{q},t). \tag{VIII.28}$$

The Fourier transformed noise,

$$\vec{\eta}(\mathbf{q},t) = \int d^d\mathbf{x}\, e^{i\mathbf{q}\cdot\mathbf{x}} \vec{\eta}(\mathbf{x},t), \tag{VIII.29}$$

has zero mean, $\langle \eta_i(\mathbf{q},t)\rangle = 0$, and correlations

$$\begin{aligned}\langle \eta_i(\mathbf{q},t)\eta_j(\mathbf{q}',t')\rangle =& \int d^d\mathbf{x} d^d\mathbf{x}'\ e^{i\mathbf{q}\cdot\mathbf{x}+i\mathbf{q}'\cdot\mathbf{x}'}\ \overbrace{\langle \eta_i(\mathbf{x},t)\eta_j(\mathbf{x}',t')\rangle}^{2D\delta_{ij}\delta^d(\mathbf{x}-\mathbf{x}')\ \delta(t-t')} \\ =& 2D\delta_{ij}\delta(t-t')\int d^d\mathbf{x}\, e^{i\mathbf{x}\cdot(\mathbf{q}+\mathbf{q}')} \\ =& 2D\delta_{ij}\delta(t-t')(2\pi)^d\delta^d(\mathbf{q}+\mathbf{q}').\end{aligned} \tag{VIII.30}$$

Each Fourier mode in eq.(VIII.28) now behaves as an independent particle connected to a spring as in eq.(VIII.6). Introducing a decay rate

$$\gamma(\mathbf{q}) \equiv \frac{1}{\tau(\mathbf{q})} = \mu(r + Kq^2), \tag{VIII.31}$$

the evolution of each mode is similar to eq.(VIII.8), and follows

$$\vec{m}(\mathbf{q},t) = \vec{m}(\mathbf{q},0)e^{-\gamma(\mathbf{q})t} + \int_0^t d\tau\ e^{-\gamma(\mathbf{q})(t-\tau)}\vec{\eta}(\mathbf{q},t). \tag{VIII.32}$$

Fluctuations in each mode decay with a different *relaxation time* $\tau(\mathbf{q})$; $\langle \vec{m}(\mathbf{q},t)\rangle = \vec{m}(\mathbf{q},0)\exp[-t/\tau(\mathbf{q})]$. When in equilibrium, the order parameter in the Gaussain model is correlated over the length scale $\xi = \sqrt{K/r}$. In considering relaxation to equilibrium, we find that at length scales larger than *xi* (or $q \ll 1/\xi$), the relaxation time saturates $\tau_{\max} = 1/(\mu r)$. On approaching the singular point of the Gaussian model at $r = 0$, the time required to reach equilibrium diverges. This phenomena is know as *critical slowing down*, and is also present for the non-linear equation, albeit with modified exponents. The critical point is thus characterized by diverging *length* and *time* scales. For the critical fluctuations at distances shorter than the correlation length ξ, the characteristic time scale grows with wavelength as $\tau(q) \approx (\mu K q^2)^{-1}$. The scaling relation between the critical length and time scales is described by a *dynamic exponent* z, as $\tau \propto \lambda^z$. The value of $z = 2$ for the critical Gaussian model is reminiscent of diffusion processes.

Time dependent correlation functions are obtained from

$$\begin{aligned}\langle m_i(\mathbf{q},t)m_j(\mathbf{q}',t)\rangle_c &= \int_0^t d\tau_1 d\tau_2 e^{-\gamma(\mathbf{q})(t-\tau_1)-\gamma(\mathbf{q}')(t-\tau_2)} \overbrace{\langle\eta_i(\mathbf{q},\tau_1)\eta_j(\mathbf{q}',\tau_2)\rangle}^{2D\delta_{ij}\delta(\tau_1-\tau_2)(2\pi)^d\delta^d(\mathbf{q}+\mathbf{q}')} \\ &= (2\pi)^d\delta^d(\mathbf{q}+\mathbf{q}')\,2D\delta_{ij}\int_0^t d\tau e^{-2\gamma(\mathbf{q})(t-\tau)} \\ &= (2\pi)^d\delta^d(\mathbf{q}+\mathbf{q}')\delta_{ij}\,\frac{D}{\gamma(\mathbf{q})}\left(1-e^{-2\gamma(\mathbf{q})t}\right) \\ &\stackrel{t\to\infty}{\longrightarrow} \quad (2\pi)^d\delta^d(\mathbf{q}+\mathbf{q}')\delta_{ij}\frac{D}{\mu(r+Kq^2)}.\end{aligned} \tag{VIII.33}$$

However, direct diagonalization of the Hamiltonian in eq.(VIII.22) with $u = 0$ gives

$$\mathcal{H} = \int \frac{d^d\mathbf{q}}{(2\pi)^d}\frac{(r+Kq^2)}{2}|\vec{m}(\mathbf{q})|^2, \tag{VIII.34}$$

leading to the equilibrium correlation functions

$$\langle m_i(\mathbf{q})m_j(\mathbf{q}')\rangle = (2\pi)^d\delta^d(\mathbf{q}+\mathbf{q}')\delta_{ij}\,\frac{k_BT}{r+Kq^2}. \tag{VIII.35}$$

Comparing equations (VIII.33) and (VIII.35) indicates that the long-time dynamics reproduce the correct equilibrium behavior if the fluctuation–dissipation condition, $D = k_BT\mu$, is satisfied.

In fact, quite generally, the single particle Fokker-Planck equation (VIII.21) can be generalized to describe the evolution of the whole probability functional, $\mathcal{P}([\vec{m}(\mathbf{x})],t)$, as

$$\frac{\partial\mathcal{P}([\vec{m}(\mathbf{x})],t)}{\partial t} = -\int d^d\mathbf{x}\frac{\delta}{\delta m_i(\mathbf{x})}\left[-\mu\frac{\delta\mathcal{H}}{\delta m_i(\mathbf{x})}\,\mathcal{P} - D\frac{\delta\mathcal{P}}{\delta m_i(\mathbf{x})}\right]. \tag{VIII.36}$$

For the equilibrium Boltzmann weight

$$\mathcal{P}_{\text{eq.}}[\vec{m}(\mathbf{x})] \propto \exp\left[-\frac{\mathcal{H}[\vec{m}(\mathbf{x})]}{k_BT}\right], \tag{VIII.37}$$

the functional derivative results in

$$\frac{\delta\mathcal{P}_{\text{eq.}}}{\delta m_i(\mathbf{x})} = -\frac{1}{k_BT}\,\frac{\delta\mathcal{H}}{\delta m_i(\mathbf{x})}\,\mathcal{P}_{\text{eq.}}. \tag{VIII.38}$$

The total probability current,

$$J[h(\mathbf{x})] = \left[-\mu\frac{\delta\mathcal{H}}{\delta m_i(\mathbf{x})} + \frac{D}{k_BT}\frac{\delta\mathcal{H}}{\delta m_i(\mathbf{x})}\right]\mathcal{P}_{\text{eq.}}, \tag{VIII.39}$$

vanishes if the fluctuation–dissipation condition, $D = \mu k_BT$, is satisfied. Once again, the Einstein equation ensures that the equilibrium weight indeed describes a steady state.

VIII.C Dynamics of a Conserved field

In fact it is possible to obtain the correct equilibrium weight with $\mathbf{q}$ dependent mobility and noise, as long as the generalized fluctuation–dissipation condition,

$$D(\mathbf{q}) = k_B T \mu(\mathbf{q}), \tag{VIII.40}$$

holds. This generalized condition is useful in considering the dissipative dynamics of a *conserved* field. The prescription that leads to the Langevin equations (VIII.23)–(VIII.25), does not conserve the field in the sense that $\int d^d\mathbf{x}\vec{m}(\mathbf{x},t)$ can change with time. (Although this quantity is on average zero for $r > 0$, it undergoes stochastic fluctuations.) If we are dealing with the a binary mixture ($n = 1$), the order parameter which measures the difference between densities of the two components is conserved. Any concentration that is removed from some part of the system must go to a neighboring region in any realistic dynamics. Let us then consider a dynamical process constrained such that

$$\frac{d}{dt}\int d^d\mathbf{x}\,\vec{m}(\mathbf{x},t) = \int d^d\mathbf{x}\,\frac{\partial\vec{m}(\mathbf{x},t)}{\partial t} = \vec{0}. \tag{VIII.41}$$

How can we construct a dynamical equation that satisfies eq.(VIII.41)? The integral clearly vanishes if the integrand is a total divergence, i.e.

$$\frac{\partial m_i(\mathbf{x},t)}{\partial t} = -\nabla\cdot\mathbf{j}_i + \eta_i(\mathbf{x},t). \tag{VIII.42}$$

The noise itself must be a total divergence, $\eta_i = -\nabla\cdot\sigma_i$, and hence in Fourier space,

$$\langle\eta_i(\mathbf{q},t)\rangle = 0, \quad \text{and} \quad \langle\eta_i(\mathbf{q},t)\eta_j(\mathbf{q}',t')\rangle = 2D\delta_{ij}q^2\delta(t-t')(2\pi)^d\delta^d(\mathbf{q}+\mathbf{q}'). \tag{VIII.43}$$

We can now take advantage of the generalized Einstein relation in eq.(VIII.40) to ensure the correct equilibrium distribution by setting,

$$\mathbf{j}_i = \mu\nabla\cdot\left(-\frac{\delta\mathcal{H}}{\delta m_i(\mathbf{x})}\right). \tag{VIII.44}$$

The standard terminology for such dynamical equations is provided by Hohenberg and Halperin: In **model A** dynamics the field $\vec{m}$ is *not conserved*, and the mobility and diffusion coefficients are constants. In **model B** dynamics the field $\vec{m}$ is *conserved*, and $\hat{\mu} = -\mu\nabla^2$ and $\hat{D} = -D\nabla^2$.

Let us now reconsider the Gaussian model ($u = 0$), this time with a conserved order parameter, with model B dynamics

$$\frac{\partial \vec{m}(\mathbf{x},t)}{\partial t} = \mu r \nabla^2 \vec{m} - \mu K \nabla^4 \vec{m} + \vec{\eta}(\mathbf{x},t). \tag{VIII.45}$$

The evolution of each Fourier mode is given by

$$\frac{\partial \vec{m}(\mathbf{q},t)}{\partial t} = -\mu q^2 (r + Kq^2)\vec{m}(\mathbf{q},t) + \vec{\eta}(\mathbf{q},t) \equiv -\frac{\vec{m}(\mathbf{q},t)}{\tau(\mathbf{q})} + \vec{\eta}(\mathbf{q},t). \tag{VIII.46}$$

Because of the constraints imposed by the conservation law, the relaxation of the field is more difficult, and slower. The relaxation times diverge even away from criticality. Depending on wavelength, we find scaling between length and time scales with dynamic exponents z, according to

$$\tau(\mathbf{q}) = \frac{1}{\mu q^2 (r + Kq^2)} \approx \begin{cases} q^{-2} & \text{for } q \ll \xi^{-1} \qquad (z = 2) \\ q^{-4} & \text{for } q \gg \xi^{-1} \qquad (z = 4) \end{cases} . \tag{VIII.47}$$

The equilibrium behavior is unchanged, and

$$\lim_{t\to\infty} \left\langle |\vec{m}(\mathbf{q},t)|^2 \right\rangle = n \frac{Dq^2}{\mu q^2 (r + Kq^2)} = \frac{nD}{\mu (r + Kq^2)}, \tag{VIII.48}$$

as before. Thus the same static behavior can be achieved by different dynamics. The static exponents (e.g. ν) are determined by the equilibrium (stationary) state and are unchanged, while the dynamic exponents may be different. As a result, dynamical critical phenomena involve many more universality classes than the corresponding static ones.

VIII.D Generic scale invariance in equilibrium systems

We live in a world full of complex spatial patterns and structures such as coastlines and river networks. There are similarly diverse temporal processes generically exhibiting "$1/f$"–noise, as in resistance fluctuations, sand flowing through an hour glass, and even in traffic and stock market movements. These phenomena lack natural length and time scales and exhibit scale invariance and self-similarity. The spacial aspects of scale invariant systems can be characterized using *fractal* geometry[1]. In this section we explore dynamical processes that can naturally result in such scale invariant patterns.

Let us assume that the system of interest is described by a scalar field $m(\mathbf{x})$, distributed with a probability $\mathcal{P}[m]$. Scale invariance can be probed by examining the correlation functions of $m(\mathbf{x})$, such as the two point correlator, $C(|\mathbf{x}-\mathbf{y}|) \equiv \langle m(\mathbf{x})m(\mathbf{y})\rangle - \langle m(\mathbf{x})\rangle \langle m(\mathbf{y})\rangle$. (It is assumed that the system has rotational and translational symmetry.) In a system with a characteristic length scale, correlations decay to zero for separations $z = |\mathbf{x}-\mathbf{y}| \gg \xi$. By contrast, if the system possesses scale invariance, correlations are homogeneous at long distances, and $\lim_{z\to\infty} C(z) \sim z^{2\chi}$.

As we have seen, in equilibrium statistical mechanics the probability is given by $\mathcal{P}_{eq} \propto \exp(-\beta\mathcal{H}[m])$ with $\beta = (k_B T)^{-1}$. Clearly at infinite temperature there are no correlations for a finite Hamiltonian. As long as the interactions in $\mathcal{H}[m]$ are *short ranged*, it can be shown by high temperature expansions that correlations at small but finite β decay as $C(z) \propto \exp(-z/\xi)$, indicating a characteristic length-scale[†]. The correlation length usually increases upon reducing temperature, and may diverge if the system undergoes a continuous (critical) phase transition. At a critical transition the system is scale invariant and $C(z) \propto z^{2-d-\eta}$. However, such scale invariance is *non-generic* in the sense that it can be obtained only by precise tuning of the system to the critical temperature. Most scale invariant processes in nature do not require such precise tuning, and therefore the analogy to the critical point is not particularly instructive[2][3].

We shall frame our discussion of scale invariance by considering the dynamics of a surface, described by its height $h(\mathbf{x}, t)$. Specific examples are the distortions of a soap film or the fluctuations on the surface of water in a container. In both cases the minimum energy configuration is a flat surface (ignoring the small effects of gravity on the soap film).

[†] It is of course possible to generate long-range correlations with *long ranged* interactions. However, it is most interesting to find out how long-range correlations are generated from local, *short ranged* interactions.

The energy cost of small fluctuations for a soap film comes from the increased area and *surface tension* σ. Expanding the area in powers of the slope results in

$$\mathcal{H}_\sigma = \sigma \int d^d\mathbf{x} \left[\sqrt{1+(\nabla h)^2} - 1\right] \approx \frac{\sigma}{2}\int d^d\mathbf{x}\,(\nabla h)^2 \ . \tag{VIII.49}$$

For the surface of water there is an additional gravitational potential energy, obtained by adding the contributions from all columns of water as

$$\mathcal{H}_g = \int d^d\mathbf{x} \int_0^{h(\mathbf{x})} \rho g h(\mathbf{x}) = \frac{\rho g}{2}\int d^d\mathbf{x} h(\mathbf{x})^2 \,. \tag{VIII.50}$$

The total (potential) energy of small fluctuations is thus given by

$$\mathcal{H} = \int d^d\mathbf{x} \left[\frac{\sigma}{2}(\nabla h)^2 + \frac{\rho g}{2}h^2\right], \tag{VIII.51}$$

with the second term absent for the soap film.

The corresponding Langevin equation,

$$\frac{\partial h(\mathbf{x},t)}{\partial t} = -\mu\rho g h + \mu\sigma\nabla^2 h + \eta(\mathbf{x},t), \tag{VIII.52}$$

is linear, and can be solved by Fourier transforms. Starting with a flat interface, $h(\mathbf{x}, t = 0) = h(\mathbf{q}, t = 0) = 0$, the profile at time t is

$$h(\mathbf{x},t) = \int \frac{d^d\mathbf{q}}{(2\pi)^d} e^{-i\mathbf{q}\cdot\mathbf{x}} \int_0^t d\tau e^{-\mu(\rho g+\sigma q^2)(t-\tau)}\eta(\mathbf{q},t). \tag{VIII.53}$$

The average height of the surface, $\bar{H} = \int d^d\mathbf{x}\,\langle h(\mathbf{x},t)\rangle\,/L^d$ is zero, while its overall width is defined by

$$w^2(t,L) \equiv \frac{1}{L^d}\int d^d\mathbf{x}\,\langle h(\mathbf{x},t)^2\rangle = \frac{1}{L^d}\int \frac{d^d\mathbf{q}}{(2\pi)^d}\,\langle |h(\mathbf{q},t)|^2\rangle\,, \tag{VIII.54}$$

where L is the linear size of the surface. Similar to Eq.(VIII.33), we find that the width grows as

$$w^2(t,L) = \int \frac{d^d\mathbf{q}}{(2\pi)^d}\,\frac{D}{\gamma(\mathbf{q})}\,\left(1 - e^{-2\gamma(\mathbf{q})t}\right). \tag{VIII.55}$$

There are a range of time scales in the problem, related to characteristic length scales as in Eq.(VIII.31). The shortest time scale, $t_{\rm min} \propto a^2/(\mu\sigma)$, is set by an atomic size a. The longest time scale is set by either the capillary length ($\lambda_c \equiv \sqrt{\sigma/\rho g}$) or the system size ($L$).

For simplicity we shall focus on the soap film where the effects of gravity are negligible and $t_{\rm max} \propto L^2/(\mu\sigma)$. We can now identify three different ranges of behavior in Eq.(VIII.55):

(a) For $t \ll t_{\rm min}$, none of the modes has relaxed since $\gamma(\mathbf{q})t \ll 1$ for all $\mathbf{q}$. Each mode grows diffusively, and

$$w^2(t,L) = \int \frac{d^d\mathbf{q}}{(2\pi)^d}\,\frac{D}{\gamma(\mathbf{q})}\,2\gamma(\mathbf{q})t \;=\; \frac{2Dt}{a^d}. \tag{VIII.56}$$

(b) For $t \gg t_{\rm max}$, all modes have relaxed to their equilibrium values since $\gamma(\mathbf{q})t \gg 1$ for all $\mathbf{q}$. The height fluctuations now saturate to a maximum value given by

$$w^2(t,L) = \int \frac{d^d\mathbf{q}}{(2\pi)^d}\,\frac{D}{\mu\sigma q^2}. \tag{VIII.57}$$

The saturated value depends on the dimensionality of the surface, and in a general dimension d behaves as

$$w^2(t,L) \propto \frac{D}{\mu\sigma}\begin{cases} a^{2-d} & \text{for } d>2, \quad (\chi=0) \\ \ln(L/a) & \text{for } d=2, \quad (\chi=0^+) \\ L^{2-d} & \text{for } d<2, \quad (\chi=\frac{2-d}{2}) \end{cases}, \tag{VIII.58}$$

where we have defined a *roughness exponent* χ that governs the divergence of the width with system size via $\lim_{t\to\infty} w(t,L) \propto L^\chi$. (The symbol 0^+ is used to indicate a logarithmic divergence.) The exponent of $\chi = 1/2$ in $d = 1$ indicates that the one dimensional interface fluctuates like a random walk.

(c) For $t_{\rm min} \ll t \ll t_{\rm max}$ only a fraction of the shorter length scale modes are saturated. The integrand in Eq.(VIII.55) (for $g = 0$) is made dimensionless by setting $y = \mu\sigma q^2 t$, and

$$\begin{aligned} w^2(t,L) &\propto \frac{D}{\mu\sigma}\int dq\; q^{d-3}\left(1-e^{-2\mu\sigma q^2 t}\right) \\ &\propto \frac{D}{\mu\sigma}\left(\frac{1}{\mu\sigma t}\right)^{\frac{d-2}{2}}\int_{t/t_{\rm max}}^{t/t_{\rm min}} dy\; y^{\frac{d-4}{2}}\left(1-e^{-2y}\right). \end{aligned} \tag{VIII.59}$$

The final integral is convergent for $d < 2$, and dominated by its upper limit for $d \geq 2$. The initial growth of the width is described by another exponent β, defined through $\lim_{t\to 0} w(t,L) \propto t^\beta$, and

$$w^2(t,L) \propto \begin{cases} \frac{D}{\mu\sigma}a^{2-d} & \text{for } d>2, \quad (\beta=0) \\ \frac{D}{\mu\sigma}\ln\left(t/t_{\rm min}\right) & \text{for } d=2, \quad (\beta=0^+) \\ \frac{D}{(\mu\sigma)^{d/2}}t^{(2-d)/2} & \text{for } d<2, \quad (\beta=(2-d)/4) \end{cases}. \tag{VIII.60}$$

The exponents χ and β also describe the height–height correlation functions which assumes the *dynamic scaling* form

$$\left\langle [h(\mathbf{x},t) - h(\mathbf{x}',t')]^2 \right\rangle = |\mathbf{x}-\mathbf{x}'|^{2\chi}\, g\left(\frac{|t-t'|}{|\mathbf{x}-\mathbf{x}'|^z}\right). \tag{VIII.61}$$

Since equilibrium equal time correlations only depend on $|\mathbf{x}-\mathbf{x}'|$, $\lim_{y\to 0} g(y)$ should be a constant. On the other hand correlations at the same point can only depend on time, requiring that $\lim_{y\to\infty} g(y) \propto y^{2\chi/z}$, and leading to the exponent identity $\beta = \chi/z$.

This scale invariance is broken when the gravitational potential energy, is added to the Hamiltonian. The correlations now decay as $C(z) \propto \exp(-z/\lambda_c)$ for distances larger than the capillary length. What is the underlying difference between these two cases? The presence of gravity breaks the translational symmetry, $\mathcal{H}[h(\mathbf{x})+c] = \mathcal{H}[h(\mathbf{x})]$. It is this continuous symmetry that forbids the presence of a term proportional to $\int d^d\mathbf{x} h(\mathbf{x})^2$ in the Hamiltonian and removes the corresponding length scale. (The coefficient of the quadratic term is usually referred to as a *mass* in field theoretical language.) The presence of a *continuous symmetry* is quite a general condition for obtaining *generic scale invariance* (GSI)[4]. As discussed in previous chapters, there are many low temperature phases of matter in which a continuous symmetry is spontaneously broken. The energy cost of small fluctuations around such a state must obey the *global* symmetry. The resulting excitations are the "massless" *Goldstone modes*. We already discussed such modes in connection with *magnons* in ferromagnets (with broken rotational symmetry), and *phonons* in solids (broken translational symmetry). All these cases exhibit scale invariant fluctuations.

In the realm of dynamics we can ask the more general question of whether temporal correlations, e.g. $C(|\mathbf{x}-\mathbf{x}'|, t-t') = \langle h(\mathbf{x},t)h(\mathbf{x}',t')\rangle_c$, exhibit a characteristic time scale τ, or are homogeneous in $t-t'$. It is natural to expect that scale invariance in the spacial and temporal domains are closely interlinked. Establishing correlations at large distances requires long times as long as the system follows *local* dynamical rules (typically $(t-t') \propto |\mathbf{x}-\mathbf{x}'|^z$). Spacial scale invariance thus implies the lack of a time scale. The converse is not true as dynamics provides an additional possibility of removing time scales through a *conservation law*. We already encountered this situation in examining the model B dynamics of the surface Hamiltonian in the presence of gravity. Equation (VIII.47) indicates that, even though the long wavelength modes are massive, the relaxation time of a mode of wavenumber $\mathbf{q}$ diverges as $1/q^2$ in the $\mathbf{q}\to\mathbf{0}$ limit.

Symmetries and conservation laws are intimately linked in equilibrium systems. Consider a *local* Hamiltonian that is invariant under the symmetry $\mathcal{H}[h(\mathbf{x}) + c] = \mathcal{H}[h(\mathbf{x})]$. Since $\mathcal{H}$ can only depend on ∇h and higher derivatives,

$$v = \mu F = -\mu \frac{\delta \mathcal{H}}{\delta h(\mathbf{x})} = \mu \nabla \cdot \frac{\partial \mathcal{H}}{\partial \nabla h} + \cdots \equiv \nabla \cdot \vec{j} \quad . \tag{VIII.62}$$

Even for model A dynamics, the deterministic part of the velocity is the divergence of a current and conserves $\int d^d\mathbf{x} h(\mathbf{x}, t)$. The conservation is only statistical and locally broken by the non-conserved noise in model A. The above result is a consequence of *Noether's theorem*.

VIII.E Non-equilibrium dynamics of open systems

We have to be cautious in applying the methods and lessons of near equilibrium dynamics to the various processes in nature which exhibit generic scale invariance. Many such systems, such as a flowing river or a drifting cloud, are very far from equilibrium. Furthermore, they are open and extended systems constantly exchanging particles and constituents with their environment. It is not clear that there is any Hamiltonian that governs the dynamics of such processes and hence the traditional approach presented earlier is not necessarily appropriate. However, the robust self-similar correlations observed in these systems[1] suggests that they can be described by stationary scale invariant probability distributions. This section outlines a general approach to the dynamics of open and extended systems that is similar in spirit to the construction of effective coarse–grained field theories described in Chapter 2. Let us again consider the dynamics of a static field, $h(\mathbf{x}, t)$:

1. The starting point in equilibrium statistical mechanics is the Hamiltonian $\mathcal{H}[h]$. Landau's prescription is to include in $\mathcal{H}$ *all terms consistent with the symmetries* of the problem. The underlying philosophy is that in a generic situation an allowed term is present, and can only vanish by accident. In the case of non-equilibrium dynamics we shall assume that the *equation of motion* is the fundamental object of interest. Over sufficiently long time scales, inertial terms ($\propto \partial_t^2 h$) are irrelevant in the presence of dissipative dynamics, and the evolution of h is governed by

$$\partial_t h(\mathbf{x}, t) = \overbrace{v\left[h(\mathbf{x}, t)\right]}^{\text{deterministic}} + \overbrace{\eta(\mathbf{x}, t)}^{\text{stochastic}} \quad . \tag{VIII.63}$$

2. If the interactions are short ranged, the velocity at $(\mathbf{x}, t)$ depends only on $h(\mathbf{x}, t)$ and a few derivatives evaluated at $(\mathbf{x}, t)$, i.e.

$$v(\mathbf{x}, t) = v\big(h(\mathbf{x}, t), \nabla h(\mathbf{x}, t), \cdots\big). \tag{VIII.64}$$

3. We must next specify the functional form of deterministic velocity, and the correlations in noise. Generalizing Landau's prescription, we assume that all terms consistent with the underlying *symmetries and conservation laws* will generically appear in v. The noise, $\eta(\mathbf{x}, t)$, may be conservative or non-conservative depending on whether there are only internal rearrangements, or external inputs and outputs.

Corollary: Note that with these set of rules there is no reason for the velocity to be derivable from a potential ($v \neq -\hat{\mu}\delta\mathcal{H}/\delta h$), and there is no fluctuation–dissipation condition ($\hat{D} \neq \hat{\mu} k_B T$). It is even possible for the deterministic velocity to be conservative, while the noise is not. Thus various familiar results of near equilibrium dynamics may no longer hold.

As an example consider the flow of water along a river (or traffic along a highway). The deterministic part of the dynamics is conservative (the amount of water, or the number of cars is unchanged). Hence the velocity is the divergence of a current, $v = -\nabla\vec{j}\,[h]$. The current, $\vec{j}$, is a vector, and must be constructed out of the other two vectorial quantities in the problem: the gradient operator ∇, and the average transport direction $\hat{t}$. (The unit vector $\hat{t}$ points along the direction of current or traffic flow.) The lowest order terms in the expansion of the current give

$$-\vec{j} = \hat{t}(\alpha h - \frac{\lambda}{2}h^2 + \cdots) + \nu_1 \nabla h + \nu_2 \hat{t}(\hat{t}\cdot\nabla)h + \cdots. \tag{VIII.65}$$

The components of current parallel and perpendicular to the net flow are

$$\begin{cases} -j_\parallel = \alpha h - \frac{\lambda}{2}h^2 + (\nu_1 + \nu_2)\partial_\parallel h + \cdots \\ -\vec{j}_\perp = \nu_1 \vec{\partial}_\perp h + \cdots \end{cases} . \tag{VIII.66}$$

The resulting equation of motion is

$$\frac{\partial h(\mathbf{x}, t)}{\partial t} = \partial_\parallel(\alpha h - \frac{\lambda}{2}h^2) + (\nu_1 + \nu_2)\partial_\parallel^2 h + \nu_1 \partial_\perp^2 h + \cdots + \eta(\mathbf{x}, t). \tag{VIII.67}$$

In the absence of external inputs and outputs (no rain, drainage, or exits), the noise is also conservative, with correlations,

$$\langle \eta(\mathbf{q}, t)\rangle = 0, \quad \text{and} \quad \langle \eta(\mathbf{q}, t)\eta(\mathbf{q}', t')\rangle = 2(D_\parallel q_\parallel^2 + D_\perp q_\perp^2)\,\delta(t - t')(2\pi)^d \delta^d(\mathbf{q} + \mathbf{q}'). \tag{VIII.68}$$

Note that the symmetries of the problem allow different noise correlations parallel and perpendicular to the net flow.

Equations (VIII.67) and (VIII.68) define a *driven diffusion system* (DDS)[5],[6]. The first term in Eq.(VIII.67) can be eliminated by looking at fluctuations in a moving frame,

$$h(x_\parallel, \mathbf{x}_\perp, t) \to h(x_\parallel - \alpha t, \mathbf{x}_\perp, t), \tag{VIII.69}$$

and shall be ignored henceforth. Neglecting the non-linear terms, these fluctuations satisfy the anisotropic noisy diffusion equation

$$\frac{\partial h(\mathbf{x},t)}{\partial t} = \nu_\parallel \partial_\parallel^2 h + \nu_\perp \partial_\perp^2 h + \eta(\mathbf{x},t), \tag{VIII.70}$$

where $\nu_\parallel = \nu_1 + \nu_2$ and $\nu_\perp = \nu_1$. The Fourier modes now relax with characteristic times,

$$\tau(\mathbf{q}) = \frac{1}{\nu_\parallel q_\parallel^2 + \nu_\perp q_\perp^2}. \tag{VIII.71}$$

Following the steps leading to Eq.(VIII.48),

$$\lim_{t\to\infty} \left\langle |h(\mathbf{q},t)|^2 \right\rangle = \frac{D_\parallel q_\parallel^2 + D_\perp q_\perp^2}{\nu_\parallel q_\parallel^2 + \nu_\perp q_\perp^2}\,. \tag{VIII.72}$$

The stationary correlation functions[†] in real space now behave as[4][6]

$$\begin{aligned}\left\langle \left(h(\mathbf{x}) - h(\mathbf{0})\right)^2 \right\rangle &= \int \frac{d^{d-1}\mathbf{q}_\perp dq_\parallel}{(2\pi)^d} \left(2 - 2\cos(q_\parallel x_\parallel + \mathbf{q}_\perp \cdot \mathbf{x}_\perp)\right) \frac{D_\parallel q_\parallel^2 + D_\perp q_\perp^2}{\nu_\parallel q_\parallel^2 + \nu_\perp q_\perp^2} \\ &\propto \left(\frac{D_\perp}{\nu_\perp} - \frac{D_\parallel}{\nu_\parallel}\right) \sqrt{\frac{\nu_\parallel^{d-1}\nu_\perp}{\left(\nu_\perp x_\parallel^2 + \nu_\parallel x_\perp^2\right)^d}}\end{aligned}. \tag{VIII.73}$$

Note that these correlations are spatially extended and scale invariant. This is again a consequence of the conservation law. Only in the special case where $D_\perp/\nu_\perp = D_\parallel/\nu_\parallel$ is the Einstein relation ($D(\mathbf{q}) \propto \nu(\mathbf{q})$) satisfied, and the fluctuations become uncorrelated ($C(\mathbf{x}) \propto \delta^d(\mathbf{x}) D/\nu$). The results then correspond to model B dynamics with a Hamiltonian $\mathcal{H} \propto \int d^d\mathbf{x} h^2$. This example illustrates the special nature of near equilibrium dynamics. The fluctuation–dissipation condition is needed to ensure approach to the equilibrium state

[†] In non-equilibrium circumstances we shall use the term *stationary* to refer to behavior at long times.

where there is typically no scale invariance. On the other hand, removing this restriction leads to GSI in a conservative system. ($D_\perp/\nu_\perp \neq D_\parallel/\nu_\parallel$ is like having two different temperatures parallel and perpendicular to the flow.)

Let us now break the conservation law stochastically by adding random inputs and outputs to the problem (in the form of rain, drainage, or exits). The properties of the noise are now modified to

$$\langle \eta(\mathbf{x},t)\rangle = 0, \quad \text{and} \quad \langle \eta(\mathbf{x},t)\eta(\mathbf{x}',t')\rangle = 2D\delta(x_\parallel - x'_\parallel)\delta^{d-1}(\mathbf{x}_\perp - \mathbf{x}'_\perp)\delta(t-t'). \quad \text{(VIII.74)}$$

In the stationary state,

$$\lim_{t\to\infty} \left\langle |h(\mathbf{q},t)|^2 \right\rangle = \frac{D}{\nu_\parallel q_\parallel^2 + \nu_\perp q_\perp^2}, \quad \text{(VIII.75)}$$

in Fourier space, and

$$\left\langle \left(h(\mathbf{x}) - h(\mathbf{0})\right)^2 \right\rangle \propto D\left(\nu_\perp x_\parallel^2 + \nu_\parallel x_\perp^2\right)^{\frac{2-d}{2}}, \quad \text{(VIII.76)}$$

in real space. Except for the anisotropy, this is the same result as in Eq.(VIII.61), with $\chi = (2-d)/2$.

How are the results modified by the nonlinear term $(-\lambda\partial_\parallel h^2/2)$ in Eq.(VIII.67)? We first perform a simple *dimensional analysis* by rescaling lengths and time. Allowing for anisotropic scalings, we set $x_\parallel \to b x_\parallel$, accompanied by $t \to b^z t$, $\vec{x}_\perp \to b^\zeta \vec{x}_\perp$, and $h \to b^\chi h$. Eq.(VIII.67) is now modified to

$$b^{\chi - z}\frac{\partial h}{\partial t} = \nu_\parallel b^{\chi-2}\partial_\parallel^2 h + \nu_\perp b^{\chi-2\zeta}\partial_\perp^2 h - \frac{\lambda}{2} b^{2\chi-1}\partial_\parallel h^2 + b^{-z/2-(d-1)\zeta/2-1/2}\eta, \quad \text{(VIII.77)}$$

where Eq.(VIII.74) has been used to determine the scaling of η. We thus identify the bare scalings for these parameters as

$$\begin{cases} \nu_\parallel \to b^{z-2}\nu_\parallel \\ \nu_\perp \to b^{z-2\zeta}\nu_\perp \\ \lambda \to b^{\chi+z-1}\lambda \\ D \to b^{z-2\chi-\zeta(d-1)-1}D \end{cases}. \quad \text{(VIII.78)}$$

In the absence of λ, the parameters can be made *scale invariant* (i.e. independent of b), by the choice of $\zeta_0 = 1$, $z_0 = 2$, and $\chi_0 = (2-d)/2$, as encountered before. However, with this choice, a small λ will grow under rescaling as

$$\lambda \to b^{y_0}\lambda, \quad \text{with} \quad y_0 = \frac{4-d}{2}. \quad \text{(VIII.79)}$$

Since the non-linearity grows larger under scaling it cannot be ignored in dimensions $d < 4$.

Equations (VIII.79) constitute a simple renormalization group (RG) that is valid close to the *fixed point* (scale invariant equation) corresponding to a linearized limit. To calculate the RG equations at finite values of nonlinearity in general requires a perturbative calculation. Sometimes there are exact *non–renormalization conditions* that simplify the calculation and lead to exponent identities. Fortunately there are enough such identities for Eq.(VIII.78) that the three exponents can be obtained *exactly*.

1. As the nonlinearity is proportional to $q_\parallel$ is Fourier space, it does not generate under RG any contributions that can modify $\nu_\perp$. The corresponding 'bare' scaling of $\nu_\perp$ in Eqs.(VIII.78) is thus always valid; its fixed point leads to the exponent identity $z - 2\zeta = 0$.
2. As the nonlinearity is in the conservative part, it does not renormalize the strength of the non–conservative noise. The non–renormalization of D leads to the exponent identity $z - 2\chi - \zeta(d-1) - 1 = 0$. (This condition has a natural counterpart in equilibrium model B dynamics, $z - 2\chi - d - 2 = 0$, leading to the well known relation, $z = 4 - \eta$.)
3. Eq.(VIII.67) is invariant under an infinitesimal reparameterization $x_\parallel \to x_\parallel - \delta\lambda t$, $t \to t$, if $h \to h + \delta$. Note that the parameter λ appears both as the coefficient of the non-linearity in Eq.(VIII.67) and as an invariant factor relating the $x_\parallel$ and h reparameterizations. Hence any renormalization of the driven diffusion equation that preserves this symmetry must leave the coefficient λ unchanged, leading to the exponent identity $z + \chi - 1 = 0$.

The remaining parameter, $\nu_\parallel$ does indeed follow a non-trivial evolution under RG. However, the above three exponent identities are sufficient to give the exact exponents in all dimensions $d \leq 4$ as[2]

$$\chi = \frac{1-d}{7-d}, \quad z = \frac{6}{7-d}, \quad \zeta = \frac{3}{7-d}. \tag{VIII.80}$$

VIII.F Dynamics of a growing surface

The rapid growth of crystals by deposition, or molecular beam epitaxy, is an important technological process. It also provides the simplest example of a non-equilibrium evolution process[7]. We would like to understand the dynamic scaling of fluctuations inherent to this type of growth. To construct the dependence of the local, deterministic velocity, v, on the surface height, $h(\mathbf{x}, t)$, note that:

(1) As long as the rearrangements of particles on the surface can result in holes and vacancies, there is no conservation law.

(2) There is a *translation symmetry*, $v[h(\mathbf{x})+c] = v[h(\mathbf{x})]$, implying that v depends only on gradients of $h(\mathbf{x})$.

(3) For simplicity, we shall focus on *isotropic* surfaces, in which all directions in $\mathbf{x}$ are equivalent[8].

(4) There is no up–down symmetry, i.e. $v[h(\mathbf{x})] \neq -v[-h(\mathbf{x})]$. The absence of such symmetry allows addition of terms of both parities.

With these conditions, the lowest order terms in the equation of motion give[9],

$$\frac{\partial h(\mathbf{x},t)}{\partial t} = u + \nu\nabla^2 h + \frac{\lambda}{2}\left(\nabla h\right)^2 + \cdots + \eta(\mathbf{x},t), \tag{VIII.81}$$

with the non-conservative noise satisfying the correlations in Eq.(VIII.74).

In Eq.(VIII.81), u is related to the average growth velocity. In fact, the coefficients of all even terms must be proportional to u as they all vanish in the symmetric case with no preferred growth direction. The constant u is easily removed by transforming to a moving frame, $h \to h - ut$, and will be ignored henceforth. The first non-trivial term is the nonlinear contribution, $\lambda(\nabla h)^2/2$. Geometrically this term can be justified by noting that growth by addition of particles proceeds through a parallel transport of the surface gradient in the normal direction. (See the inset to Fig. 9.1.) This term cannot be generated from the variations of any Hamiltonian, i.e. $v \neq -\mu\delta\mathcal{H}[h]/\delta h$. Thus, contrary to the equilibrium situation (Noether's theorem), the translational symmetry does not imply a conservation law, $v \neq -\nabla j$.

Further evidence of the relevance of Eq.(VIII.81) to growth phenomena is provided by examining *deterministic growth*. Consider a slow and uniform snowfall, on an initial profile which at $t = 0$ is described by $h_0(\mathbf{x})$. The nonlinear equation can in fact be *linearized* with the aid of a "Cole–Hopf" transformation,

$$W(\mathbf{x},t) = \exp\left[\frac{\lambda}{2\nu}h(\mathbf{x},t)\right]. \tag{VIII.82}$$

The function $W(\mathbf{x},t)$ evolves according to the diffusion equation with *multiplicative noise*,

$$\frac{\partial W(\mathbf{x},t)}{\partial t} = \nu\nabla^2 W + \frac{\lambda}{2\nu}W\eta(\mathbf{x},t). \tag{VIII.83}$$

In the absence of noise, $\eta(\mathbf{x},t) = 0$, Eq.(VIII.83) can be solved subject to the initial condition $W(\mathbf{x},t=0) = \exp[\lambda h_0(\mathbf{x})/2\nu]$, and leads to the growth profile,

$$h(\mathbf{x},t) = \frac{2\nu}{\lambda} \ln \left\{ \int d^d\mathbf{x}' \exp\left[-\frac{|\mathbf{x}-\mathbf{x}'|^2}{2\nu t} + \frac{\lambda}{2\nu} h(\mathbf{x},t) \right] \right\}. \qquad \text{(VIII.84)}$$

It is instructive to examine the $\nu \to 0$ limit, which is indeed appropriate to snow falls since there is not much rearrangement after deposition. In this limit, the integral in Eq.(VIII.84) can be performed by the saddle point method. For each $\mathbf{x}$ we have to identify a point $\mathbf{x}'$ which maximizes the exponent, leading to a collection of paraboloids described by

$$h(\mathbf{x},t) = \max_{\mathbf{x}'} \left\{ h_0(\mathbf{x}') - \frac{|\mathbf{x}-\mathbf{x}'|^2}{2\lambda t} \right\}. \qquad \text{(VIII.85)}$$

Such parabolic sequences are quite common in many layer by layer growth processes in nature, from biological to geological formations. The patterns for $\lambda = 1$ are identical to those obtained by a geometrical method of Huygens, familiar from optics. The growth profile (wave front) is constructed from the outer envelop of circles of radius λt drawn from all points on the initial profile. The nonlinearity in Eq.(VIII.81) algebraically captures this process of expanding wave fronts.

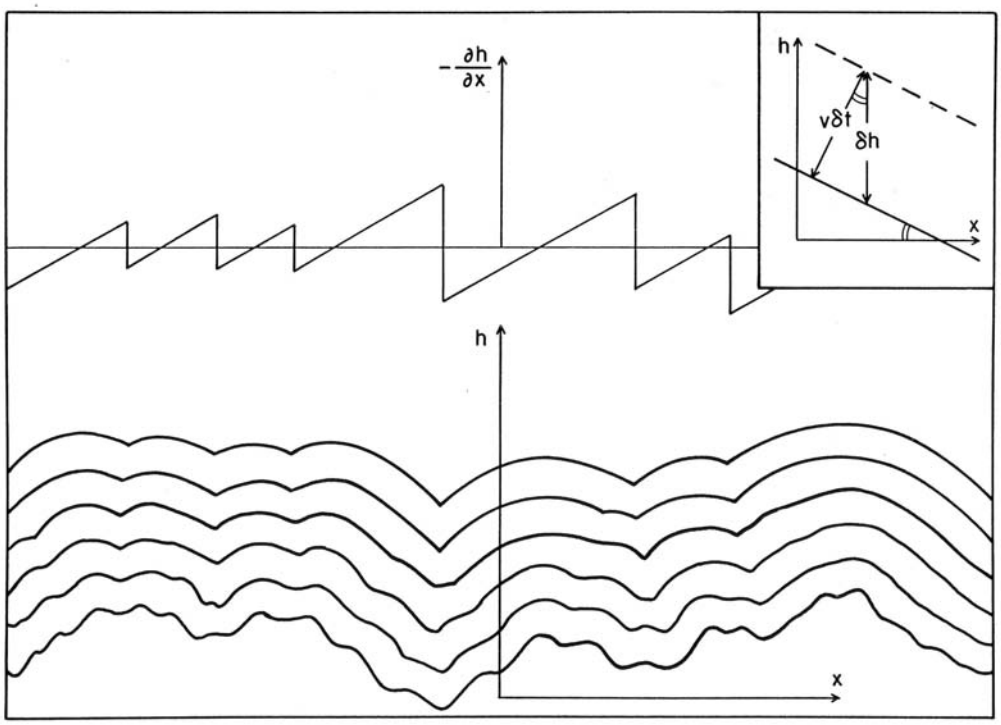

VIII.1. Deterministic growth according to eq,(VIII.81) leads to a pattern of coarsening paraboloids. In one dimension, the slope of the interface forms 'shock fronts.' Inset depicts projection of lateral growth on the vertical direction.

As growth proceeds, the surface smoothens by the *coarsening* of the parabolas. What is the typical size of these features at time t? In maximizing the exponent in Eq.(VIII.85), we have to balance a reduction $|\mathbf{x}-\mathbf{x}'|^2/2\lambda t$, by a possible gain from $h_0(\mathbf{x}')$ in selecting a point away from $\mathbf{x}$. The final scaling is controlled by the roughness of the initial profile. Let us assume that the original pattern is a *self-affine fractal* of roughness χ, i.e.

$$\overline{|h_0(\mathbf{x})-h_0(\mathbf{x}')|} \sim |\mathbf{x}-\mathbf{x}'|^{\chi}. \tag{VIII.86}$$

(According to Mandelbrot, $\chi \approx 0.7$ for mountains[1].) Balancing the two terms in Eq.(VIII.85) gives

$$(\delta x)^{\chi} \sim \frac{(\delta x)^2}{t} \quad \Longrightarrow \quad \delta x \sim t^{1/z}, \quad \text{with} \quad z+\chi = 2. \tag{VIII.87}$$

For example, if the initial profile is like a random walk in $d=1$, $\chi = 1/2$, and $z = 3/2$. This leads to the spreading of information along the profile by a process that is faster than diffusion, $\delta x \sim t^{2/3}$.

Note that the slope, $\vec{v}(\mathbf{x},t) = -\lambda\vec{\nabla}h(x,t)$, satisfies the equation,

$$\frac{D\vec{v}(\mathbf{x},t)}{Dt} \equiv \frac{\partial \vec{v}}{\partial t} + \vec{v}\cdot\vec{\nabla}\vec{v} = \nu\nabla^2\vec{v} - \lambda\nabla\eta. \tag{VIII.88}$$

The above is the Navier–Stokes equation for the velocity of a fluid of viscosity ν, which is being randomly stirred by a conservative force[10], $\vec{f} = -\lambda\nabla\eta$. However, the fluid is vorticity free since

$$\vec{\Omega} = \vec{\nabla}\times\vec{v} = -\lambda\nabla\times\nabla h = 0. \tag{VIII.89}$$

This is the *Burgers' equation*[11], which provides a simple example of the formation of shock waves in a fluid. The gradient of Eq.(VIII.85) in $d=1$ gives a saw tooth pattern of shocks which coarsen in time. Further note that in $d=1$ Eq.(VIII.88) is also equivalent to the driven diffusion equation of (VIII.67), with $\vec{v}$ playing the role of h.

To study stochastic roughening in the presence of the nonlinear term, we carry out a scaling analysis as in Eq.(VIII.77). Under the scaling $\mathbf{x}\to b\mathbf{x}$, $t\to b^z t$, and $h\to b^{\chi}h$, Eq.(VIII.81) transforms to

$$b^{\chi-z}\frac{\partial h}{\partial t} = \nu b^{\chi-2}\nabla^2 h + \frac{\lambda}{2}b^{2\chi-2}\left(\nabla h\right)^2 + \eta\left(b\mathbf{x}, b^z t\right). \tag{VIII.90}$$

The correlations of the transformed noise, $\eta'(\mathbf{x},t) = b^{z-\chi}\eta(b\mathbf{x}, b^z t)$, satisfy

$$\begin{aligned}\langle \eta'(\mathbf{x},t)\eta'(\mathbf{x}',t')\rangle =& b^{2z-2\chi}\, 2D\, \delta^d(\mathbf{x}-\mathbf{x}')b^{-d}\delta(t-t')b^{-z} \\ =& b^{z-d-2\chi}\, 2D\, \delta^d(\mathbf{x}-\mathbf{x}')\delta(t-t')\end{aligned} \quad . \tag{VIII.91}$$

Following this scaling the parameters of Eq.(VIII.81) are transformed to

$$\begin{cases} \nu \to b^{z-2}\nu \\ \lambda \to b^{\chi+z-2}\lambda \\ D \to b^{z-2\chi-d}D \end{cases} \quad . \tag{VIII.92}$$

For $\lambda = 0$, the equation is made scale invariant upon the choice of $z_0 = 2$, and $\chi_0 = (2-d)/2$. Close to this linear fixed point, λ scales to $b^{z_0+\chi_0-2}\lambda = b^{(2-d)/2}\lambda$, and is a relevant operator for $d < 2$. In fact a perturbative dynamic renormalization group suggests that it is *marginally relevant* at $d = 2$, and that in all dimensions a sufficiently large λ leads to new scaling behavior. (This will be discussed further in the next chapter.)

Are there any non–renormalization conditions that can help in identifying the exponents of the full nonlinear stochastic equation? Note that since Eqs.(VIII.81) and (VIII.88) are related by a simple transformation, they must have the same scaling properties. Since the Navier–Stokes equation is derivable from Newton's laws of motion for fluid particles, it has the Galilean invariance of changing to a uniformly moving coordinate frame. This symmetry is preserved under renormalization to larger scales and requires that the ratio of the two terms on the left hand side of Eq.(VIII.88) ($\partial_t \vec{v}$ and $\vec{v}\cdot\nabla\vec{v}$) stays at unity. In terms of Eq.(VIII.81) this implies the non–renormalization of the parameter λ, and leads to the exponent identity

$$\chi + z = 2. \tag{VIII.93}$$

Unfortunately there is no other non–renormalization condition except in $d = 1$. Following Eq.(VIII.36), we can write down a Fokker–Planck equation for the evolution of the configurational probability as,

$$\frac{\partial \mathcal{P}([h(\mathbf{x})],t)}{\partial t} = -\int d^d\mathbf{x} \frac{\delta}{\delta h(\mathbf{x})}\left[\left(\nu\nabla^2 h + \frac{\lambda}{2}(\nabla h)^2\right)\mathcal{P} - D\frac{\delta \mathcal{P}}{\delta h(\mathbf{x})}\right]. \tag{VIII.94}$$

Since Eq.(VIII.81) was not constructed from a Hamiltonian, in general we do not know the stationary solution at long times. In $d = 1$, we make a guess and try a solution of the form

$$\mathcal{P}_0[h(x)] \propto \exp\left[-\frac{\nu}{2D}\int dx (\partial_x h)^2\right]. \tag{VIII.95}$$

Since

$$\frac{\delta \mathcal{P}_0}{\delta h(x)} = -\partial_x \frac{\delta \mathcal{P}_0}{\delta(\partial_x h)} = \frac{\nu}{D}\left(\partial_x^2 h\right)\mathcal{P}_0, \tag{VIII.96}$$

Eq.(VIII.94) leads to,

$$\begin{aligned}\frac{\partial \mathcal{P}_0}{\partial t} =& -\int dx \frac{\delta \mathcal{P}_0}{\delta h(x)}\left(\nu\partial_x^2 h + \frac{\lambda}{2}(\partial_x h)^2 - D\frac{\nu}{D}\partial_x^2 h\right) \\ =& -\frac{\lambda}{2}\mathcal{P}_0 \int dx \frac{\nu}{D}(\partial_x^2 h)(\partial_x h)^2 = -\frac{\lambda\nu}{2D}\mathcal{P}_0 \int dx \partial_x\left(\frac{(\partial_x h)^3}{3}\right) = 0.\end{aligned} \tag{VIII.97}$$

We have thus identified the stationary state of the one dimensional equation. (This procedure does not work in higher dimensions as it is impossible to write the final result as a total derivative.) Surprisingly, the stationary distribution is the same as the one in equilibrium at a temperature proportional to D/ν. We can thus immediately identify the roughness exponent $\chi = 1/2$, which together with the exponent identity in Eq.(VIII.93) leads to $z = 3/2$, i.e. super-diffusive behavior.

The values of the exponents in the strongly non-linear regime are not known exactly in higher dimensions. However, extensive numerical simulations of growth have provided fairly reliable estimates[7]. In the physically relevant case ($d = 2$) of a surface grown in three dimensions, $\chi \approx 0.39$ and $z \approx 1.61$[12]. A rather good (but not exact) fit to the exponents in a general dimension d is the following estimate by Kim and Kosterlitz[13],

$$\chi \approx \frac{2}{d+3} \quad \text{and} \quad z \approx \frac{2(d+2)}{d+3}. \tag{VIII.98}$$

References

[1] B.B. Mandelbrot, *The Fractal Geometry of Nature* (Freeman, San Francisco, 1982).

[2] T. Hwa and M. Kardar, Phys. Rev. A **45**, 7002 (1992).

[3] Similar motivations underlie the development of the concept of Self-Organized Criticality by P. Bak, C. Tang and K. Wiesenfeld, Phys. Rev. Lett. **59**, 381 (1987). The distinctions and similarities to generic scale invariance are discussed in Ref.[2].

[4] G. Grinstein, S. Sachdev, and D.H. Lee, Phys. Rev. Lett. **64**, 1927 (1990).

[5] H.K. Janssen and B. Schmitttman, Z. Phys. B **63**, 517 (1986).

[6] P.L. Garrido, J.L. Lebowitz, C. Maes, and H. Spohn, Phys. Rev. A **42**, 1954 (1990); Z. Cheng, P.L. Garrido, J.L. Lebowitz, and J.L. Valles, Europhys. Lett. **14**, 507 1991).

[7] *Dynamics of Fractal Surfaces*, edited by F. Family and T. Vicsek, World Scientific, Singapore (1991).

[8] See, however, D. Wolf, Phys. Rev. Lett. **67**, 1783 (1991).

[9] M. Kardar, G. Parisi, and Y.-C. Zhang, Phys. Rev. Lett. **56**, 889 (1986); E. Medina, T. Hwa, M. Kardar, and Y.-C. Zhang, Phys. Rev. A **39**, 3053 (1989).

[10] D. Forster, D.R. Nelson, and M.J. Stephen, Phys. Rev. A **16**, 732 (1977).

[11] J.M. Burgers, *The Nonlinear Diffusion Equation* (Riedel, Boston, 1974).

[12] B.M. Forrest and L.-H. Tang, Phys. Rev. Lett. **64**, 1405 (1990)

[13] J.M. Kim and J.M. Kosterlitz, Phys. Rev. Lett. **62**, 2289 (1989).